Particle Detectors

Lecture at the African School for Fundamental Physics
Kumasi, Ghana 2012

- **Introduction:**
  - From visual to electronic detectors
  - Some generalities
- **The “building blocks”**
  - Gas detectors
  - Scintillators
  - Semiconductors
  - Calorimeters
  - Cerenkov and transition radiation detectors
- **Detector systems, some examples**
  - (Dark matter searches)
  - (Detectors in Space)
  - Nuclear physics
  - Experiments at the LHC
  - (Neutrino experiments)
  - Astroparticle physics experiments
  - (Applications in medicine and other fields, see later during this school)
- **Large collaborations: Where are the students?**
- **Conclusions or recommendations**

UNIVERSITÉ DE STRASBOURG

Who am I?

Ulrich.Goerlach@iphc.cnrs.fr

IPHC Institut Pluridisciplinaire Hubert CURIEN STRASBOURG

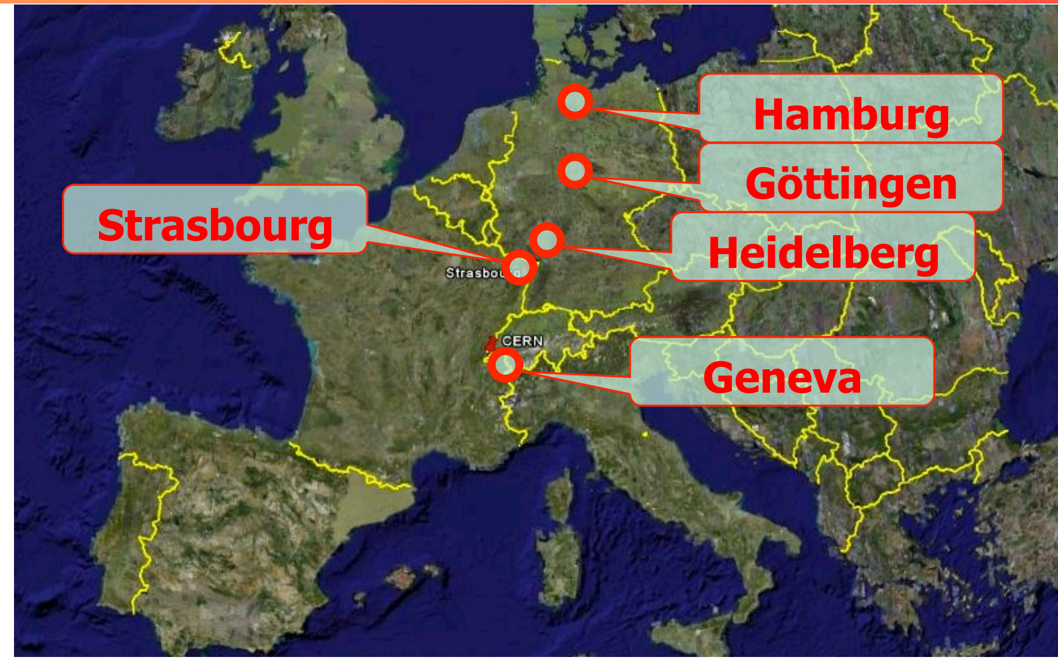

- Born in Göttingen, Germany

  interested in science at the age of about 14
- Physics (and Math) studies at the Universities Göttingen and Heidelberg
- Diploma (now Master) and PhD at the Max Planck Institute for Nuclear Physics in Heidelberg
- Post-doc (particle physics) at CERN, Geneva
- Researcher at University Heidelberg
- Researcher at CERN Geneva
- Researcher at DESY, Hamburg
- University Professor at the UdS, (Université de Strasbourg), IPHC
- Responsible for the Master in subatomic Physics

CMS experiment at the LHC

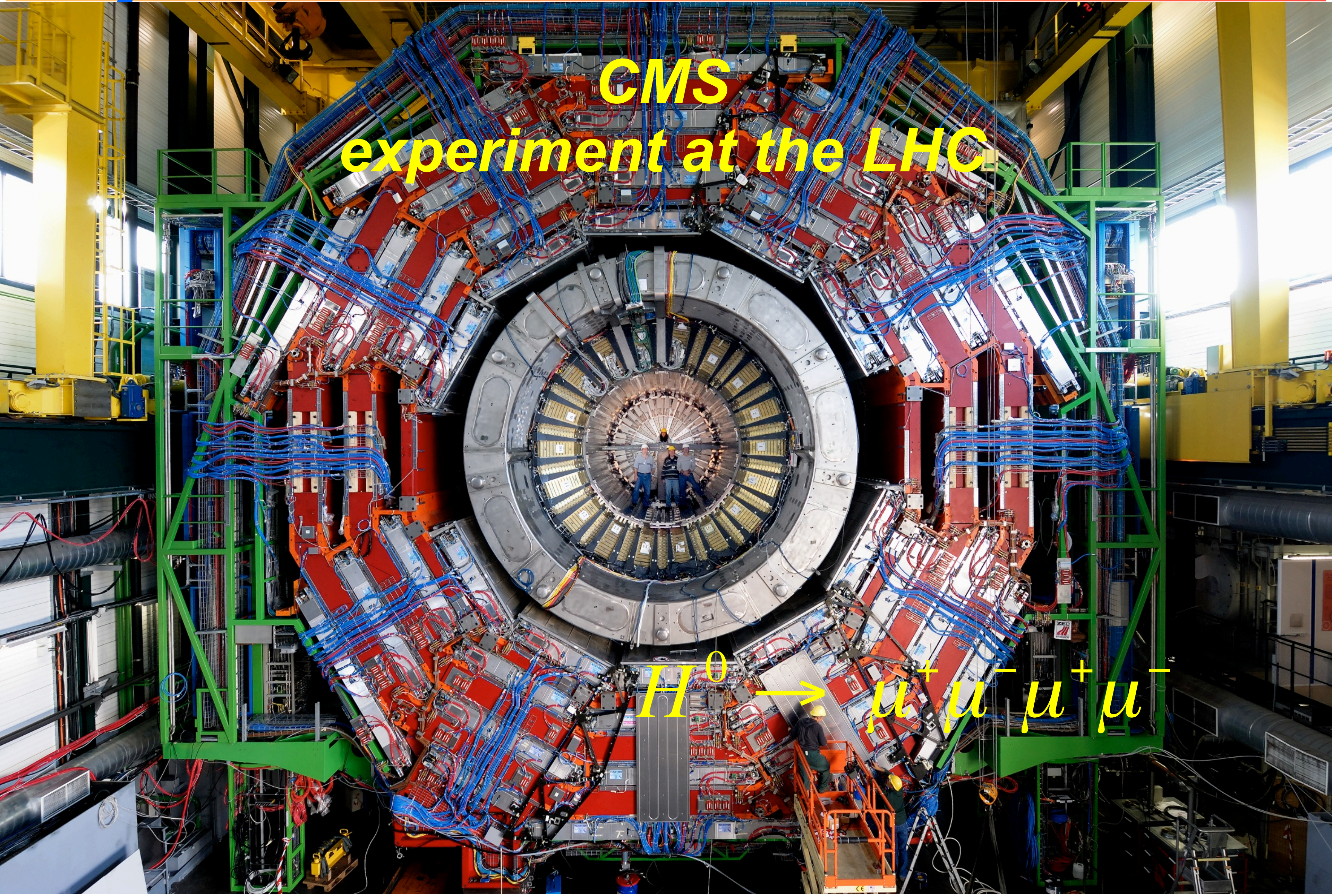

$$H^0 \rightarrow \mu^+\mu^-\mu^+\mu^-$$

CMS experiment at the LHC

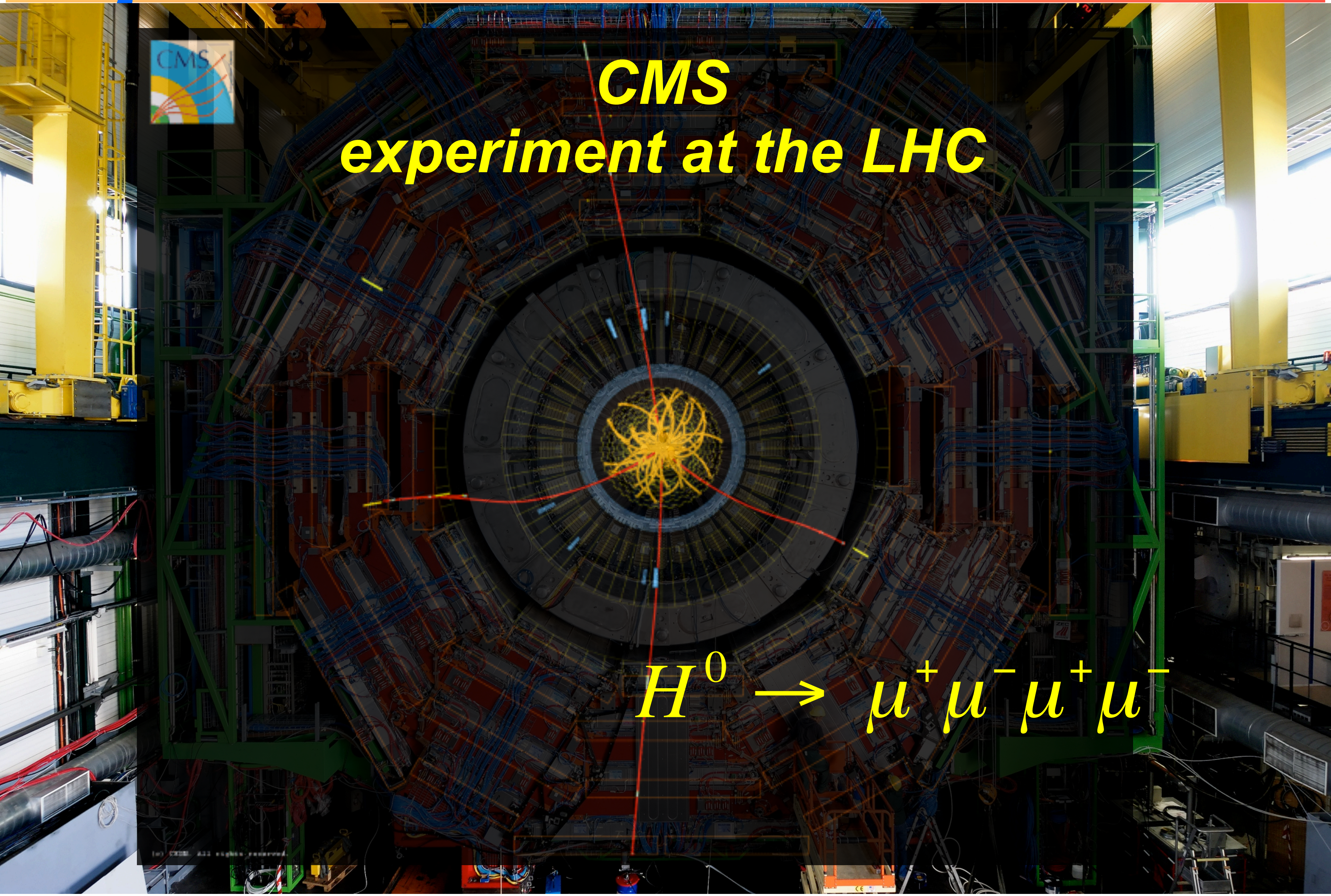

$$H^0 \rightarrow \mu^+\mu^-\mu^+\mu^-$$

UNIVERSITÉ DE STRASBOURG

Bibliography

Text books :

– C. Grupen, Particle Detectors, Cambridge University Press, 1996
– G. Knoll, Radiation Detection and Measurement, 3rd ed. Wiley, 2000
– W. R. Leo, Techniques for Nuclear and Particle Physics Experiments, Springer, 1994
– K. Kleinknecht, Detectors for particle radiation , 2nd edition, Cambridge Univ. Press, 1998
- G. Lutz, Semiconductor Radiation Detectors, Springer, 1999
- W. Blum, L. Rolandi, Particle Detection with Drift Chambers, Springer, 1994
– R. Wigmans, Calorimetry, Oxford Science Publications, 2000

Review Articles

– Experimental techniques in high energy physics, T. Ferbel (editor), World Scientific, 1991.
– Instrumentation in High Energy Physics, F. Sauli (editor), World Scientific, 1992.
– Many excellent articles can be found in Ann. Rev. Nucl. Part. Sci.

Other sources

– Particle Data http://pdg.lbl.gov/pdg.html
– R. Bock, A. Vasilescu, Particle Data Briefbook
http://www.cern.ch/Physics/ParticleDetector/BriefBook/
– Summer student lectures and academic training at CERN, DESY, Fermilab, GSI

Summer student lectures and academic training

- **Particle Detectors - Principles and Techniques: C. D'Ambrosio, T. Gys, C. Joram, M. Moll and L. Ropelewski, CERN Academic Training Programme 2004/2005**
- **Summer Student Lectures 2010, Werner Riegler, CERN,**
- **Summer Student Lectures 2012, Detectors for Particle Physics, D. Bortoletto, Purdue University**
- **Particle detection and reconstruction at the LHC (I), African School of Physics, Stellenbosch, South Africa, August 2010 (D. Froidevaux, CERN)**
- **Particle detectors and large HEP experiments, L. Serin LAL/Orsay & IN2P3/ CNRS, lecture at the European Summer Campus 2011, Strasbourg France**
- **Physics of Particle Detection, ICFA, Instrumental school, South Africa 2001, Claus Grupen, University of Siegen**
- **….**

Acknowledgements

- Many thanks to all my colleagues who have prepared lectures like this one in the past and from which I profited a lot!!!
- I tried to quote the authorship of the slides I took from theses lectures and I apologize for the cases in which I forgot

What do we want to observe?

- Collisions, interactions, creation and decay of particles (elementary or composed), which are invisible from first principles, even under a big microscope
- These particles are characterised by their masses, electric charges, spin, polarization.
- Their energy can vary from keV (Dark Matter searches, Nuclear physics) to GeV or TeV (particle physics) up to ZeV (10^{21}eV cosmic rays)
- Measure precisely the particle 4-vectors $\left(E/c,\vec{p}\right)$ and all other quantities

NOBEL PRIZES FOR INSTRUMENTATION

http://www.lhc-closer.es/php/index.php?i=1&s=9&p=2&e=0

D. Bortoletto

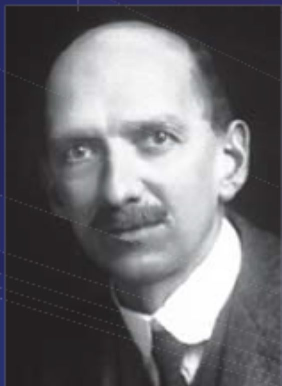

1927: C.T.R. Wilson, Cloud Chamber

1939: E. O. Lawrence, Cyclotron

1948: P.M.S. Blacket, Cloud Chamber

1950: C. Powell, Photographic Method

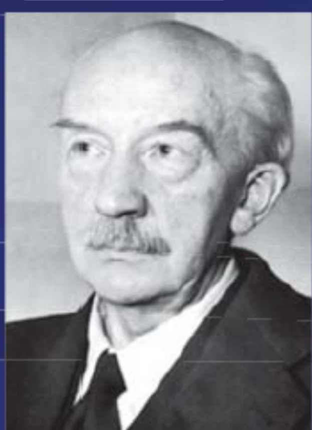

1954: Walter Bothe, Coincidence method

1960: Donald Glaser, Bubble Chamber

1968: L. Alvarez, Hydrogen Bubble Chamber

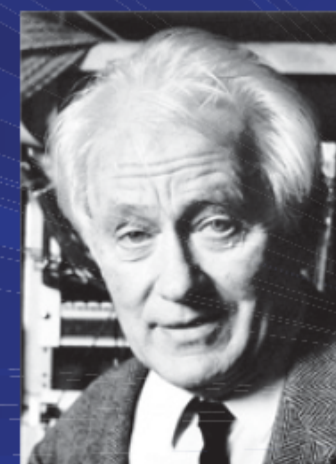

1992: Georges Charpak, Multi Wire Proportional Chamber

Seeing particles:
Rutherford scattering
Experiment by Hans Geiger and Ernest Marsden 1909

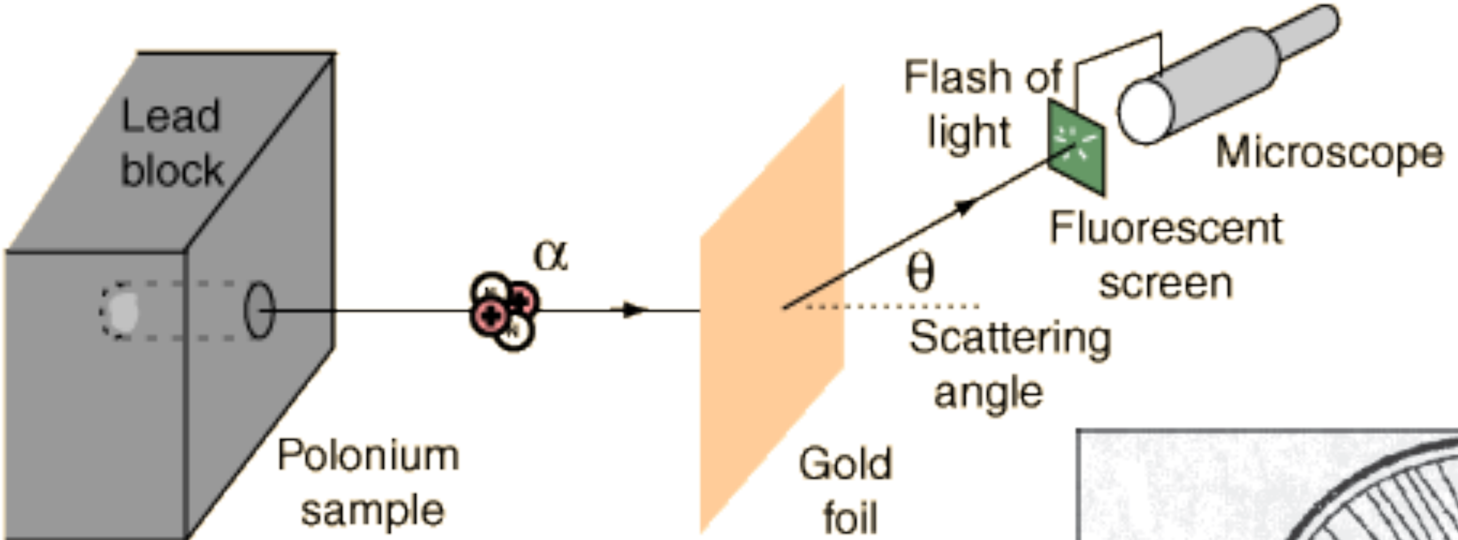

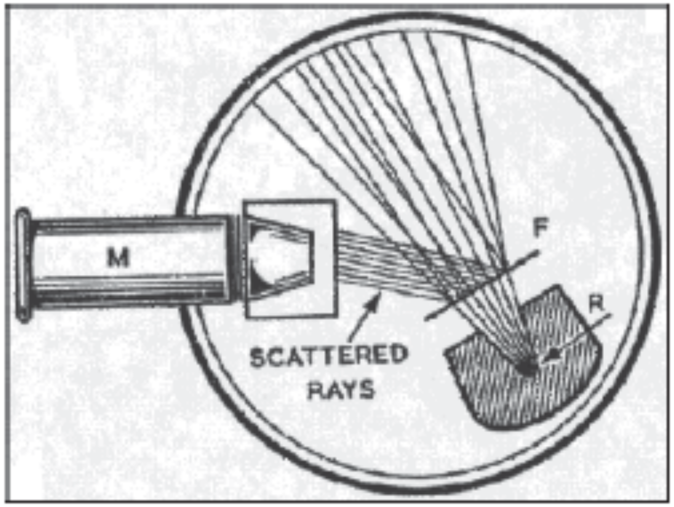

e^+ 63 MeV

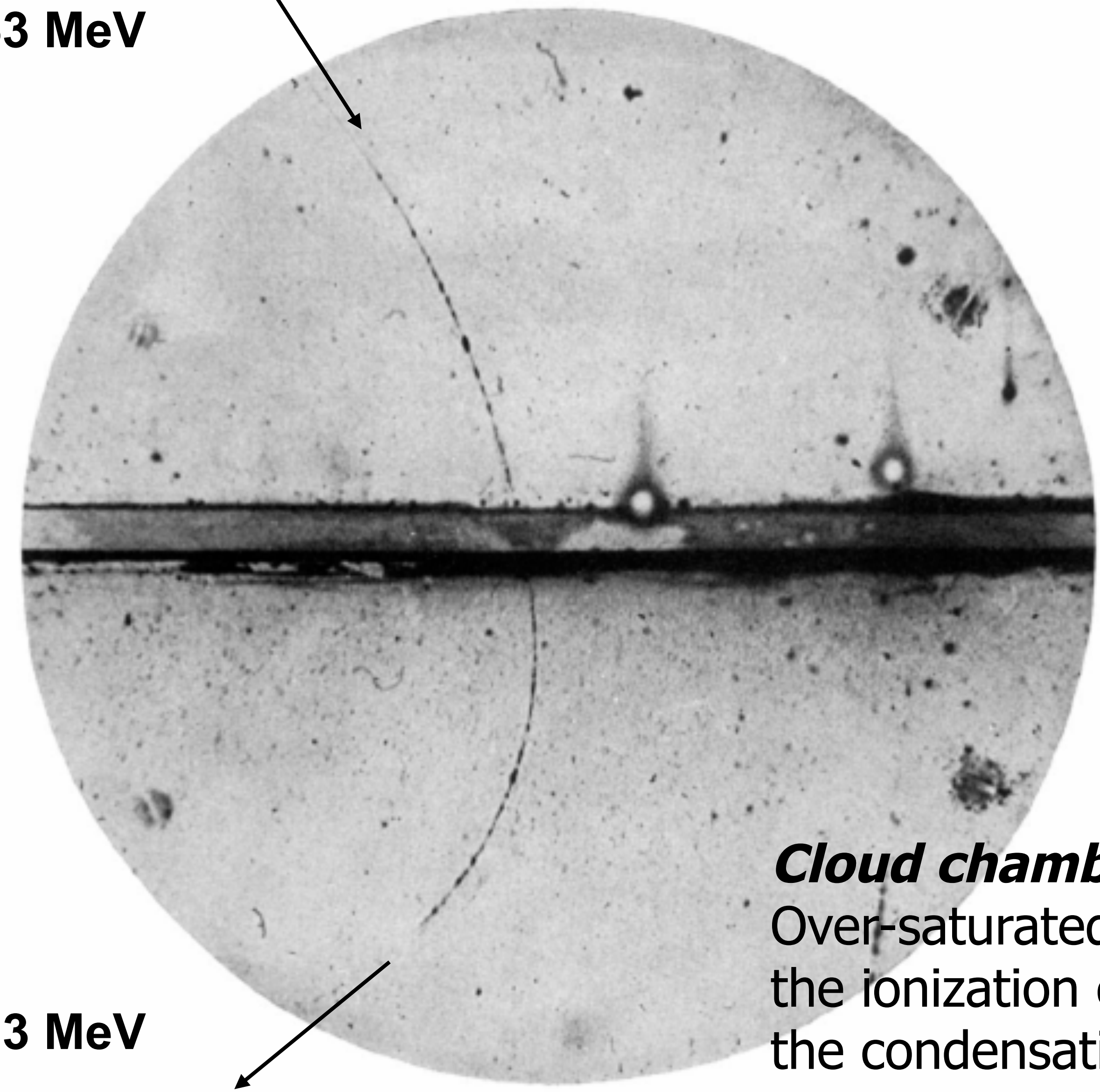

e^+ 23 MeV

1932
Discovery of the positron by C.D.Anderson

6 mm Pb

Cloud chamber (C.T.R. Wilson)
Over-saturated vapour :
the ionization clusters become the condensation nuclei

Emulsions

- The grains of AgBr (Ø 0.1-0.2 µm) are disolved in a gel;
- Ionization reduction → Ag
- → the film becomes black
- Very high spatial resolution

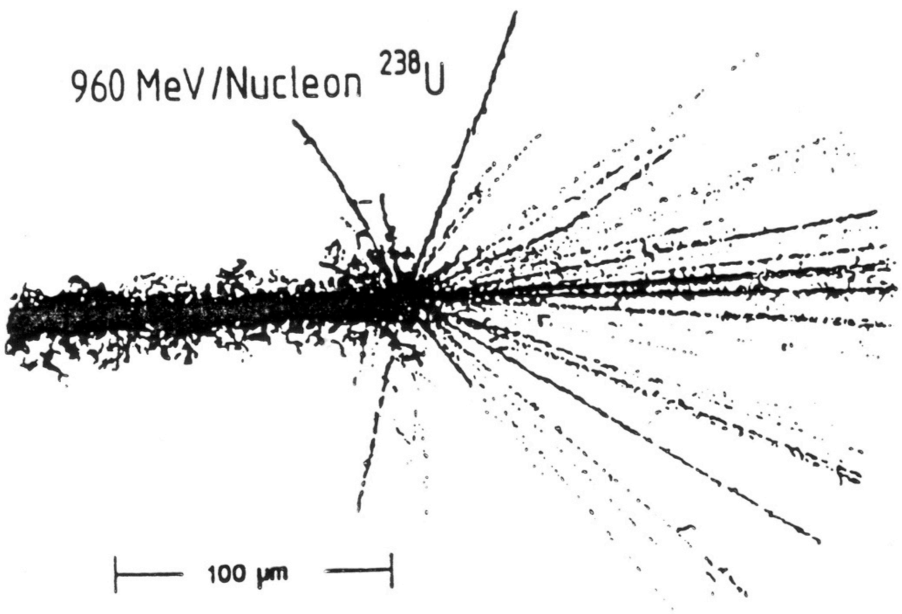

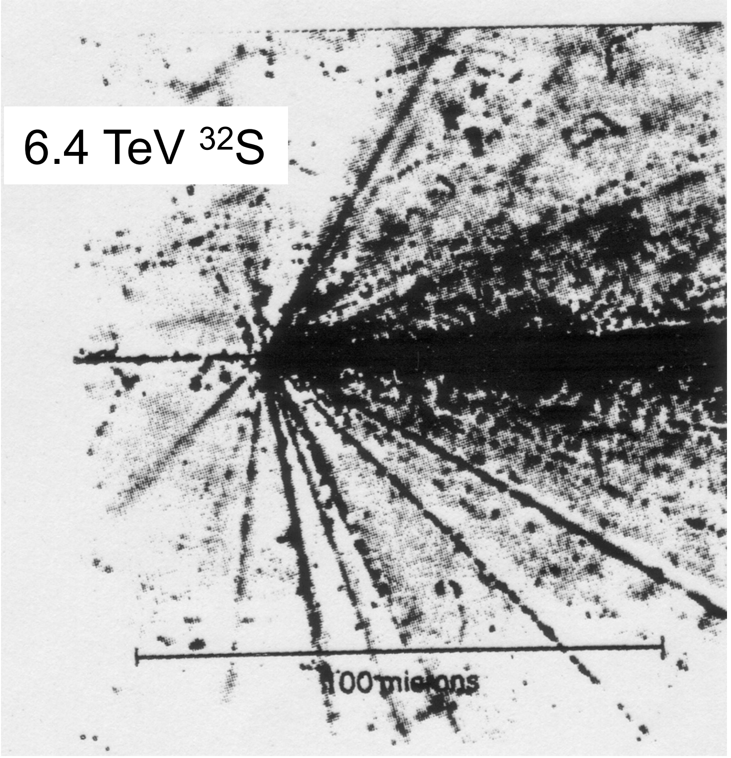

Bubble chambers

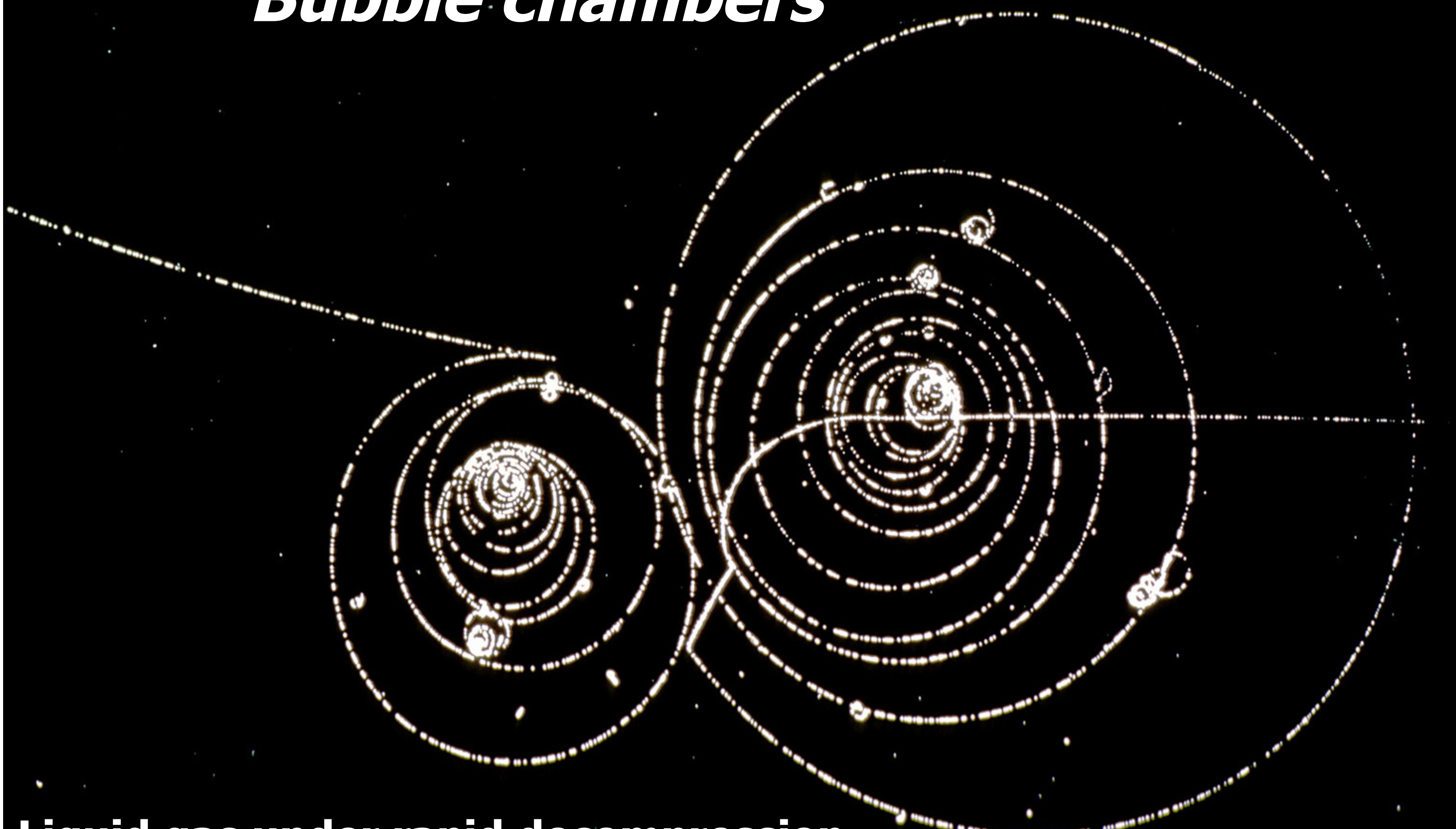

Liquid gas under rapid decompression

Ionization clusters → bubbles


VUB
CERN

Chambre à bulles

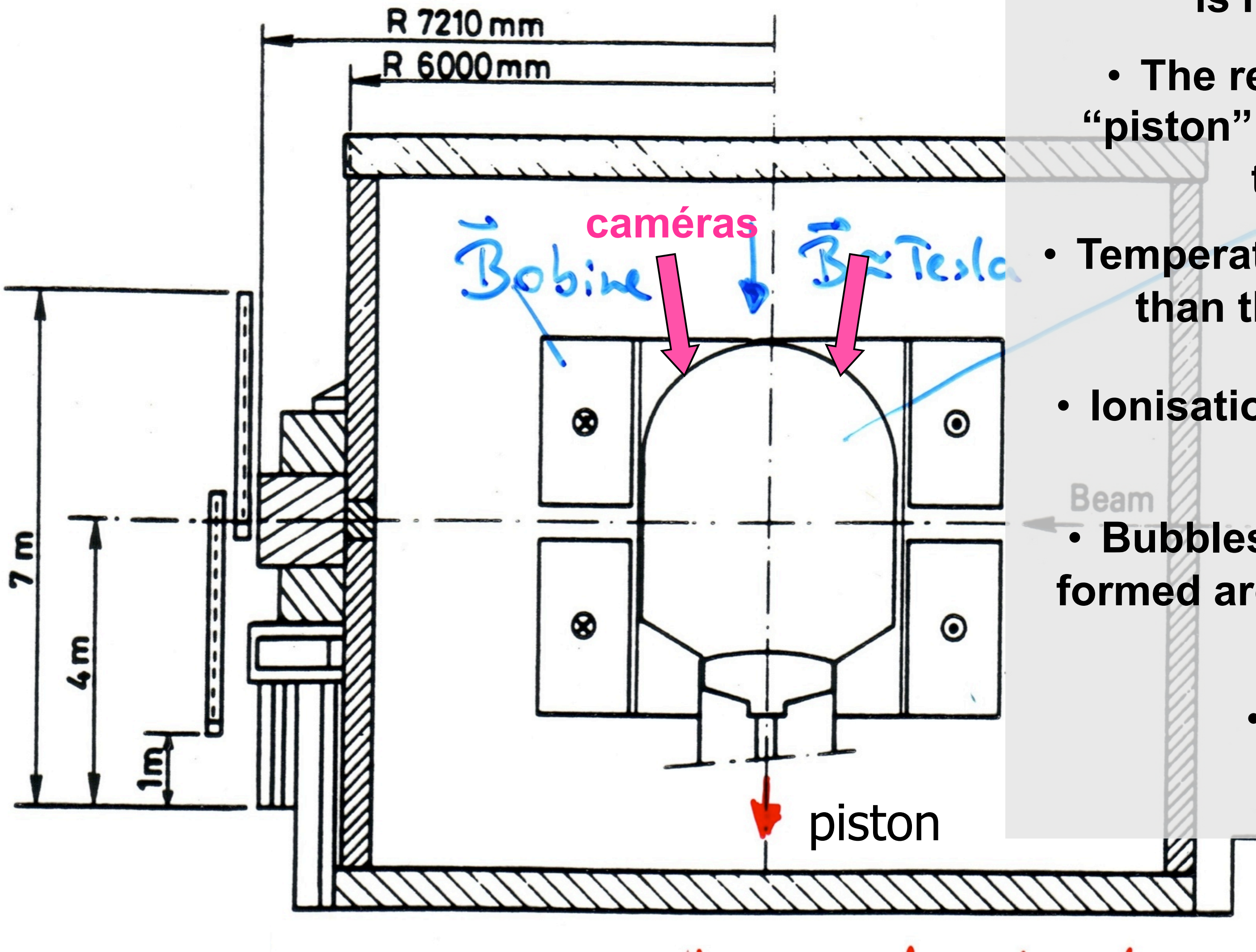

- Liquid gas under over pressure (H, D, He, ...
- Boiling point under pressure is much higher
- The retraction of the "piston" will de-compress the gas ⇒
- Temperature will be higher than the boiling point
- Ionisation of the gas ($\tau \approx 10^{-10}$s)
- Bubbles (boiling) will be formed around the ionization clusters
- Photo !

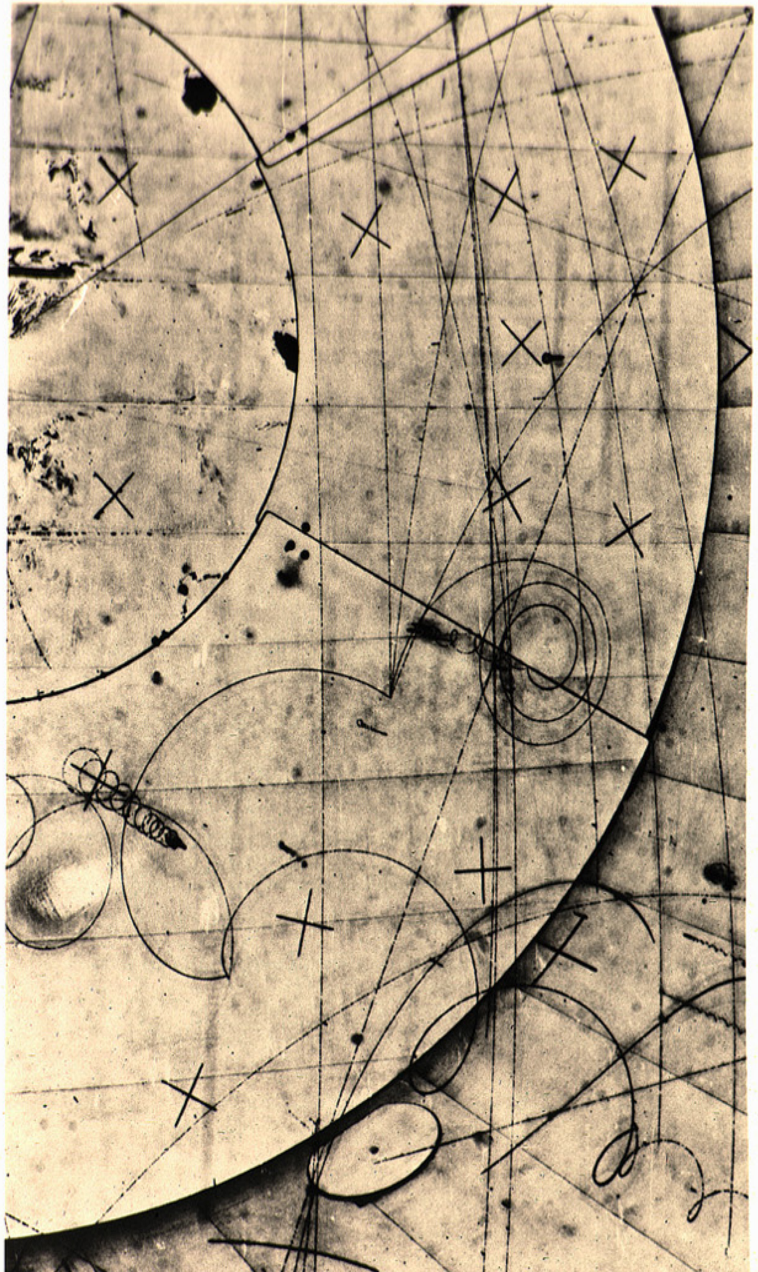

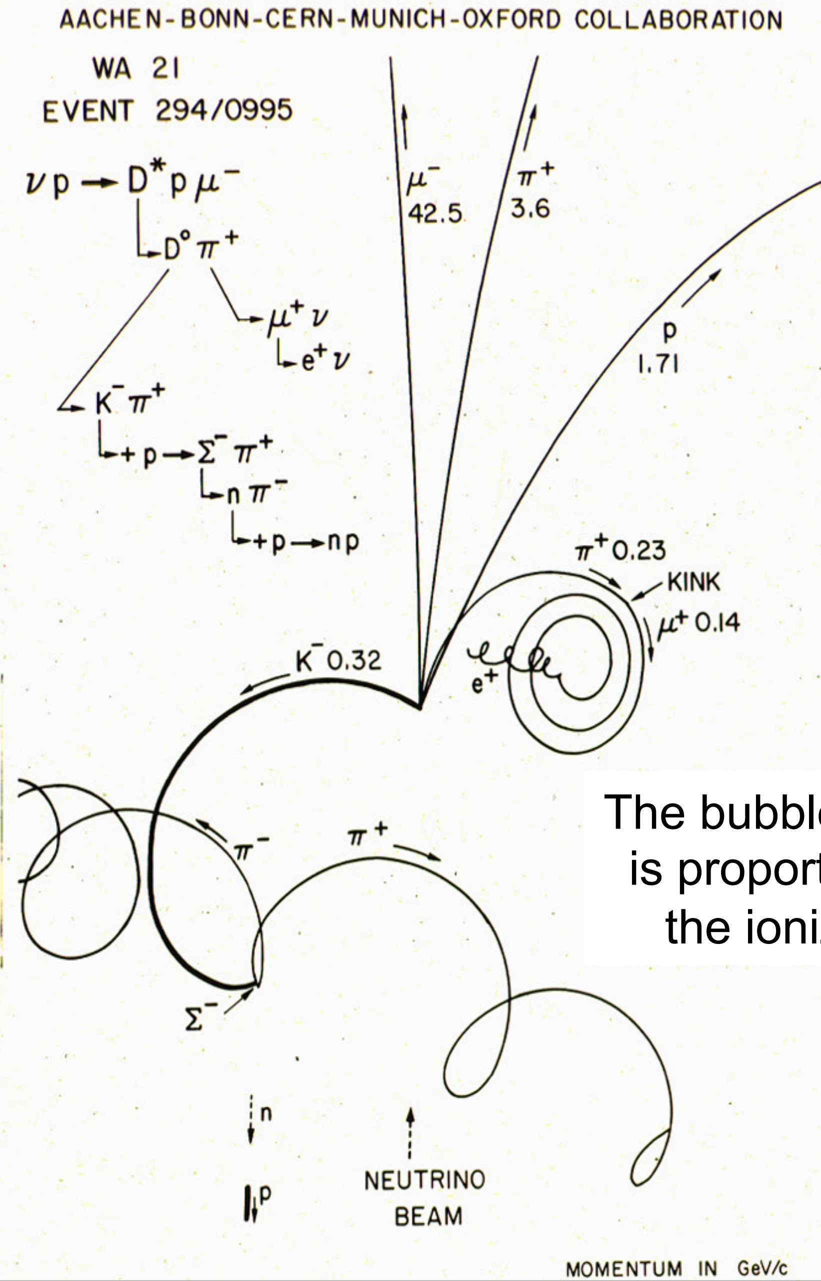

The bubble density is proportional to the ionization

Ulrich.Goerlach@iphc.cnrs.fr, ASP Particle detectors 2012

The spark chamber
»How to see the invisible"

- **A historic instrument used in the years 1960-1980 at accelerators**
- **Some important discoveries were made with this detector, like the discovery of the muon-neutrino**

- **One sees "live" the passage of the particles (like the muons induced by cosmic rays, about 100/m²/sec)**

The spark chamber, how does it work ?

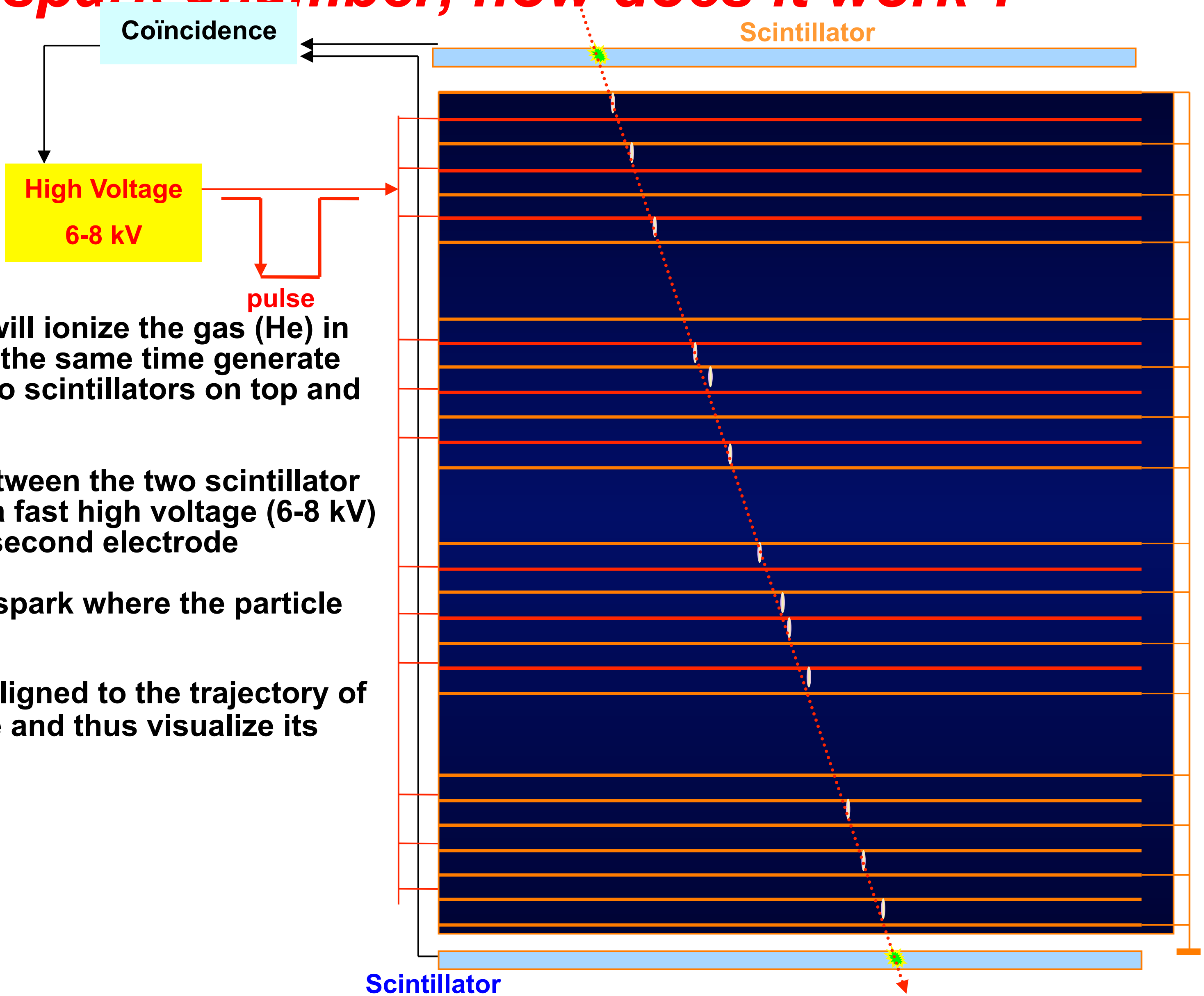

1. A charged particle will ionize the gas (He) in the chamber and at the same time generate some light in the two scintillators on top and bottom.
2. The coincidence between the two scintillator signals will trigger a fast high voltage (6-8 kV) pulse sent to each second electrode
3. This will provoke a spark where the particle had ionized the gaz.
4. The sparks will be aligned to the trajectory of the charged particle and thus visualize its passage.

And you will see this

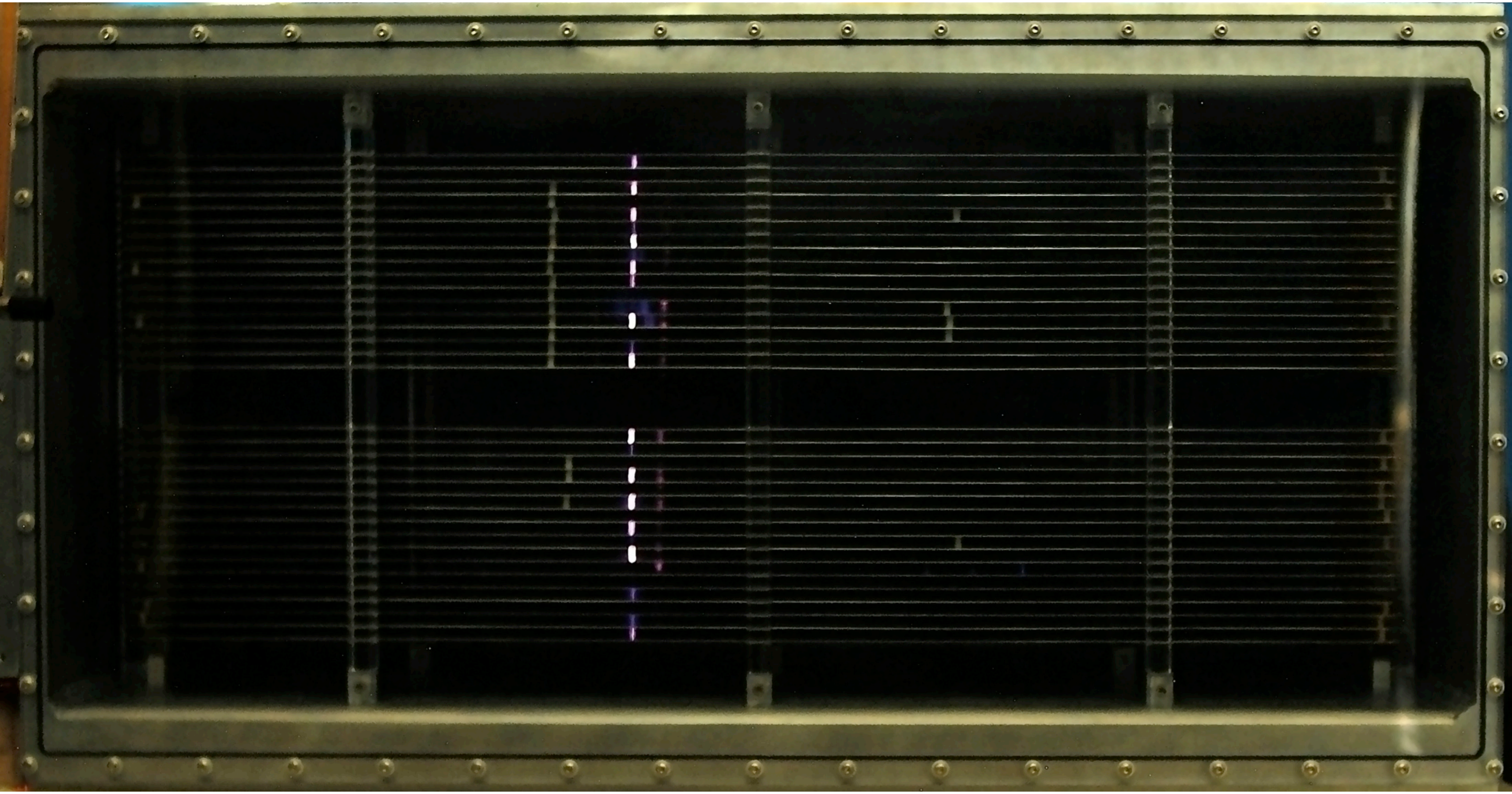

Deep inelastic electron-proton scattering

H1 Experiment at the HERA (e-p) collider, DESY - Hamburg

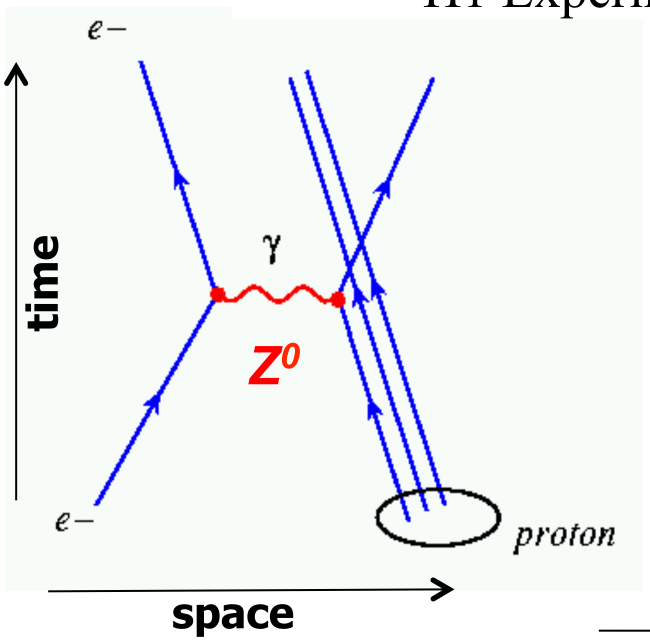

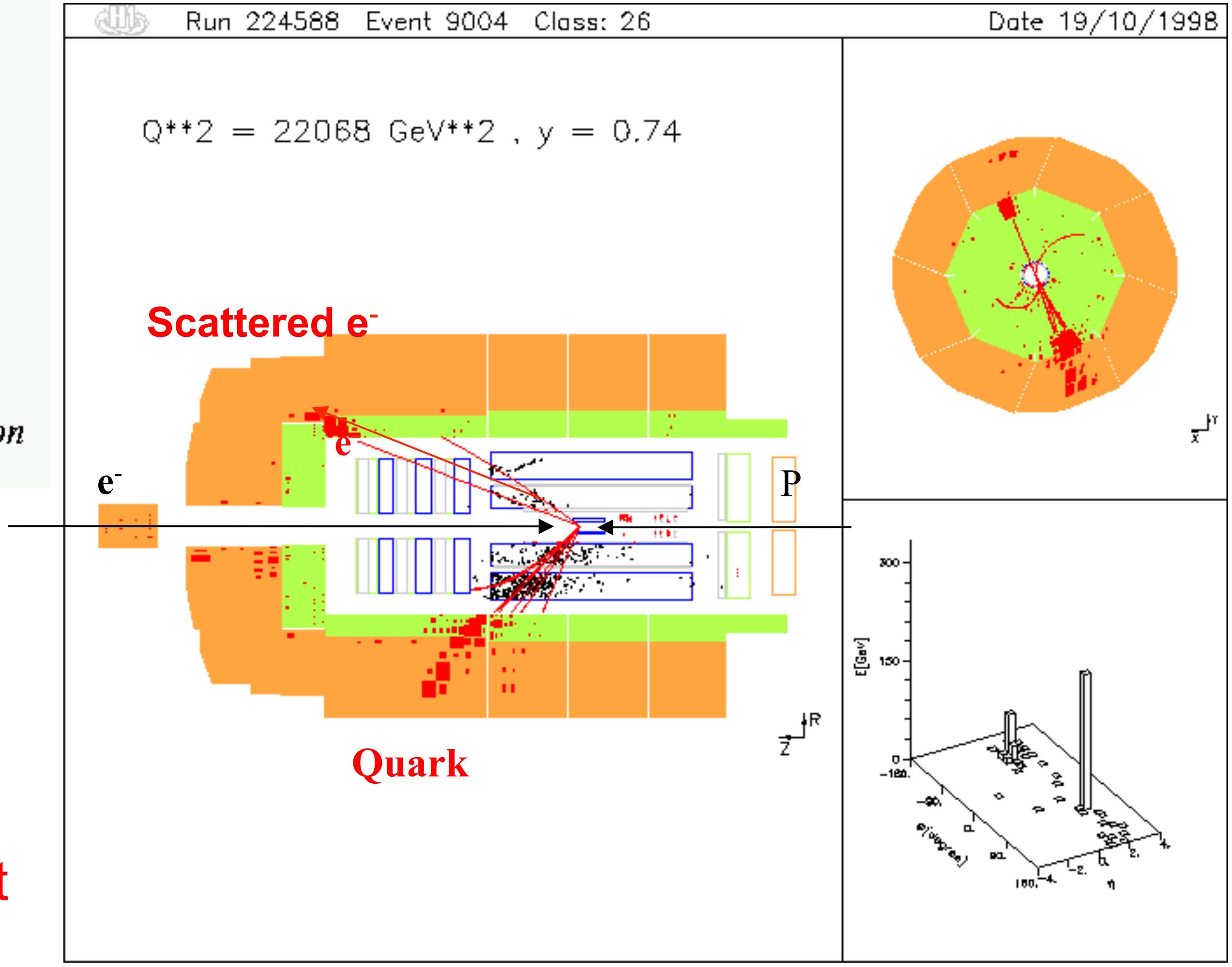

energy (e-) = 30 GeV
energy (p) = 900 GeV

Neutral current event

Deep inelastic electron-proton scattering

H1 Experiment at the HERA (e-p) collider, DESY - Hamburg

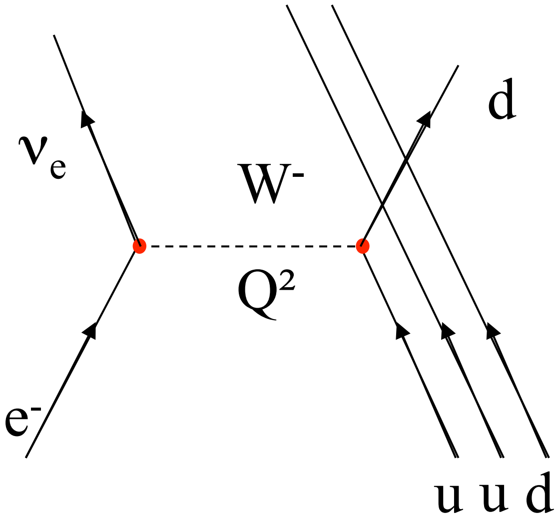

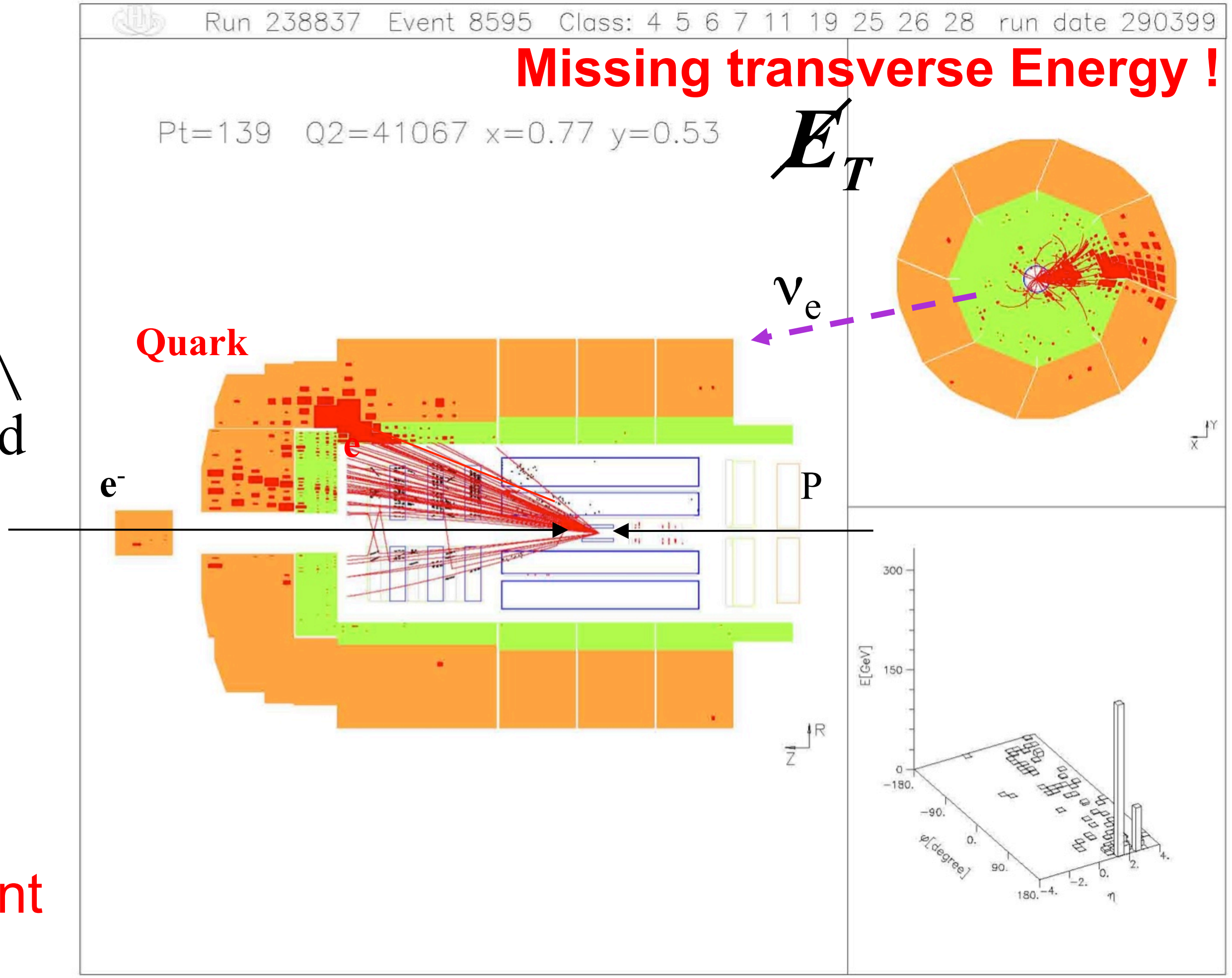

energy (e^-) = 30 GeV
energy (p) = 900 GeV

Charged current event

UNIVERSITÉ DE STRASBOURG

Some basics of particle detection

- Energy loss of charged particles by ionization
  - Non-relativistic, minimum ionizing and relativistic
- Nuclear interactions of hadrons (nuclear interaction length)
- Bremsstrahlung of electrons (and muons)
  - Critical energy and radiation length
- Photo effect, Compton scattering and conversion of gammas to electron-positron pairs
- ⇒ electromagnetic and hadronic showers
- Cerenkov effect and transition radiation

Some general characteristics of electronic detectors

Single detector (the building blocks)

- Energy-response function and linearity
- Time-response and dead time
- Energy, spatial or angular and time resolution
- Efficiency of a detector
- Availability and price !!!
- …

Combination of many detectors → experiment

- Propagation of charged particles in a magnetic field, reconstructing their trajectories

$$p_T(\text{GeV}/c) = 0.3\, B(\text{Tesla})\, R(\text{m})$$

- Measure the energy of electrons, photons and jets
- Detect muons as penetrating particles
- Particle identification!
- Trigger (event selection) and Data acquisition (DAQ)

Gas detectors

- Ionisation chambers
- Proportional counters
- Multi Wire Proportional chambers
- Drift chambers and Time Projection Chambers
- Many many more …..

$$-\frac{1}{\rho}\frac{dE}{ds} = -\frac{dE}{dx} = \underbrace{4\pi N_{Av} r_e^2 m_e c^2}_{0.3071 MeV/(g/cm^2)} \frac{Z}{A} z^2 \frac{1}{\beta^2}\left[\frac{1}{2}\ln\frac{2m_e c^2\gamma^2\beta^2 \cdot T_e^{max}}{I^2} - \ldots\right]$$

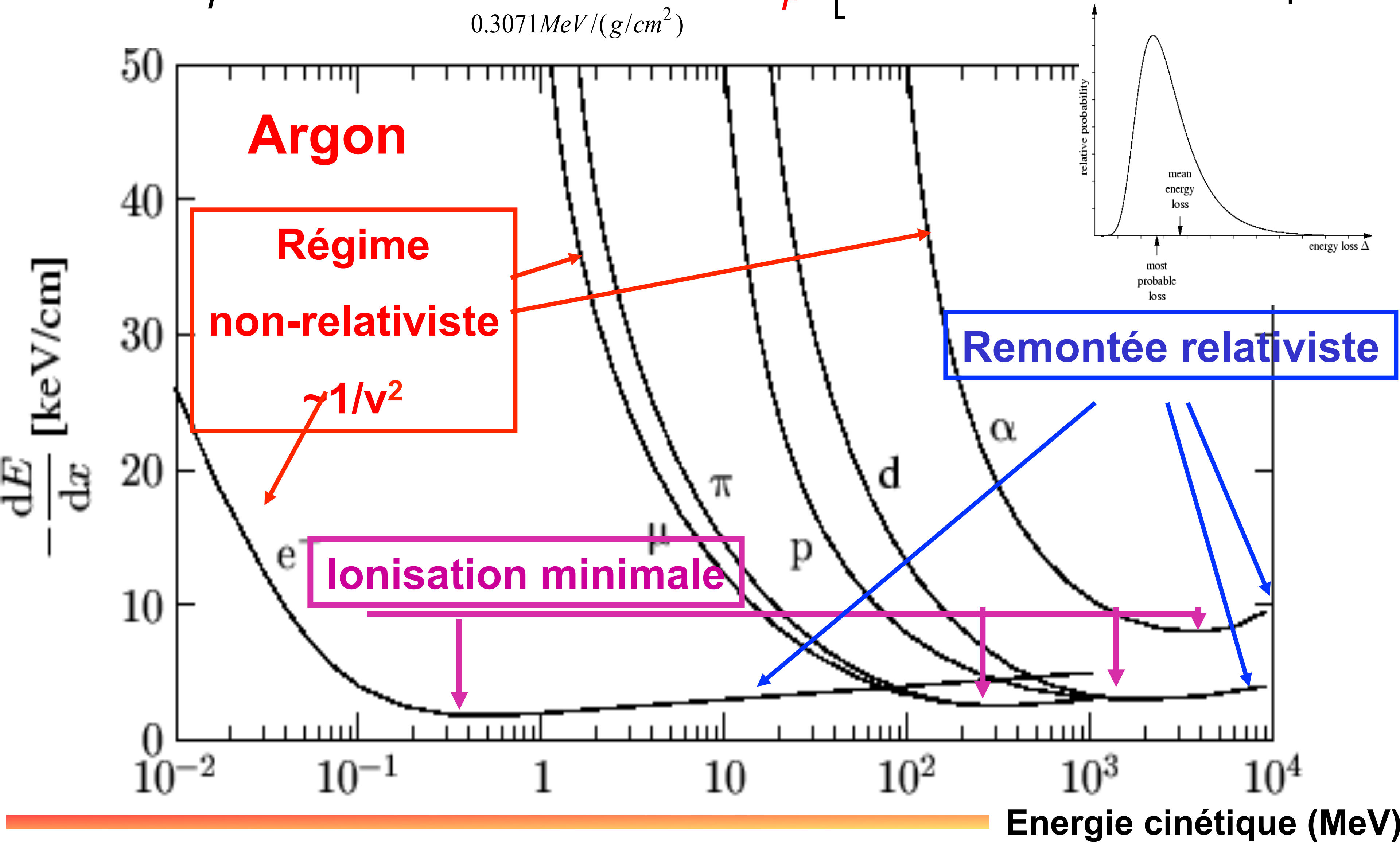

Ionisation and excitation in a gas

- **Excitation : $X+p \rightarrow X^{*}+p$**
  - $\sigma \approx 10^{-17}$ cm²
- **Ionisation : $X+p \rightarrow X^{+}+p + e^{-}$**
  - $\sigma \approx 10^{-16}$ cm²
  - Primary and secondary (δ-electrons)
  - Penning effect: $Ne^{*} + Ar \rightarrow Ne + Ar^{+} + e^{-}$
  - Formation of molecular ions: $He^{+} + He \rightarrow He_2^{+}$

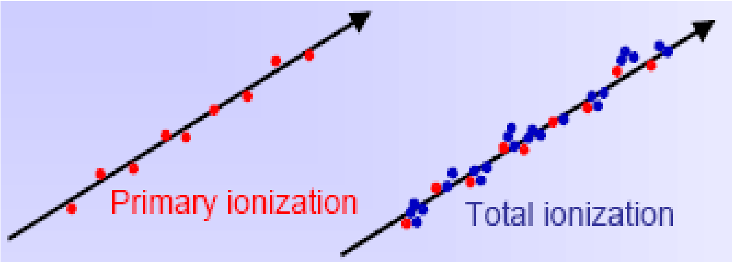

- **Recombination**
  - $X^{+} + e^{-} \rightarrow X +$
  - $X^{-}+Y^{+} \rightarrow XY +$
- **Electron attachement :**

$X+ e^{-} \rightarrow X^{-} + h\nu$

Electrons are not free anymore !

$n_{primary} \approx n_{total}$ x1/3

Gaz	Excitation (eV)	Ionisation (eV)	Energie moyenne pour (e-, ion) (eV)	(e-,ion+) /cm au minimum d'ionisation n_{total}
H_2	10.8	15.4	37	14
He	19.8	24.6	41	16
Ne	16.6	21.6	35	42
Ar	11.6	15.8	26	103
CO_2	10.0	13.7	33	62
CH_4		13.1	33	107
C_4H_{10}		10.8	23	113

UNIVERSITÉ DE STRASBOURG

Mobility and collection of charge

$v_D = \mu \cdot E$; E = electric field; p = pressure

in general it's more complicated $\mu = \mu(E, p)$

$v_D(\text{electrons}) \gg v_D(\text{ions}) \sim E/p$

Drift velocity for ions

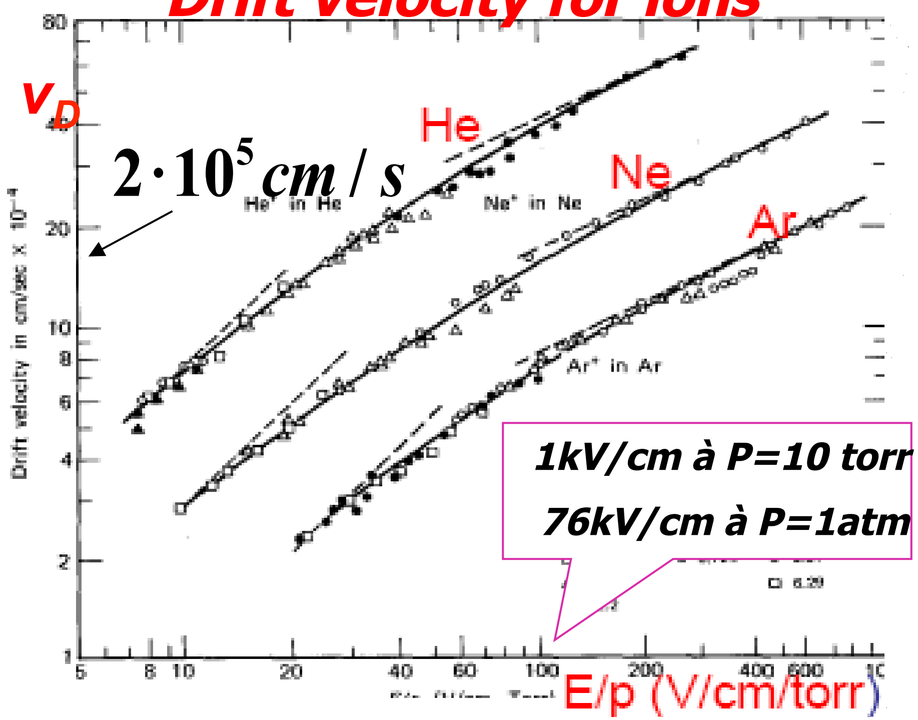

Drift velocity for electrons

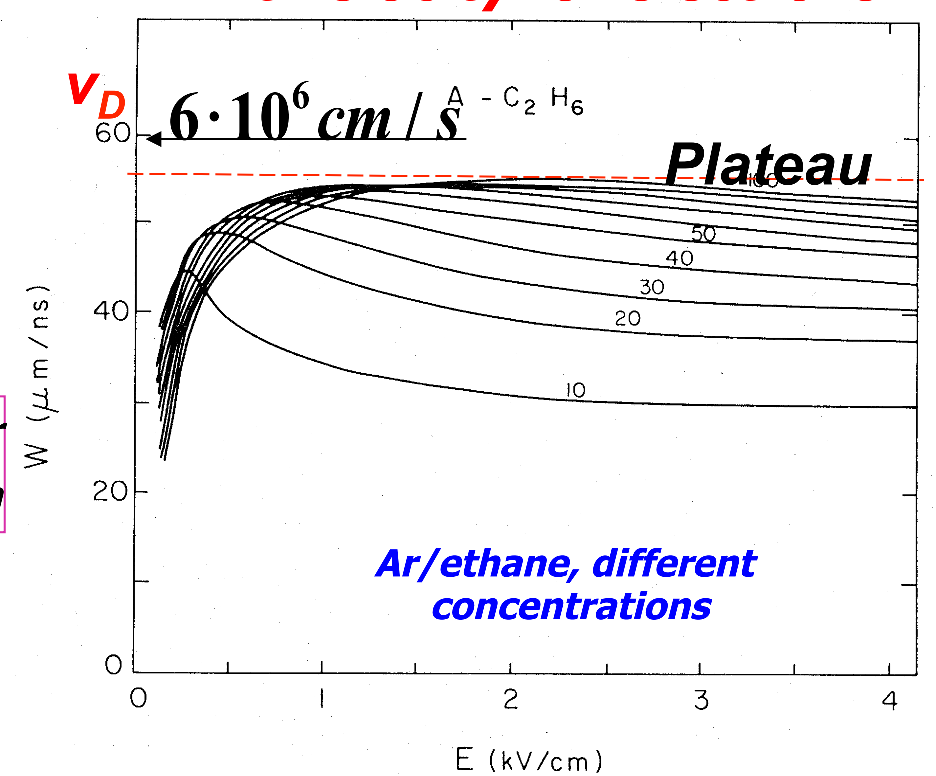

Ionisation chamber

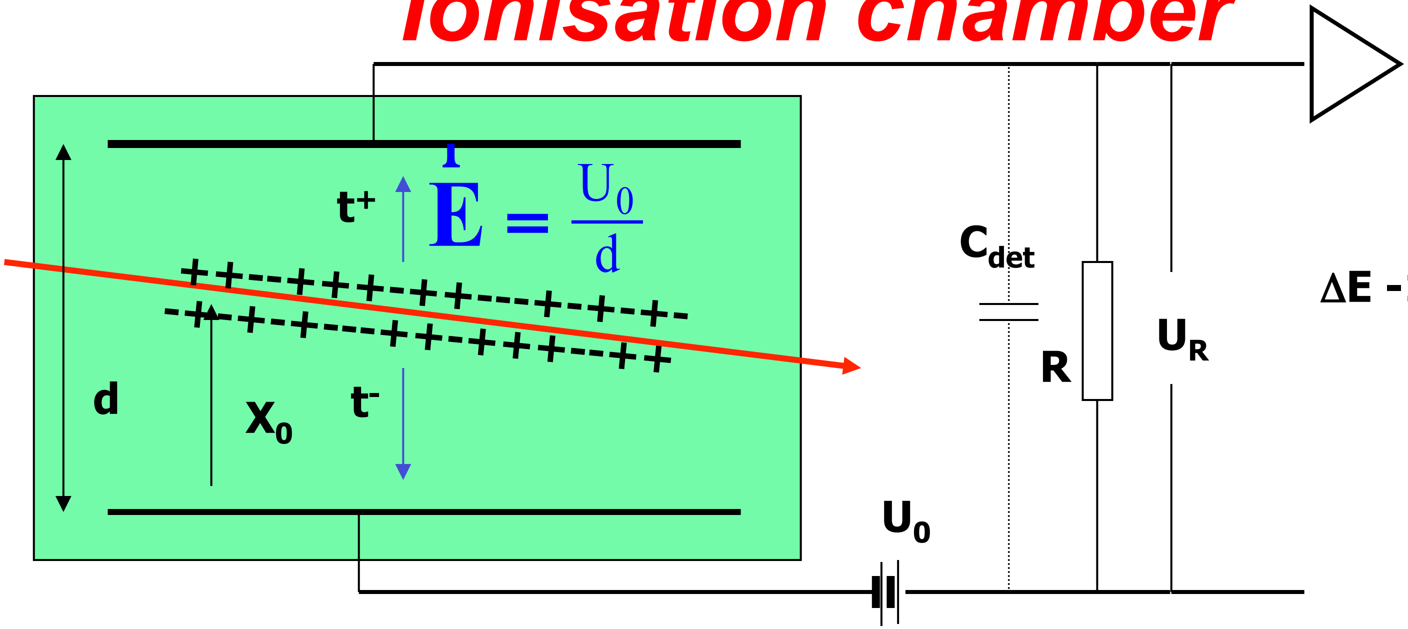

$\Delta E \rightarrow$ charges $\Delta Q^+ = Ne$
and $\Delta Q^- = -Ne$

Drift velocity v_D

$v_D(e^-) >> v_D(ions)$

$\Delta U_{max} = \Delta Q/C$

$v_D \sim E/p$

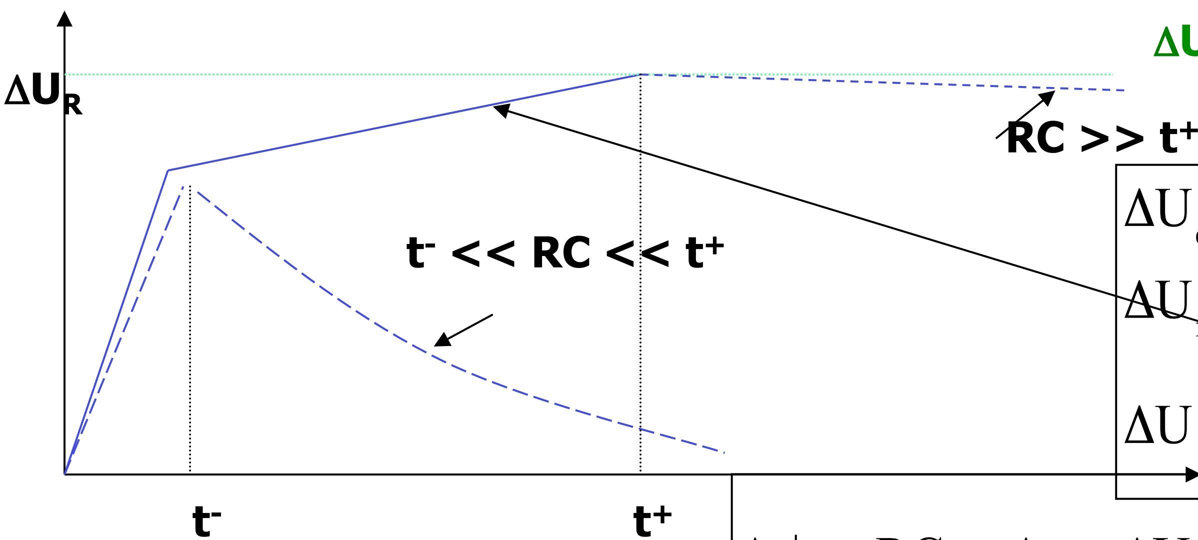

$$\Delta U_{el} = \frac{Ne}{Cd}(-x_0)$$

$$\Delta U_{ion} = \frac{-Ne}{Cd}(d - x_0)$$

$$\Delta U = \Delta U_{el} + \Delta U_{ion} = -\frac{Ne}{C} = \Delta Q / C$$

$$\Delta t^+ \gg RC \gg \Delta t^-; \quad \Delta U = -\frac{Ne}{d}\left(\frac{x_0}{C} - v^+R\left(1 - e^{-\Delta t^+/RC}\right)\right)$$

Signal formation in a planar drift chamber

$$\left|\vec{E}\right| = U_0 / d$$

$$Energy:\ \tfrac{1}{2}CU_0^2 \to \tfrac{1}{2}CU^2 = \tfrac{1}{2}CU_0^2 - N\int_{x_0}^{x} qE\,dx$$

$$\tfrac{1}{2}CU^2 - \tfrac{1}{2}CU_0^2 = \tfrac{1}{2}C\left(U+U_0\right)\left(U-U_0\right) = -NqE\left(x-x_0\right)$$

$$U \approx U_0;\ U+U_0 \approx 2U_0;\ U-U_0 = \Delta U;$$

$$\tfrac{1}{2}C\cdot 2U_0\cdot\Delta U = -Nq\frac{U_0}{d}\left(x-x_0\right)$$

$$\Delta U = -\frac{N}{C}\frac{q}{d}\left(x-x_0\right);\quad q=+e\ (ions)\quad q=-e\ (electr.)$$

$$\left(x-x_0\right) = v^{\pm}\Delta t^{\pm};\quad v^+ \ll v^-$$

$$\Delta U^- \xrightarrow{x\to 0} = -\frac{N}{C}\frac{e}{d}x_0$$

$$\Delta U^+ \xrightarrow{x\to d} = -\frac{N}{C}\frac{e}{d}\left(d-x_0\right)$$

$$\Delta U = \Delta U^- + \Delta U^+ = -\frac{Ne}{C} = \Delta Q / C$$

$$\Delta t^+ \gg RC \gg \Delta t^-;\ \Delta U = -\frac{Ne}{d}\left(\frac{x_0}{C} - v^+R\left(1-e^{-\Delta t^+/RC}\right)\right)$$

Ulrich.Goerlach@iphc.cnrs.fr, ASP Particle detectors 2012

Cylindrical ionisation chamber

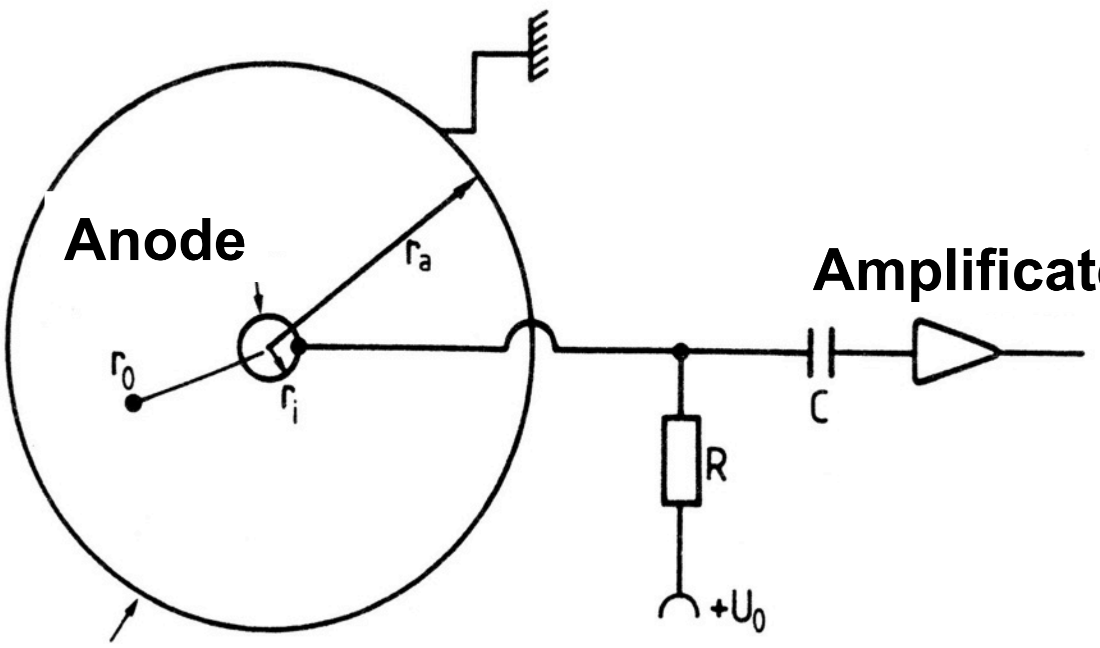

- Non-uniform electric field

$$\left|\vec{E}\right| = \frac{U_0}{r \ln\left(r_a / r_i\right)}$$

- Drift velocity is not constant

$$v^- = -\mu^- E$$

- $\Delta U^+ < \Delta U^-$ The electron signal dominates

$$\frac{\Delta U^+}{\Delta U^-} = \left. \frac{\ln\left(r_a / r_0\right)}{\ln\left(r_0 / r_i\right)} \right|$$

$$r_a = 1cm,\ r_i = 30\mu m \Rightarrow \Delta U^+ / \Delta U^- = 0.12$$

Electric field in a cylindrical geometry

Poisson's equation:

$\Delta V = 0;\quad V(x) =$ **Potential; cylindrical coordinates :**

$$\frac{1}{r}\frac{\partial}{\partial r}\left(r\frac{\partial V}{\partial r}\right) + \underbrace{\cancel{\frac{1}{r^2}\frac{\partial^2 V}{\partial \varphi^2}} + \cancel{\frac{\partial^2 V}{\partial z^2}}}_{\text{symetry}} = 0; \Rightarrow \frac{1}{r}\frac{\partial}{\partial r}\left(r\frac{\partial V}{\partial r}\right) = 0$$

$$V(r = r_a) = 0; V(r = r_i) = U_0; \quad \Rightarrow V = U_0 \frac{\ln\left(r / r_a\right)}{\ln\left(r_1 \;/ r_a\right)}$$

$$\vec{E} = -\vec{\nabla} V; \Rightarrow \left|\vec{E}\right| = \frac{U_0}{r \ln\left(r_a / r_i\right)}$$

$v^- = -\mu^- E;$ **but in general :** $\mu^- = \mu^-(E)$

$$\Delta t^- = \int_{r_0}^{r_i} \frac{dr}{v^-} = -\int_{r_0}^{r_i} \frac{dr}{\mu^- E} = -\int_{r_0}^{r_i} \frac{dr}{\mu^- U_0} r \ln\left(r_a / r_i\right) = \frac{\ln\left(r_a / r_i\right)}{2\mu^- U_0}\left(r_0^2 - r_i^2\right)$$

Signal in a cylindrical ionisation chamber

$$\left|\vec{E}(r)\right| = \frac{U_0}{r\ln\left(r_a/r_i\right)}$$

$$Energie:\ \tfrac{1}{2}CU_0^2 \rightarrow \tfrac{1}{2}CU^2 = \tfrac{1}{2}CU_0^2 - N\int_{r_0}^{r_{i,a}} q\frac{U_0}{r\ln\left(r_a/r_i\right)}dr$$

$$\left.\begin{aligned}\Delta U^- &\xrightarrow{r\to r_i} = -\frac{Ne}{C}\frac{\ln\left(r_0/r_i\right)}{\ln\left(r_a/r_i\right)}\\ \Delta U^+ &\xrightarrow{r\to r_a} = -\frac{Ne}{C}\frac{\ln\left(r_a/r_0\right)}{\ln\left(r_a/r_i\right)}\end{aligned}\right\}\frac{\Delta U^+}{\Delta U^-} = \left.\frac{\ln\left(r_a/r_0\right)}{\ln\left(r_0/r_i\right)}\right|_{r_0=r_a/2} = \frac{\ln 2}{\ln\left(r_a/2r_i\right)}$$

$$r_a \gg 2r_i \Rightarrow \Delta U^+ < \Delta U^-;\ r_a = 1cm,\ r_i = 30\mu m \Rightarrow \Delta U^+/\Delta U^- = 0.12$$

Ulrich.Goerlach@i

Proportional Counters

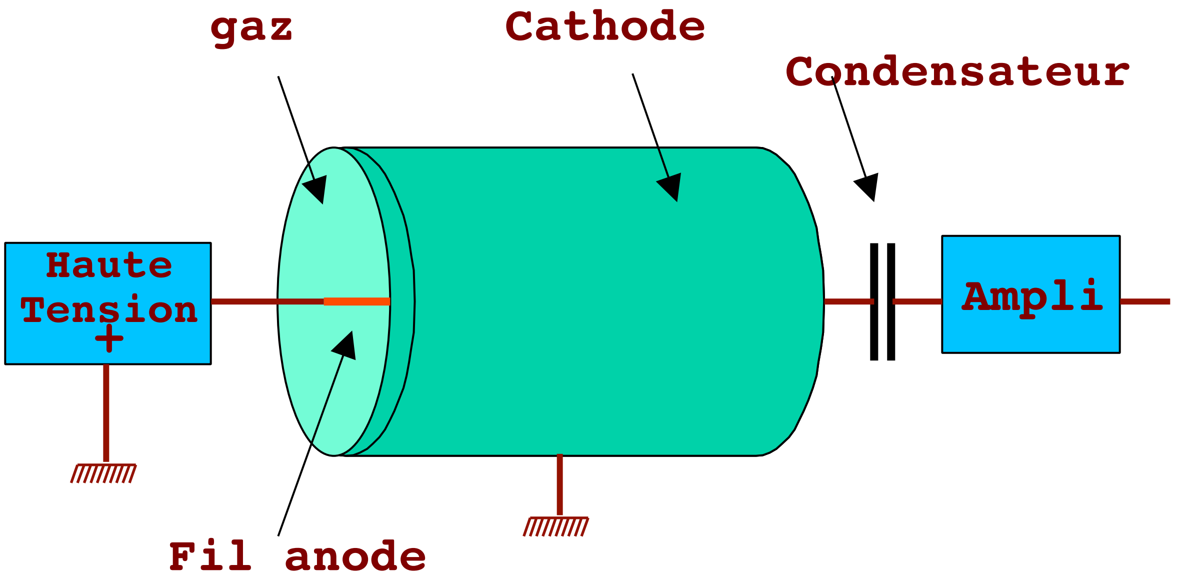

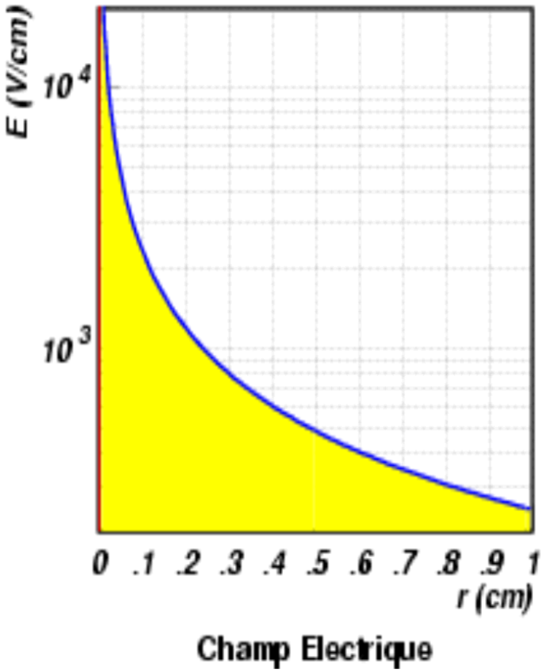

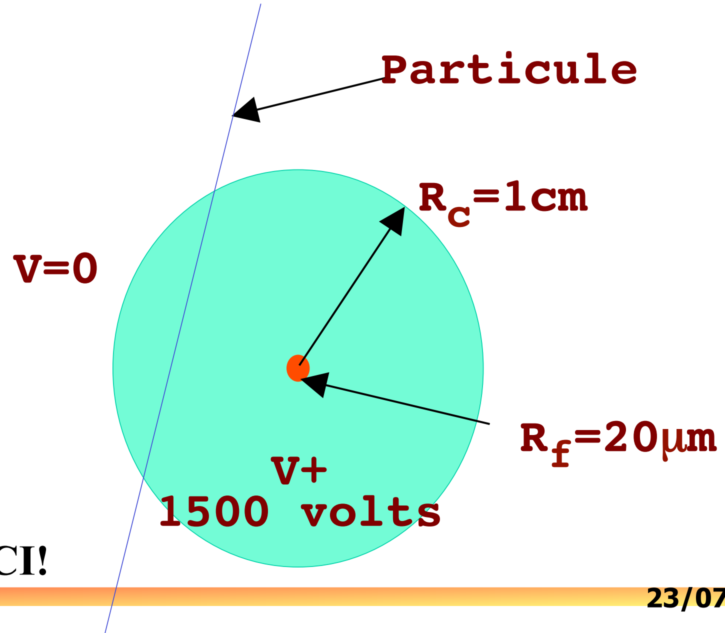

Après B.Jean-Marie, Roscoff 2000, école IN2P3, MERCI!

T=0

Passage of a charged particle

Creation of paires ion-electron.

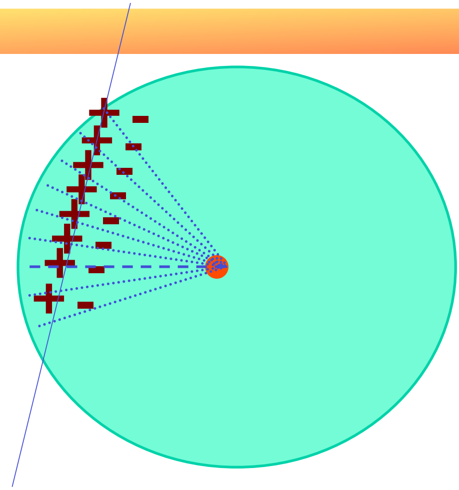

T~100ns

The primary electrons have sufficient energy to ionize the gas. This multiplication happens close to the wire, where the field is very high and stops when all electrons have reached the wire

T de 0 à 100ns

Ions and electrons are separated by the electric field.

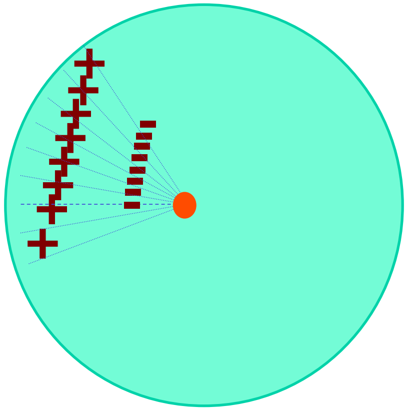

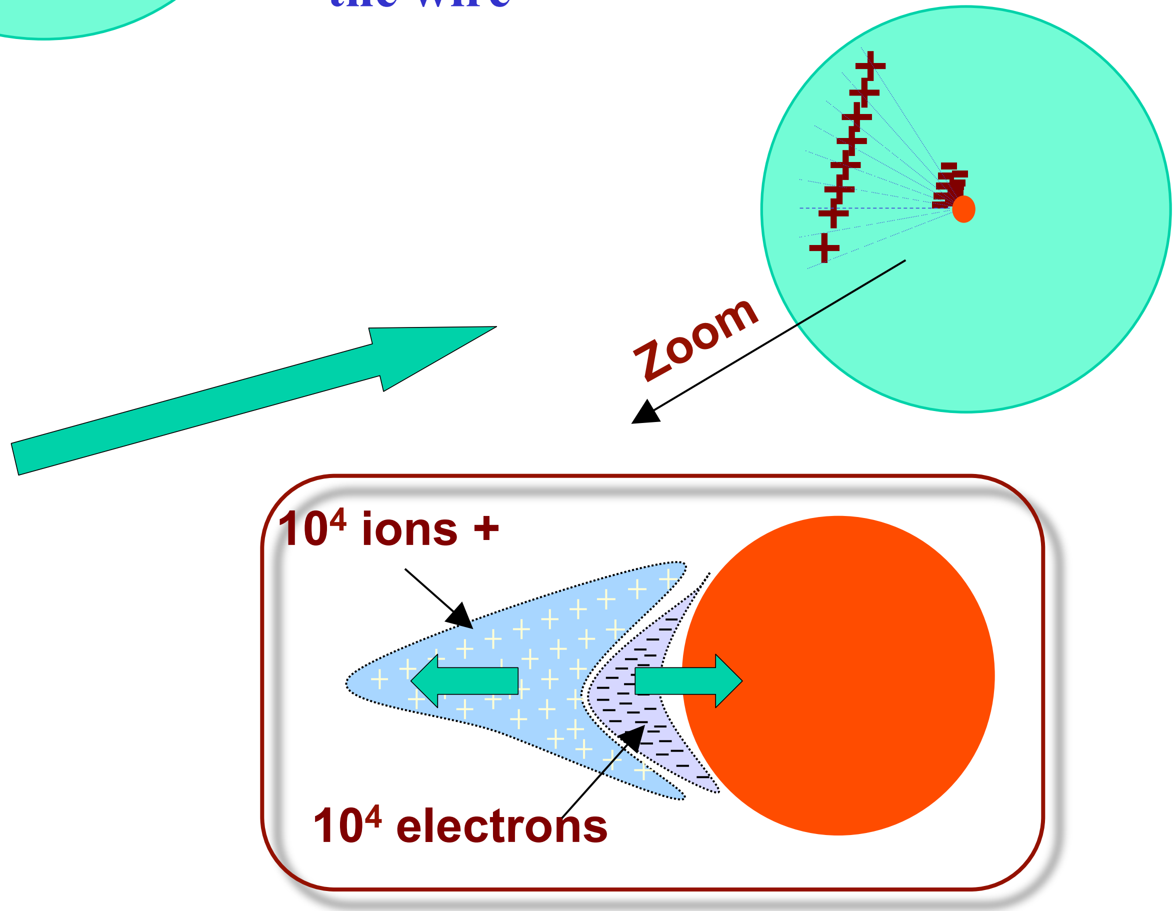

T~150ns

The electrons have been collected by the wire, all ions (primary and secondary) migrate slowly to the cathode. An electric signal is produced by this mouvement of the charges

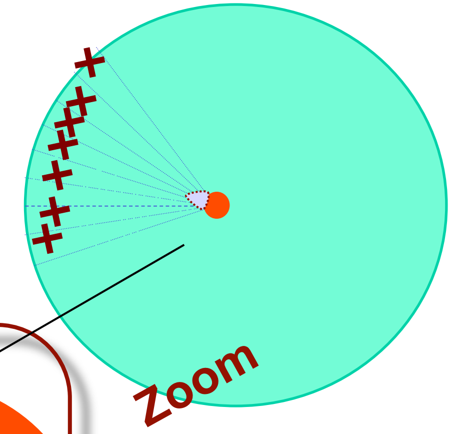

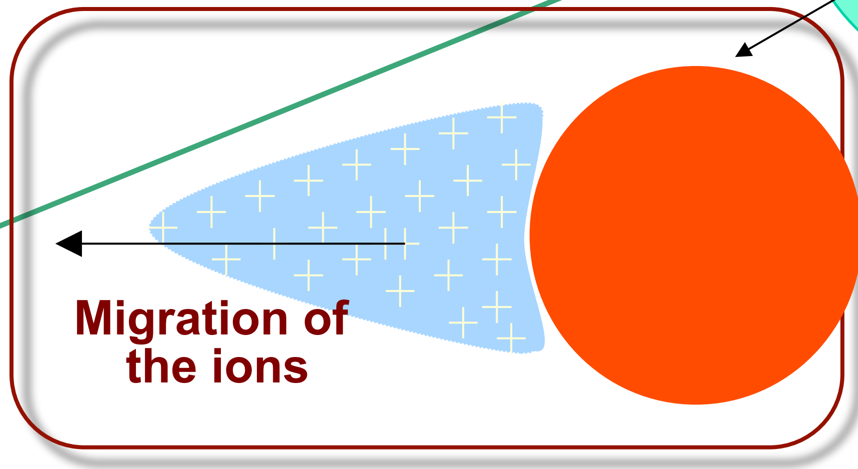

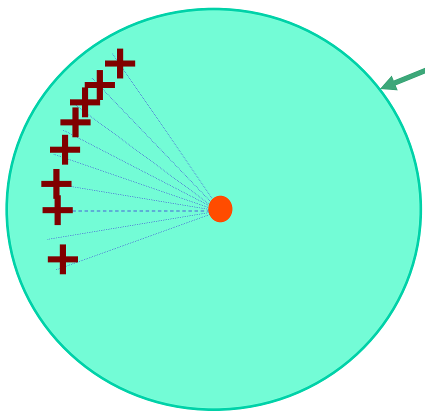

T some ms

The secondary ions from the avalanche have reached the cathode, the counter is ready for the next particle .

The essential points:

⇒ **Very high field close to the anode wire**
⇒ **Creation af an avalanche around the anode**
⇒ **Slow motion of the ions**
⇒ **The gas is at the same time the detecting and amplifying material**

Avalanche development

- Time development of avalanche near the wire of a proportional counter

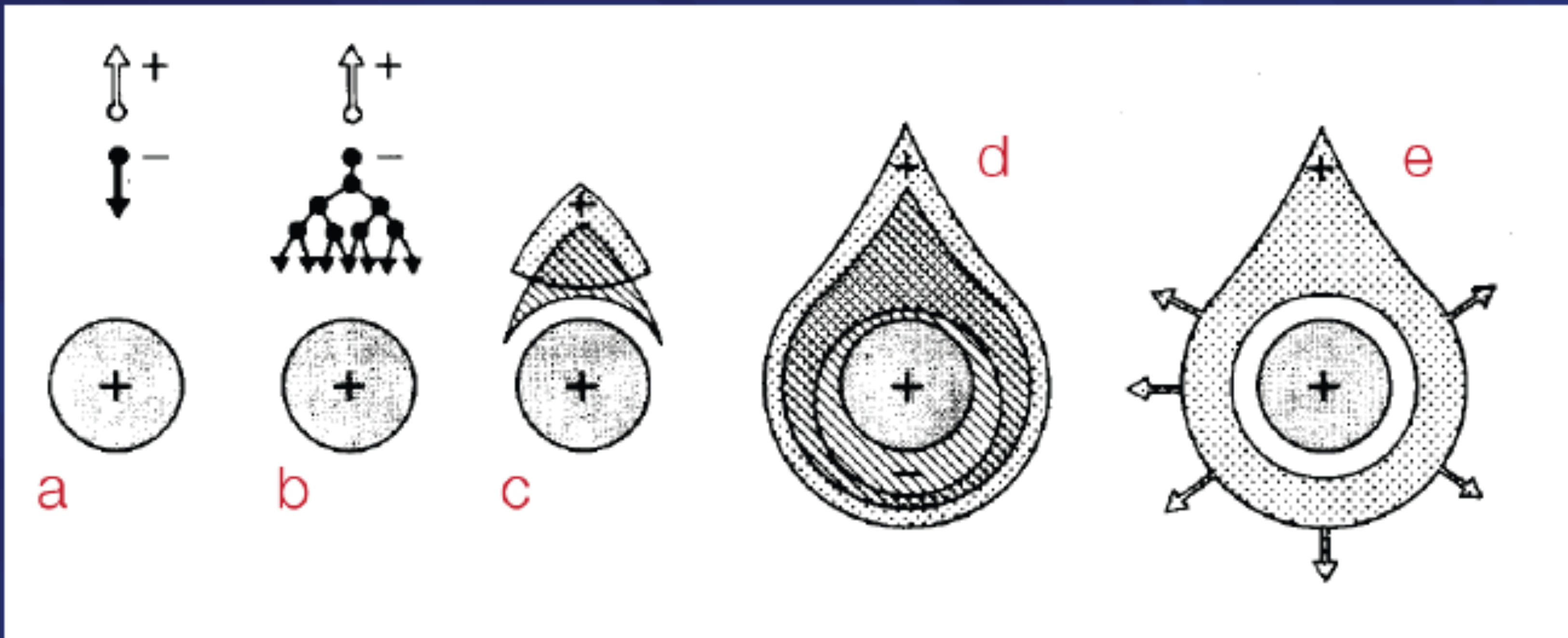

a) single primary electron proceeds towards the wire anode,
b) In the region of increasingly high field avalanche multiplication starts
c) electrons and ions are subject to lateral diffusion,
d) a drop-like avalanche develops which surrounds the anode wire,
e) the electrons are quickly collected (~1ns) while the ions begin drifting
f) towards the cathode generating the signal at the electrodes

Simulation of an avalanche

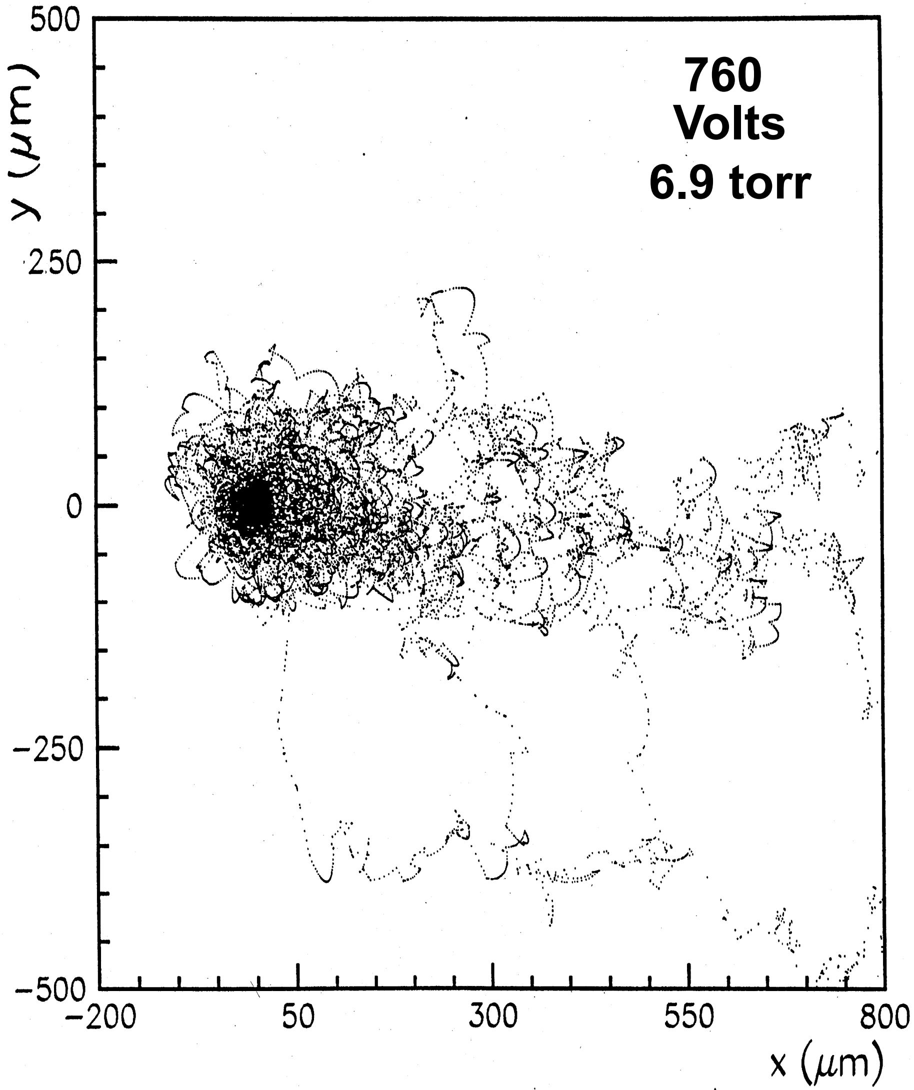

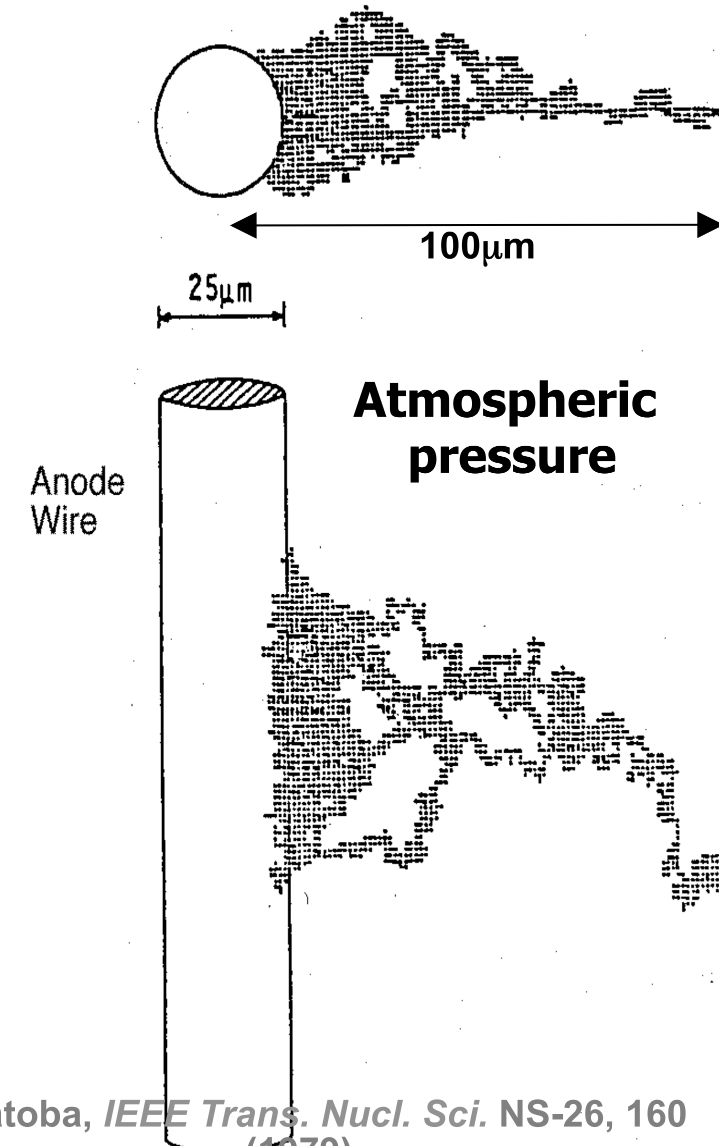

M. Matoba, *IEEE Trans. Nucl. Sci.* NS-26, 160 (1979)

The role of the gas

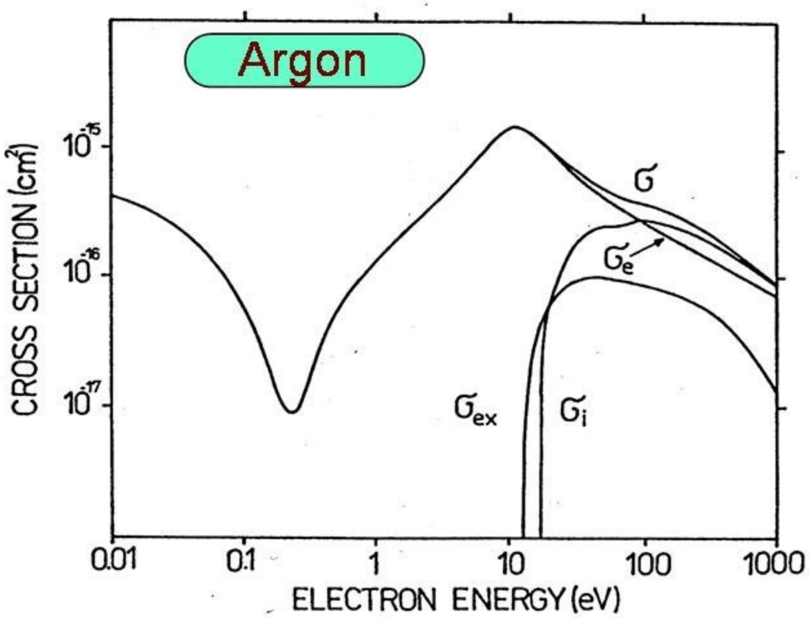

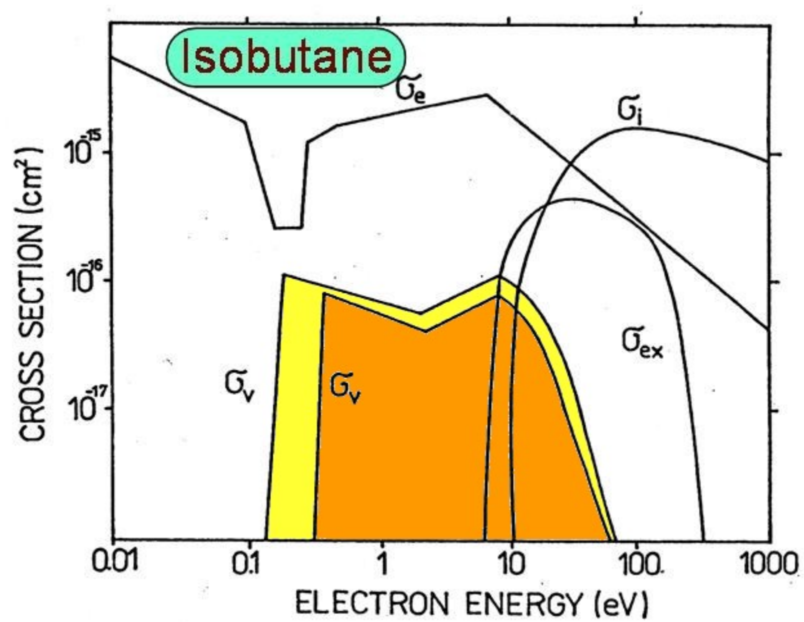

In practice one uses a mixture of gases, a noble gas and a molecular gas:

Noble gas: Ar, He, neon, xenon, krypton to favour ionisation.

High excitation energies, the photons from the de-excitation can generate new electrons by photoelectric effect on the cathode, which will provoke a second avalanche and so on. The detector is not stable

A molecular gas: CO_2, CH_4, C_2H_6, C_4H_{10}, have a lot of vibrational and rotational degrees of freedom. These exitations can absorbe some of these photons.

Ulrich.Goerlach@iphc.cnrs.fr, ASP Particle detectors 2012

Townsend coefficient

1atm = 1,013x10^5 pascal
= 1013 Hecto pascal
= 1,013 bar
= 760 Torr
1pascal= 10^{-4} N/cm^2
= 7,501 10^{-3} mm Hg
1 torr = 1 mm Hg = 133,3 pascal

The Townsend coefficient α describes the multiplication of an electron in a gaz .

α = Number of electrons produced in 1cm

$\lambda = 1/\alpha$ is the mean free path of the electron

The growth of the number of electrons is

$$\alpha = \sigma_{ionisation} \frac{N_A}{V_{Mol}}$$

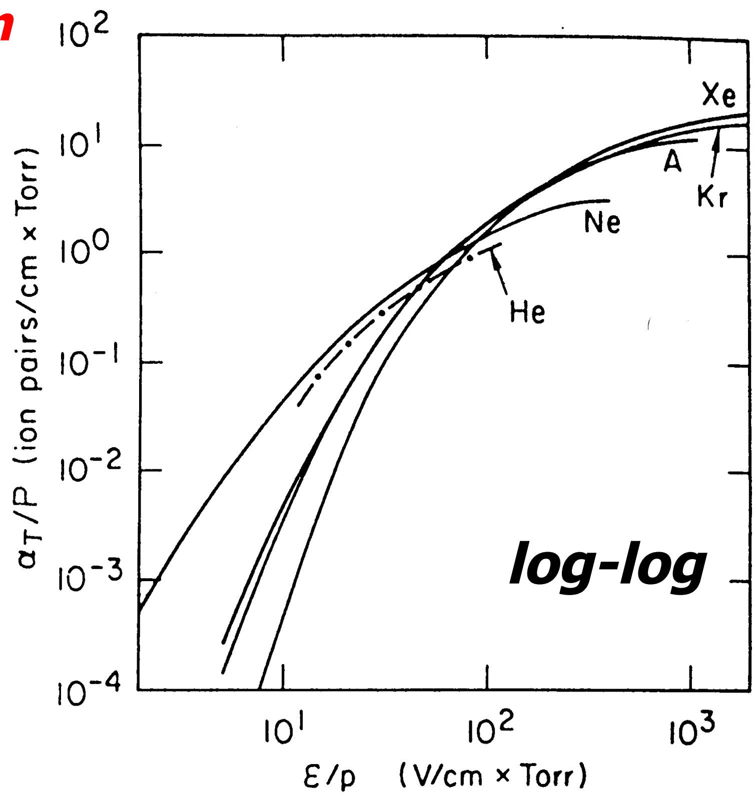

The Townsend coefficient α

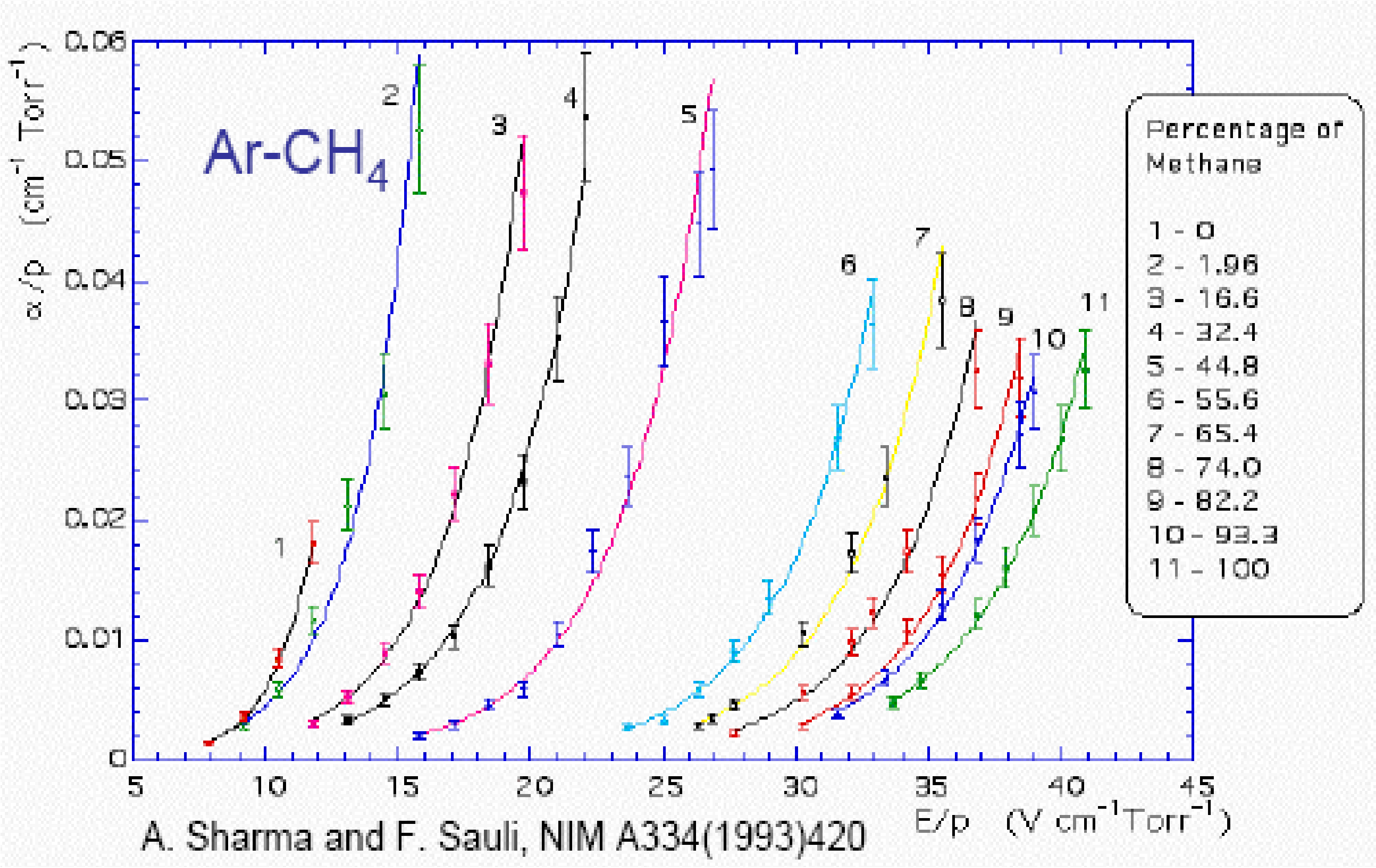

lin-lin

UNIVERSITÉ DE STRASBOURG

The gain

If the probability of ionisation is proportional to the electron energy, the coefficient α depends linear on the energy, this is the case in noble gases and if the gain does not exceed 10^4.

$$dN = N_0 \cdot \alpha \cdot dx; \quad N(x) = N_0 \underbrace{e^{\alpha x}}_{\approx G}$$

$$\Rightarrow G = \exp(\alpha \cdot x) \sim \exp(keV)$$

Otherwise

$$N(x) = N_0 \underbrace{e^{\alpha x}}_{\approx G} \xrightarrow{\alpha=\alpha(E,x)} N(x) = N_0 \underbrace{\exp\left(\int_{r_{E>E_{avalanche}}}^{r_{fil}} \alpha(r)\, dr \right)}_{G}$$

Simplified scheme of different regimes of gas counters

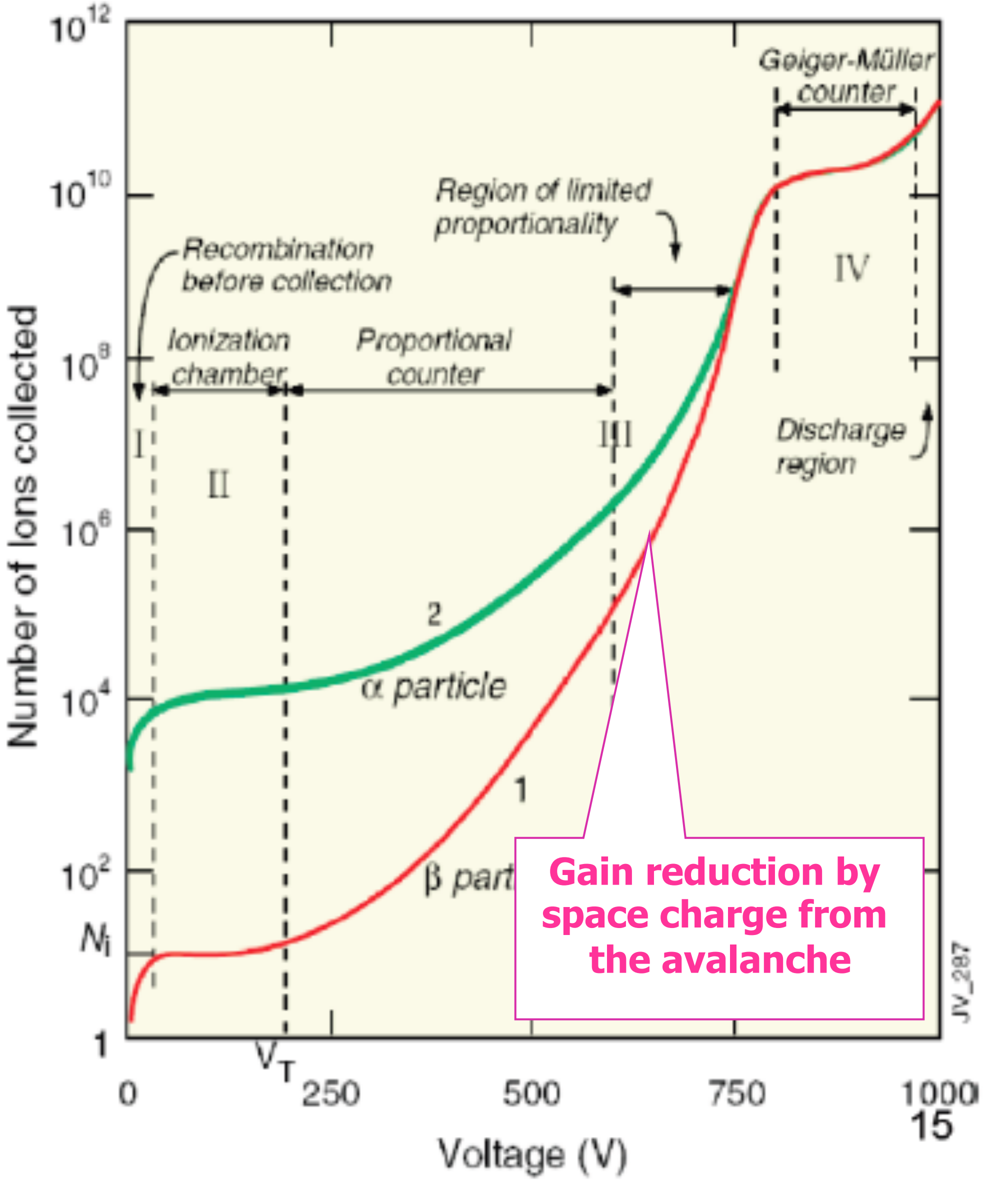

15

I. ionization mode: full charge collection, but no multiplication;

II. proportional mode: multiplication of ionization; detected signal proportional to original ionization → possible energy measurement (dE/dx); secondary avalanches are quenched; gain ~ 10^4 – 10^5

III. limited proportional mode (saturated, streamer) strong photoemission; secondary avalanches merging with original avalanche; requires strong quenchers or pulsed HV; large signals → simple electronics; gain ~ 10^{10}

IV. Geiger mode – massive photoemission; full length of the anode wire affected; discharge stopped by HV cut; strong quenchers needed as well

CERN Academic Training Programme 2004/2005

Ulrich.Goerlach@iphc.cnrs.fr, ASP Particle detectors 2012

Geiger Müller (1928)

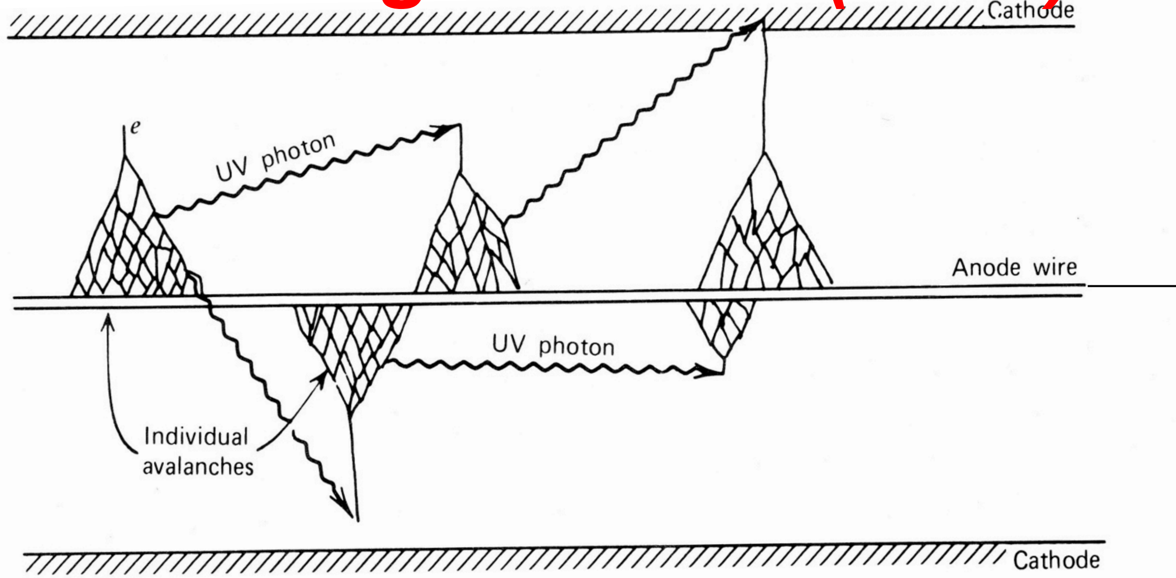

Figure 7-1 The mechanism by which additional avalanches are triggered in a Geiger discharge.

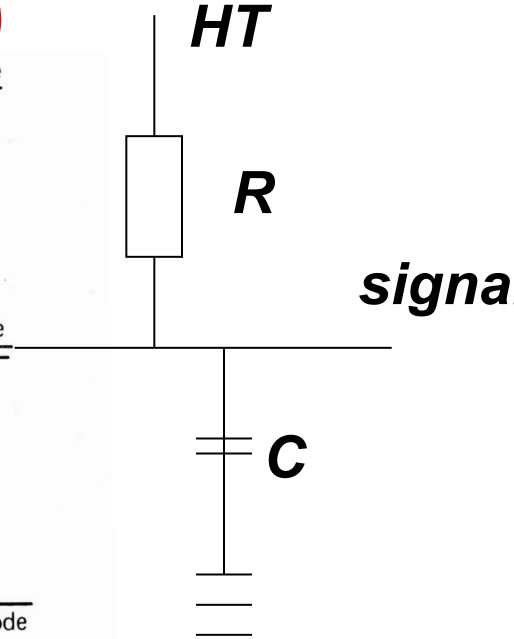

- **Multiplication with very high gain, *G=10^6-8^***
- **Secondary avalanches, triggered by UV photons can completely cover the wire**
- **Space charge *Q=10^10^* will stop avalanche independant of initial charge**
- **« Quenching » with a gaz or limit high voltage with R**
- **output amplitude is contant**
- **Very high dead time,**

Response time

- Interaction of particle or photon in the detector
- Formation of charges or of scintillation light
- Collection of charges / photons
- Amplification and integration
- Read-out

⇒ << ps → ms

Dead time

- Time necessary in order to be « ready » for the next event. During this time the detector (or it's read-out electronics is partially or completely insensitive to new particles.
- Restoration time: time until the detector has completely recovered.
- « pile-up » : superposition of pulses
- One has to understand, to measure and correct

Response and dead time

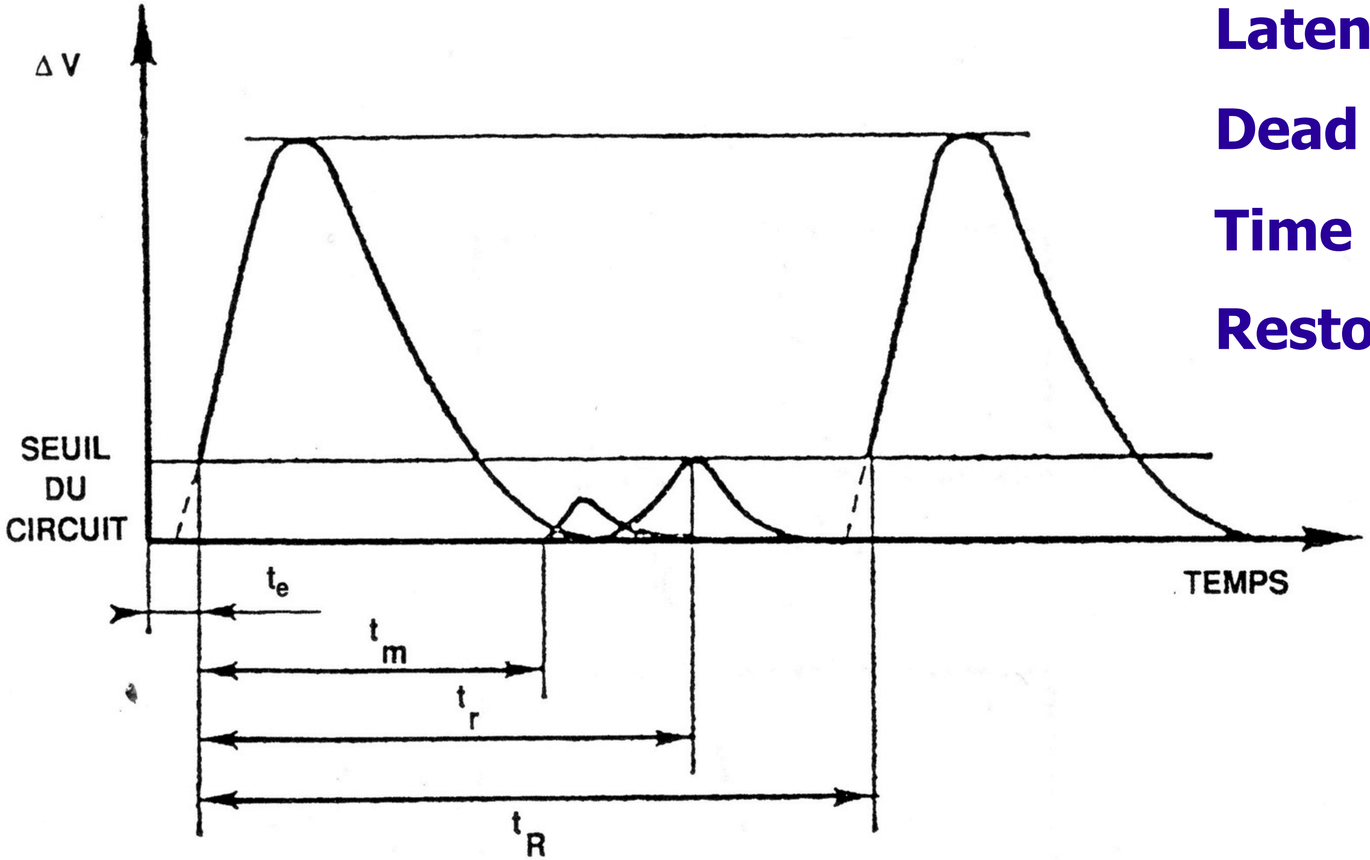

Figure 6.4 : *Séquence des impulsions délivrées par un compteur Geiger-Müller*

Latency t_e

Dead time t_m

Time resolution t_r

Restoration time t_R

Temps mort

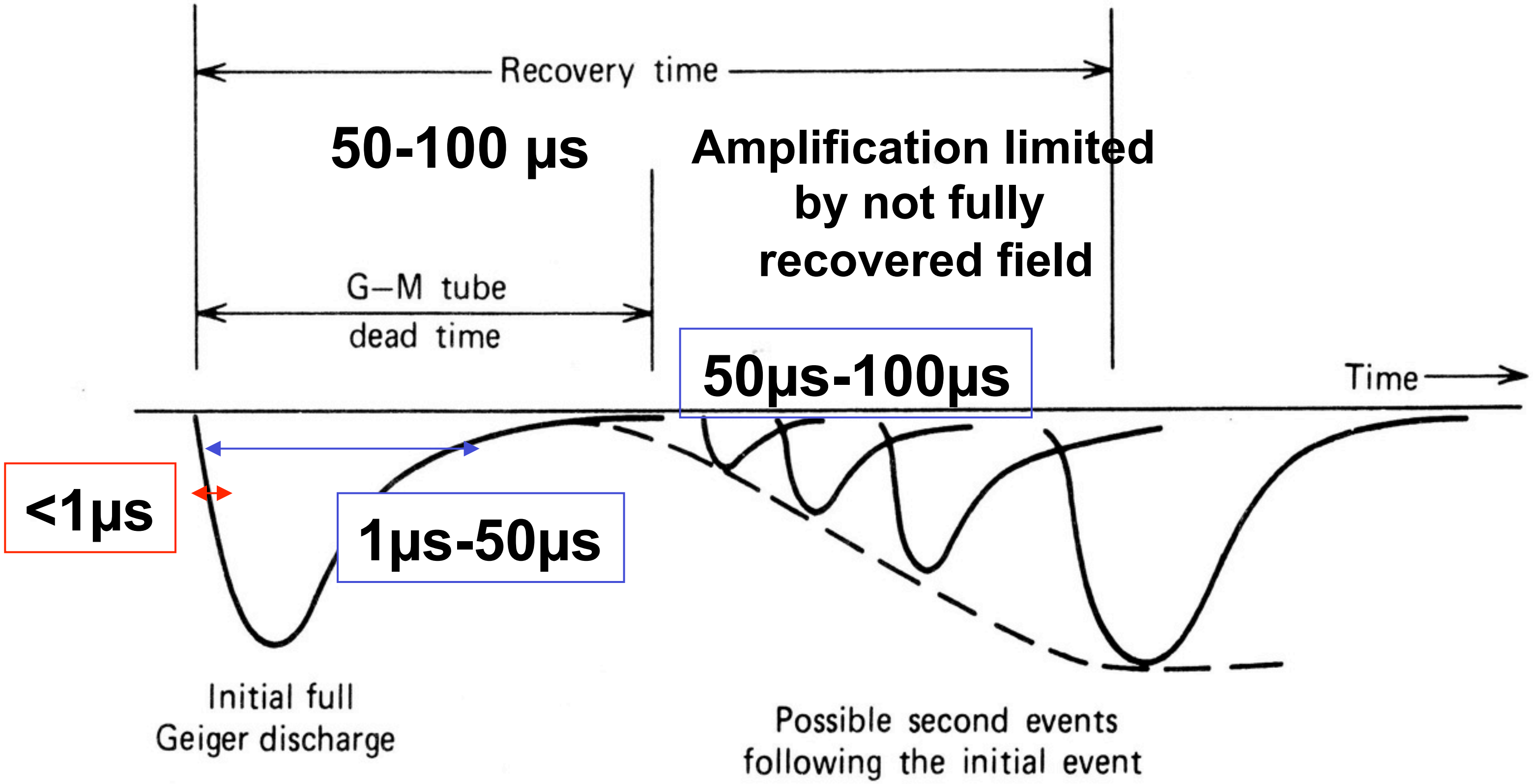

Figure 7-4 Illustration of the dead time of a G-M tube. Pulses of negative polarity conventionally observed from the detector are shown.

Dead time and efficiency

- If the counting rate is larger then (dead-time)$^{-1}$ you have to correct!

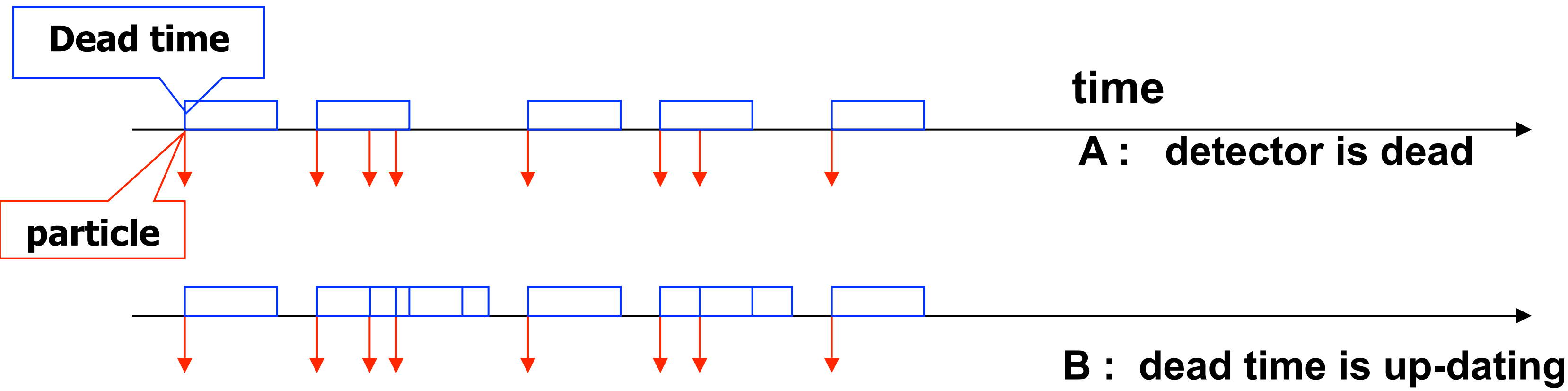

Cas A : f = real rate of N particles hitting the detector within time interval T

f' = measured rate of N' particles registered during interval T

each hit will cause a dead time τ

$N'\tau$ = total dead time ; during this time you loose $N'\cdot\tau\cdot f$ particles

$$N = f\cdot T = N' + N'\cdot\tau\cdot f$$

$$f = \frac{N'/T}{1-(N'/T)\tau} = \frac{f'}{1-f'\tau}$$

Dead time and efficiency

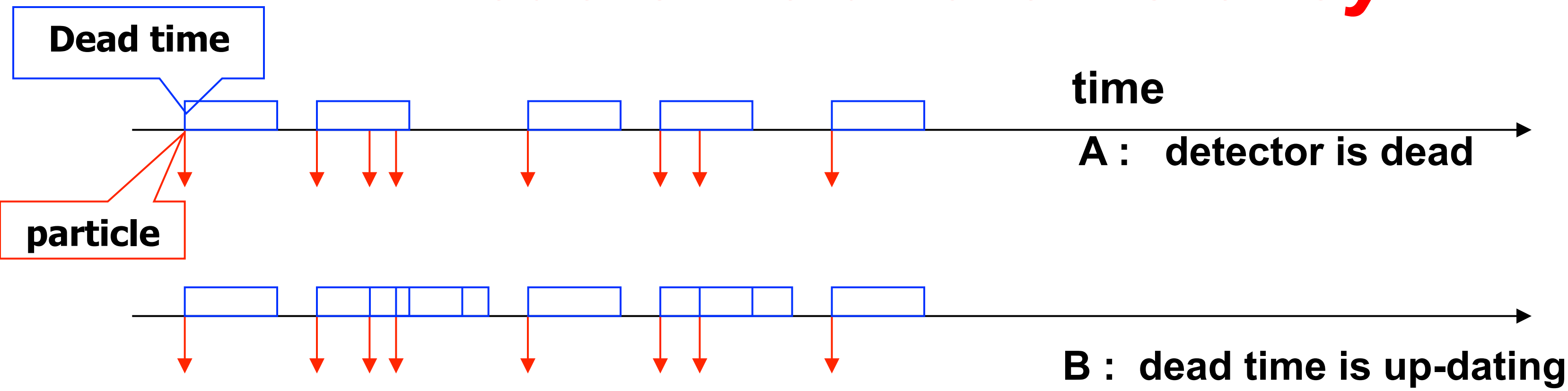

Cas B :

f = real rate ; f' = measured rate: N' registered events in time T; dead time τ

Only particles which arrive within an interval $> \tau$ are registered

Distribution of the intervals t between two particles

$$P_{distrib}(t) = f \cdot \exp(-ft)$$

$$\mathrm{P}(t > \tau) = \int_{\tau}^{\infty} P_{distrib}(t)\,dt = \exp(-f\tau)$$

is the probability that two particles are seperated by a time $t > \tau$

measured events N' is then:

$N'(\tau) = N \cdot \exp(-f\tau)$ to solve numerically

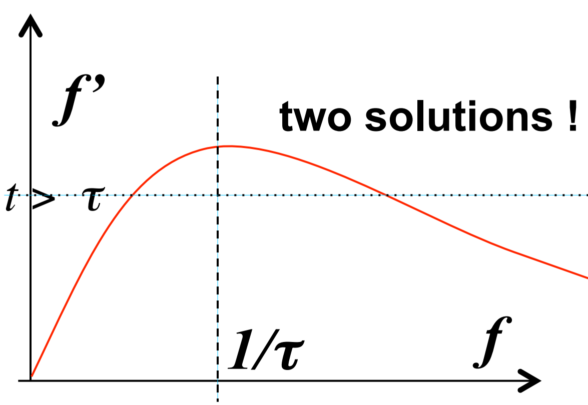

RPC – Resistive Plate Chamber

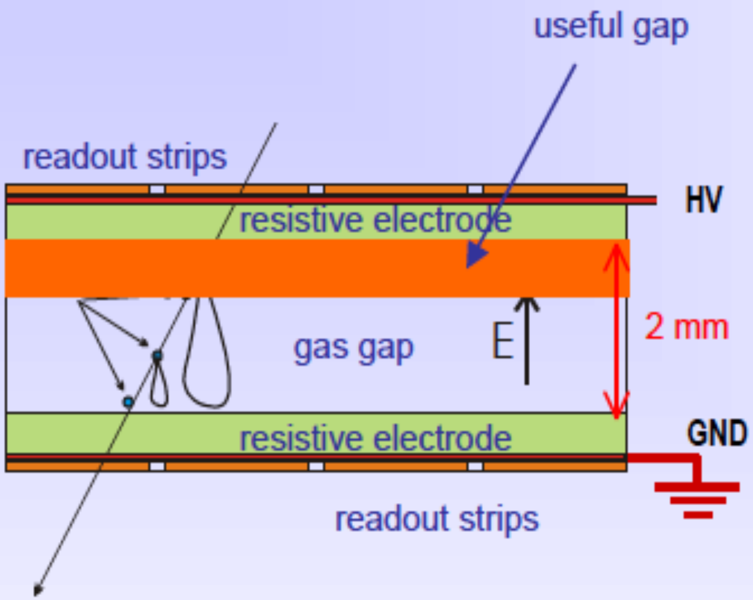

Rate capability strong function of the resistivity of electrodes in streamer mode.

MRPC

Multigap RPC - exceptional time resolution suited for the trigger applications

A. Akindinov et al., NIM A456(2000)16

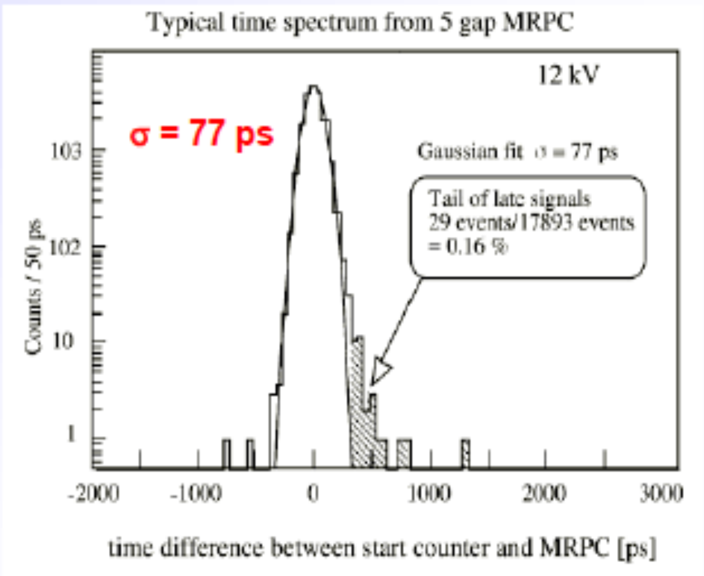

Time resolution

UNIVERSITÉ DE STRASBOURG

Return proportional mode

Cylindrical proportional chamber

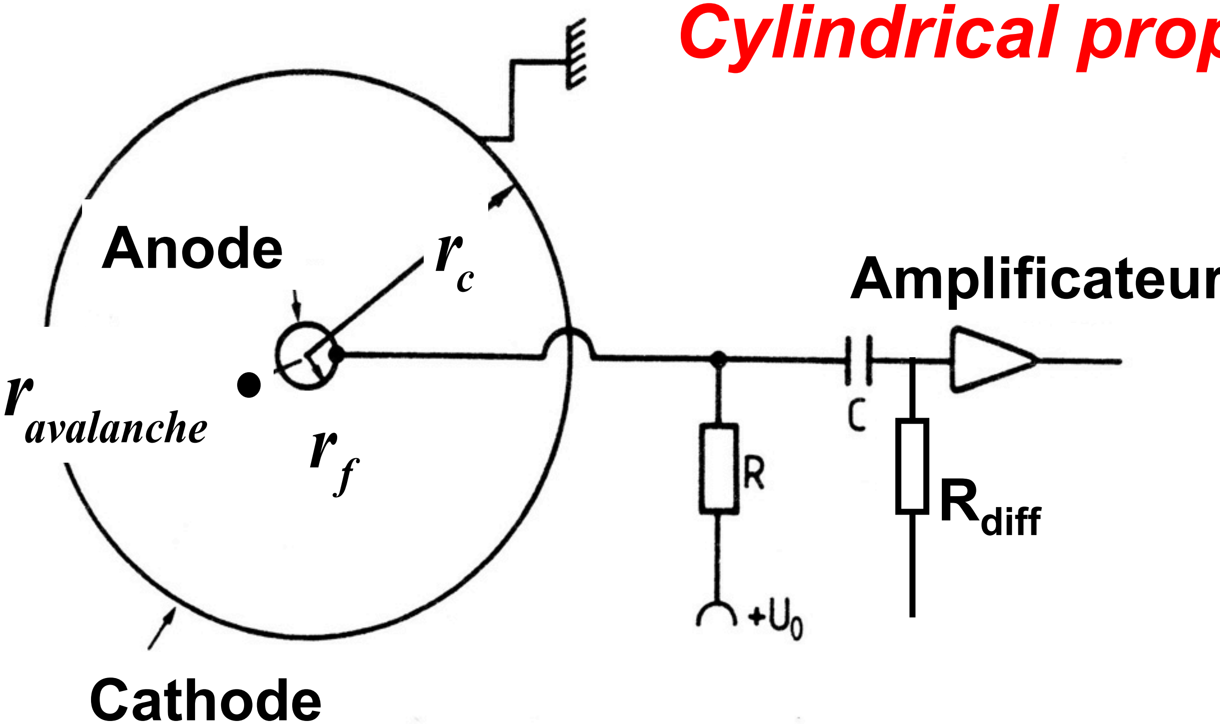

$$\left|\vec{E}\right| = \frac{U_0}{r \ln\left(r_c / r_f\right)}$$

- For a cylindrical proportionel chamber the majority of the signal comes from the slow moving ions. The electrons contribute only ≈ 1%

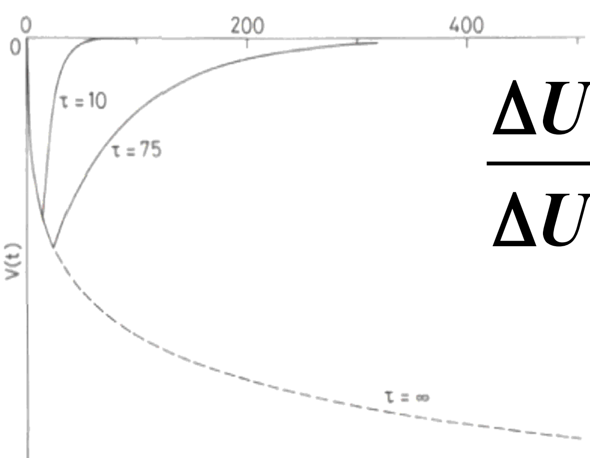

$$\frac{\Delta U^+}{\Delta U^-} = \left.\frac{\ln\left(r_c / r_{avalanche}\right)}{\ln\left(r_{avalanche} / r_f\right)}\right|_{r_{ava} \geq r_f}$$

$$\frac{\Delta U^+}{\Delta U^-} \gg 1$$

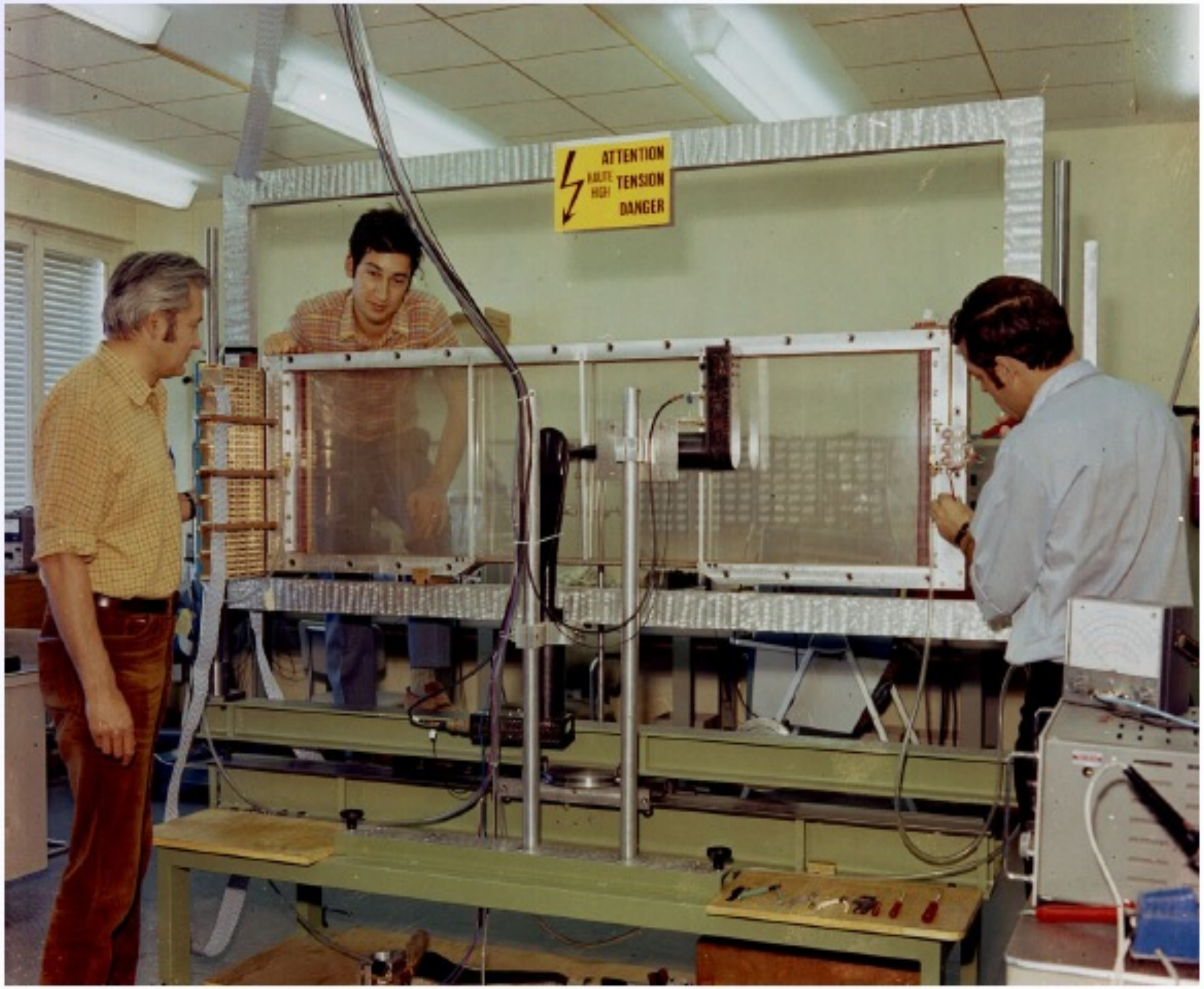

G. Charpak, F. Sauli and J.C. Santiard

Multi Wire Proportional Chamber (MWPC)

Proposed by G. Charpak in 1967

- **Wire:** tungsten 30-50μm,
- **Surface :** 10x10cm² → 4×4m²,
  t= 100ns
- **Counting:** 10^5/fil, **signal:** qq mV,
- **gas:** argon+n-pentane.
- **Each wire is connected to an amplifier**

Cathod grid

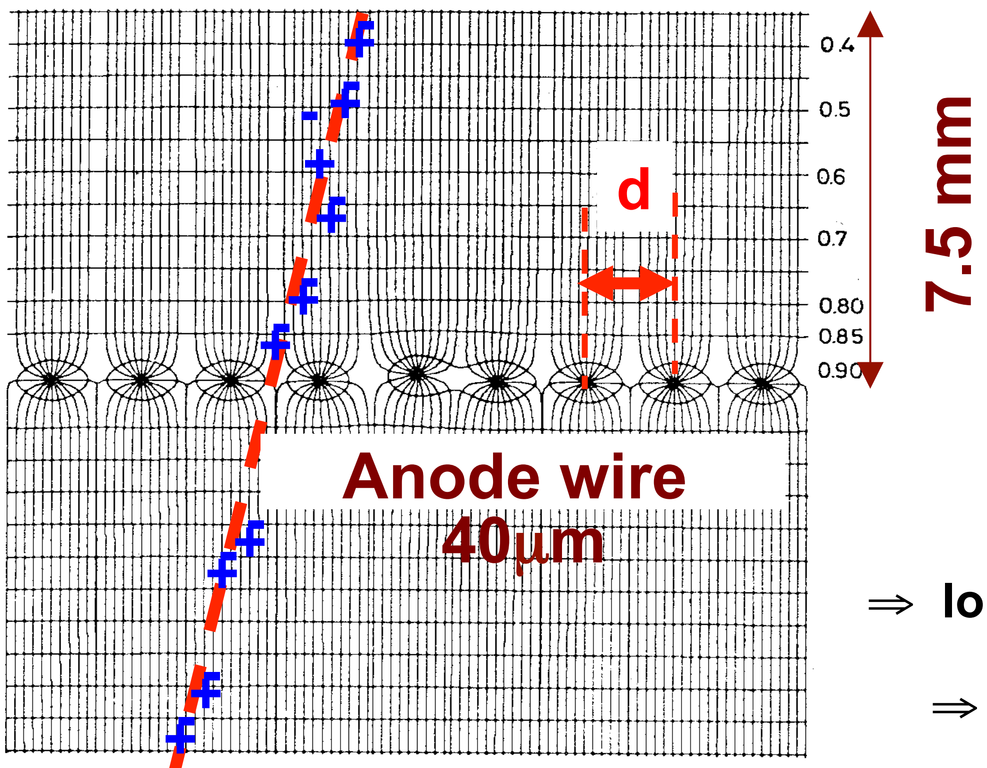

(a)

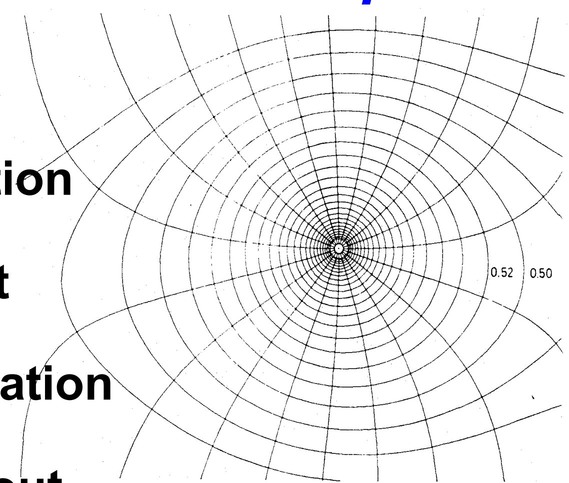

(b)

⇒ Ionisation

⇒ Drift

⇒ Amplification

⇒ Read-out

Spacial Resolution: d/√12

Multi Wire Proportional Chamber (MWPC)

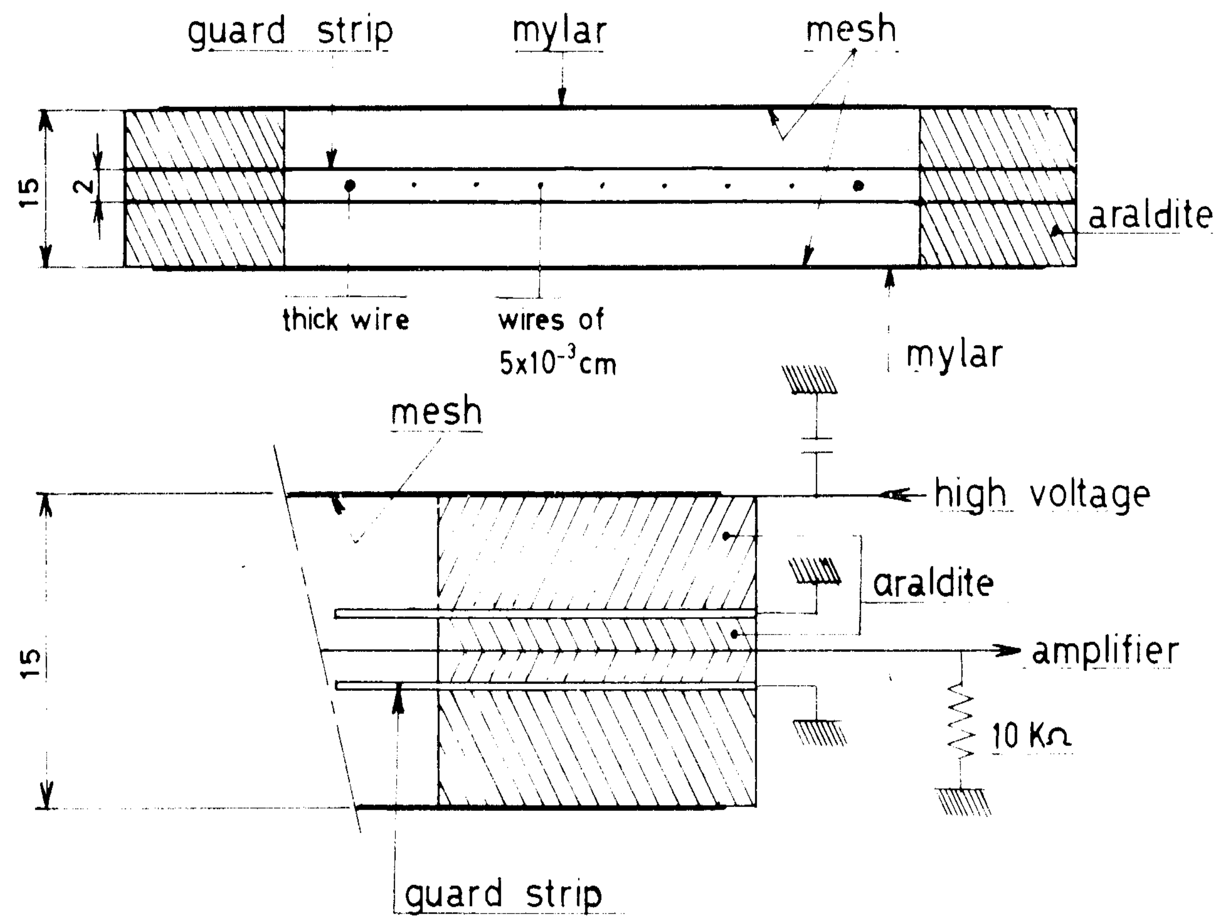

Cylindrical proportional chamber

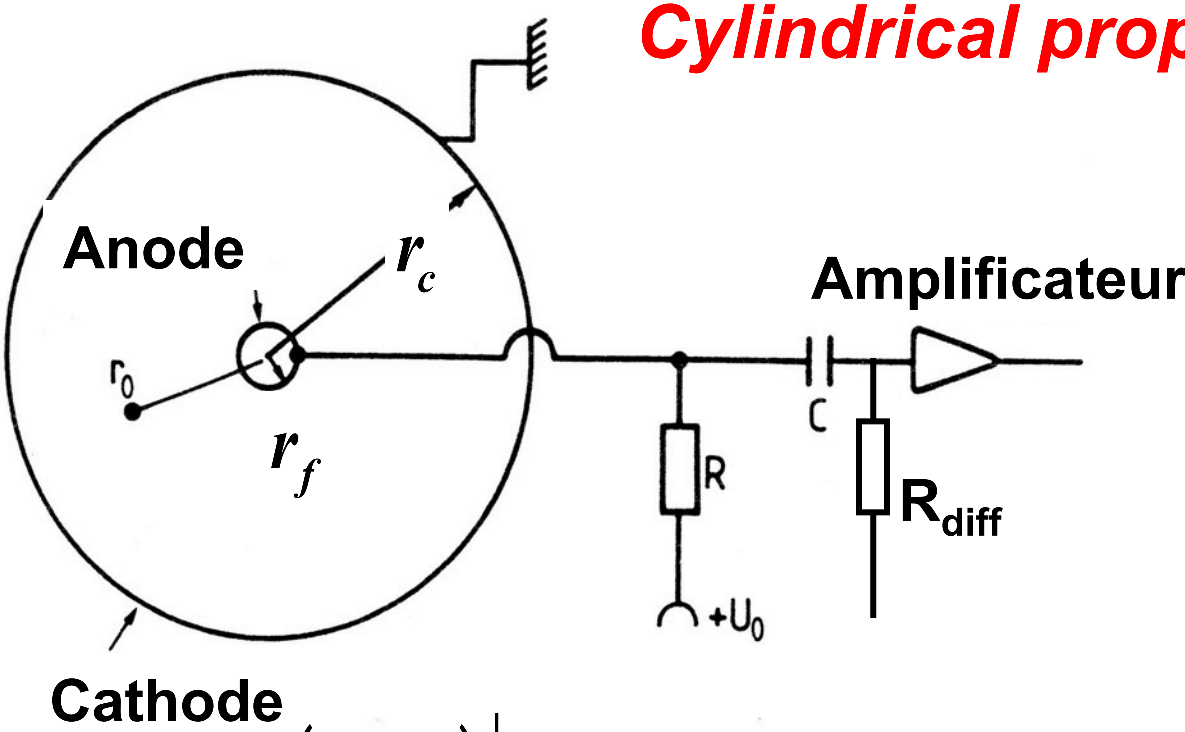

$$\left|\vec{E}\right| = \frac{U_0}{r \ln\left(r_c / r_f\right)}$$

- Most of the signal comes from the ions Electrons contribut only ≈ 1%
- k = number of mean free path λ

$$\frac{\Delta U^+}{\Delta U^-} = \left.\frac{\ln\left(r_c / r_0\right)}{\ln\left(r_0 / r_f\right)}\right|; \; r_0 = r_f + k\lambda; \; r_f \gg k\lambda$$

$$= \frac{\ln r_c - \ln\left(r_f + k\lambda\right)}{\ln\left[\left(r_f + k\lambda\right) / r_f\right]} \approx \frac{\ln\left(r_c / r_f\right)}{k\lambda / r_f} \gg 1$$

Cylindrical proportional chamber : signal formation

$$U^{(+)}(t) = \int_{r_0=r(t_0)}^{r(t)} \frac{dU}{dr} dr = -\frac{Ne}{C} \frac{\ln(r(t)/r_0)}{\ln(r_c/r_f)}$$

$$r_0 \approx r_f; \;\; C/l = \frac{2\pi\varepsilon}{\ln(r_c/r_f)}$$

$$U^{(+)}(t) = -\frac{Ne}{2\pi\varepsilon l} \ln(r(t)/r_f)$$

$$\frac{dr}{dt} = \mu E(r) = \frac{\mu C U_0}{2\pi\varepsilon} \frac{1}{r};$$

$$r dr = \frac{\mu C U_0}{2\pi\varepsilon} dt; \text{ integration between } r_f \text{ and } r$$

$$r(t) = \sqrt{r_f^2 + \frac{\mu C U_0}{\pi\varepsilon} t}$$

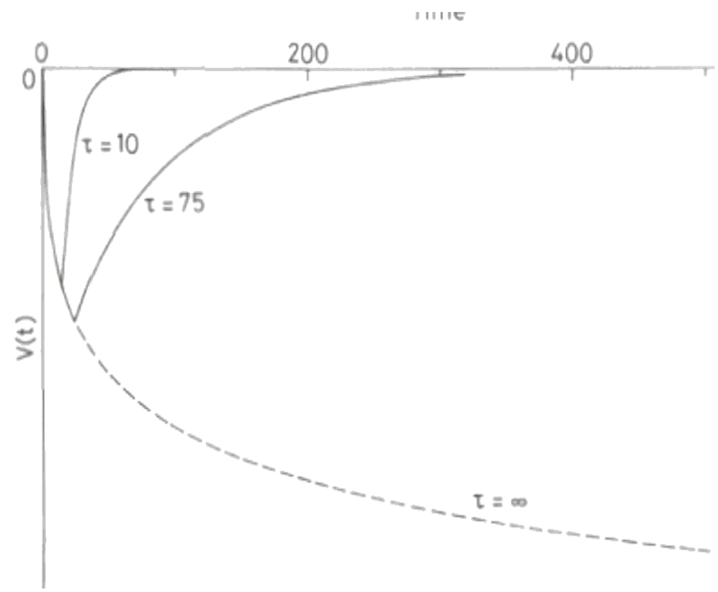

$$U(t) = -\frac{Ne}{4\pi\varepsilon l} \ln\left(1 + \frac{\mu C U_0}{\pi\varepsilon r_f^2} t\right) = -\frac{Ne}{4\pi\varepsilon l} \ln\left(1 + \frac{t}{t_0}\right); \; t_0 = \frac{\pi\varepsilon r_f^2}{\mu C U_0}$$

$$T_{total} = \frac{t_0}{r_f^2}\left(r_c^2 - r_f^2\right) = \frac{\pi\varepsilon}{\mu C U_0}\left(r_c^2 - r_f^2\right)$$

UNIVERSITÉ DE STRASBOURG

MWPC

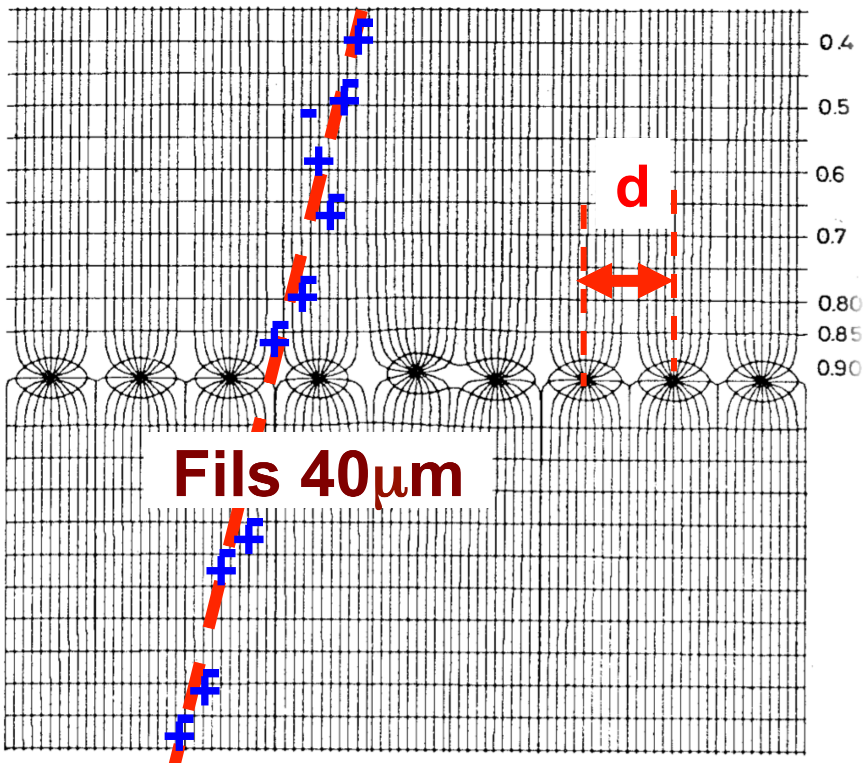

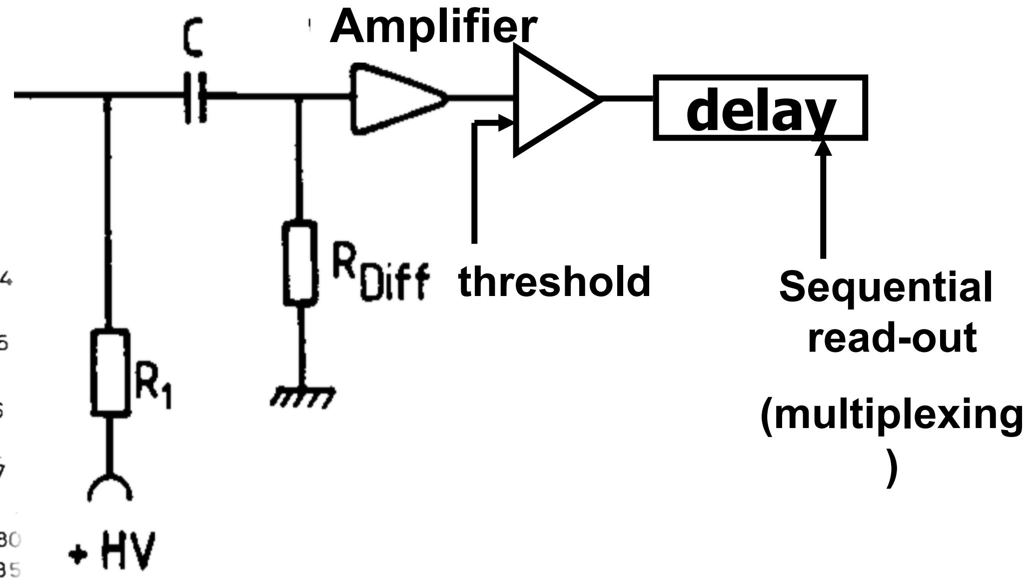

efficiency

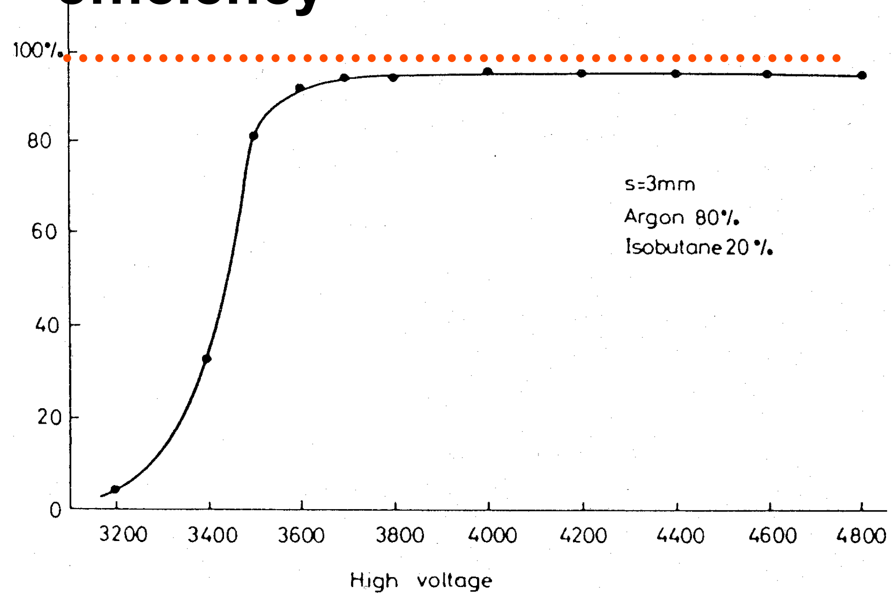

Binary read-out :

Resolution:

$d/\sqrt{12}$; d=2mm → $\sigma \approx 0{,}6$ mm

Two-dimensional read-out via cathodes

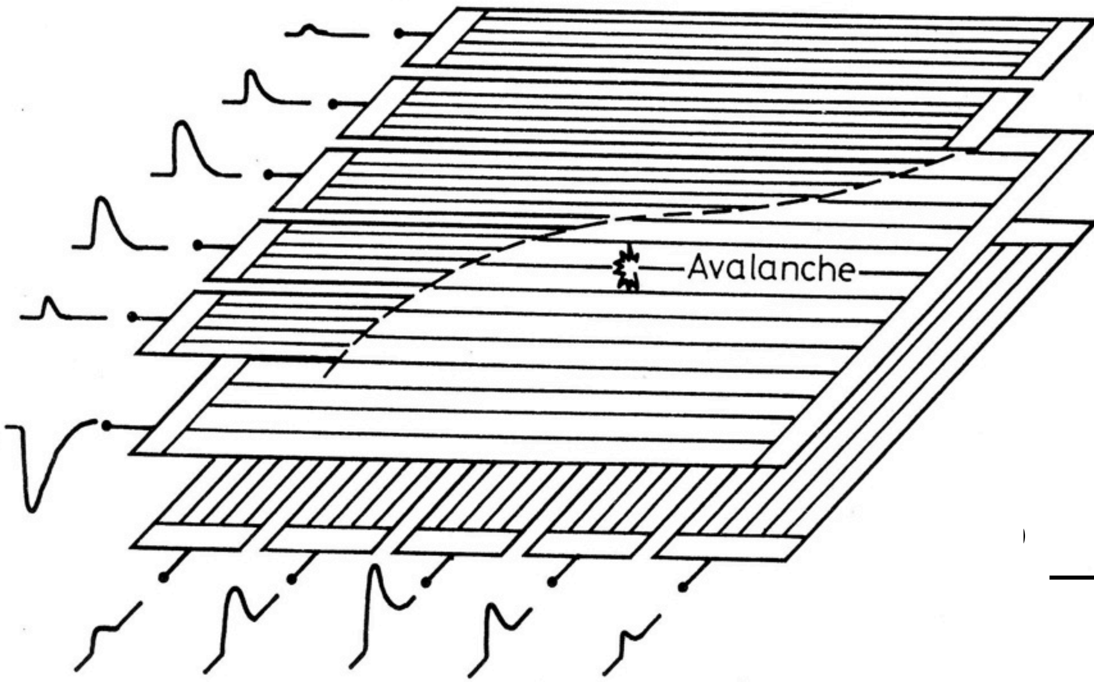

Fig. 6.11. Bidimensional readout using cathode strips (from *Breskin* et al. [6.18]). The signals from each strip are stored and the center of gravity of the distribution calculated to yield the position of the avalanche

$$y = \frac{\sum (Q_i - b) y_i}{\sum (Q_i - b)},$$

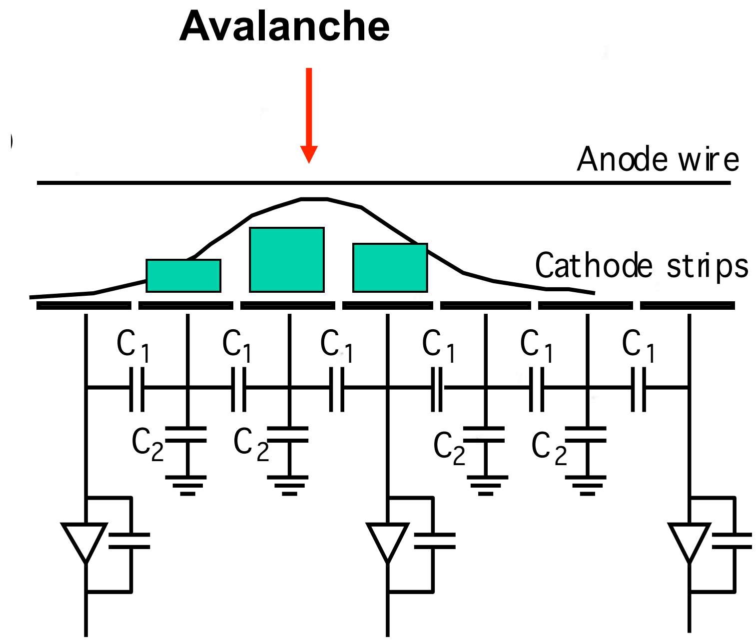

CSC – Cathode Strip Chamber

Precise measurement of the second coordinate by interpolation of the signal induced on pads.
Closely spaced wires makes CSC fast detector.

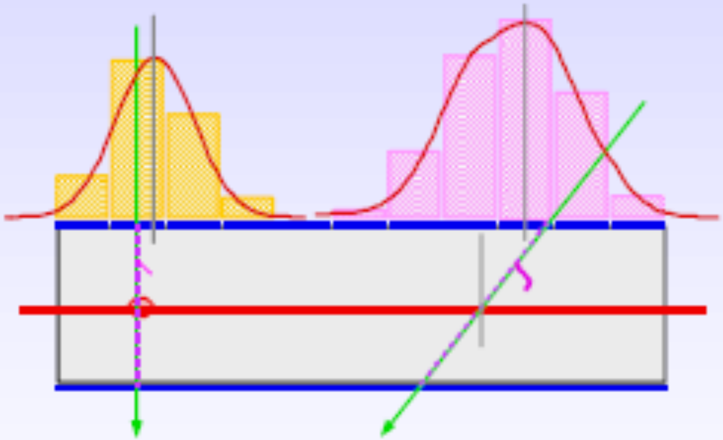

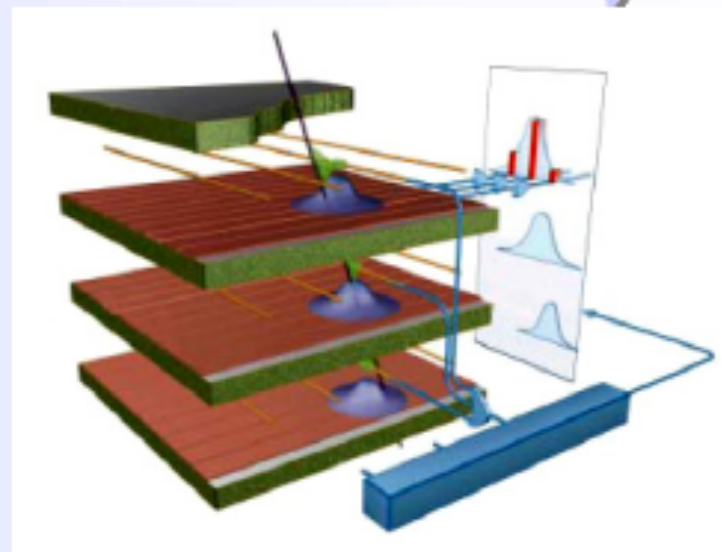

Center of gravity of induced signal method.

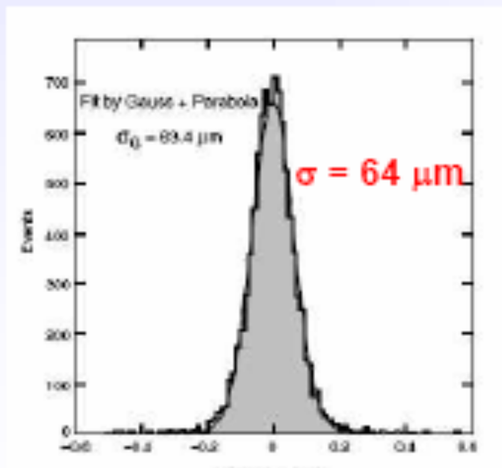

Space resolution

CMS

RPC – Resistive Plate Chamber

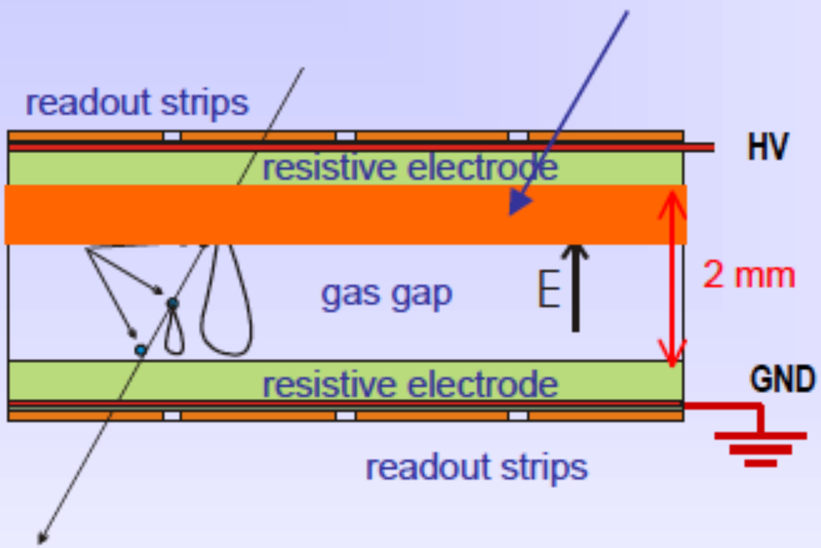

Rate capability strong function of the resistivity of electrodes in streamer mode.

MRPC

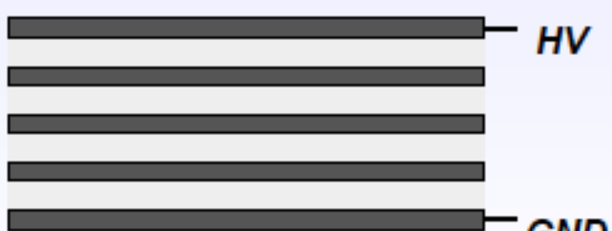

Multigap RPC - exceptional time resolution suited for the trigger applications

A. Akindinov et al., NIM A456(2000)16

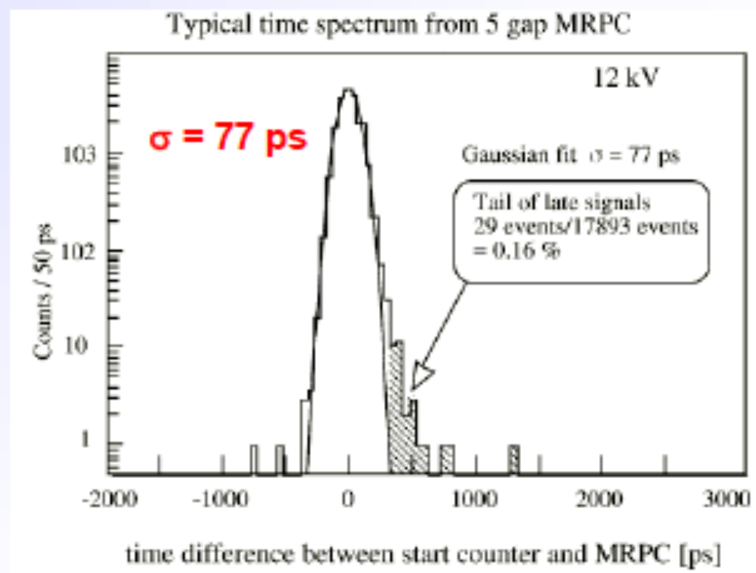

Time resolution

Drift Chambers

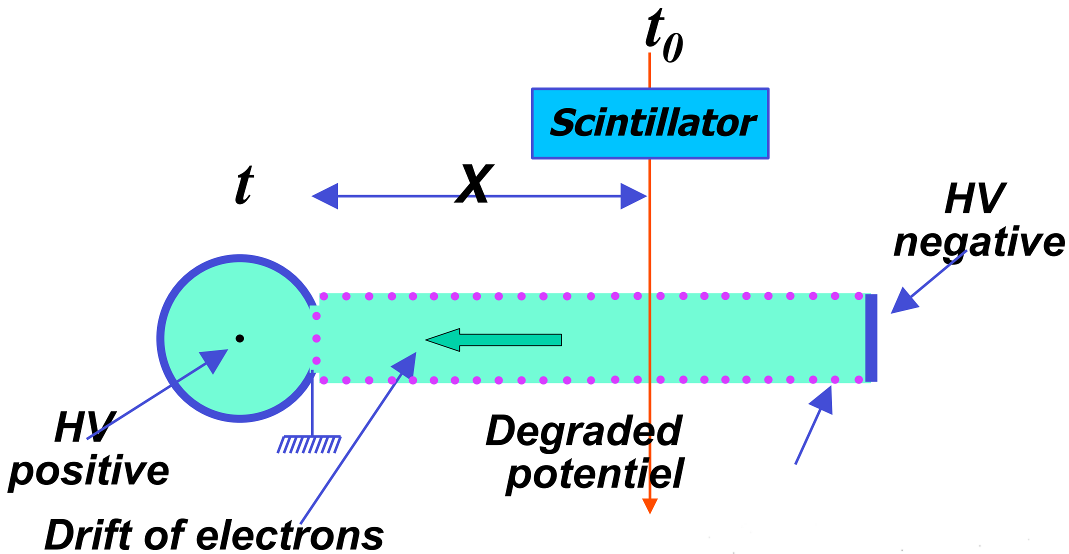

Drift velocity of electrons:

50 µm/ns

Spacial resolution 100-200 µm

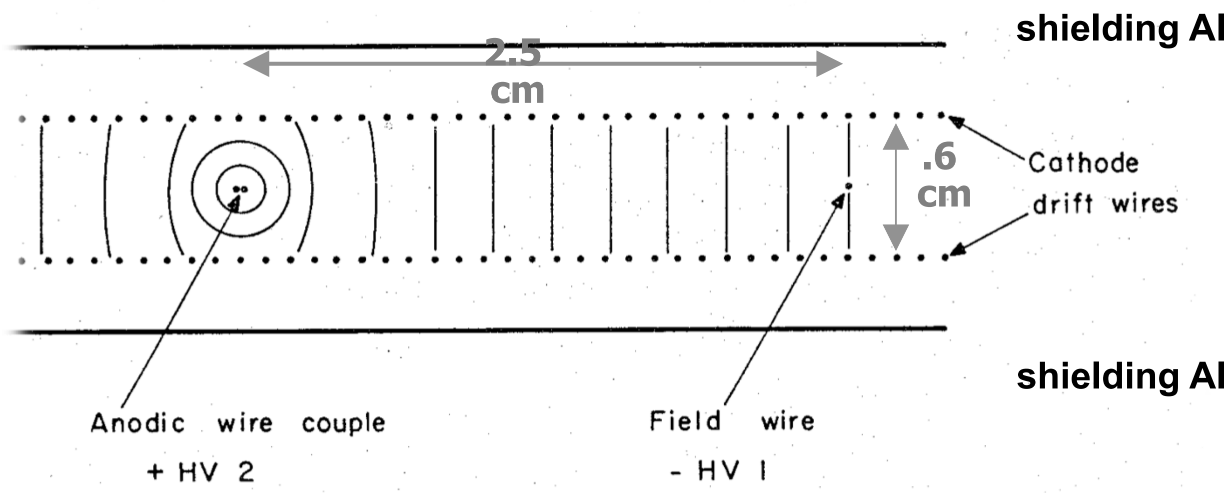

A. Breskin et al Nucl. Instr. Meth.A124 (1975) 189

Chambre_a_derive_2.pct

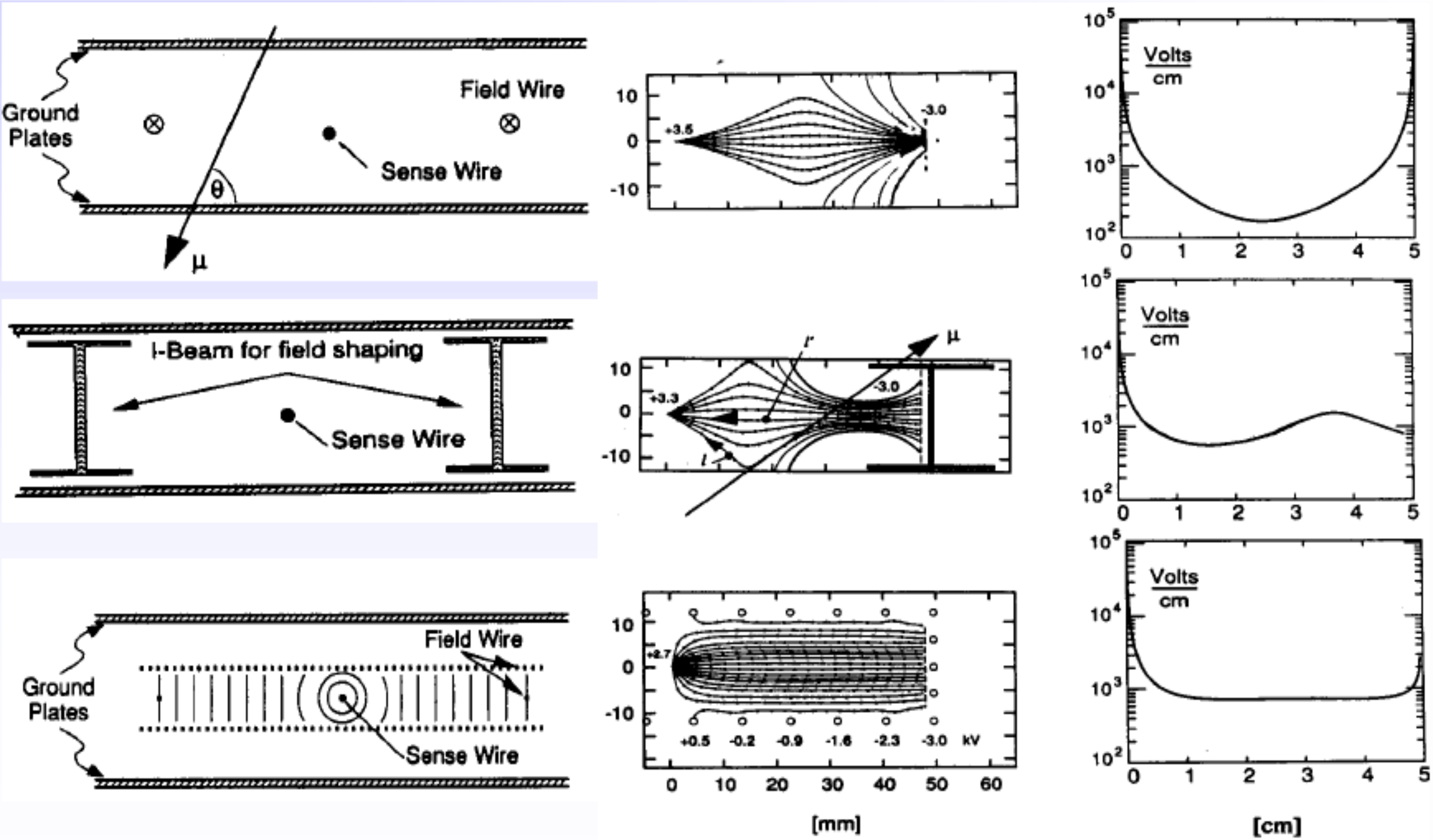

U. Becker in Instrumentation in High Energy Physics, World Scientific

UNIVERSITÉ DE STRASBOURG

CMS Muon chambers

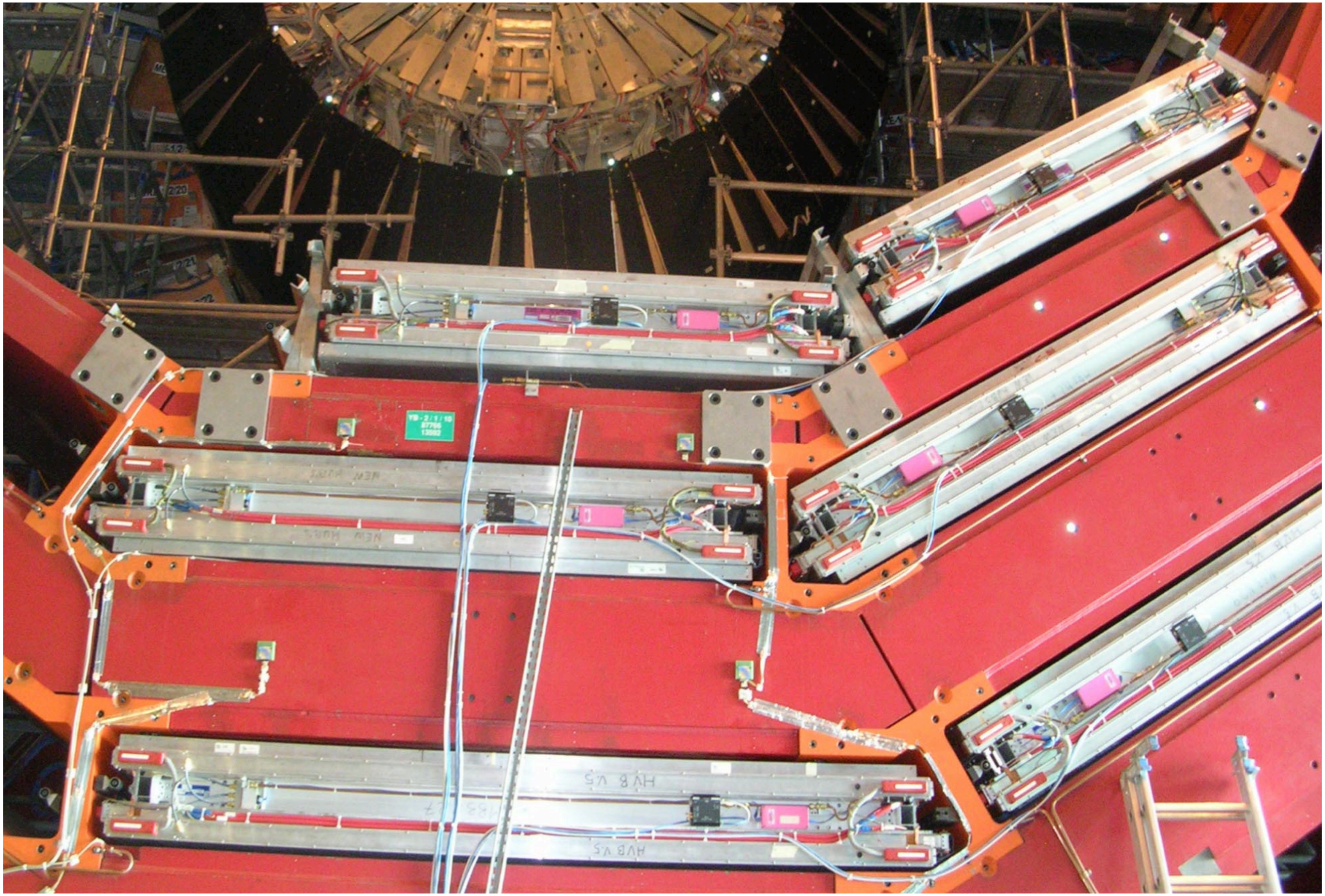

CMS Muon chambers

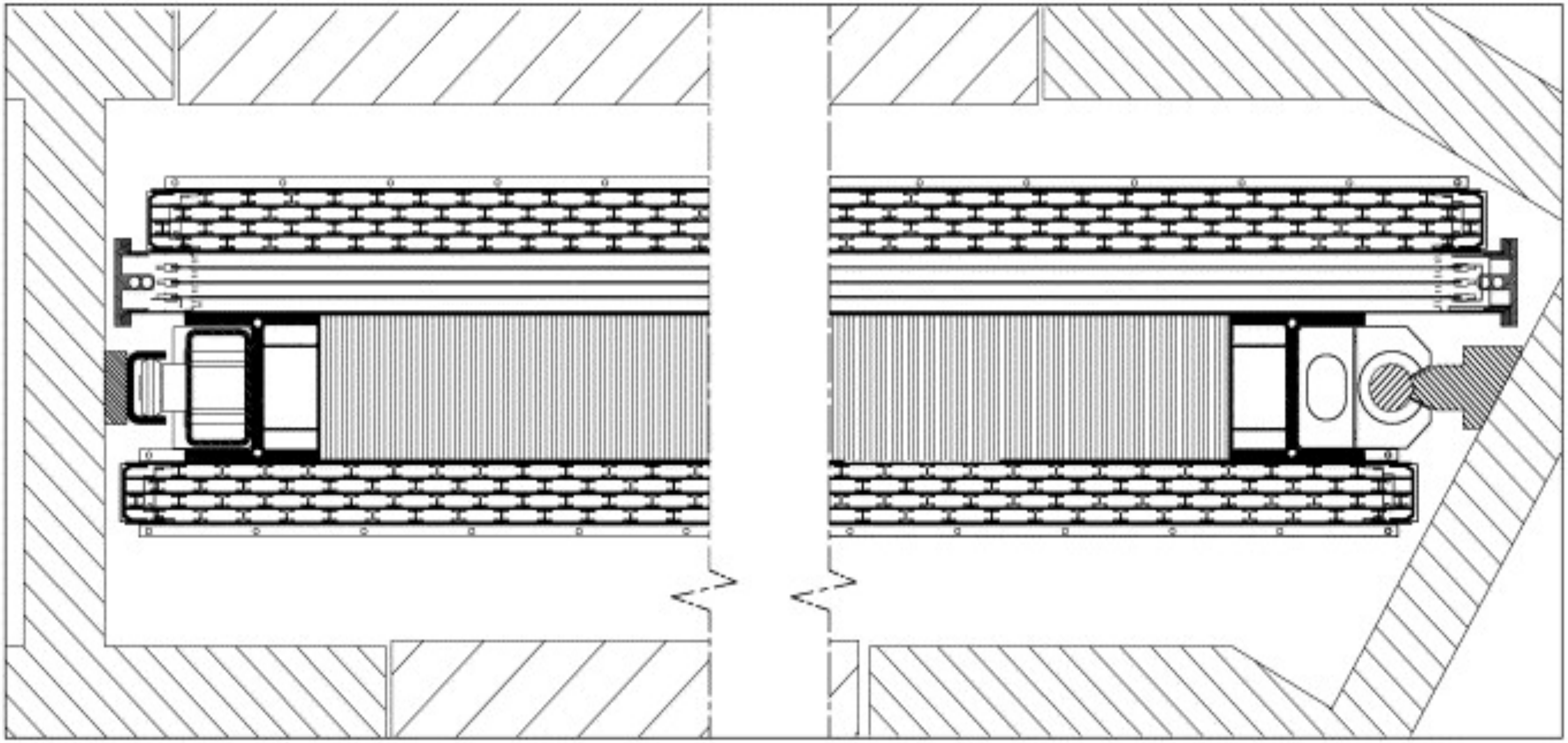

Cut view of a drift tube chamber in its final position inside the CMS iron yoke. Two superlayers with wires along the beam direction and a third crossed one can be seen as well as the honeycomb panel providing rigidity to the chamber.

Ulrich.Goerlach@iphc.cnrs.fr, ASP Particle detectors 2012

CMS Muon chambers

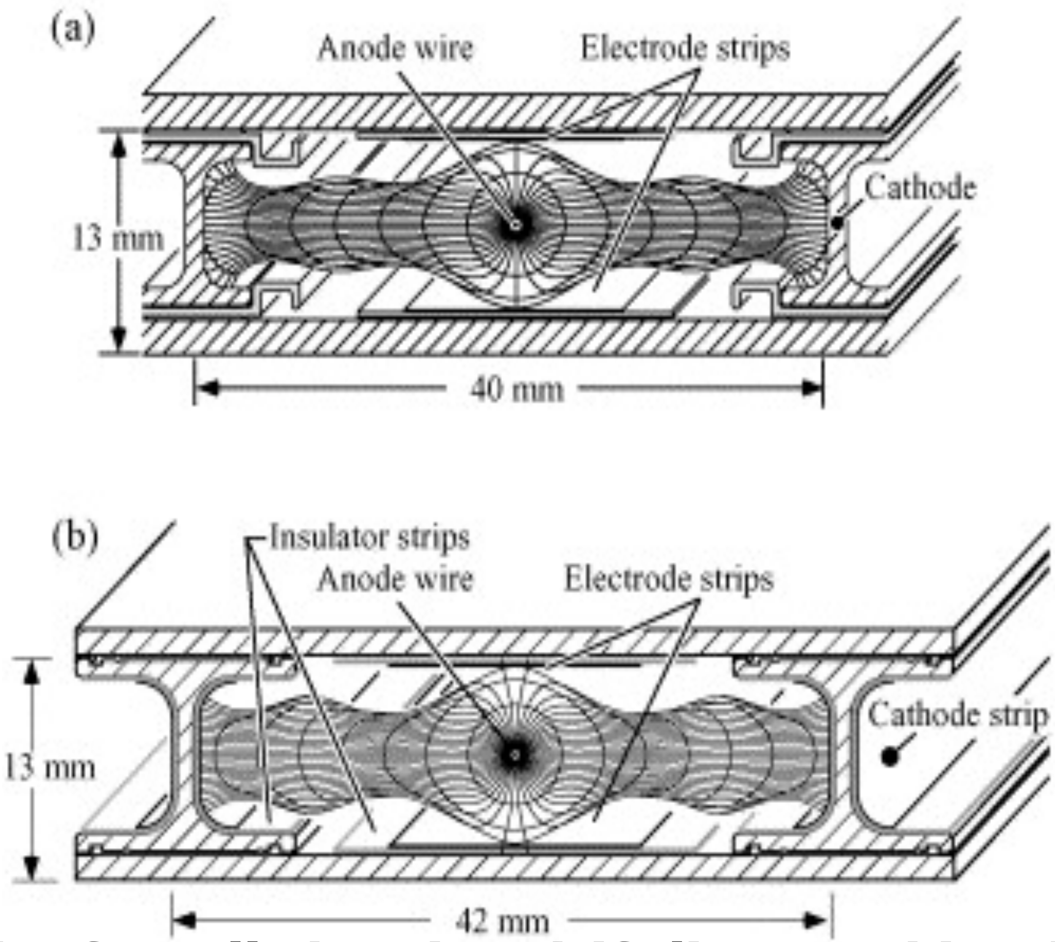

Sketch of a cell showing drift lines and isochrones: (a) corresponds to the old design [1], and (b) corresponds to the new design used in Q4. The plates at the top and bottom of the cell are at ground potential.

Drift Tubes (DT) in ATLAS: inner detector and muon spectrometer

- **Classical detection technique for charged particles based on gas ionisation and drift time measurement**

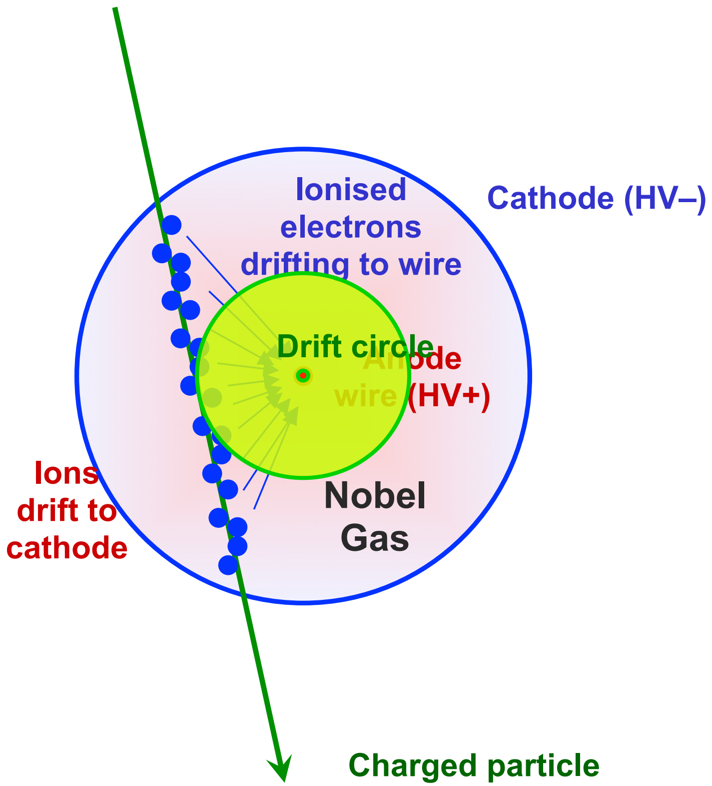

TRT: Kapton tubes,	∅ = 4 mm
MDT: Aluminium tubes,	∅ = 30 mm

From D. Froidevaux, ASP 2010

- **DTs used in muon systems and ATLAS TRT**
- **Primary electrons drift towards thin anode wire**
- **Charge amplification during drift ($\gtrsim 10^4$) in high E field in vicinity of wire: $E(r) \propto U_0 / r$**
- **Signal rises with number of primary e's (dE/dx) [signal dominated by ions → need differentiator]**
- **Macroscopic drift time: $v_D / c \sim 10^{-4}$ → ~30 ns / mm**
- **Determine v_D from difference between DT signal peaking time and expected particle passage**

➡ **Spatial resolution of O(100 μm)**

Drift Tubes (DT) in ATLAS: inner detector and muon spectrometer

- **Classical detection technique for charged particles based on gas ionisation and drift time measurement**

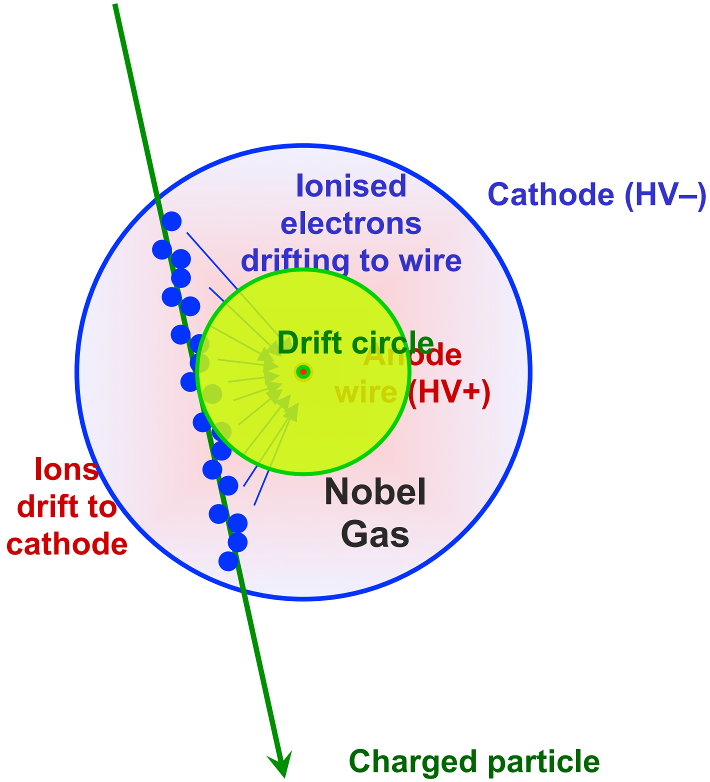

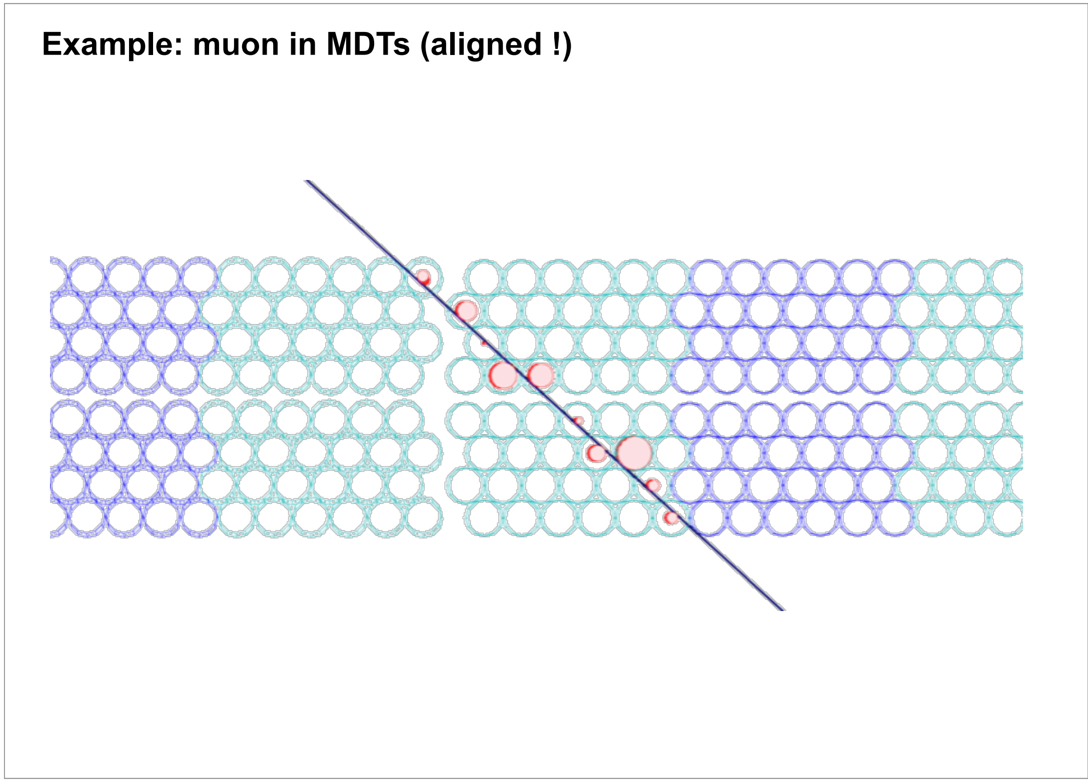

TRT: Kapton tubes,	∅ = 4 mm
MDT: Aluminium tubes,	∅ = 30 mm

From D. Froidevaux, ASP 2010

signal peaking time and expected particle passage

➧ **Spatial resolution of *O*(100 μm)**

The ATLAS Muon Spectrometer

Big wheel, Feb 2007

From D. Froidevaux, ASP 2010

Ulrich.Goerlach@iphc.cnrs.fr, ASP Particle detectors 2012

Time Projection Chamber (TPC):

Gas volume with parallel E and B Field.

B for momentum measurement. Positive effect:
Diffusion is strongly reduced by E//B (up to a factor 5).

Drift Fields 100-400V/cm. Drift times 10-100 μs.

Distance up to 2.5m !

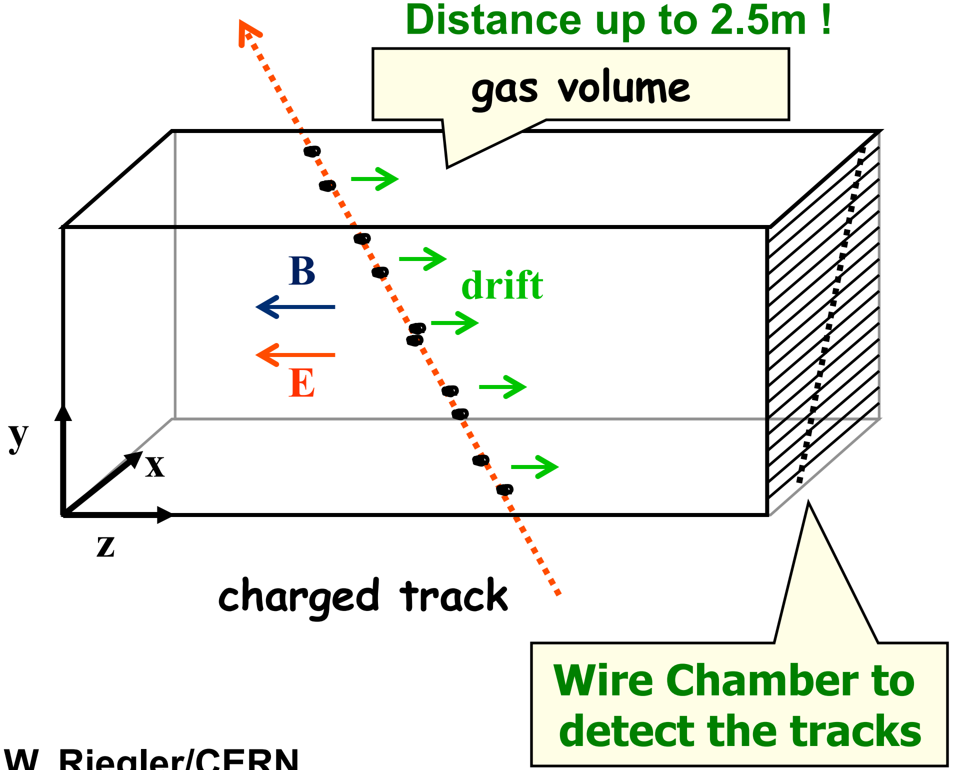

W. Riegler/CERN

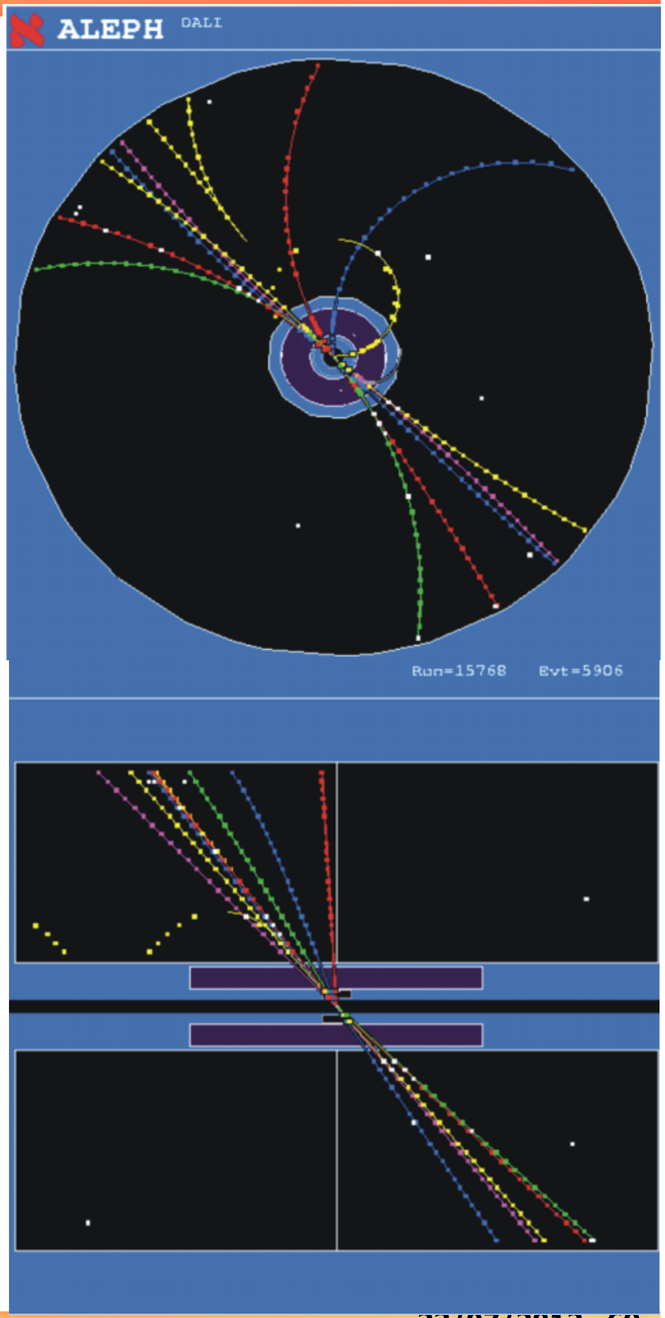

O.Ullaland CERN 2005

UNIVERSITÉ DE STRASBOURG

Time Projection (

Gas volume with pa

B for momentum measu
Diffusion is strongly reduc

Drift Fields 100-400V/cr

Distance u

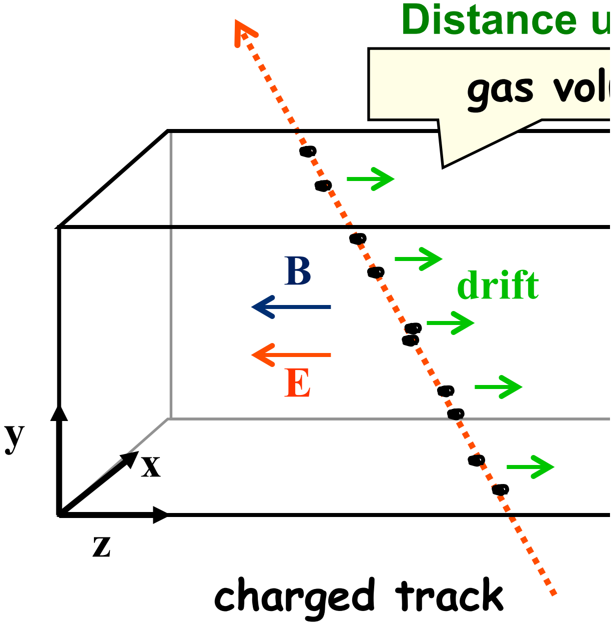

Wi
de

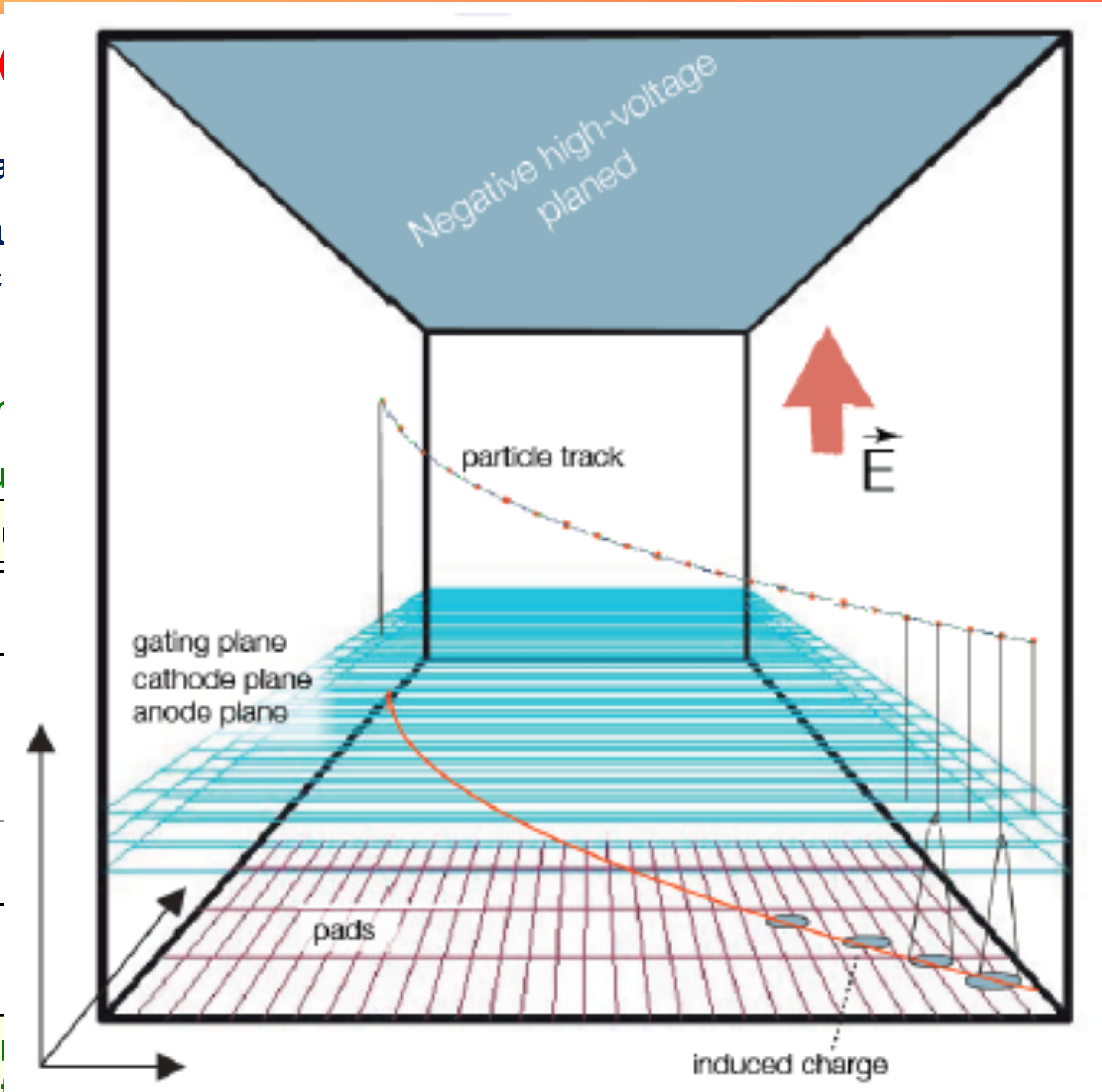

W. Riegler/CERN

O.Ullaland CERN 2005

TPC DELPHI

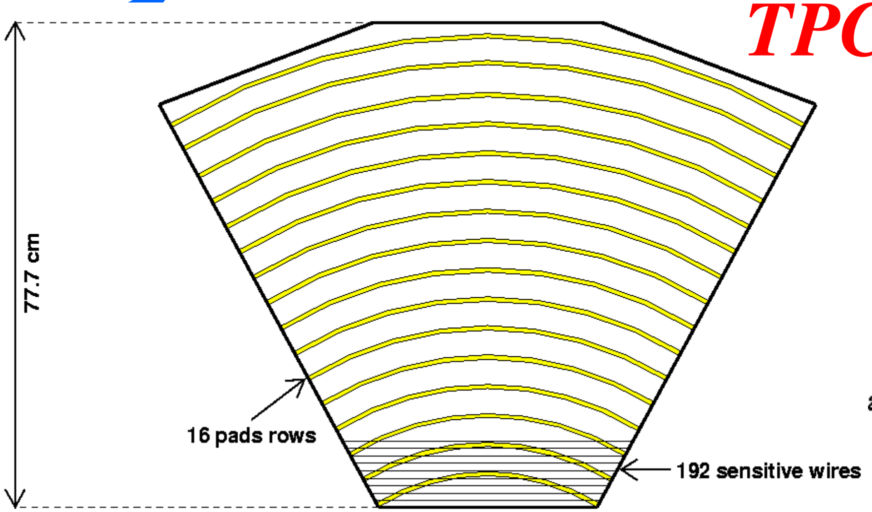
77.7 cm
16 pads rows
192 sensitive wires


ALEPH

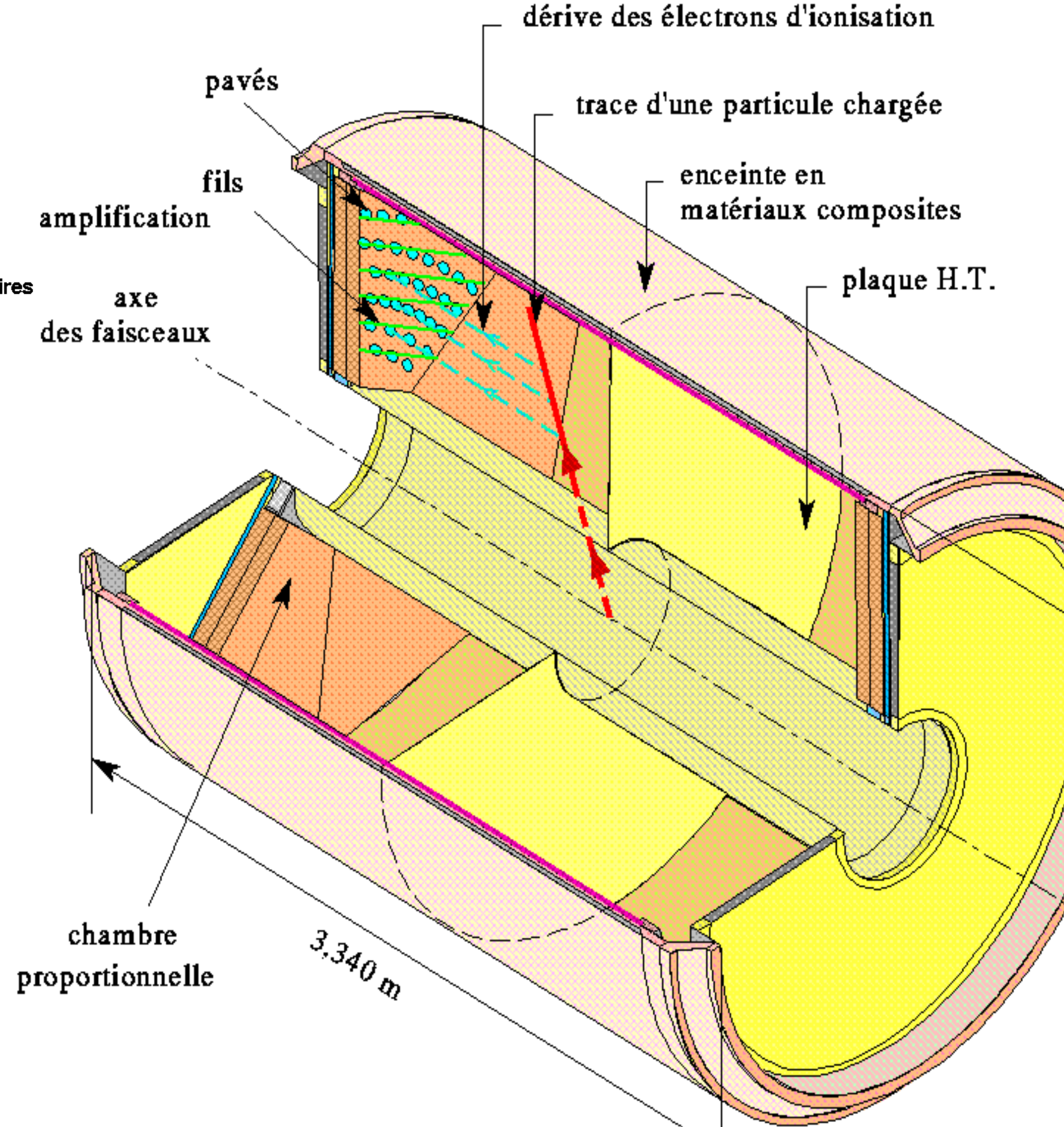
dérive des électrons d'ionisation
pavés
trace d'une particule chargée
fils
amplification
enceinte en
matériaux composites
axe
des faisceaux
plaque H.T.
chambre
proportionnelle
3,340 m

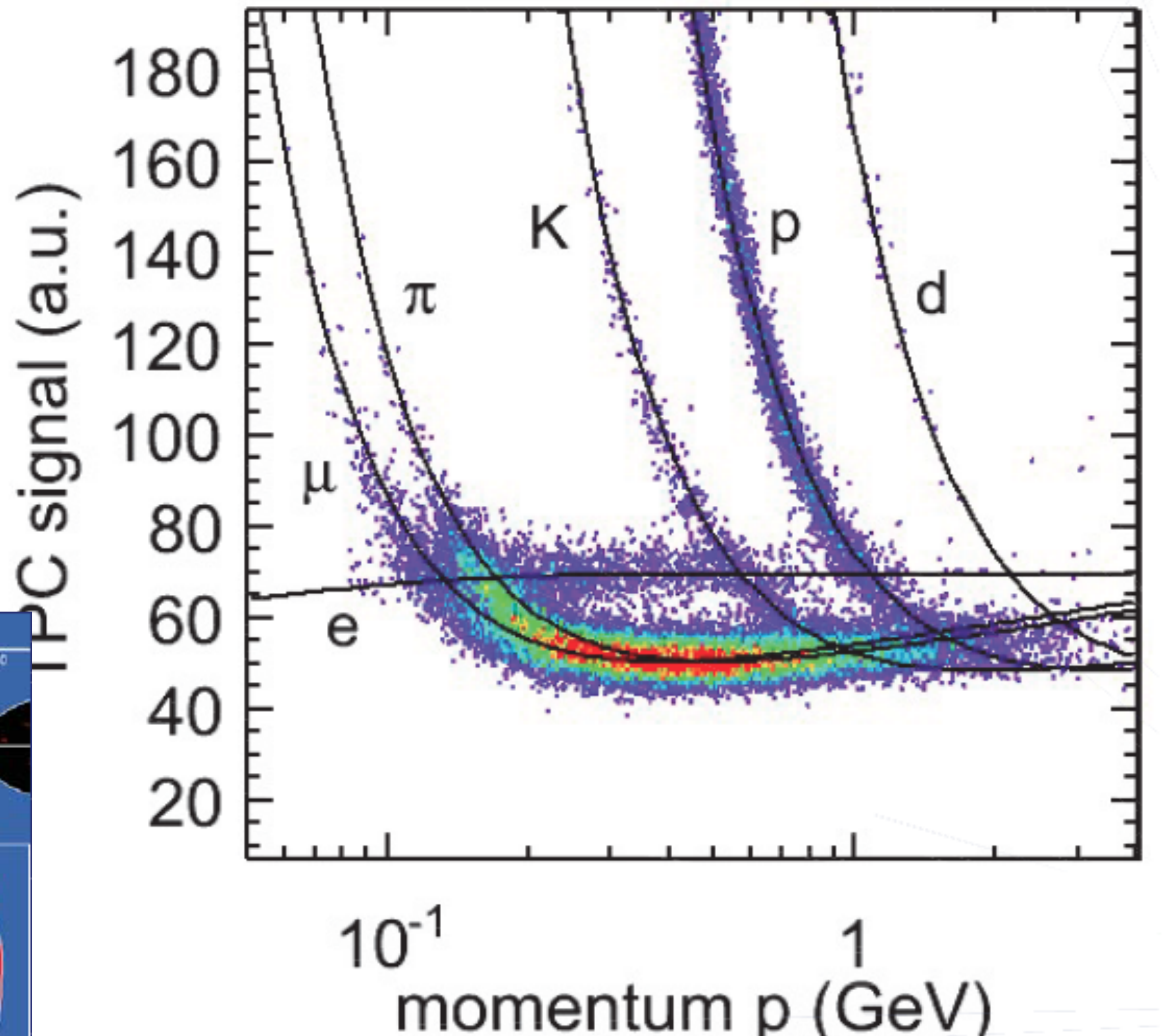
TPC signal (a.u.)
180
160
140
120
100
80
60
40
20
μ
π
K
p
d
e
10^{-1}
1
momentum p (GeV)

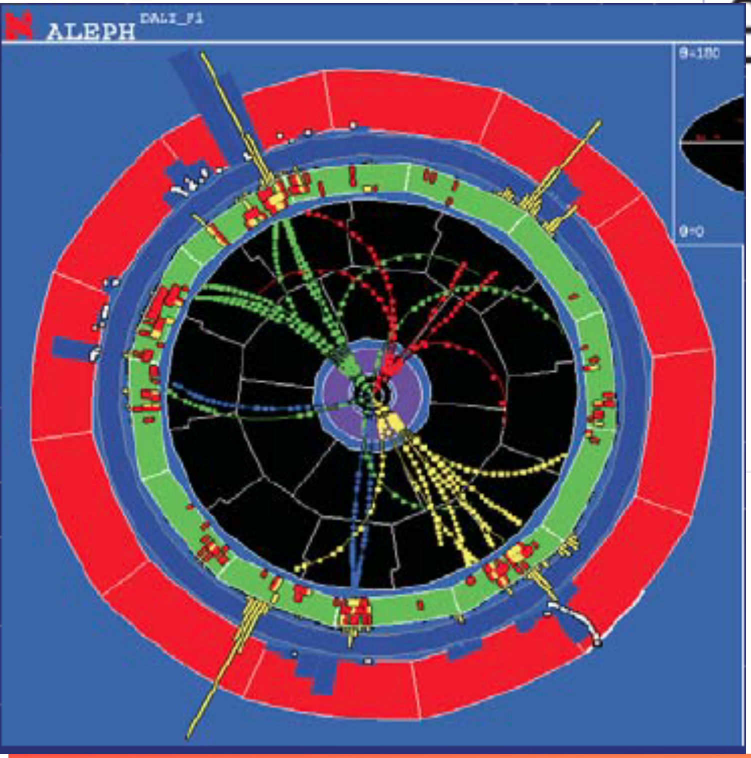
ALEPH

ALICE TPC: Detector Parameters

Largest TPC:

- Length 5m
- Diameter 5m
- Volume 88m3
- Detector area 32m2
- Channels ~570 000

- Gas Ne/ CO_2 90/10%
- Field 400V/cm
- Gas gain >10^4
- Position resolution σ= 0.25mm
- Diffusion: σ_t= 250μm
- Pads inside: 4x7.5mm
- Pads outside: 6x15mm
- B-field: 0.5T

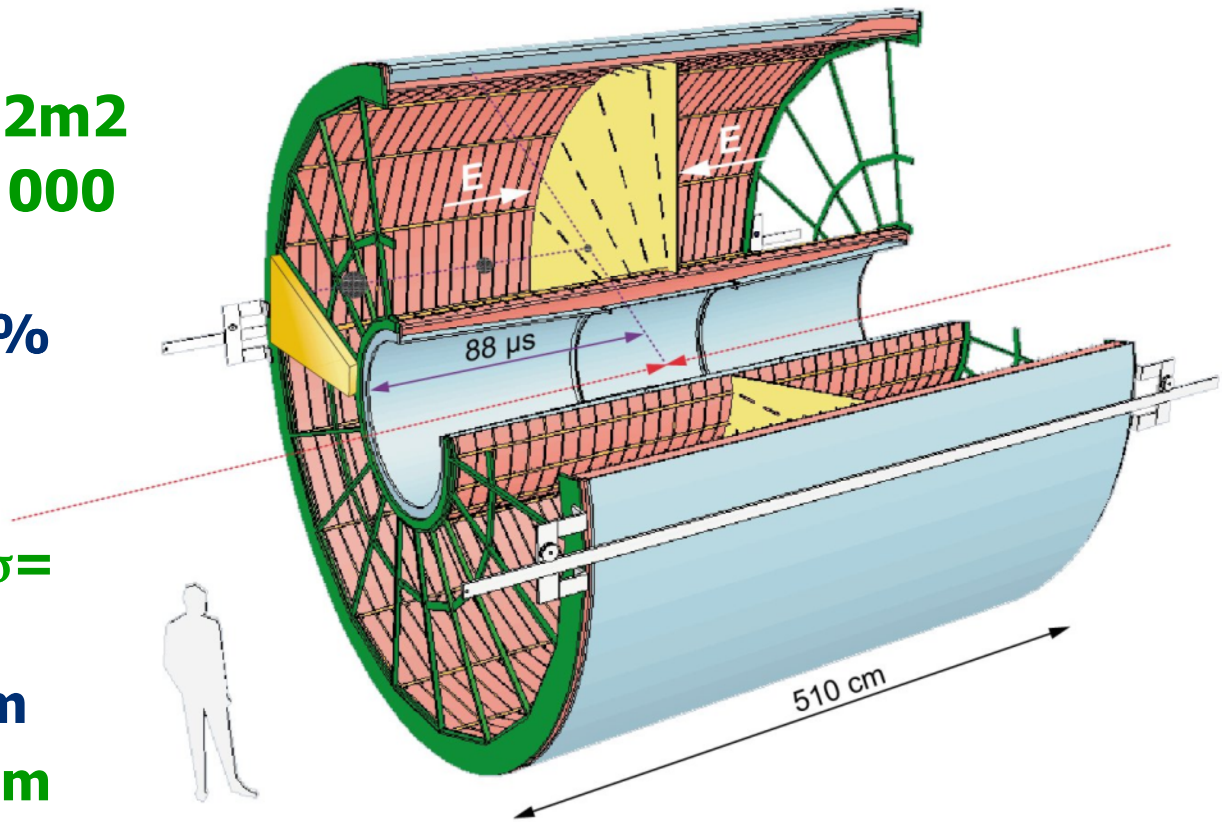

Ulrich.Goerlach@iphc.cnrs.fr, ASP Particle detectors 2012

TPC installed in the ALICE Experiment

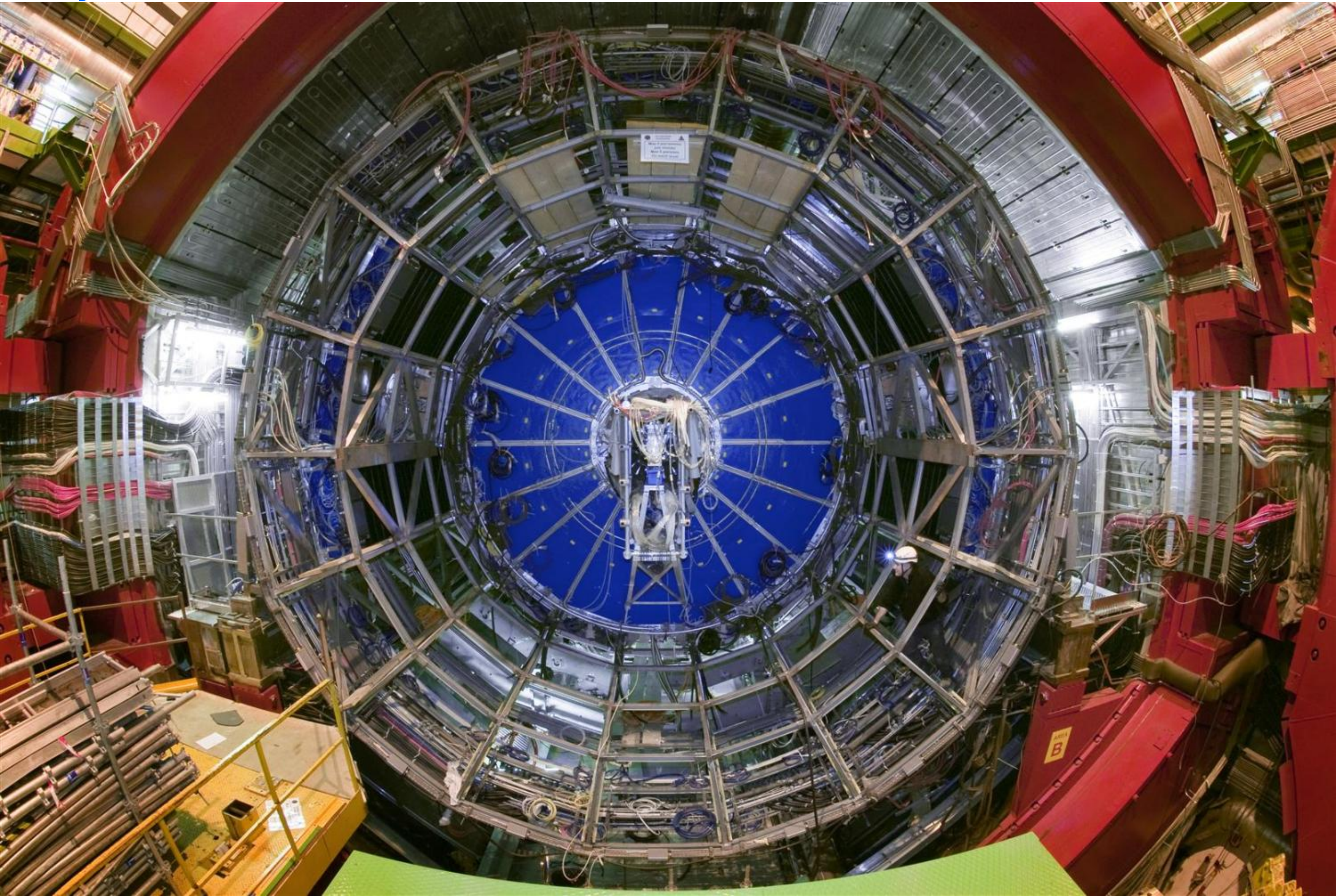

UNIVERSITÉ DE STRASBOURG

First Pb Pb Collisions in the ALICE TPC in Nov 2010 !

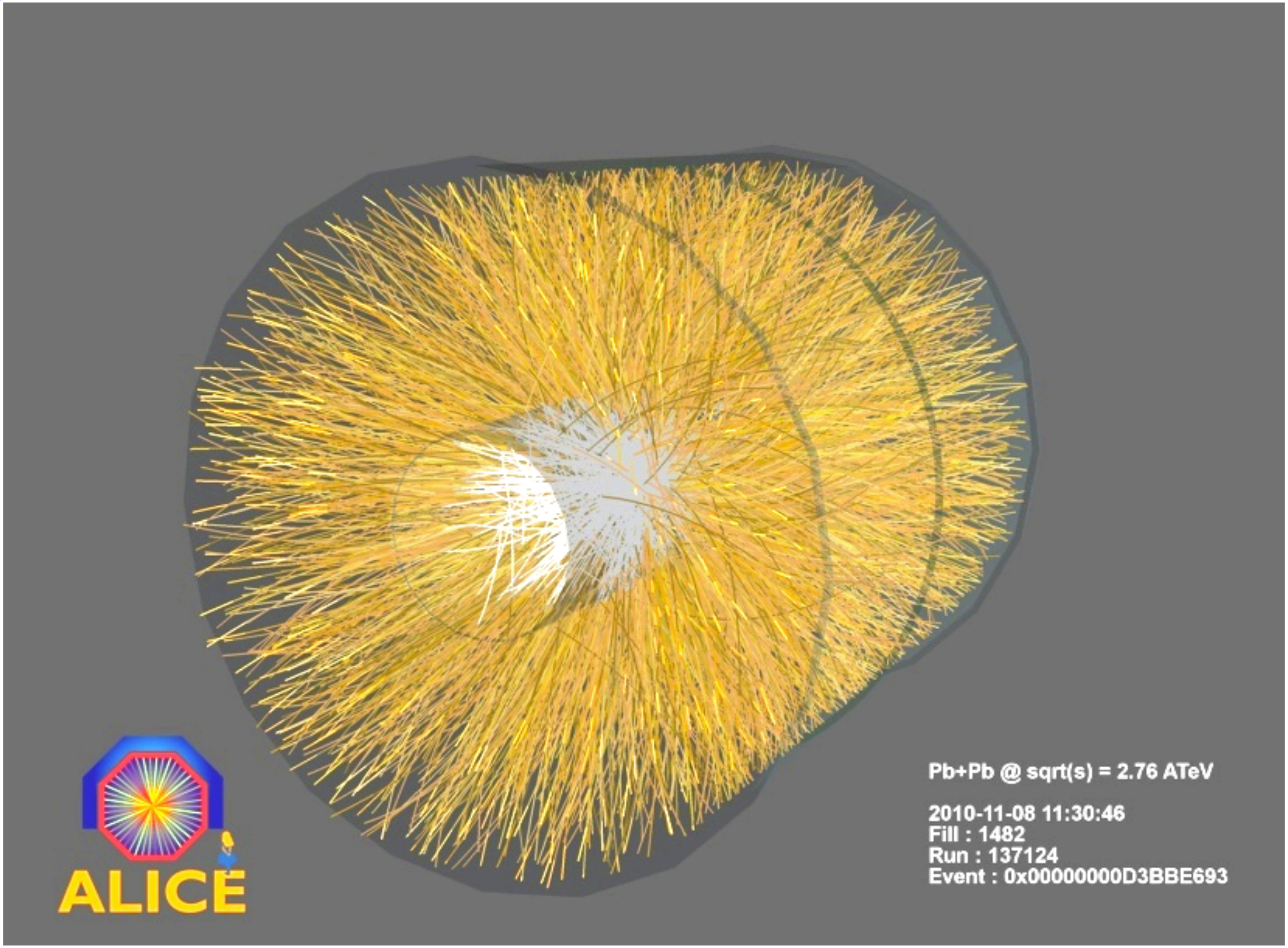

23/07/12

Scintillators

Scintillators

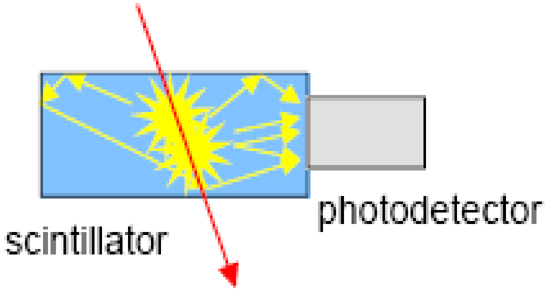

- Organic scintillators (molecules)
- Inorganic scintillators (crystals)
- Gas scintillators (atoms)

A good scintillator :

1. Number of produced photons should be high
2. And should be proportional to the deposited energy.
3. Transparent.
4. Short signals.
5. Good optical properties.
6. Refraction close to 1.5 .

Scintillators

Fluorescence : < 10 ns
Phosphorescence >> 10 ns

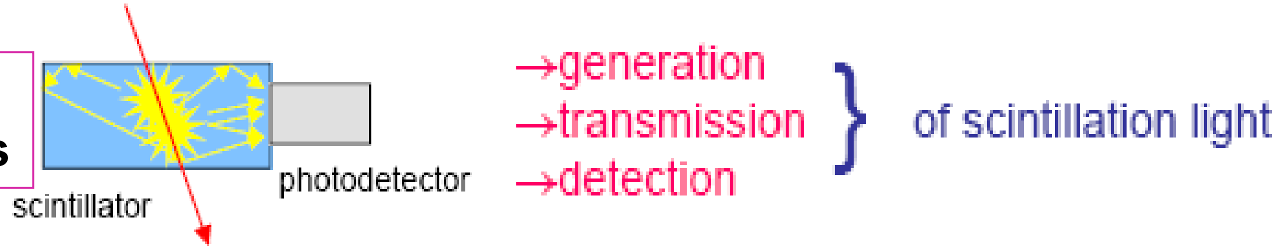

- **Inorganic Scintillators Crystal structure**
  - → 40 000 *hν*/MeV
  - High Z material,
  - High density
  - Time constants of ns - µs
  - High price!
  - ~ radiation hard

  Used for
  - Gamma detection
  - Medical imaging
  - Electromagnetic calorimeters

- **Organic scintillator plastic or liquid**
  - → 10 000 *hν*/MeV
  - low *Z*,
  - Low density ≈ 1g/cm³
  - Large choice of emission spectra
  - Time constants of typically ns
  - "low" price
  - Sensitive to radiation

  Used for
  - Charged particle detection
  - TOF, Veto counters, calorimeters

Scintillator crystal

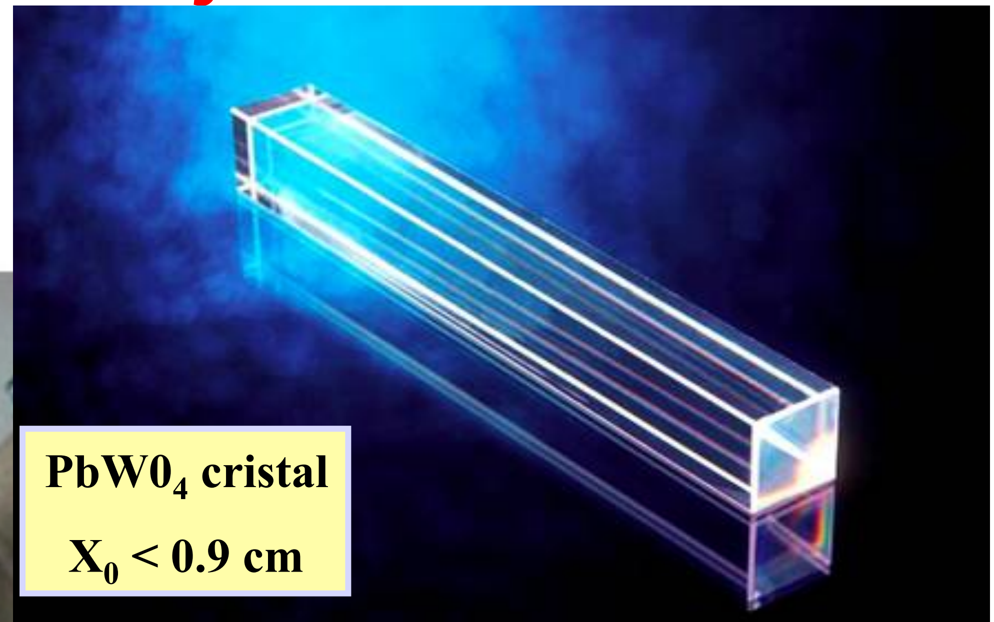

CMS

UNIVERSITÉ DE STRASBOURG

Scintillator - crystals

Three steps!

1. Absorption ⇒excitons/ionisation
2. Transfer to activator
3. Fluorescence of the activator

Excitons:

Pairs (e-,trou) (⇒ band below conduction band), but mobile within the crystal, will hit the activator atoms :

Transfer of energy

→ Excitation of activator atom

→ Radiative transition: lumière

→ Non-radiative transitions: vibrations (phonons) of the whole crystal, (energy loss)

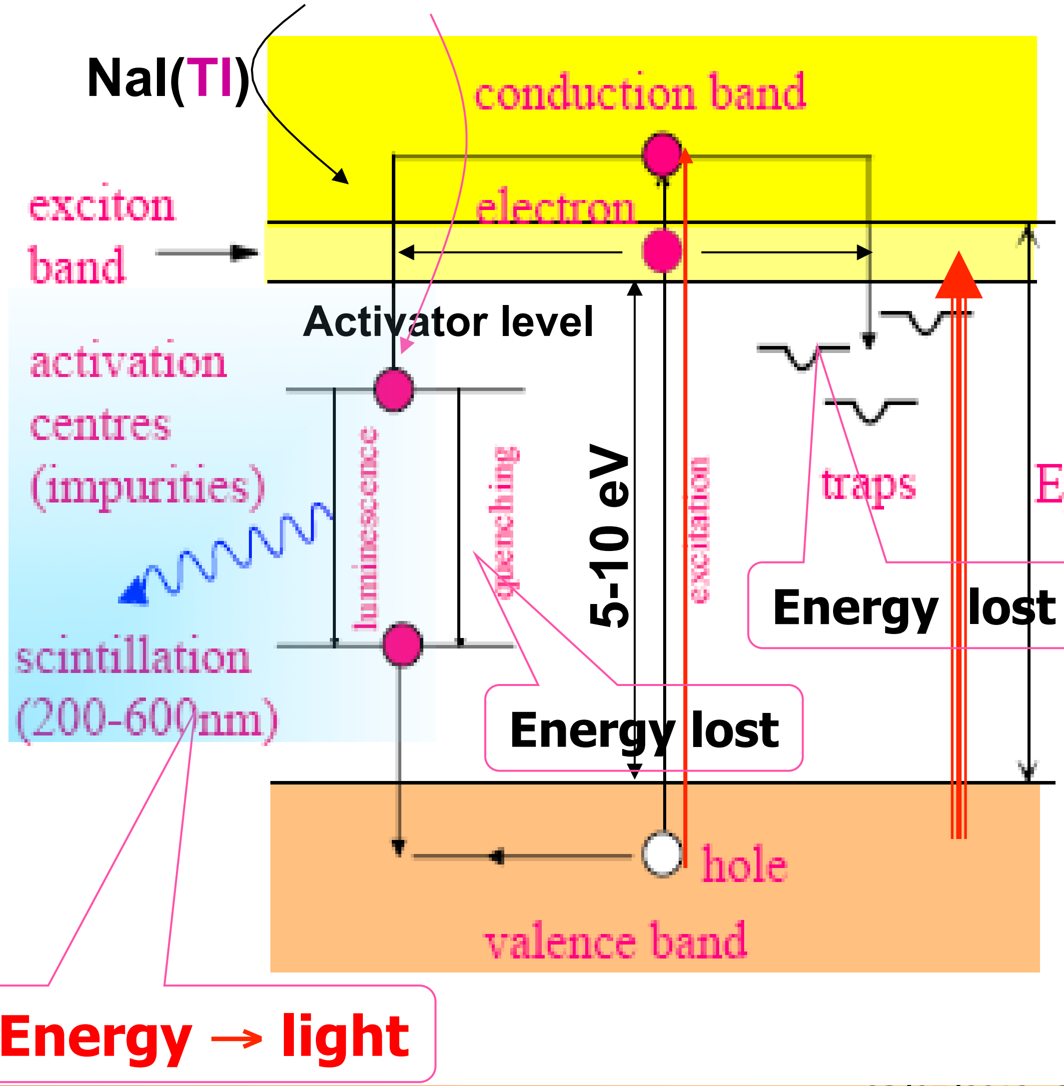

Light emission of energy $E = h\nu$

$$E = h\nu < E_{gap};\ \tau_d = 0.02 - 1\ \mu s$$

$$\frac{dN(t)}{dt} = \frac{N_0}{\tau_d} \exp\left(-t/\tau_d\right)$$

$$\lambda_{max} \approx 410 - 600\ \text{nm}$$

Ulrich.Goerlach@iphc.cnrs.fr, ASP Particle detectors 2012

Properties of inorganic scintillators

Properties of Common Inorganic Scintillators

Material	Specific Gravity	Wavelength of Maximum Emission (nm) λ_{max}	Index of Refraction at λ_{max}	Principal Decay Constant (μs)	Pulse 10–90% Rise Time (μs)	Total Light Yield in Photons/MeV	Absolute Scintillation Efficiency for Fast Electrons	Relative γ-Ray Pulse Height with Bialkali PM Tube
NaI(Tl)	3.67	415	1.85	0.23	0.5	38000	11.3%	1.00
CsI(Tl)	4.51	540	1.80	1.0	4	52000	11.9	0.49
CsI(Na)	4.51	420	1.84	0.63	4	39000	11.4	1.11
LiI(Eu)	4.08	470	1.96	1.4	—	11000	2.8	0.23
BGO	7.13	505	2.15	0.30	0.8	8200	2.1	0.13
BaF_2 slow component	4.89	310	1.49	0.62	3	10000	4.5	0.13
BaF_2 fast component	4.89	220	—	0.0006	—	—	—	0.03[a]
ZnS(Ag) (polycrystalline)	4.09	450	2.36	0.2	—	—	—	1.30[b]
CaF_2(Eu)	3.19	435	1.44	0.9	4	24000	6.7	0.78
CsF	4.11	390	1.48	0.004	—	—	—	0.05
Li glass[c]	2.5	395	1.55	0.075	—	—	1.5	0.10
For comparison, a typical organic (plastic) scintillator:								
NE 102A	1.03	423	1.58	0.002		10000	3.0	0.25

[a] Using UV-sensitive PM tube.
[b] For alpha particles.
[c] Properties vary with exact formulation. Also see Table 15-1.

Source: Data derived primarily from Refs. 56–58.

Scintillator composition	Density (g/cm^3)	Index of refraction	Wavelength of max.Em. (nm)	Decay time Constant (µs)	Scinti Pulse height[1)]	Notes
NaI(Tl)	3.67	1.9	410	0.25	100	2)
CsI	4.51	1.8	310	0.01	6	3)
CsI(Tl)	4.51	1.8	565	1.0	45	3)
$CaF_2(Eu)$	3.19	1.4	435	0.9	50	
BaF_2	4.88	1.5	190/220 310	0,0006 0.63	5 15	
BGO	7.13	2.2	480	0.30	10	
$CdW0_4$	7.90	2.3	540	5.0	40	
$PbWO_4$	8.28	2.1	440	0.020	0.1	
CeF_3	6.16	1.7	300 340	0.005 0.020	5	
GSO	6.71	1.9	430	0.060	40	
LSO	7	1.8	420	0.040	75	
YAP	5.50	1.9	370	0.030	70	

1) Relative to NaI(Tl) in %; 2) Hygroscopic; 3) Water soluble

Emission spectra of inorganic scintillators

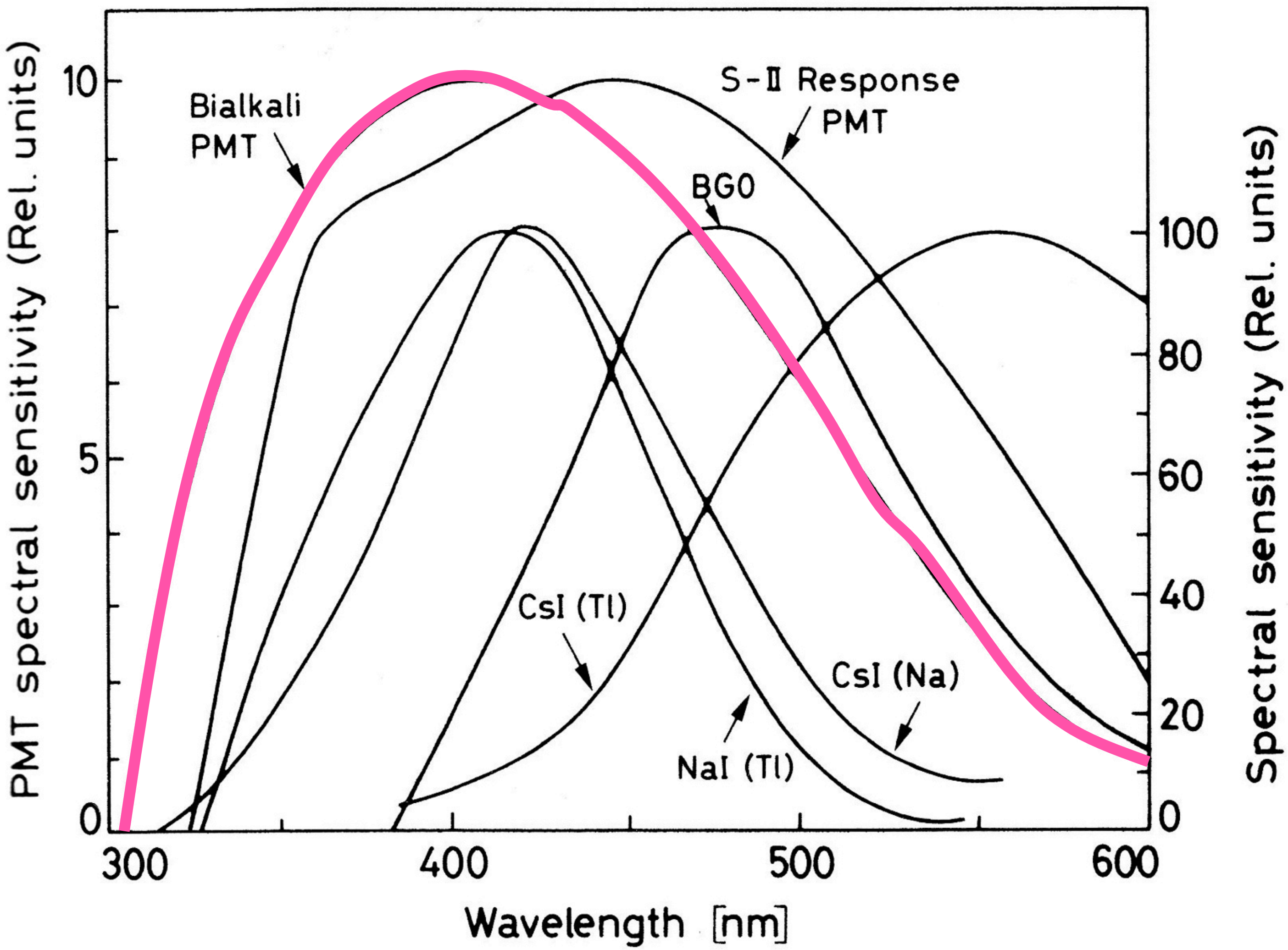

Efficiency of a detector

- **Absolute or total efficiency**

$$\varepsilon_{tot} = \frac{\text{(particles or gammas) registered}}{\text{(particles or gammas) emmitted}}$$

  – This depends on the geometry between the source and the detector

$$\boxed{\varepsilon_{tot} \cong \varepsilon_{\text{int}} \times \varepsilon_{geom}}$$

$$\varepsilon_{tot} = \underbrace{\left[1 - \exp\left(\frac{-S_p}{\lambda}\right)\right]}_{\text{probability of an interaction}} \cdot \underbrace{\frac{\Delta\Omega}{4\pi}}_{\text{probability of an emission in direction } \theta}$$

$$\lambda = \text{attenuation length}; \left\{\frac{1}{\lambda} = \sigma \cdot n_b\right\}; \; S_p = \text{Depth of the detector}$$

- **Intrinsic efficiency**

$$\varepsilon_{\text{int}} = \frac{\text{(particles or gammas) "registered"}}{\text{(particles or gammas) in the acceptance of the detector}}$$

NaI (Tl)

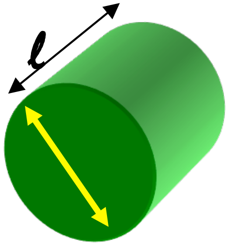

- Reference/standard of efficiency: $\varepsilon = 1{,}22 \times 10^{-3}$
  - Cylindrical detector NaI(Tl), 7,62(∅) x 7,62(ℓ) cm^3
  - Source of ^{60}Co (1,33 MeV) at 25 cm

Exercise : verify the efficiency!

Properties of NaI:

- Z = 53 high ⇒ good efficiency
- Relatively short decay time (230 ns)
- intense signal
- Relative good energy resolution
- But NaI is very hygroscopic!!

$\mu = 0.6\ cm^{-1}$

$\mu = 0.18\ cm^{-1}$

$\mu = 0.007\ cm^{-1}$

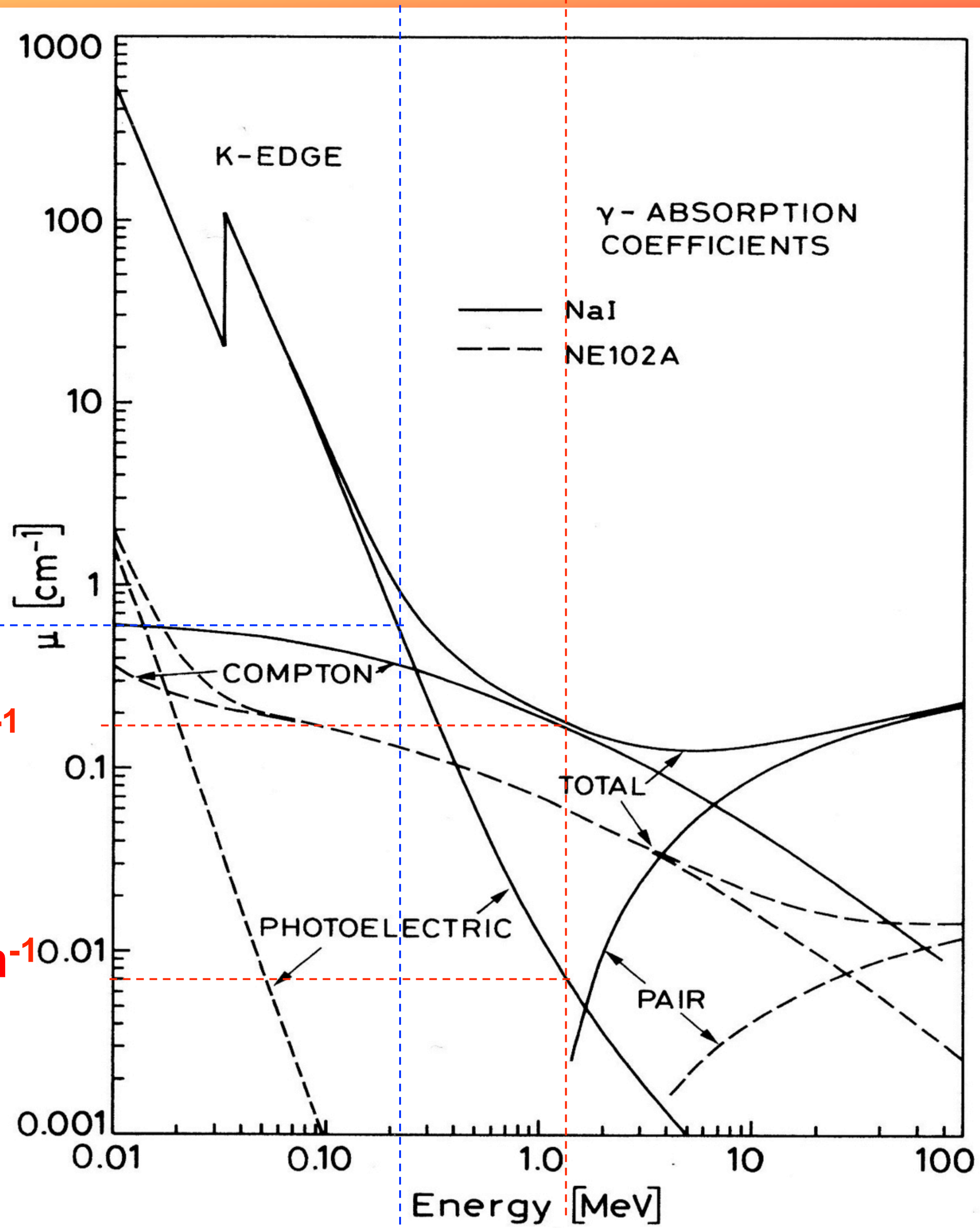

Respone of NaI

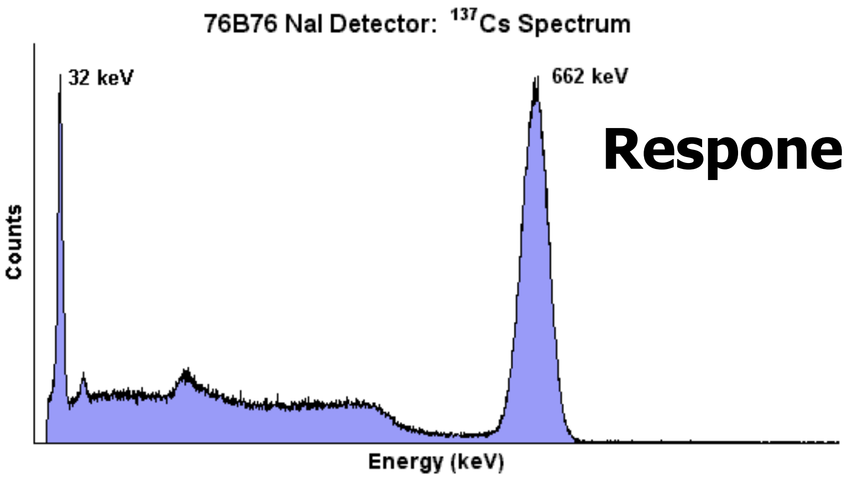

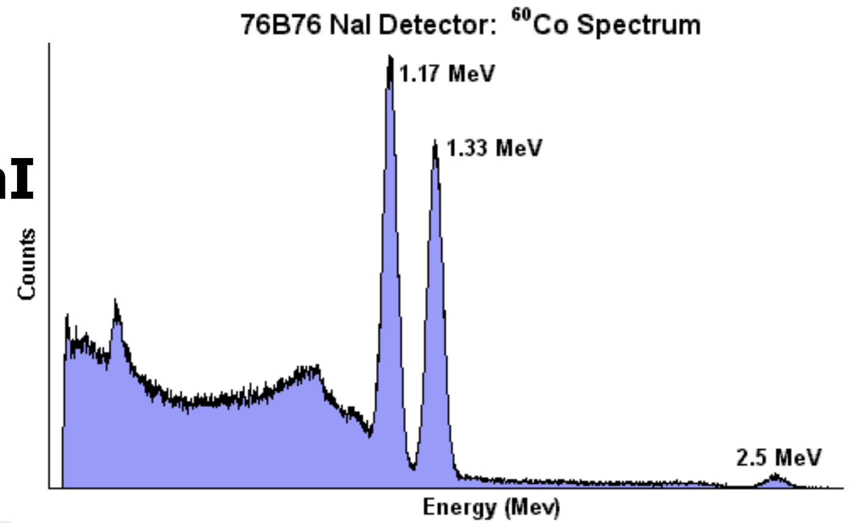

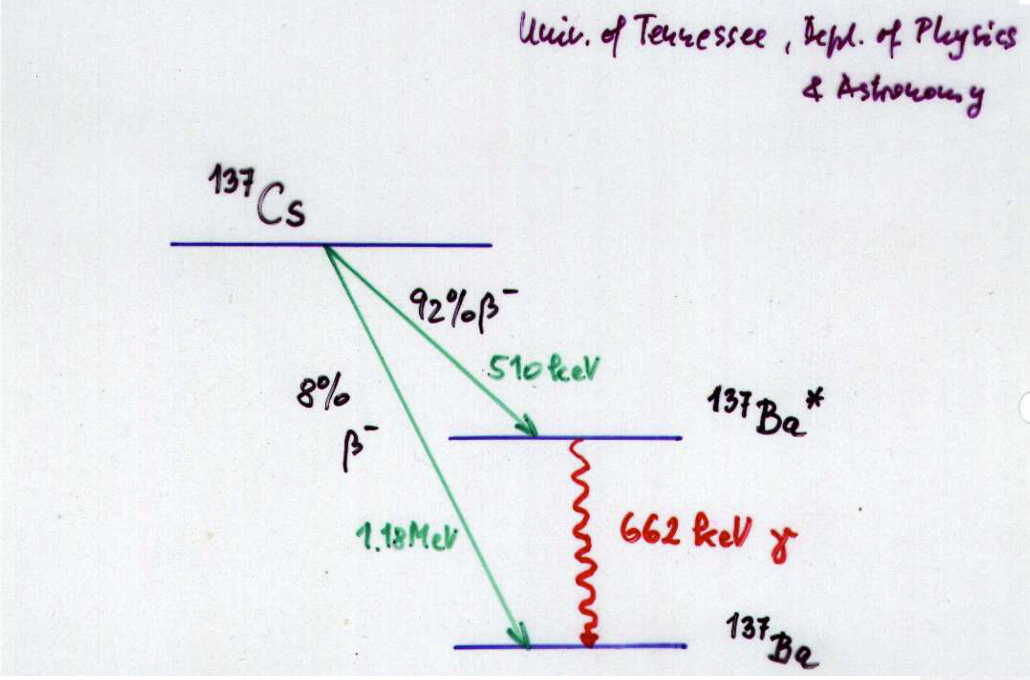

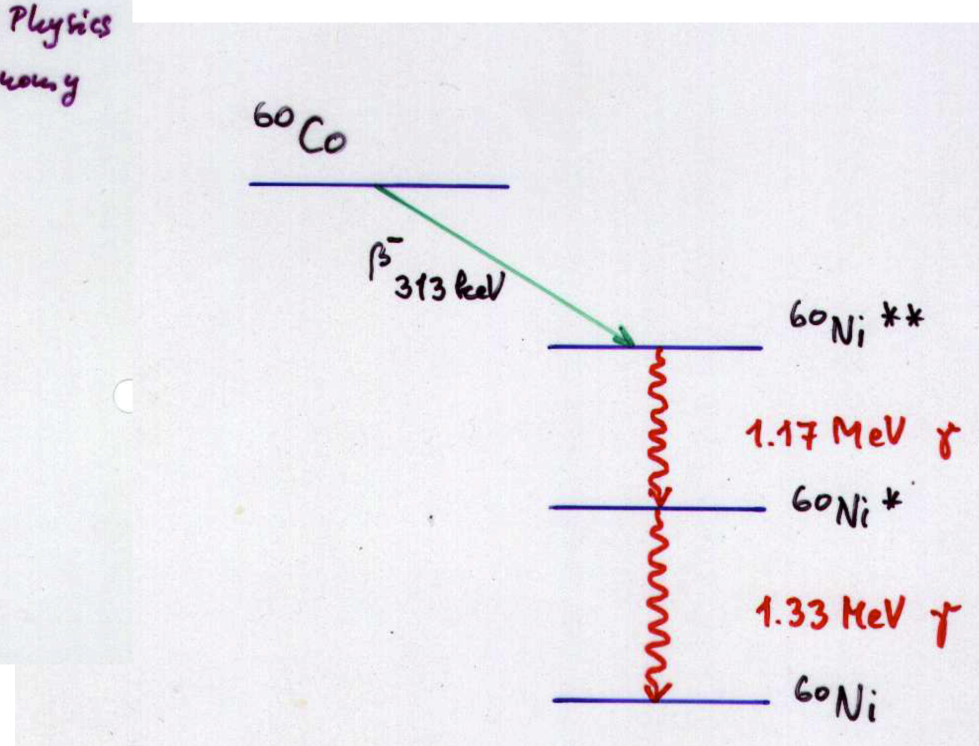

K. Grupen, Univ Siegen

Energy Resolution

Detector response :

- **For a fixed energy the detector will respond each time slightly different**
- **All measurements will be distributed around a mean value with a certain width**
- **This distribution can be approximated by a Gaussian with**
  - **Mean μ and**
  - **A width FWHM**
- **The resolution *R* is defined by**

$$R := \frac{\text{FWHM}}{\mu} = 2.35\frac{\sigma}{\mu}$$

μ, σ^2 = mean and variance of the distribution

- **Two energies closer than FWHM cannot be resolved anymore**

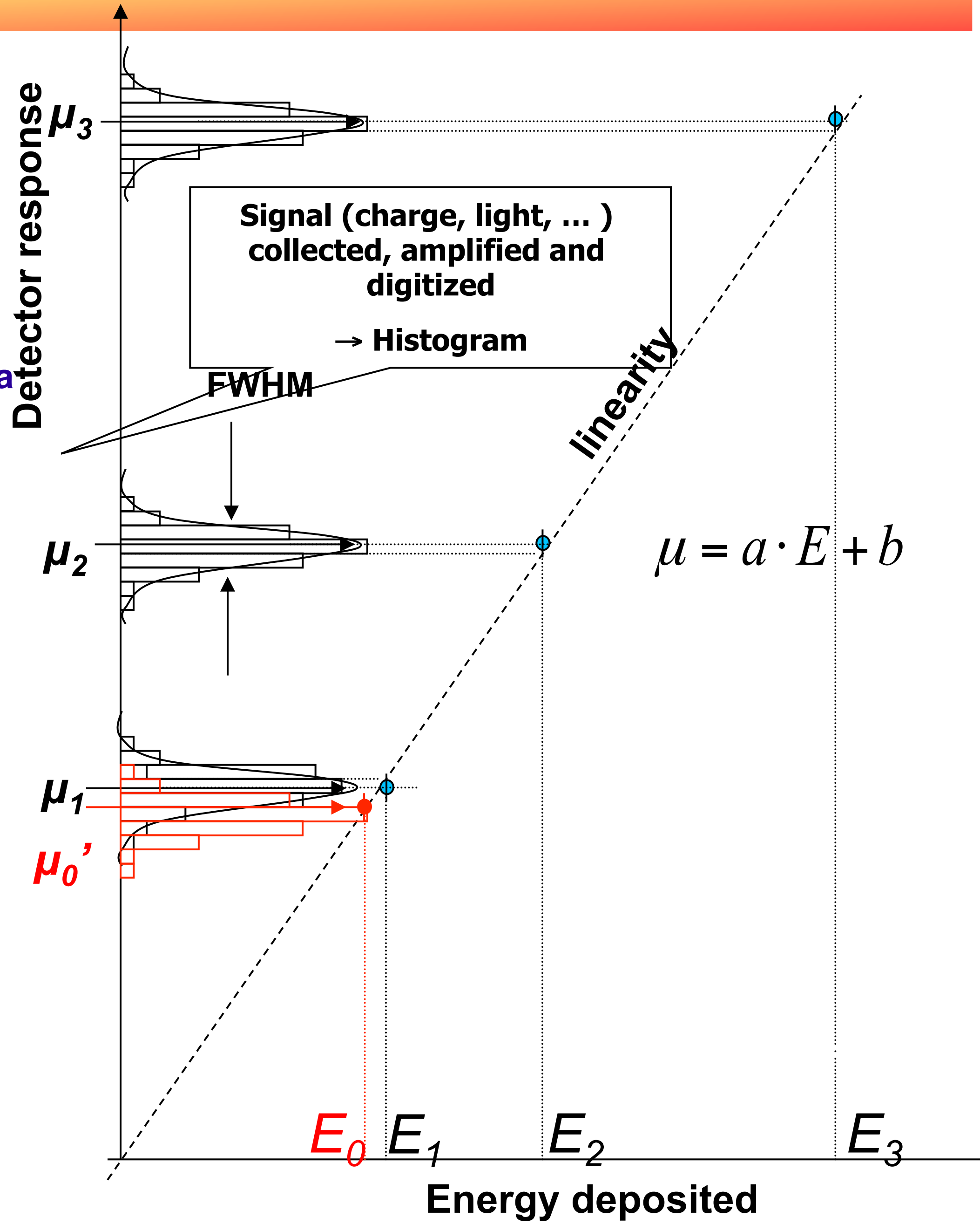

Energy Resolution

$$R := \frac{\text{FWHM}}{\mu} = 2.35\frac{\sigma}{\mu} = 2.35\frac{\sigma_N}{\mu_N} = 2.35\sqrt{\frac{w}{E}}$$

μ, σ^2 = mean, variance of peak in histogram

$\mu = \alpha \cdot \mu_N;$

$\sigma = \alpha \cdot \sigma_N;$ *with*

α = calibration factor (electronic gain etc)

$\mu_N = E / w;$ avec

w = mean energy to create one "charge or photon"

$\mu_N,\ \sigma_N^2$ = Mean number of measured quantities (charges or photons created)

Poissons law: $\sigma_N^2 = \mu_N;$

$$\Rightarrow \sigma_N / \mu_N = 1/\sqrt{\mu_N} = \sqrt{w/E}$$

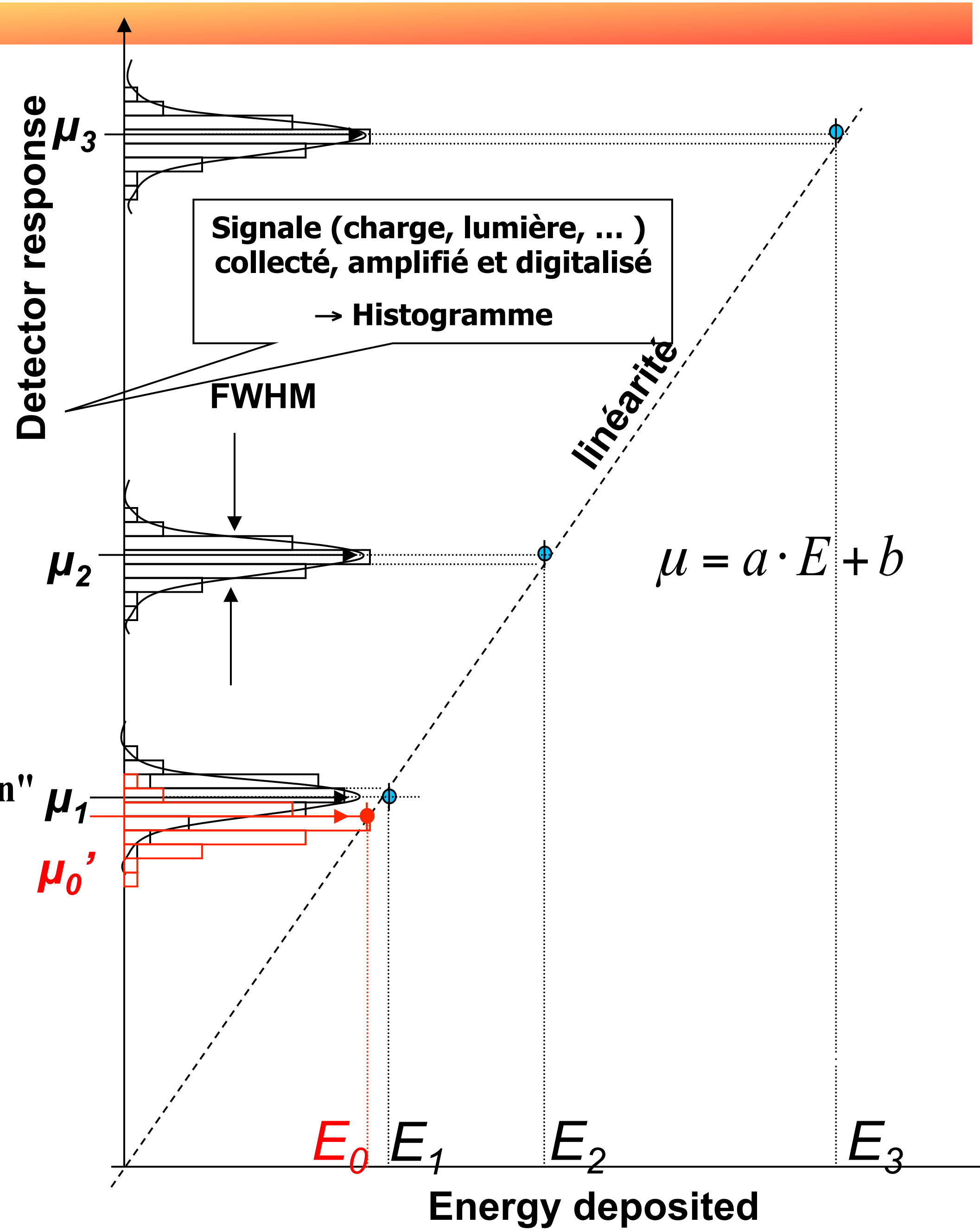

Gaussien or normal distribution

±1σ = 68.3% confidence level

±2σ = 95.5%

±3σ = 99.7%

$$P(x) = \frac{1}{\sigma\sqrt{2\pi}} \exp\left(-\frac{(x-\mu)^2}{2\sigma^2}\right);$$

μ = *mean*

σ^2 = variance;

FWHM = 2.35 σ

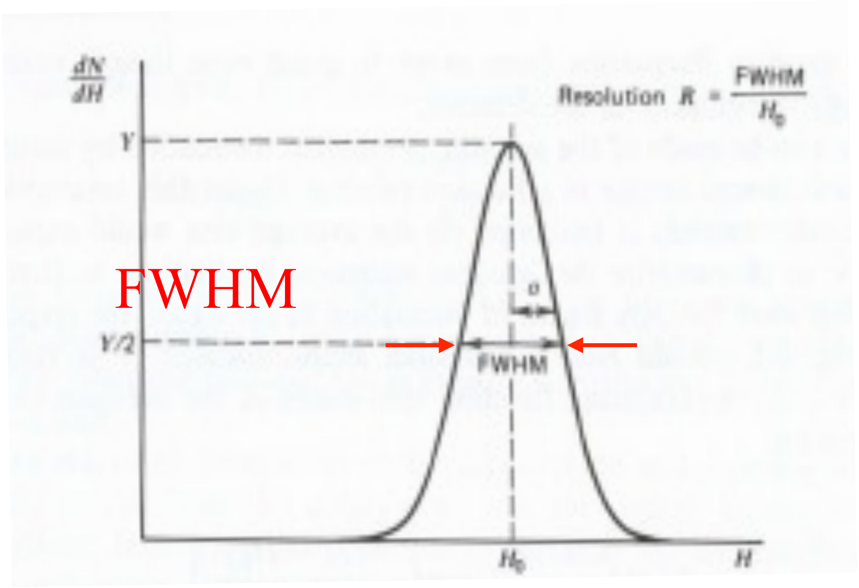

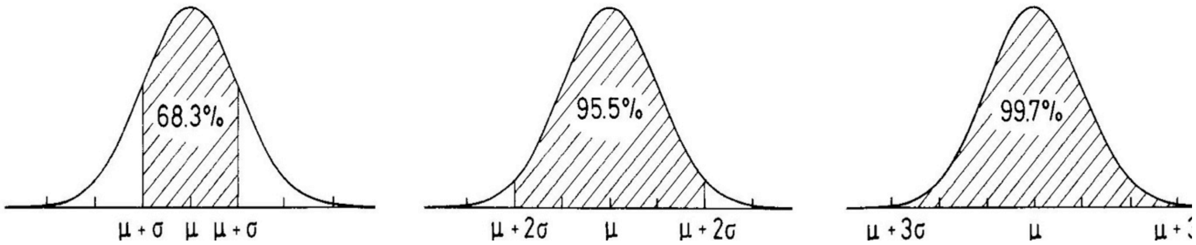

Resolution

$$R := \frac{FWHM}{\mu}$$

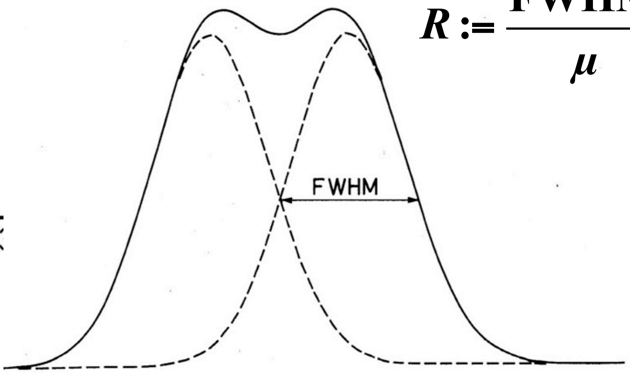

Impossible to separate two signals closer than FWHM

Ulrich.Goerlach@iphc.cnrs.fr, ASP Particle detectors 2012

Resolution

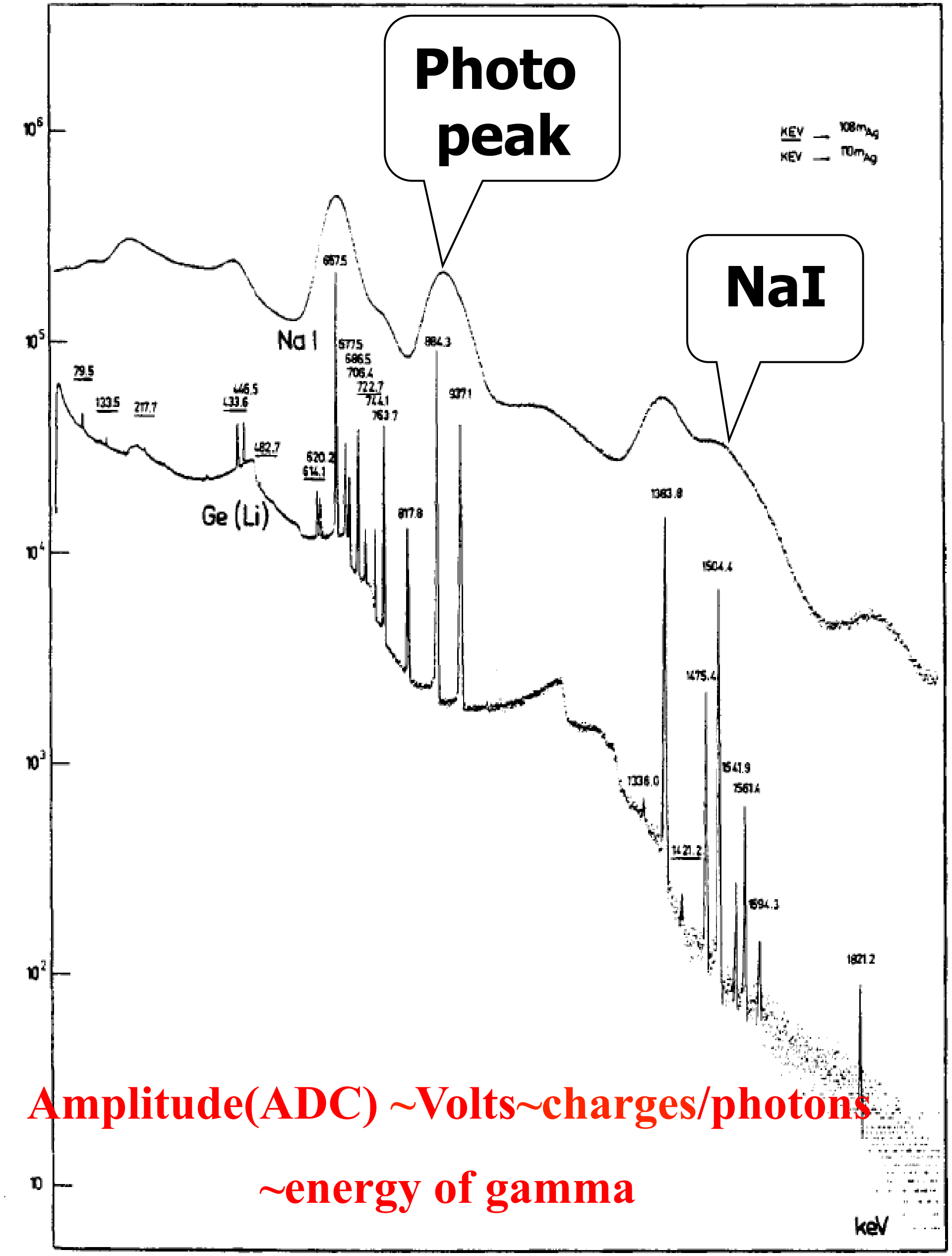

$$N_{h\nu} = \frac{E}{w};\ dN_{h\nu} = \sqrt{N_{h\nu}} = \sqrt{\frac{E}{w}}$$

Statistics strictly Poisson $\Rightarrow \sigma^2 = \mu;$

$$dE/E = dN_{h\nu}/N_{h\nu} \sim \frac{1}{\sqrt{N_{h\nu}}}$$

$NaI: w \approx 25\,eV / photon_{\text{scint}} \Rightarrow 40000\,h\nu / MeV$

Incomplete collection of scintillation photons and finite quantum efficiency will reduce the mean number of photo-electrons

$$N_{pe} = N_{h\nu} \times \varepsilon_{collection} \cdot \varepsilon_{quantic};$$

$$dN_{pe} = \sqrt{N_{pe}} = \sqrt{N_{h\nu} \times \varepsilon_{coll.} \cdot \varepsilon_{quant.}}$$

$$\varepsilon_{coll.} \approx 0.2 - 0.8;\ \varepsilon_{quant.} \approx 0.2\,(PM)$$

$$dE/E = dN_{pe}/N_{pe} \cong \frac{1}{\sqrt{N_{pe}}} = \frac{1}{\sqrt{N_{h\nu} \times \varepsilon_{coll.} \cdot \varepsilon_{quant.}}}$$

$$F \approx 1;\ \varepsilon_{coll.} \approx 0.4;\ \varepsilon_{quant.} \approx 0.2\,(PM)$$

$$\Rightarrow dE/E = \sigma_E/E \approx 1.5\%\ \text{à}\ 1.333\ MeV$$

$$R = 2.35 \times 1.5\% = 3.6\% \xrightarrow{\text{experimental}} (5-8)\%$$

Organic scintillators

- Liquids and plastics
- Solvent which absorbs the energy
- The excitation energy of the solvent is transferred to the dopant
- Emission, reabsorption and re-emission of light
- Shift towards longer wave lengths
- Fast response, about 5ns
- Liquids :
  - Solvents liquids: xylene, tolene,benzene,phenylcyclohexane,triethylbenzene,decaline
  - Dopants for liquids: p-Terphenyl ($C_{18}H_{14}$), PBD($C_{20}H_{14}N_2O$), PPO($C_{15}H_{11}NO$), POPOP ($C_{24}H_{16}N_2O_2$), ≈ 3g/l
- Solids:
  - Solvents plastics polyvinyltoluene, polyphenilbenzene, polystyrene.
  - Primary dopants for plastics : PBD, p-Terphenyl, PBO, 10g/l
  - Secondary dopant POPOP to shift the light to longer wavelengths.
- Quality depends largely on low level of impurities

Ulrich.Goerlach@iphc.cnrs.fr, ASP Particle detectors 2012

Organic Scintillators

fluorescence

Prompt emission.

- fluorescence (durée ∼ ns-μs)
- phosphorescence (durée ∼ μs-min)

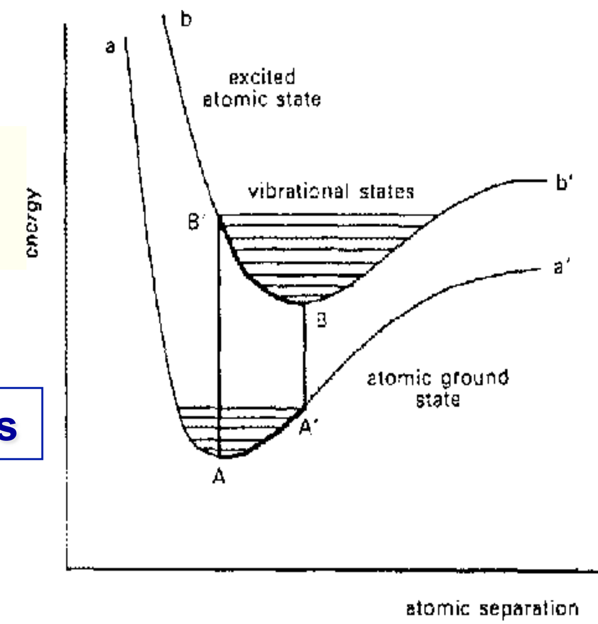

Valence electrons of the π-orbitals

Radiation less transitions

(Förster)

The energy absorbed by the solvent is transferred to the dopant without radiation

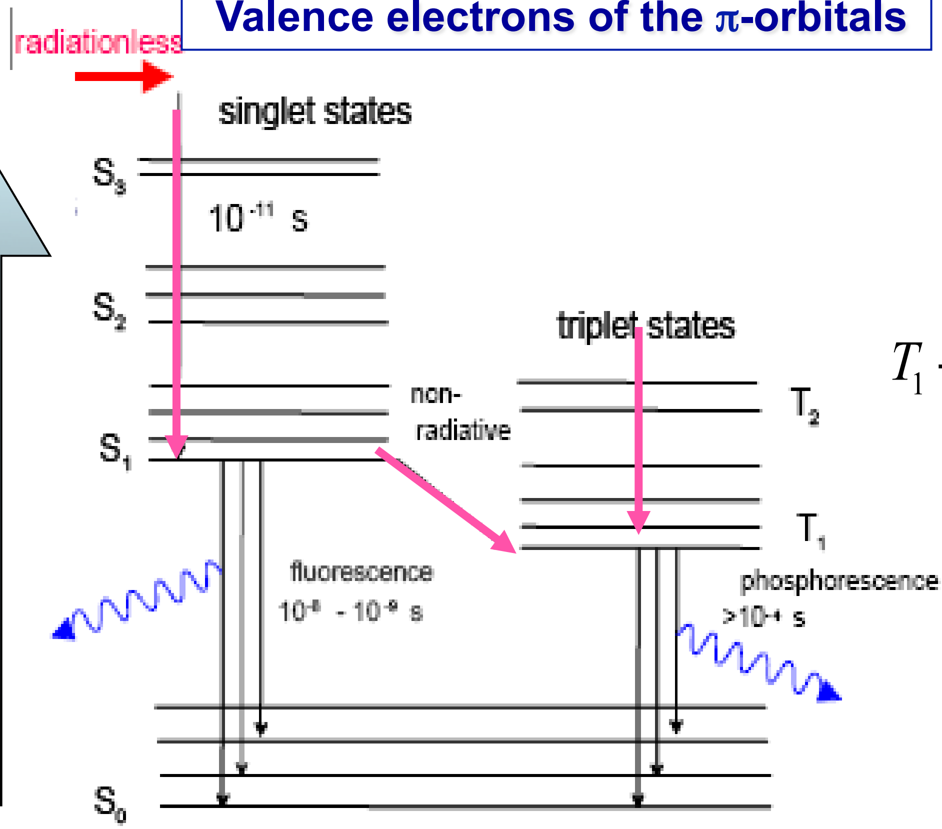

$$T_1 + T_1 \rightarrow S_0 + S_1 + phonons$$

Phosphorescence : Slow emission

Organic Scintillators

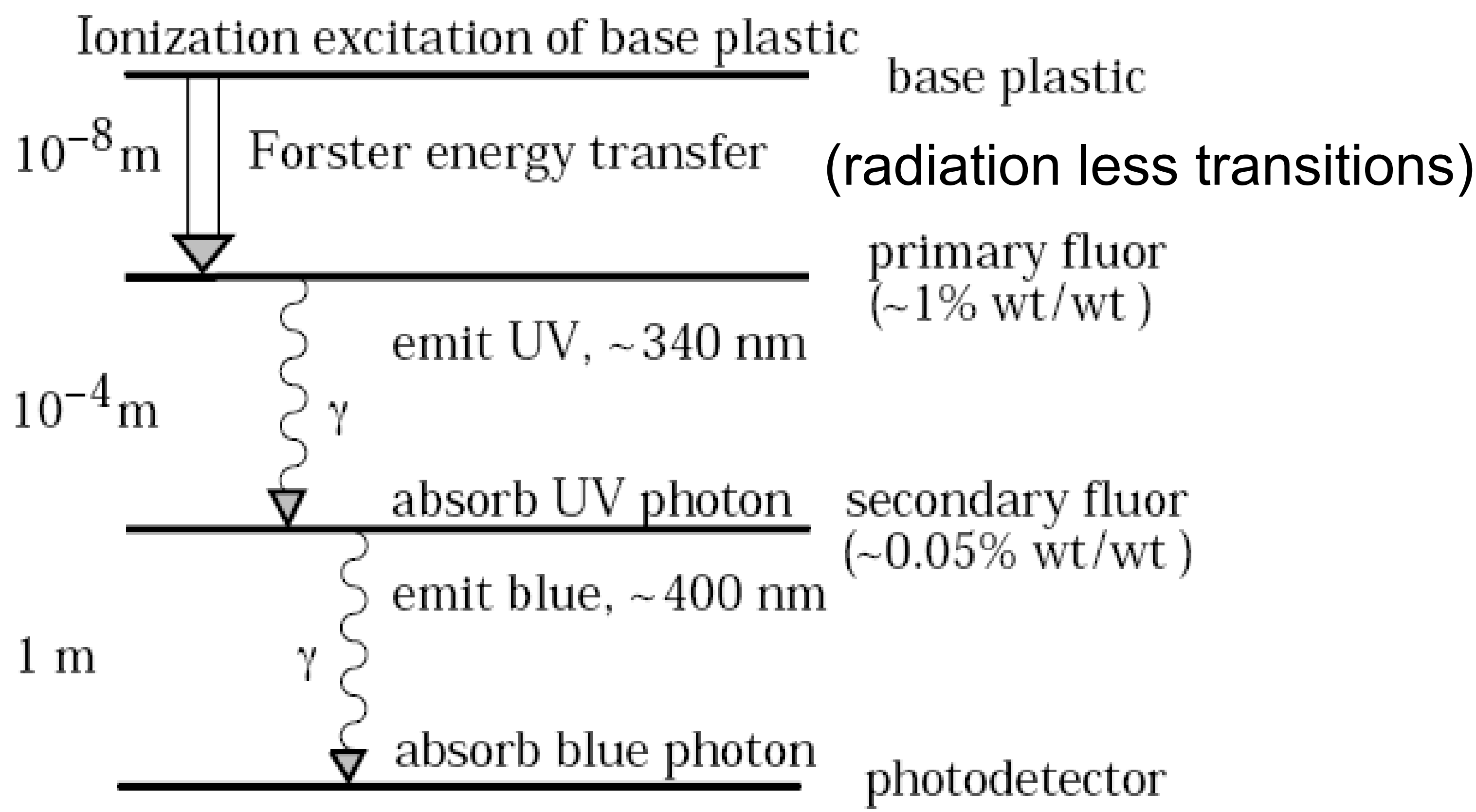

Figure 28.1: Cartoon of scintillation "ladder" depicting the operating mechanism of plastic scintillator. Approximate fluor concentrations and energy transfer distances for the separate sub-processes are shown.

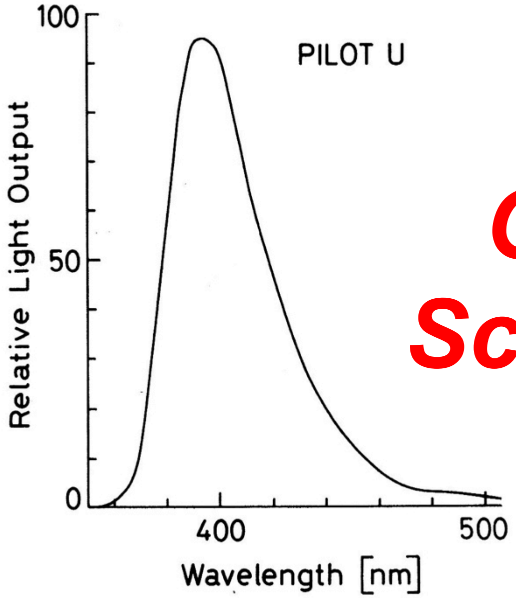

Organic Scintillators

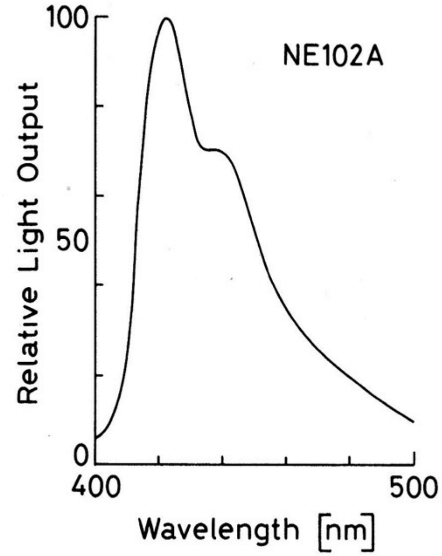

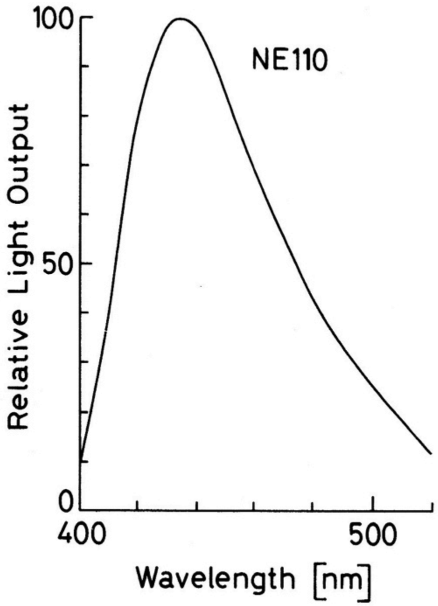

emission spectra

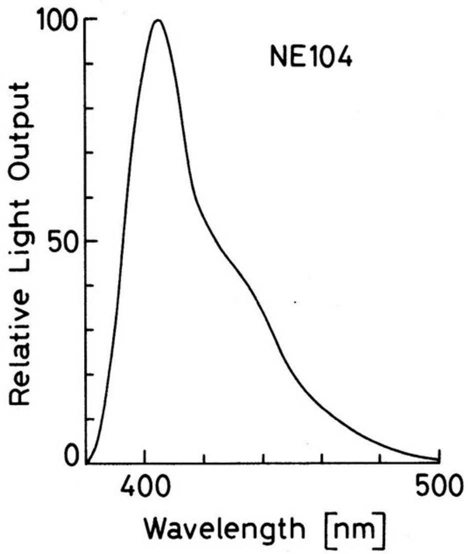

Absorption and emission

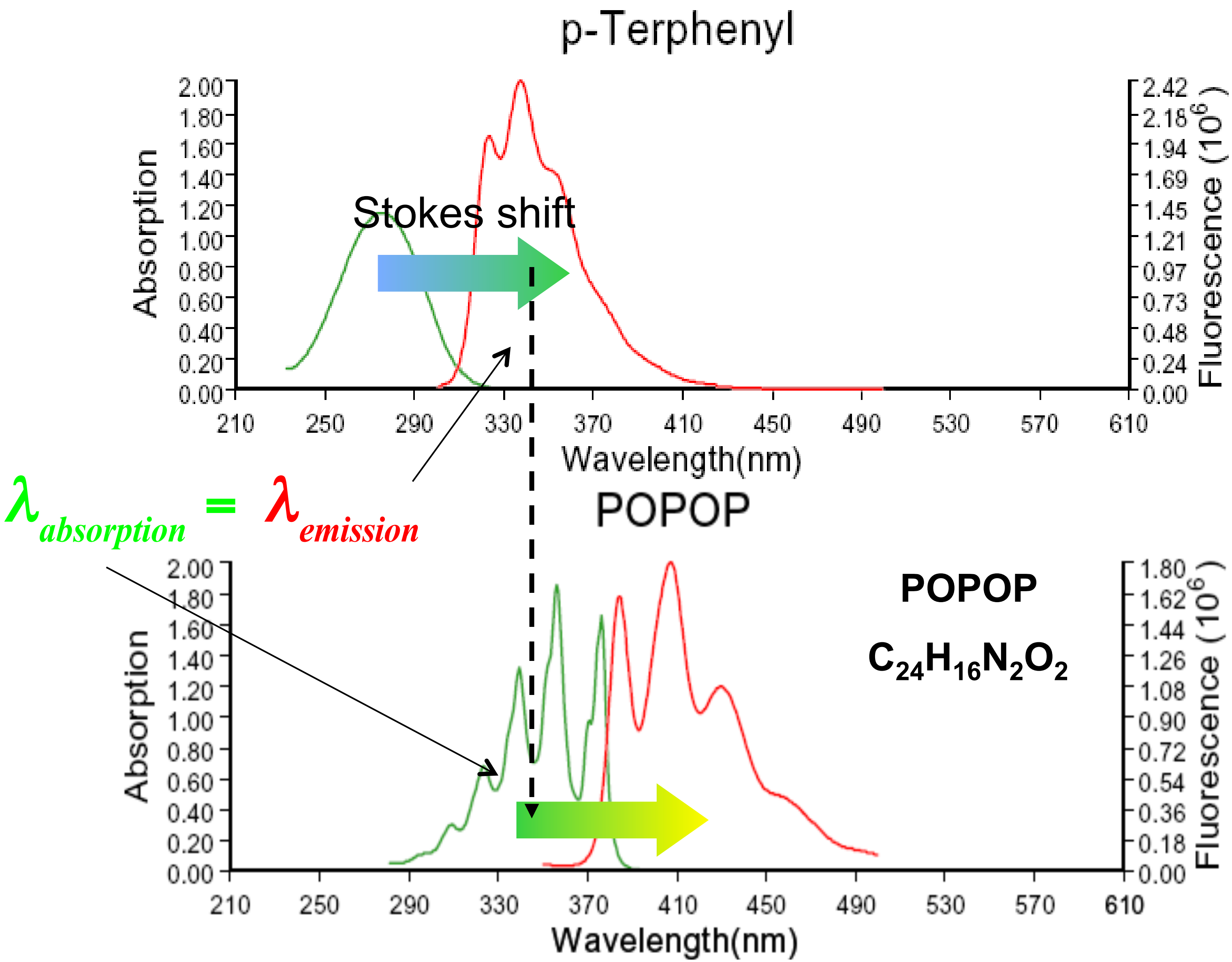

Abs. and emission spectra

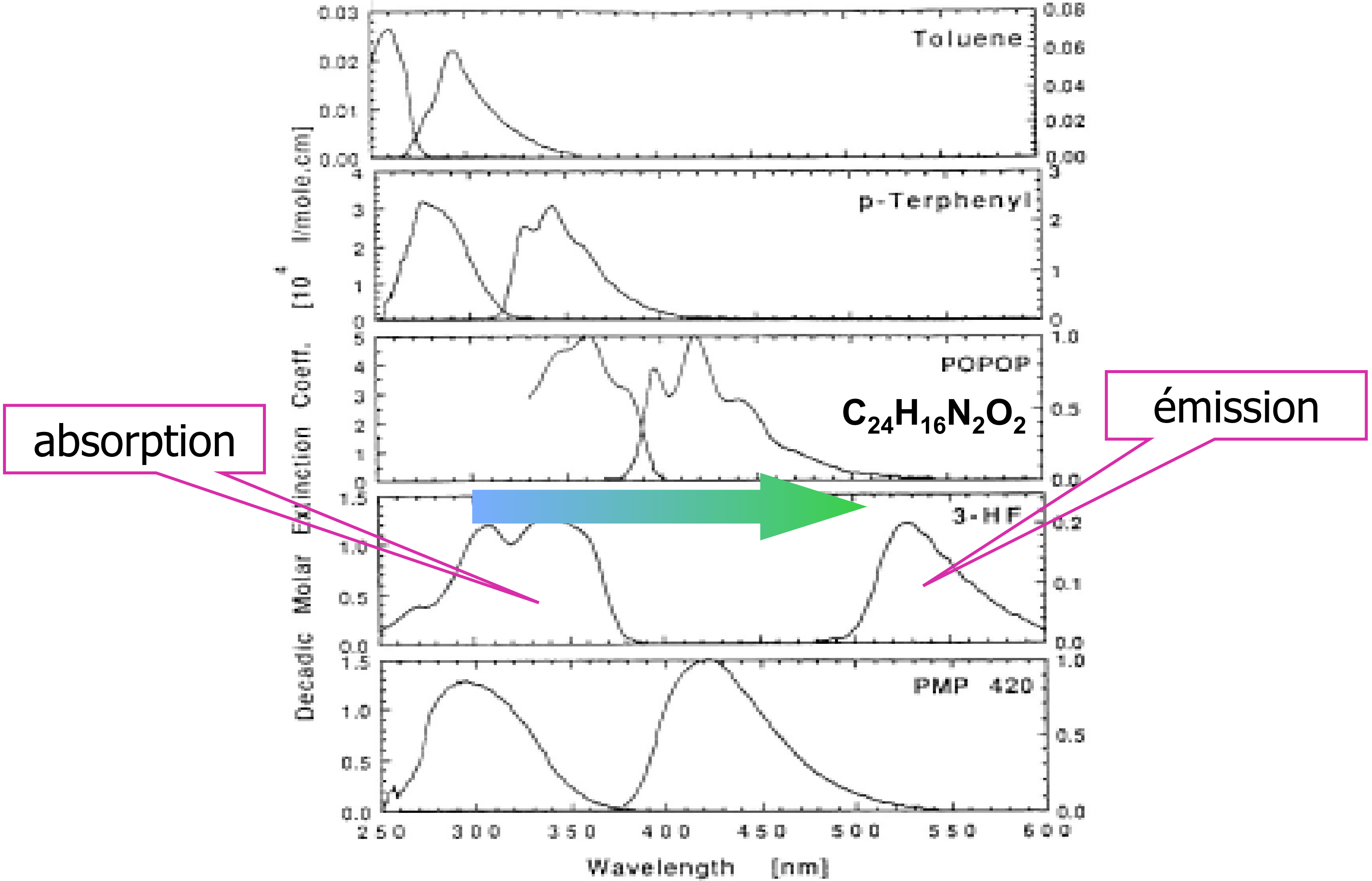

Light guides

Geometrical adaptation:

- Light guides: transfer by total internal reflection (+outer reflector)

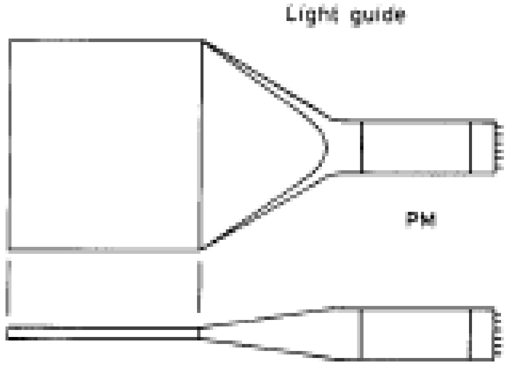

"fish tail"

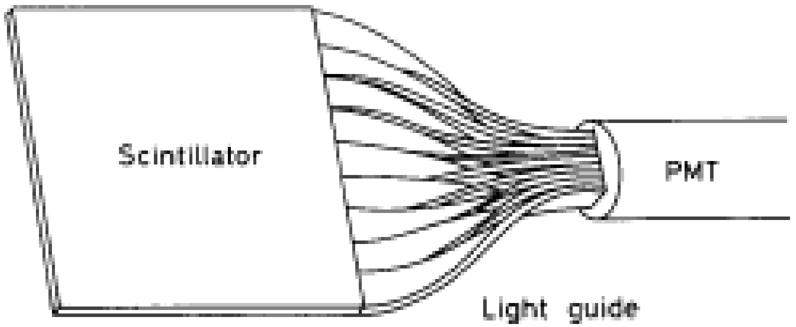

adiabatic

- wavelength shifter (WLS) bars

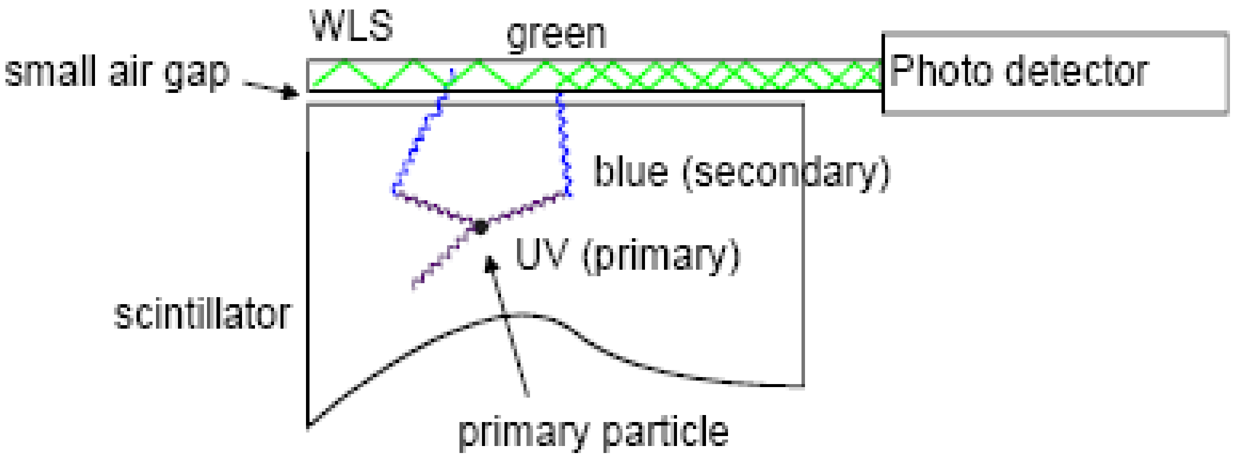

Adiabatic light guides

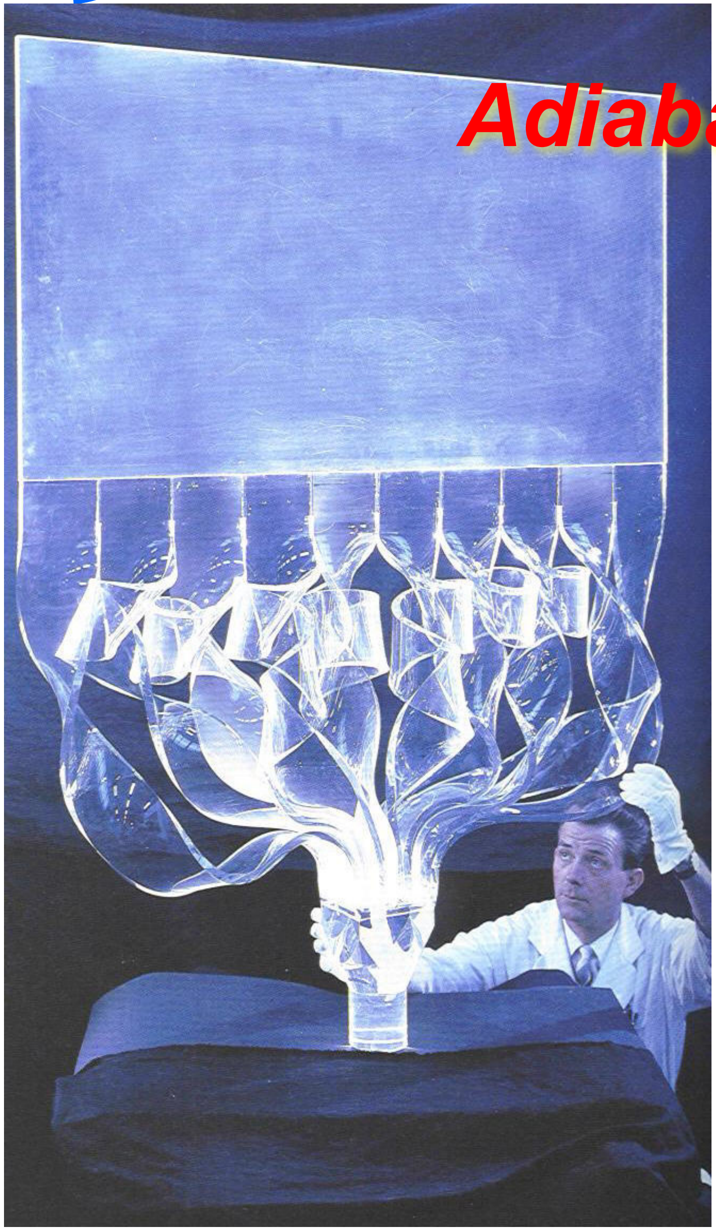

Photomultiplier

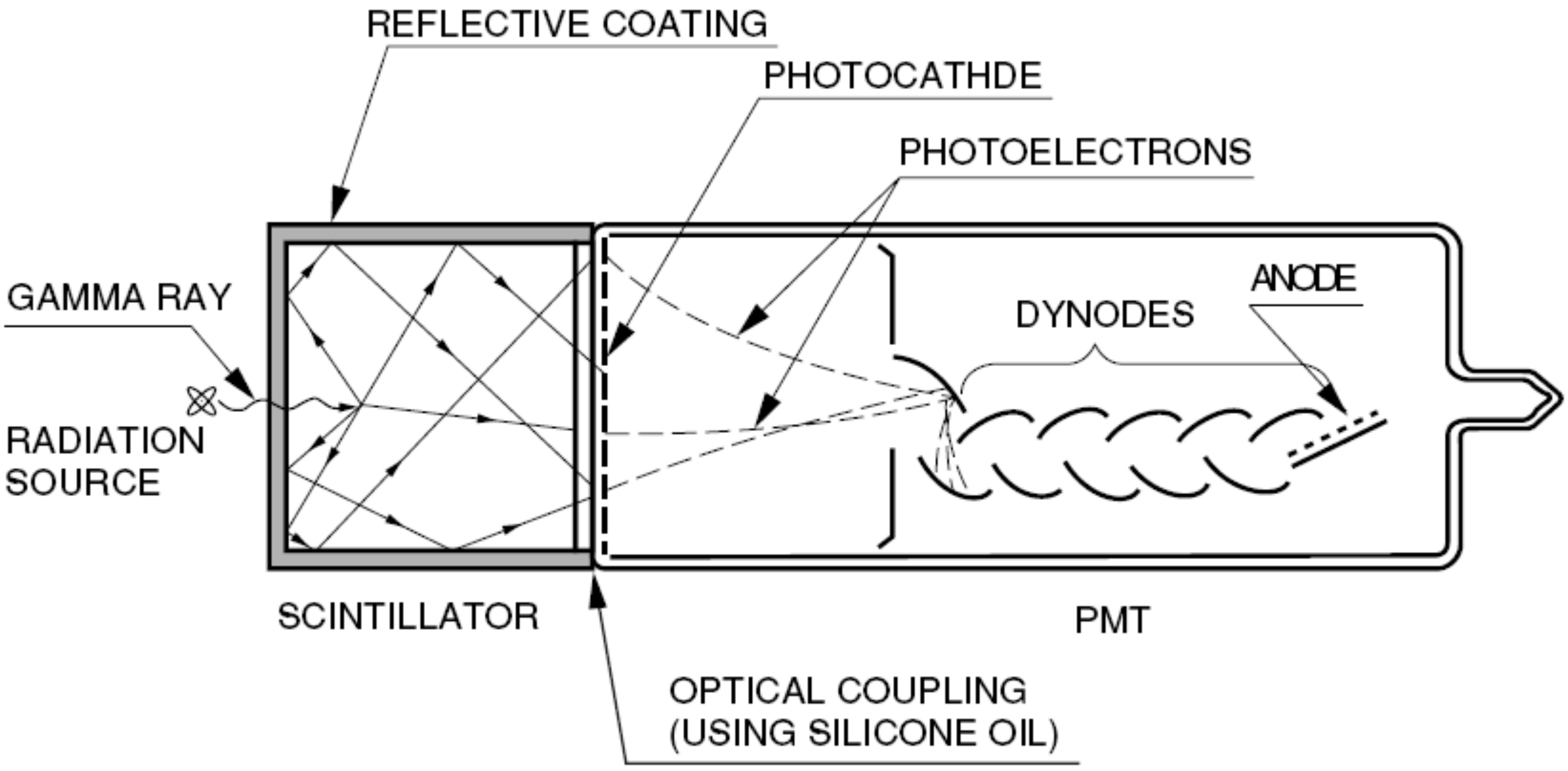

UNIVERSITÉ DE STRASBOURG

Response function of a Scintillator

Two examples of how a scintillator responds to mono-energetic photons

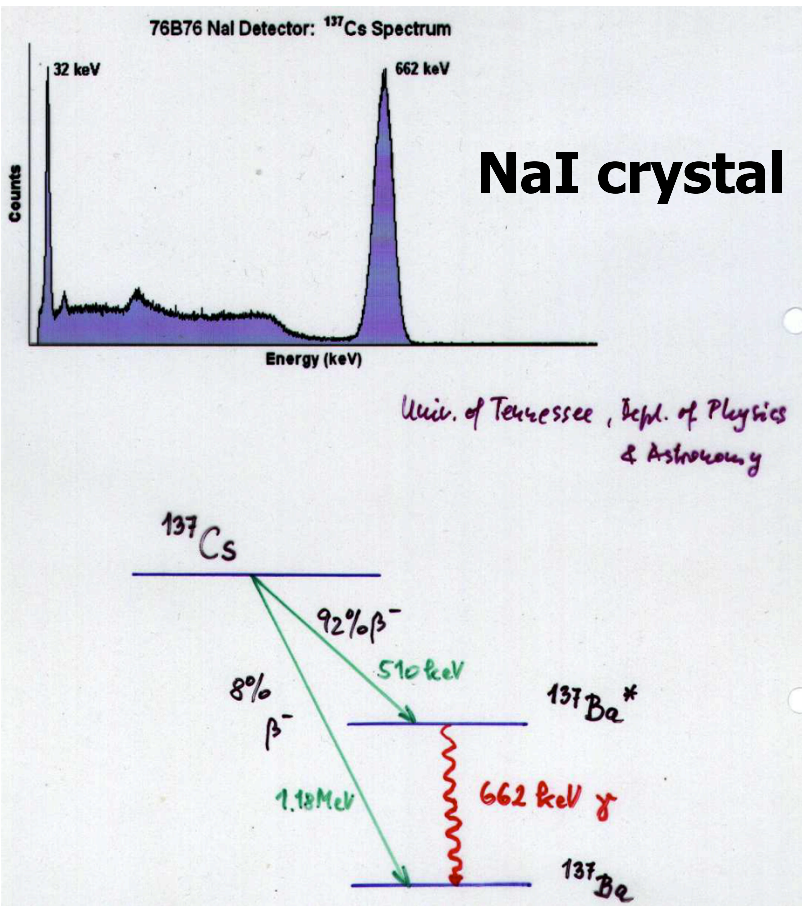

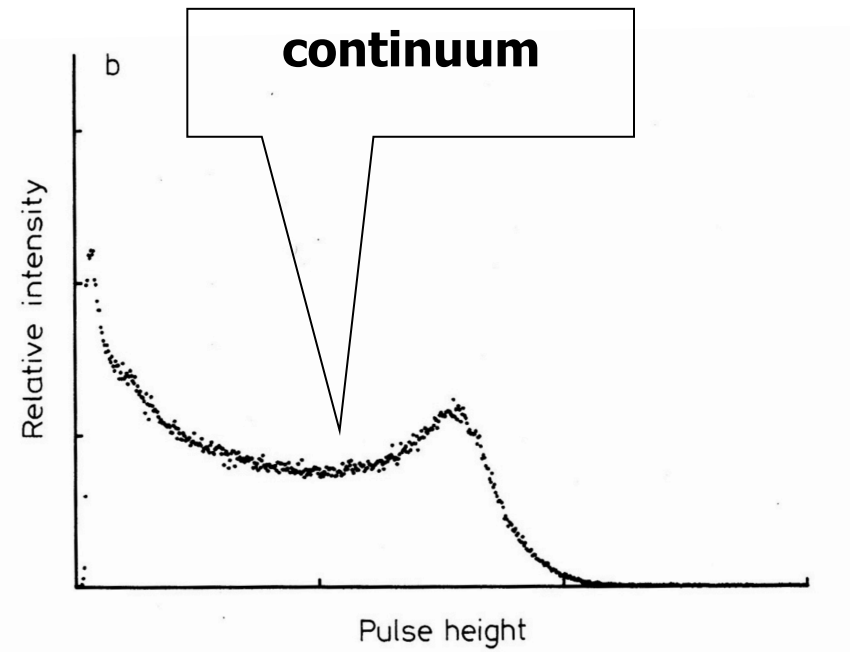

Plastic Scintillator

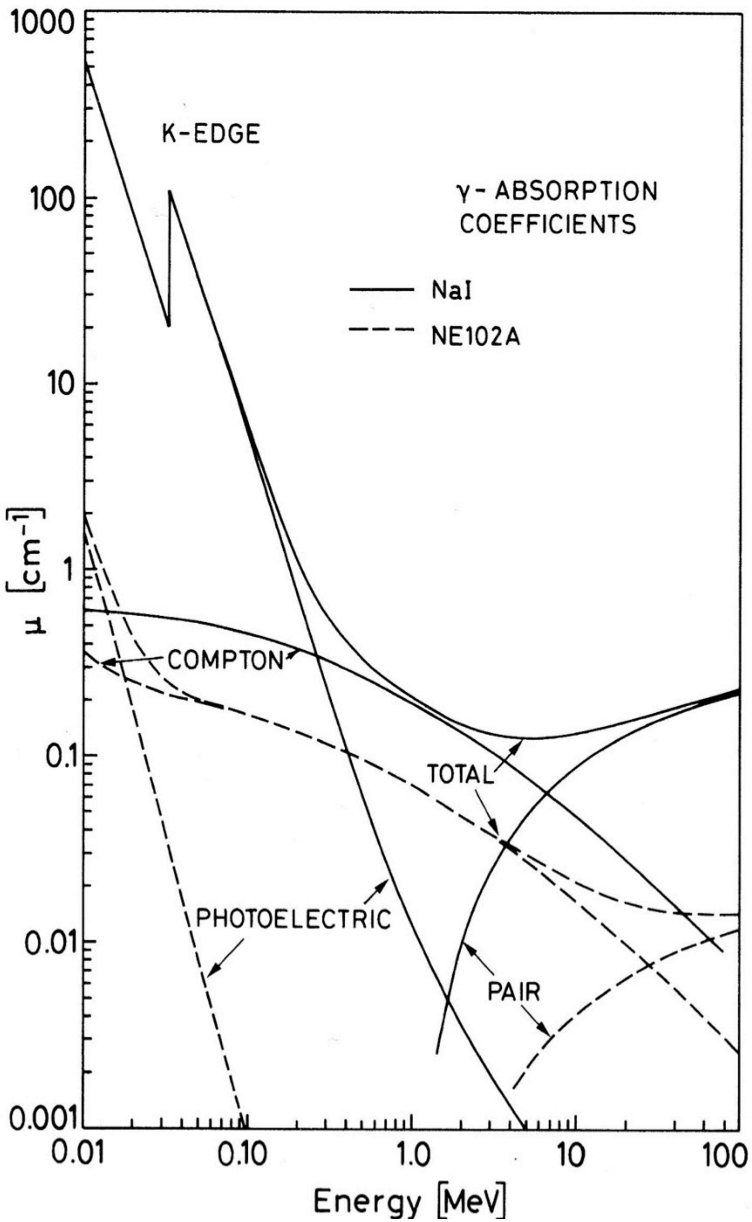

Photo-electric Effect

Absorption of γ $E_\gamma \leq$ 0.1-0.5 MeV

Compton effect

Scattering $\gamma \rightarrow \gamma'$ $0.1 \leq E_\gamma \leq$ 10 MeV

Pair production (e^+e^-)

Absorption of γ $E_\gamma \geq$ 1.022 MeV

Scintillating fibers

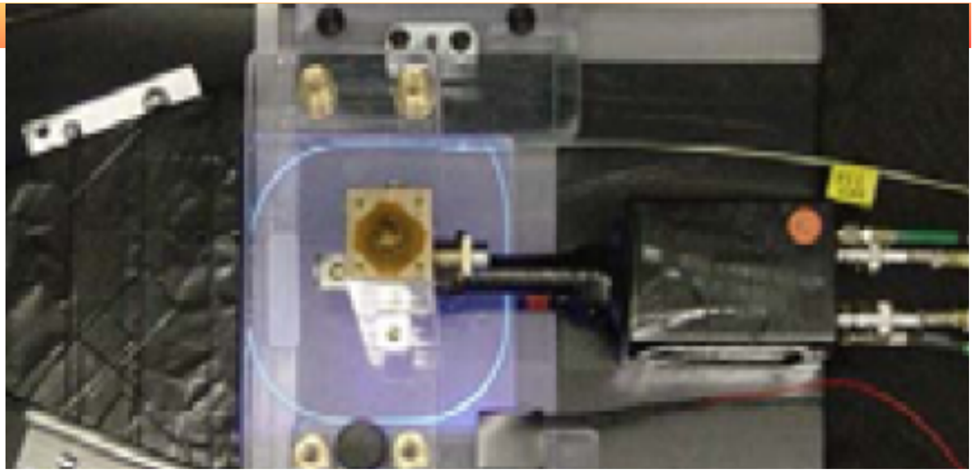

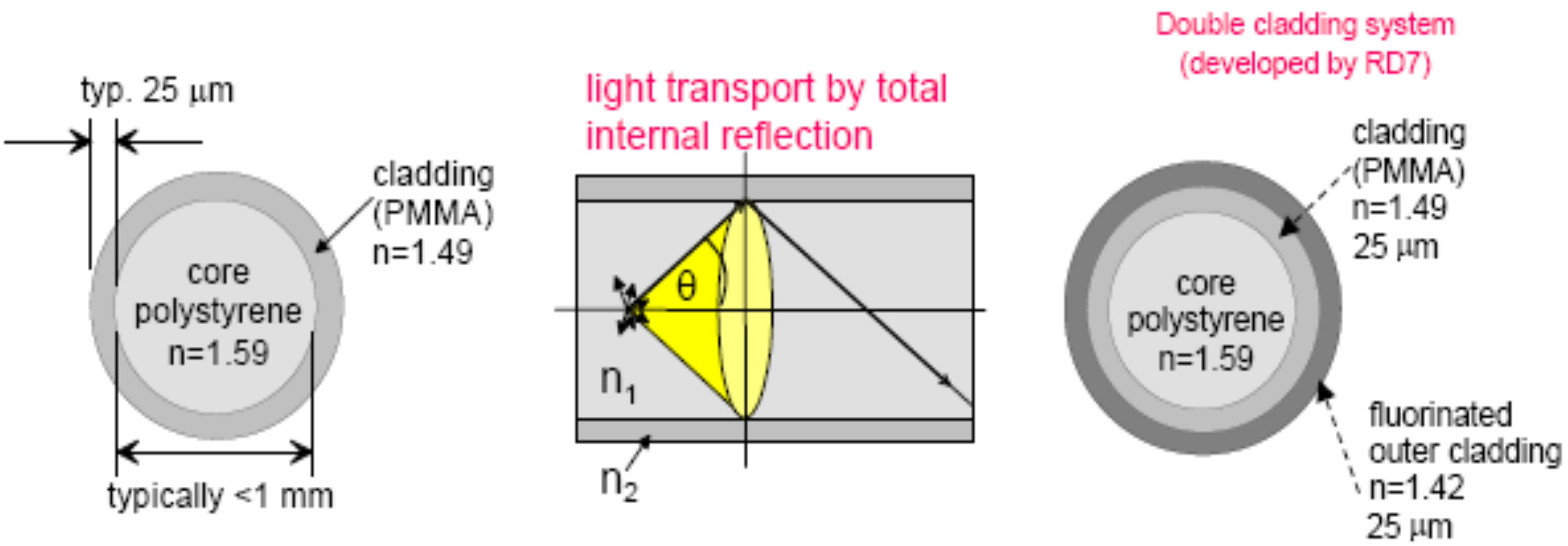

$$\cos\theta = \sin\alpha_1 = \frac{n_2}{n_1} = 0.937 \Rightarrow \theta = 20.5°;\ \frac{d\Omega}{4\pi} = \tfrac{1}{2}\sin^2\theta = \tfrac{1}{2}\left(1-\cos^2\theta\right) = 0.06$$

$$\frac{n_2}{n_1} = 0.893 \Rightarrow \theta = 26.7°;\ \frac{d\Omega}{4\pi} = 0.10$$

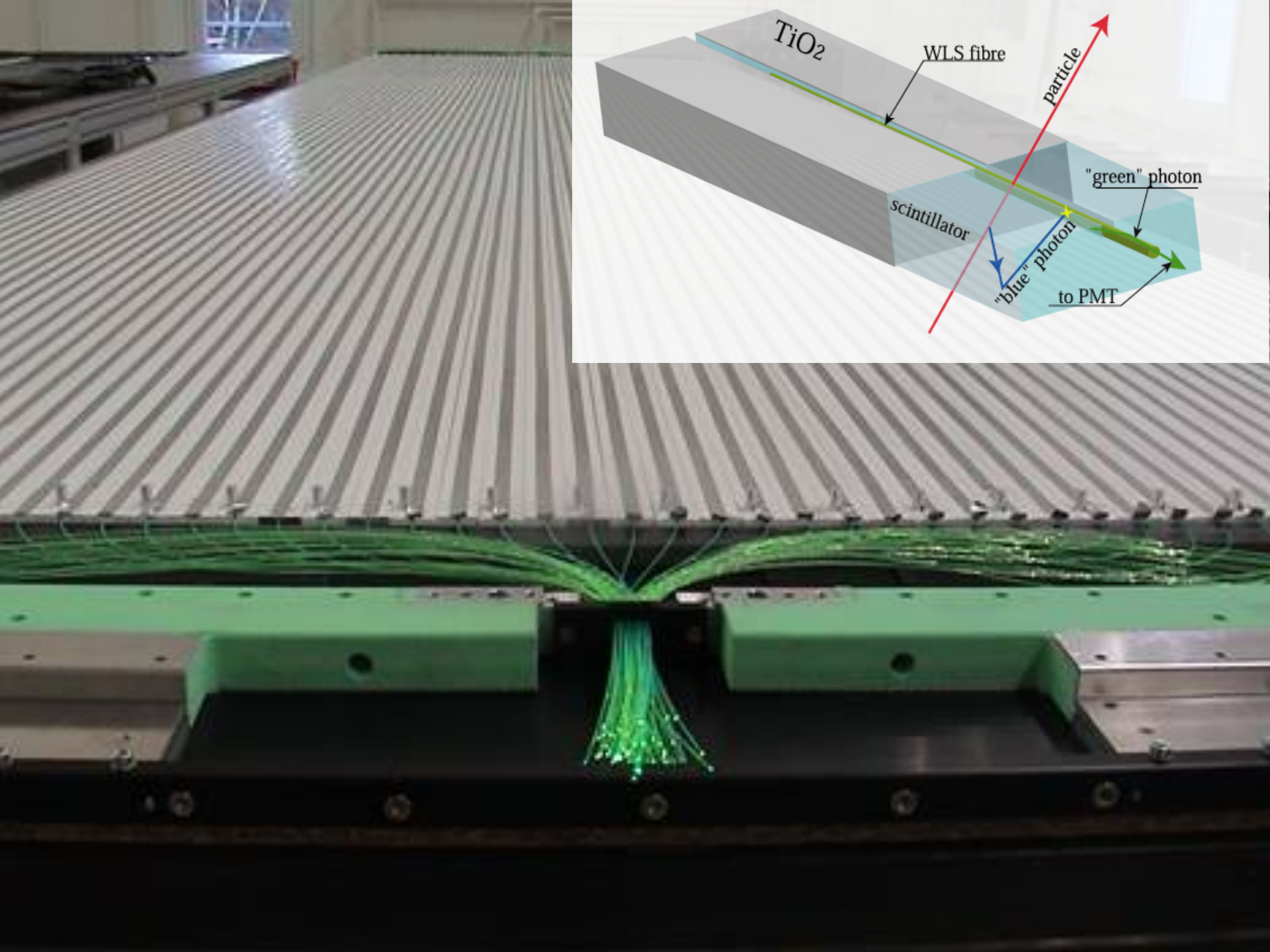
TiO2
WLS fibre
particle
"green" photon
scintillator
"blue" photon
to PMT

Semiconductor detectors

Semi-conductors

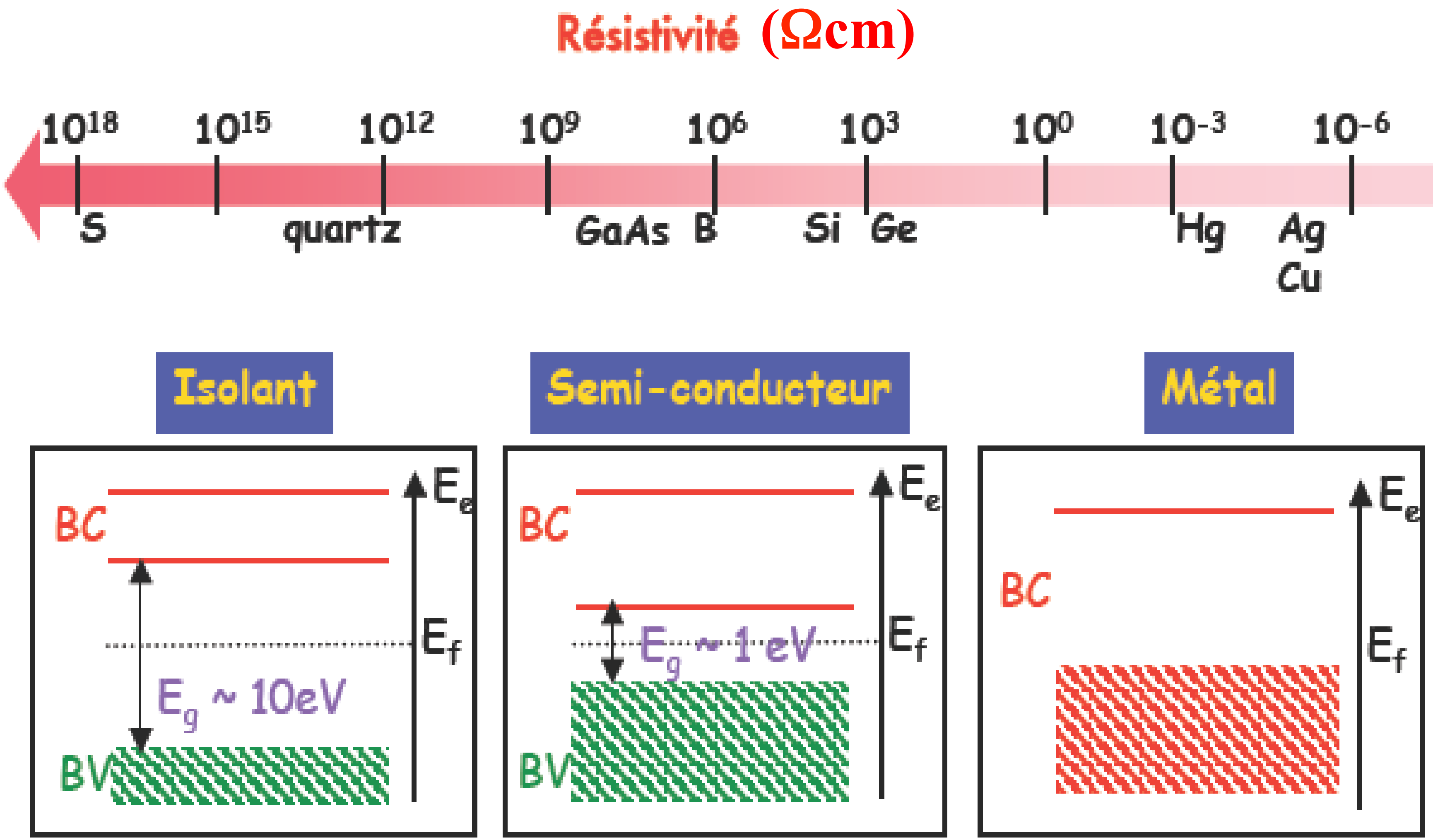

Semi-conductors

- **Advantages**
  - Higher density
    - ρ_{air} = 0.0012 g/cm³
    - $\rho_{plastique,\ scint.}$ = 1.032 g/cm³; ρ_{NaI} = 3.67 g/cm³
    - ρ_{Si} = 2.33 g/cm³ ρ_{Ge} = 5.32 g/cm³
  - Energy to produce a pair (electron, hole) is very low
    - w_{air} = 33.8 eV
    - $w_{plastique,\ scint}$ = 100 eV par photon; w_{NaI} = 26.3 eV per photon;
    - w_{Si} = 3.6 eV
    - ⇒ better energy resolution :

$$\frac{dN}{N} = \frac{1}{\sqrt{N}} \;;\; E \sim N;$$

$$N = \text{numb. of (e,h), h}\nu\text{, (e,ion}^{+}\text{)}$$

- **Disadvantages**
  - Needs very high purity
  - price
  - Crystal structure sensitive to radiation

Charge mobility

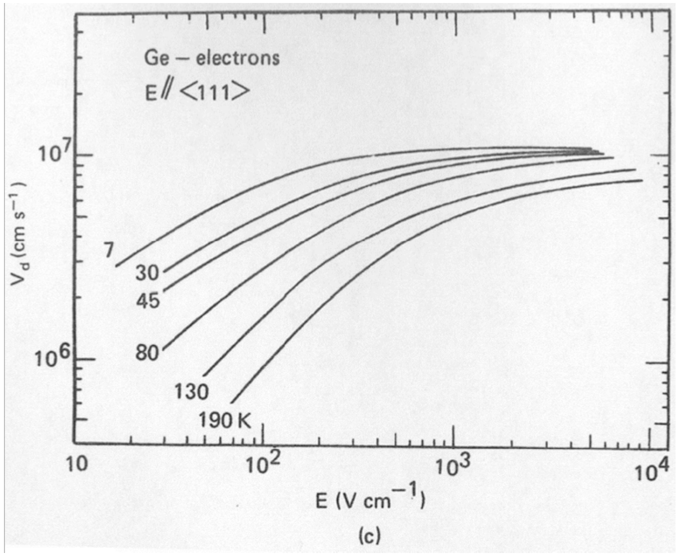

(c)

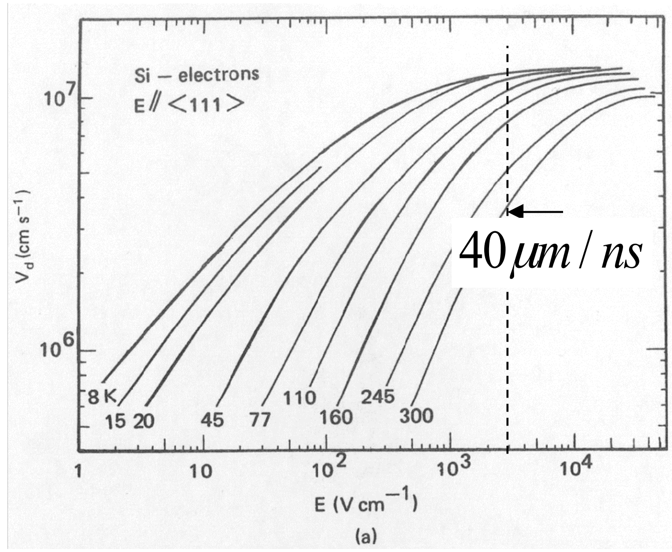

(a)

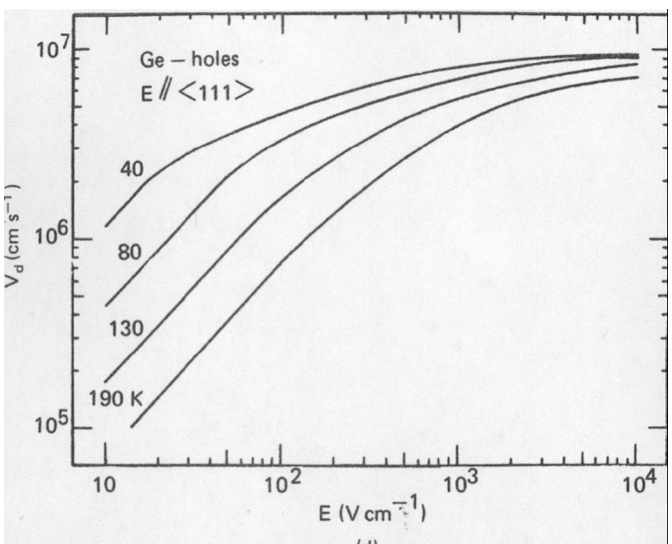

(d)

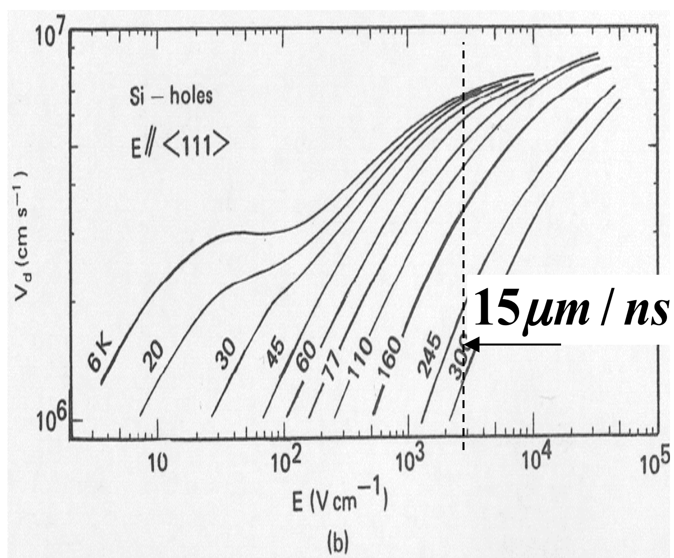

(b)

Mobility μ is defined

$$v_{e-,h} = \mu_{e,h} E$$

~ identical for holes and e$^-$

Saturation at higher fields*(v~10^7 cm/s)* i.e. semi-conductors are fast

Semi-conductor detectors

Material	E_g [eV]	w [eV]	Mobility (velocity/*E*)		τ_e [s]	τ_h [s]	density	Z [a.m.u]
			μ_e [cm^2/Vs]	μ_h [cm^2/Vs]			g/cm^3	
C (diamond)	5.5	13	1800	1200	$2\ 10^{-9}$	$2\ 10^{-9}$	3.515	6
Si	1.12	3.61	1350	480	$5\ 10^{-3}$	$5\ 10^{-3}$	2.33	14
Ge	0.67	2.98	3900	1900	$2\ 10^{-5}$	$2\ 10^{-5}$	5.32	32
GaAs	1.42	4.70	8500	450	$5\ 10^{-8}$	$5\ 10^{-8}$	5.32	31,33
CdTe	1.56	4.43	1050	100	$1\ 10^{-6}$	$1\ 10^{-6}$		48,52
HgI_2	2.13	4.20	100	_	$1\ 10^{-6}$	$2\ 10^{-6}$		53,80

Parameters Values for Materials Used in Fabricating Semiconductor Radiation Sensors [3]

W.Dulinski

„Doped“ Semi-conductors

concentrations of

$n(e^-)$ and $p(holes^+)$:

$$n \cdot p = n_i^2 = AT^3 \exp\left(-\frac{E_g}{kT}\right)$$

$$N_D + p = N_A + n \text{ (el. neutral)}$$

$$N_A \approx 0 \quad n \gg p \quad (\text{n-type})$$

$$n \approx N_D \Rightarrow p \approx n_i^2 / N_D$$

$$1/\rho = \sigma \approx e N_D \mu_e$$

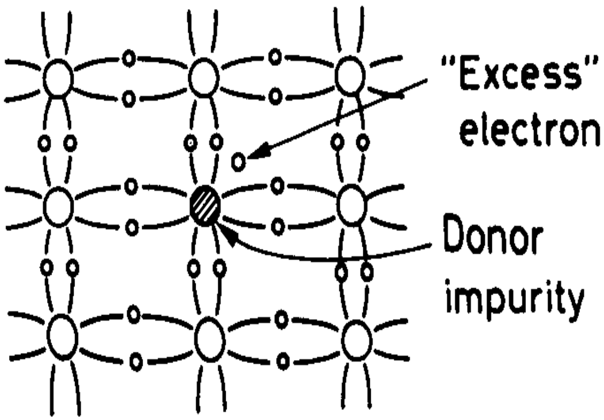

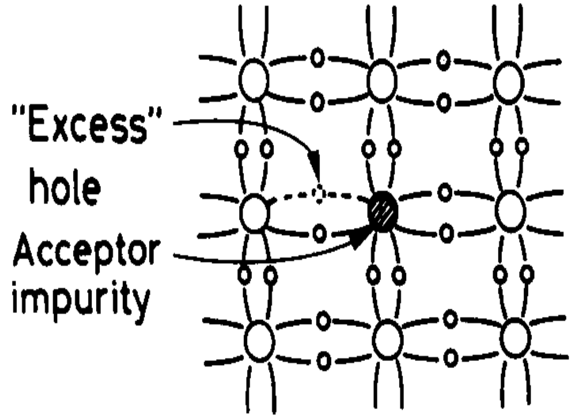

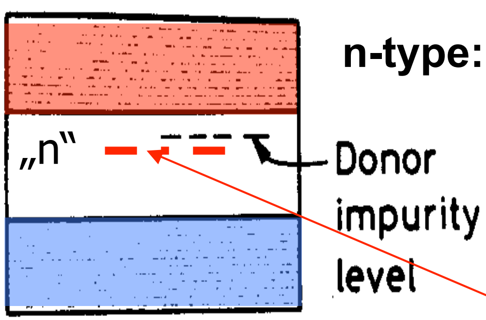

n-type: $N_D > N_A \approx 0$

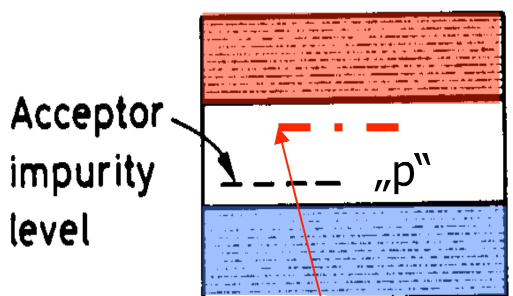

p-type: $N_A > N_D \approx 0$

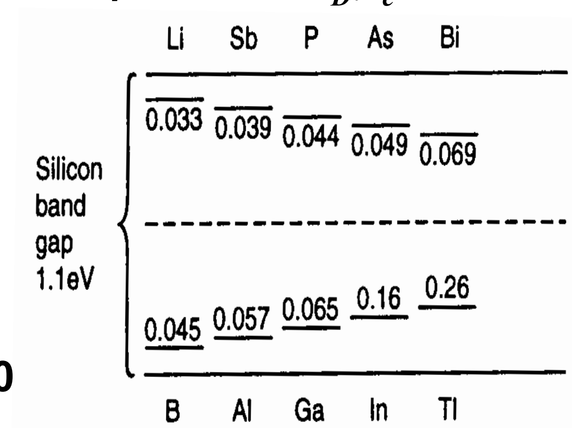

Energy levels within the band gap corresponding to various n- and p-type dopants [6]

Intrinsic: $1.5\ 10^{10}/\text{cm}^3$ ($N_A = 6.022\ 10^{23}/\text{cm}^3$!!)
n, p : $10^{13}/\text{cm}^3$
n^+, p^+ : $10^{20}/\text{cm}^3$

Impurities

- traps
- recombination

W.Dulinski

Junction p-n

Formation of a depletion zone

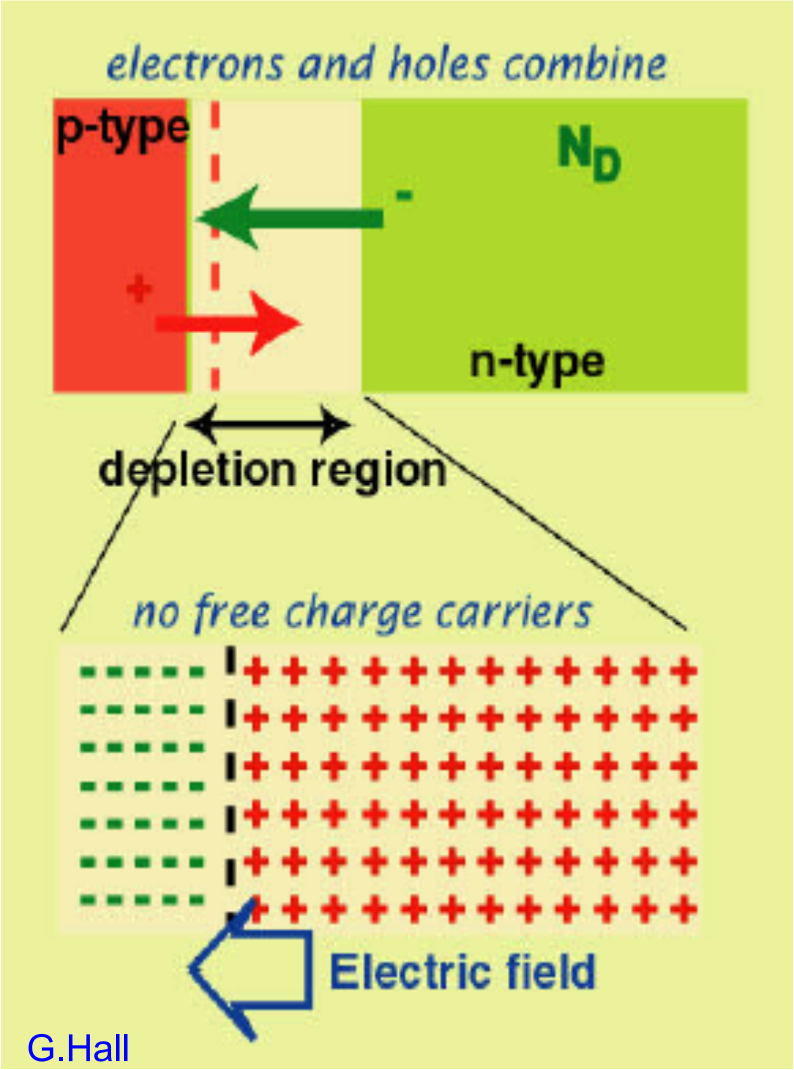

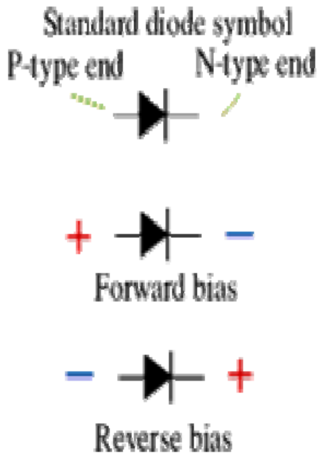

Direct Polarisation

- **conduction**
- $I \sim I_0[\exp(qV/kT) - 1]$

Inverse Polarisation

- **increase of depletion zone**
- **reduction of capacitance**

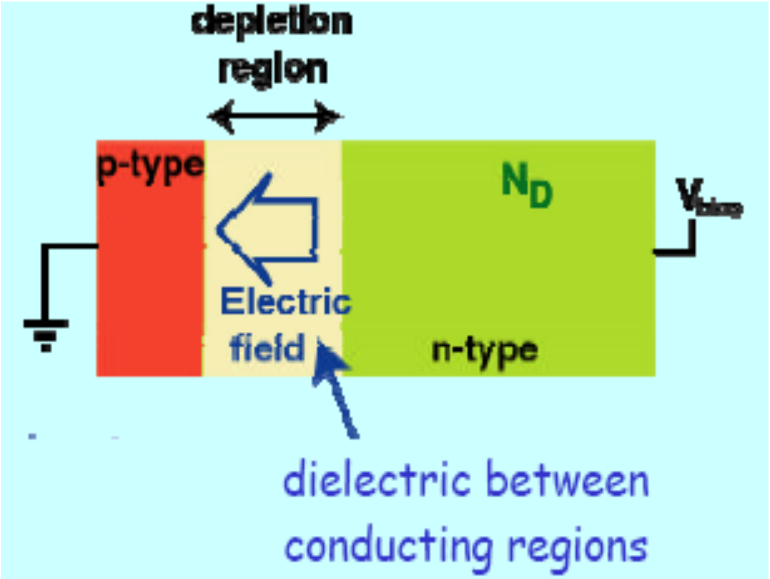

Depth of the depletion zone

$$N_A \gg N_D$$

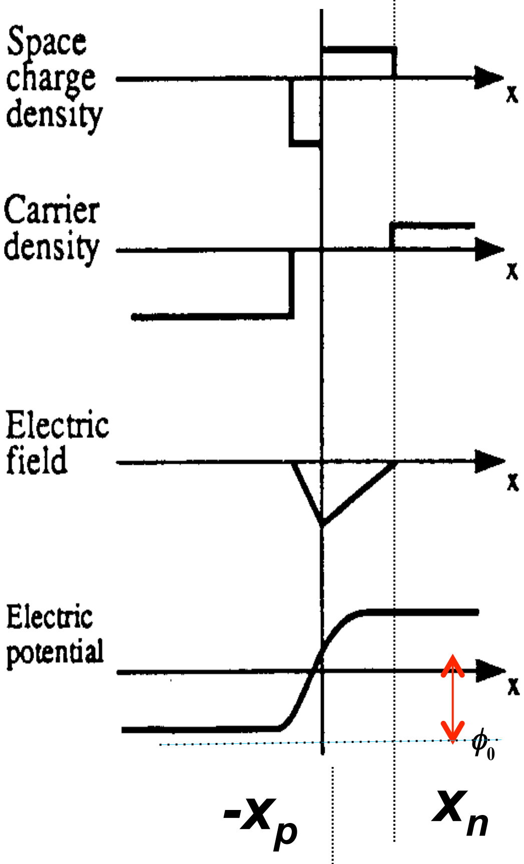

$$\frac{d^2\phi}{dx^2} = -\rho(x)/\varepsilon \; ; \; \rho(x) = \begin{cases} eN_D & 0 < x < x_n \\ -eN_A & -x_p < x < 0 \end{cases}$$

$$N_A x_p = N_D x_n$$

$$-E(x) = \frac{d\phi}{dx} = \begin{cases} -\frac{eN_D}{\varepsilon} x + C_n \; ; \\ \frac{eN_A}{\varepsilon} x + C_p \; ; \end{cases} \Rightarrow \begin{cases} -\frac{eN_D}{\varepsilon}(x - x_n) \; ; \; 0 < x < x_n \\ \frac{eN_A}{\varepsilon}(x + x_p) \; ; \; -x_p < x < 0 \end{cases}$$

$$[d\phi / dx = 0 \;\; à \;\; x = x_n \quad et \;\; à \;\; x = -x_p]$$

$$\phi(x) = \begin{cases} -\frac{eN_D}{\varepsilon}\left(x^2/2 - x \cdot x_n\right) + C \; ; \; 0 < x < x_n \\ \frac{eN_A}{\varepsilon}\left(x^2/2 + x \cdot x_p\right) + C' \; ; \; -x_p < x < 0 \end{cases}$$

continuity à $x = 0 \Rightarrow \; C = C'$;

à $x = x_n, \phi(x) = \phi_0$ = contact potentiel; $\phi(x = -x_p) = 0$

$$\phi_0 = \frac{eN_D}{2\varepsilon} x_n^2 + C \quad et \quad 0 = -\frac{eN_A}{2\varepsilon} x_p^2 + C$$

$$\phi_0 = \frac{e}{2\varepsilon}\left(N_D x_n^2 + N_A x_p^2\right)$$

Depth of the depletion zone

$N_A \gg N_D$

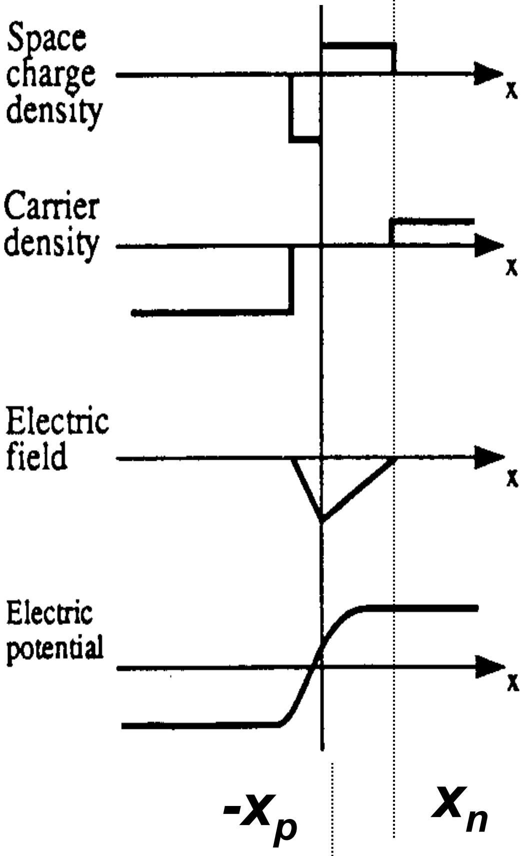

$$\phi_0 = \frac{e}{2\varepsilon}\left(N_D x_n^2 + N_A x_p^2\right)$$

$$x_n = \sqrt{\frac{2\varepsilon\phi_0}{eN_D\left(1+N_D/N_A\right)}} \; ; \; x_p = \sqrt{\frac{2\varepsilon\phi_0}{eN_A\left(1+N_A/N_D\right)}} \; ;$$

$$d = x_n + x_p = \sqrt{\frac{2\varepsilon\phi_0}{e}\frac{\left(N_A+N_D\right)}{N_A N_D}}$$

$N_D \gg N_A \; (x_p \gg x_n) \Rightarrow$ **depletion in p**

$$x_n = \frac{1}{N_D}\sqrt{\frac{2\varepsilon\phi_0}{e}N_A} \; ; \; x_p = \sqrt{\frac{2\varepsilon\phi_0}{eN_A}} \; ;$$

$$d \simeq x_p \simeq \sqrt{\frac{2\varepsilon\phi_0}{eN_A}} = \sqrt{2\varepsilon\rho_p\mu_h\phi_0} \approx 0.32\sqrt{\rho_p\phi_0}\,\mu m \quad (Si)$$

$N_A \gg N_D \; (x_n \gg x_p) \Rightarrow$ **depletion in n**

$$x_n = \sqrt{\frac{2\varepsilon\phi_0}{eN_D}} \; ; \qquad x_p = \frac{1}{N_A}\sqrt{\frac{2\varepsilon\phi_0}{e}N_D} \; ;$$

$$d \simeq x_n \simeq \sqrt{\frac{2\varepsilon\phi_0}{eN_D}} = \sqrt{2\varepsilon\rho_n\mu_e\phi_0} \approx 0.53\sqrt{\rho_n\phi_0}\,\mu m \quad (Si)$$

$$\rho \sim 20\,000\,\Omega cm, \; \phi_0 \sim 1 Volt \Rightarrow d \sim 75\,\mu m$$

Inverse Polarisation

$$d\big|_{V_{bias}} = x_n + x_p = \sqrt{\frac{2\varepsilon(\phi_0 + V_{bias})}{e}\frac{(N_A + N_D)}{N_A N_D}}$$

Holes move to « - »

electrons move to contact "+"

$N_A \gg N_D$

depletion in n-type

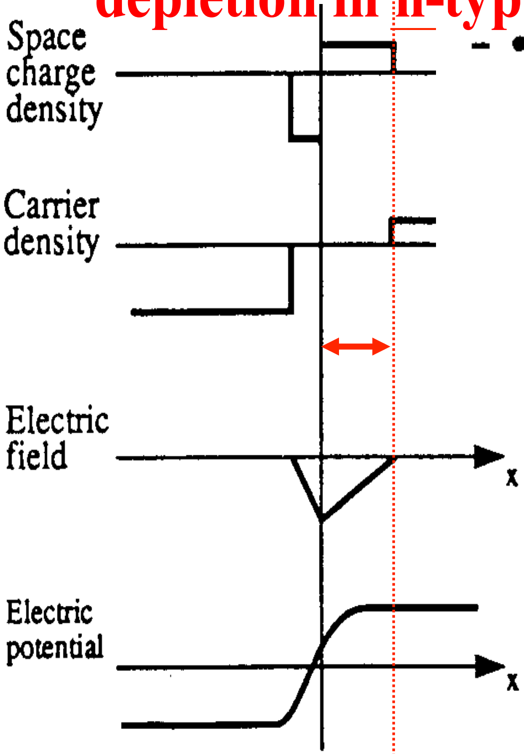

-x_p x_n

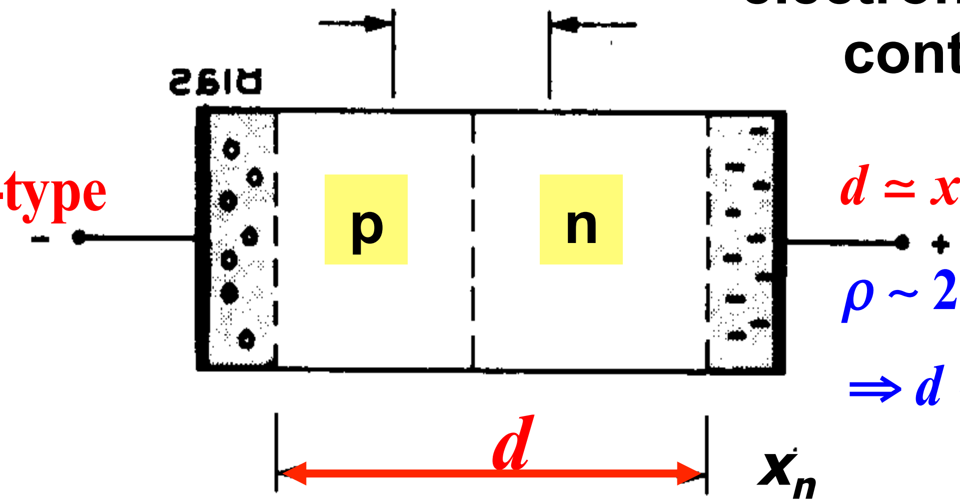

Depletion zone

$d \simeq x_n \approx 0.53\sqrt{\rho_n \phi_0}\ \mu m$

$\rho \sim 2 \cdot 10^4\ \Omega cm,\ \phi_0 \sim 1V$

$\Rightarrow d \sim 75\ \mu m$

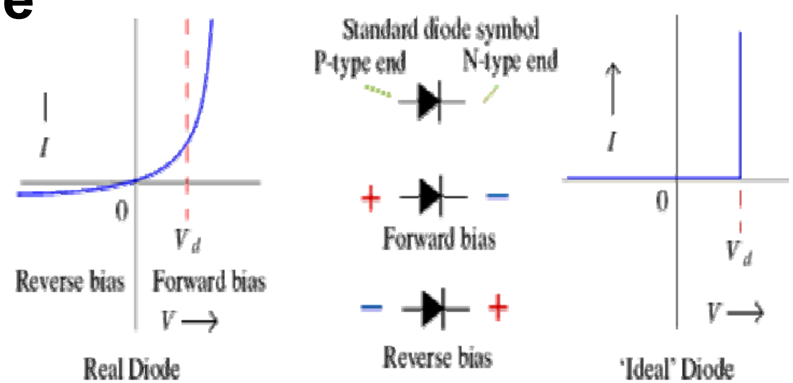

Zone désertée

$$d\Big|_{V_{bias}} = x_n + x_p = \sqrt{\frac{2\varepsilon\left(\phi_0 + V_{bias}\right)}{e}\frac{\left(N_A + N_D\right)}{N_A N_D}} \xrightarrow{N_A \gg N_D} \sqrt{\frac{2\varepsilon}{e}\frac{1}{N_D}}\sqrt{V_{bias}}$$

Capacitance $C \propto 1/d \quad \Rightarrow \frac{1}{C^2} \propto V_{bias}$

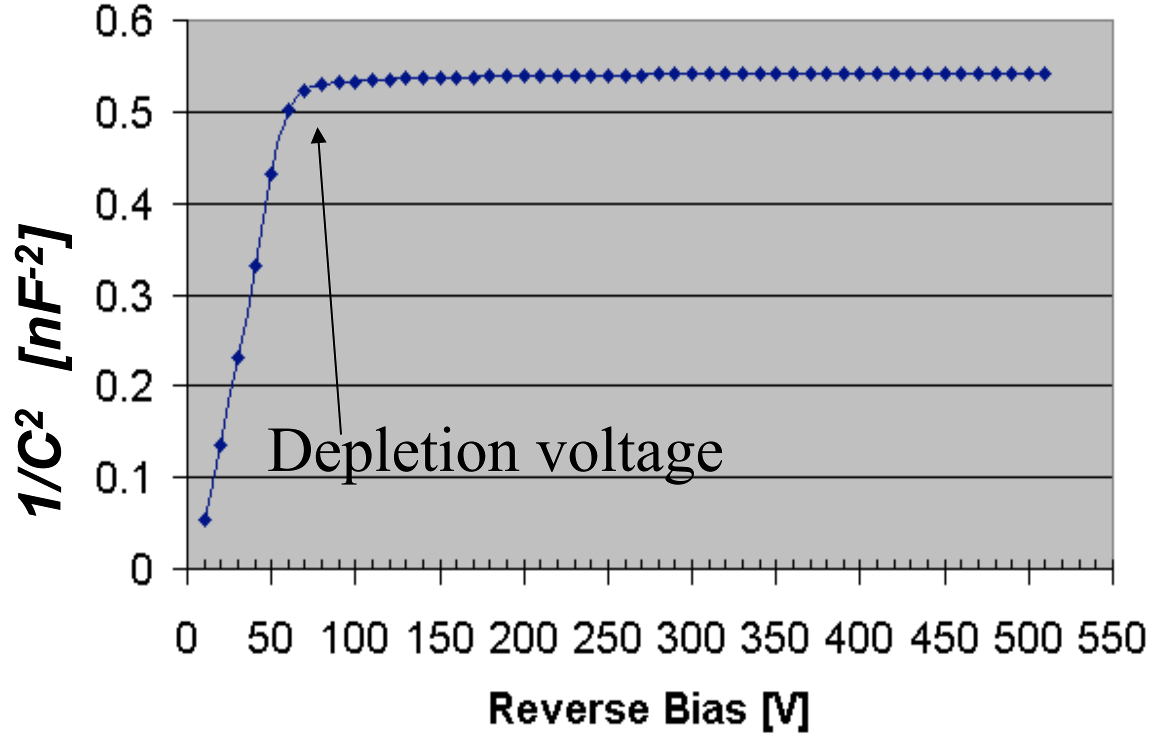

Junction p-n

0.1-2µm ⇒ perte d'énergie

Diffused or Ion implanted

Diffused & Ion implanted

oxide window

robust, flexible geometry

Shottky barrier

Shottky barrier

metal-silicon junction

thin metal contact more fragile

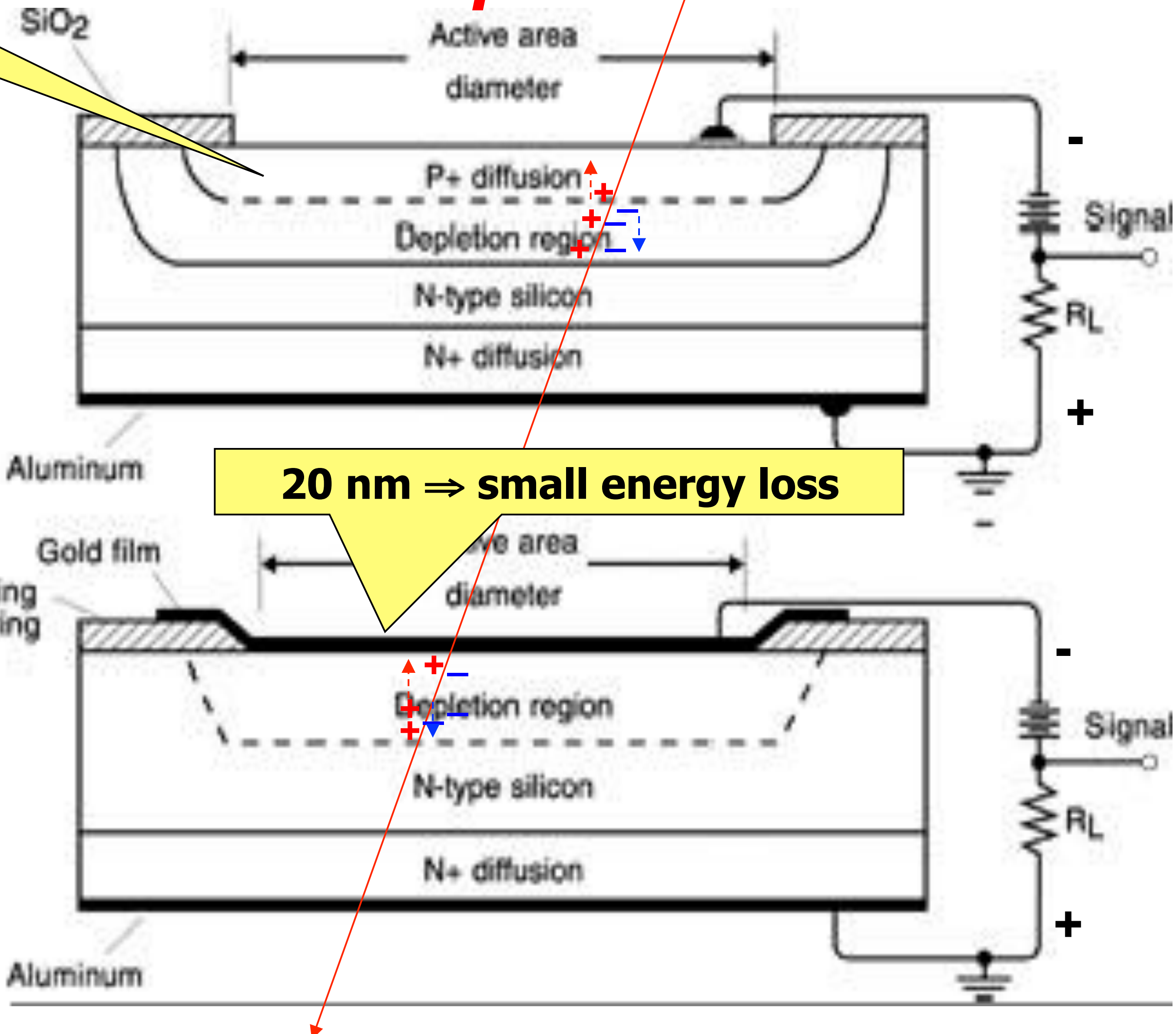

G.Hall

Surface barrier detectors

Signal formation (diode)

$$Q_{tot} \sim \Delta E^{\text{déposée}}_{\text{énergie}};$$

$$U = \frac{Q}{C} = \eta \frac{E_{\text{nergie}}}{wC} e\,;\ \eta = coll.eff.$$

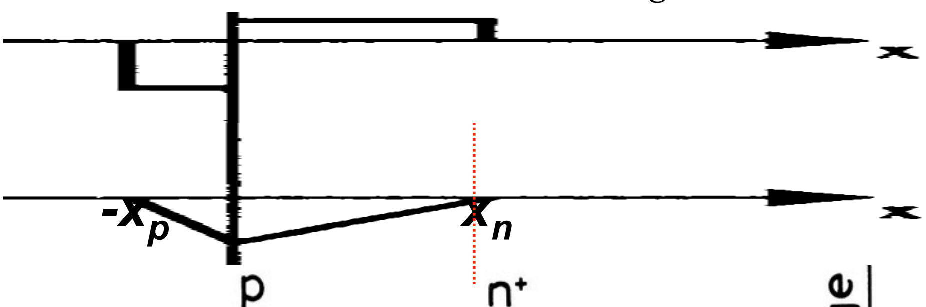

μ_e [cm²/Vs]	μ_h [cm²/Vs]
1350	480

E=3kV/cm $40\,\mu m/ns$ $15\,\mu m/ns$

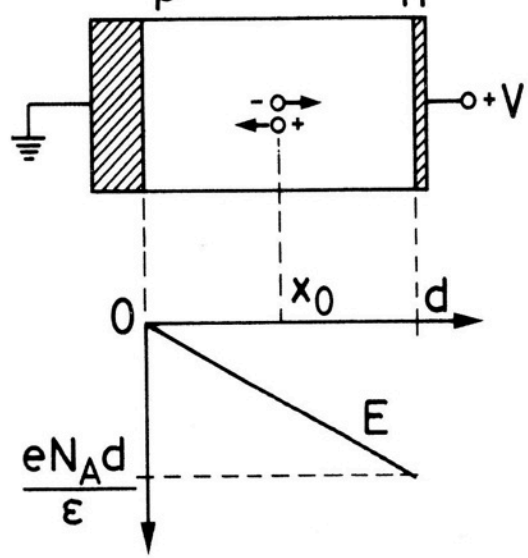

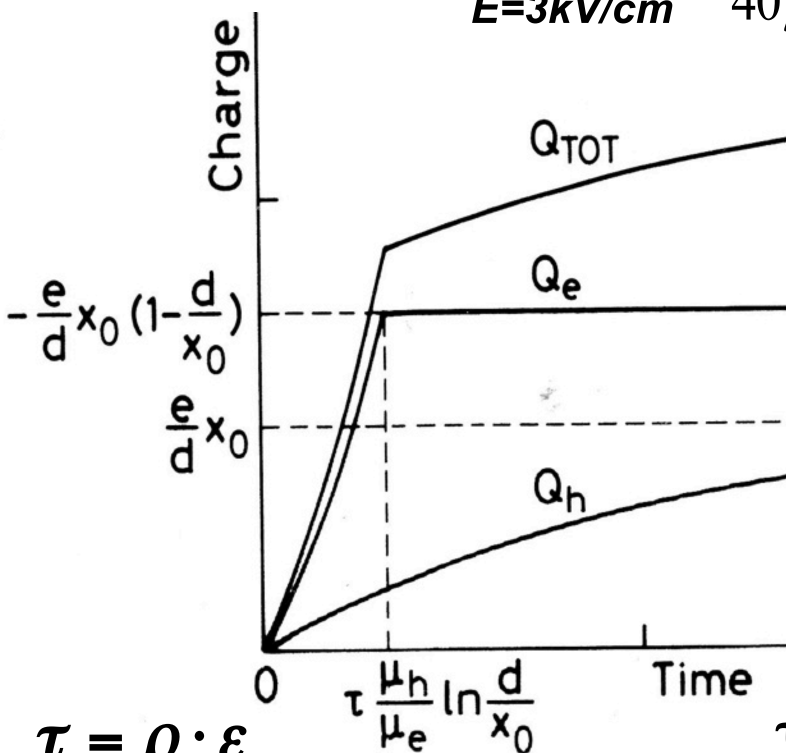

$$v = \frac{dx}{dt} = -\mu_e E = \frac{\mu_e}{\mu_h}\frac{x}{\tau}$$

$$t = \tau \frac{\mu_e}{\mu_h} \ln \frac{d}{x_0}$$

$$Q_e(t) = \frac{e}{d} x_0 \left(1 - \exp\left(\frac{\mu_e}{\mu_h} t\right)\right)$$

$$Q_h(t) = -\frac{e}{d} x_0 \left(1 - \exp\left(\frac{-t}{\tau}\right)\right)$$

Champ électrique

$$\tau = \rho \cdot \varepsilon$$

τ~10 nsec

Signal Formation

PIN diode electric field E= constante

$$\left|\vec{E}\right| = U_0 / d$$

$$Energy:\ \tfrac{1}{2}CU_0^2 \rightarrow \tfrac{1}{2}CU^2 = \tfrac{1}{2}CU_0^2 - N\int_{x_0}^{x} qE\,dx$$

$$\tfrac{1}{2}CU^2 - \tfrac{1}{2}CU_0^2 = \tfrac{1}{2}C\left(U+U_0\right)\left(U-U_0\right) = -NqE\left(x-x_0\right)$$

$$U \approx U_0;\ U+U_0 \approx 2U_0;\ U-U_0 = \Delta U;$$

$$\tfrac{1}{2}C\cdot 2U_0\cdot\Delta U = -Nq\frac{U_0}{d}\left(x-x_0\right)$$

$$\Delta U = -\frac{N}{C}\frac{q}{d}\left(x-x_0\right);\quad q=+e\ (holes)\quad q=-e\ (electr.)$$

$$\left(x-x_0\right) = v^{\pm}\Delta t^{\pm};\quad v^{+} < v^{-}\quad v = \text{drift velocity}$$

$$\Delta U^{-} \xrightarrow{x\rightarrow d} = -\frac{N}{C}\frac{e}{d}\left(d-x_0\right)$$

$$\Delta U^{+} \xrightarrow{x\rightarrow 0} = -\frac{N}{C}\frac{e}{d}x_0$$

$$\Delta U = \Delta U^{-} + \Delta U^{+} = -\frac{Ne}{C} = \Delta Q / C$$

Interaction des particules chargées avec le silicium

Data Taken from C.F. Williamson, J.P. Boujot and J. Picard, CEA-R-3042 (July 1966)

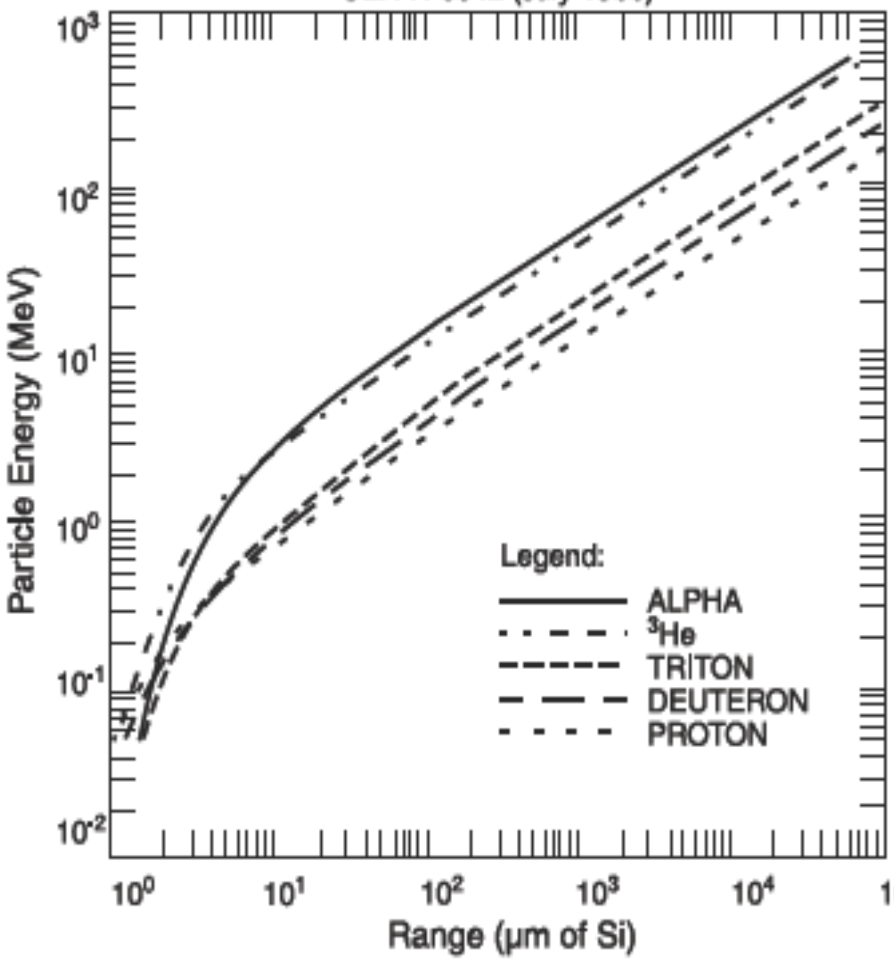

Figure 1.10 Range-Energy Curves in Silicon

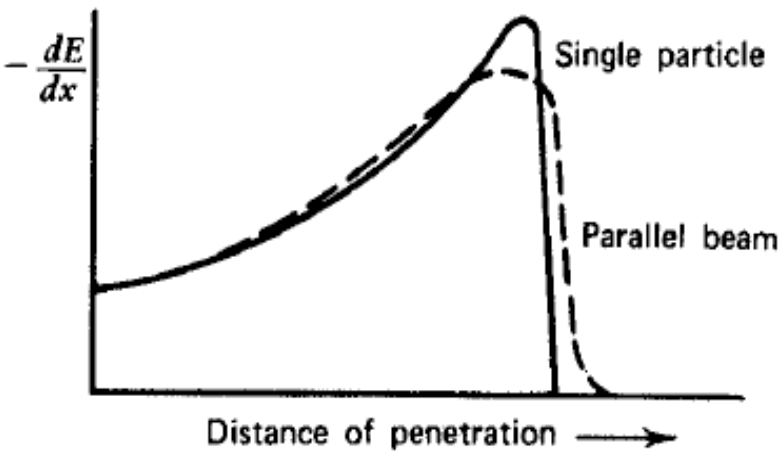

Fission fragments spectrum

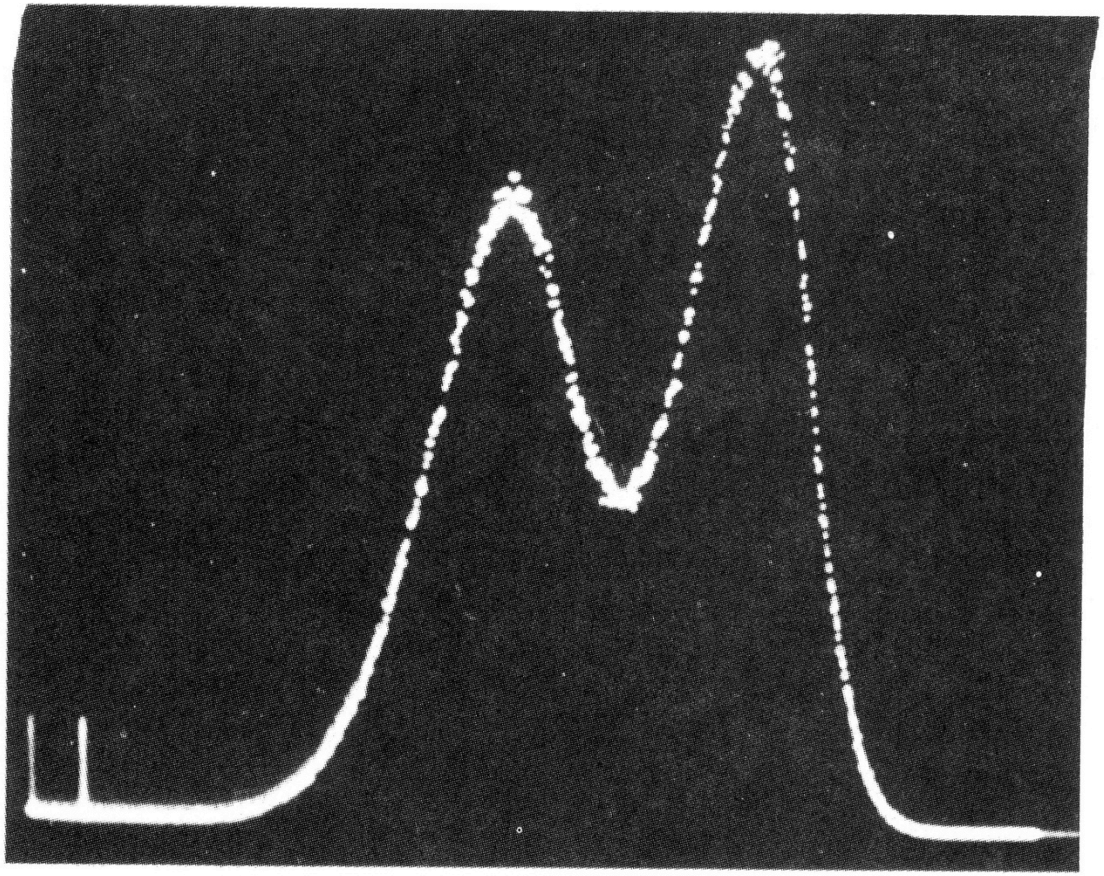

Figure 11-15 ^{252}Cf fission fragment pulse height spectrum. The spectrum parameters defined on the diagram can be used for energy calibration and detector evaluation (see text). (From Bozorgmanesh[75] and Schmitt and Pleasonton.[83])

Identification of masses

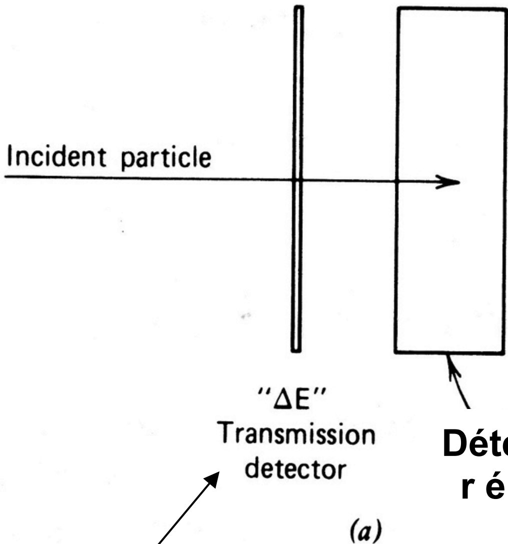

Détecteur épais

E

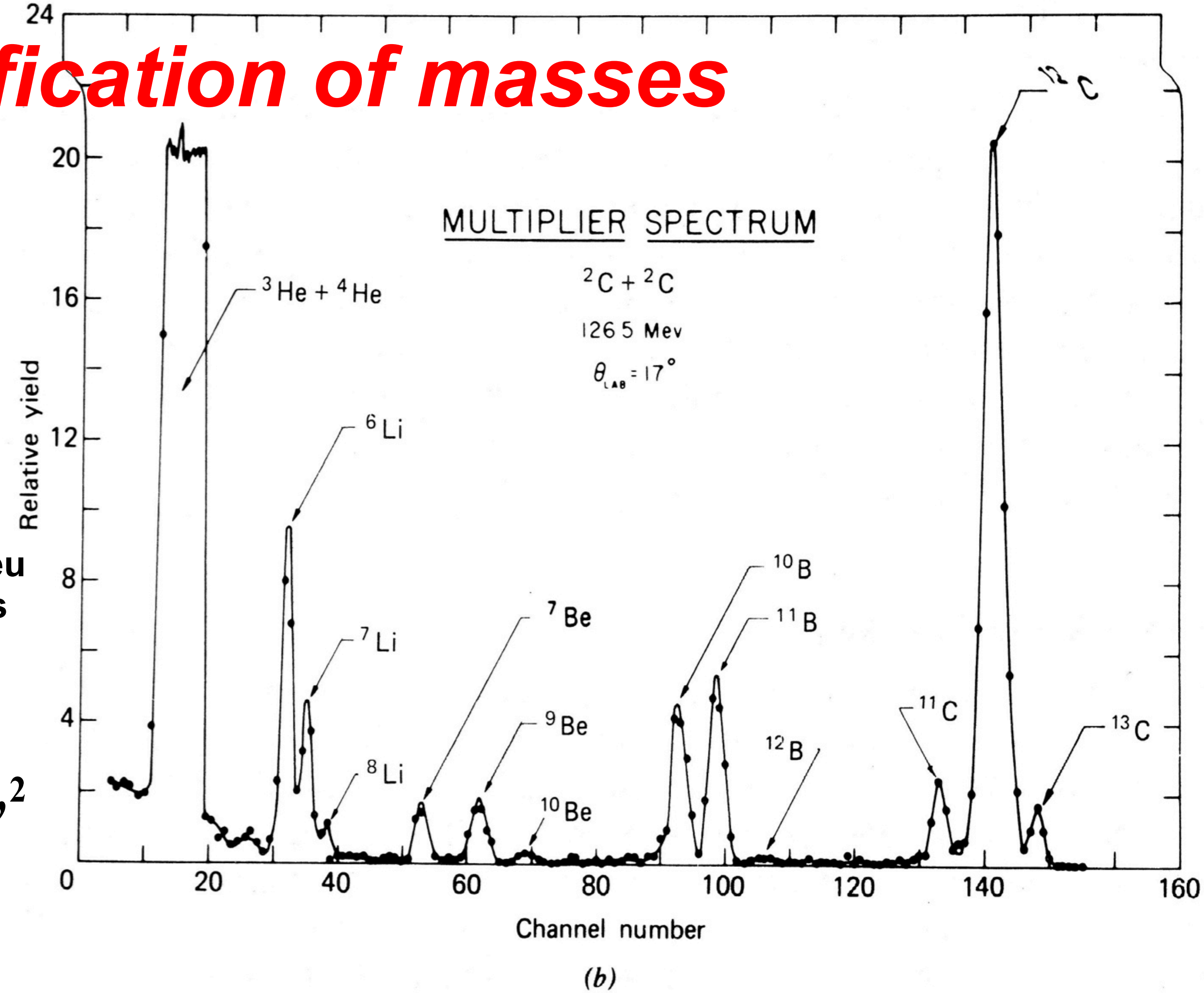

$$\frac{dE}{dx} \propto \frac{1}{v^2}; \quad E_{cin} = \frac{1}{2} m v^2$$

$$\Rightarrow$$

$$\frac{dE}{dx} \times E_{cin} \propto m$$

Figure 11-16 (a) A particle identifier arrangement consisting of tandem ΔE and E detectors operated in coincidence. (b) Experimental spectrum obtained for the $\Delta E \cdot E$ signal product for a mixture of different ions. (From Bromley.[90])

High energies

Silicon microstrip detectors

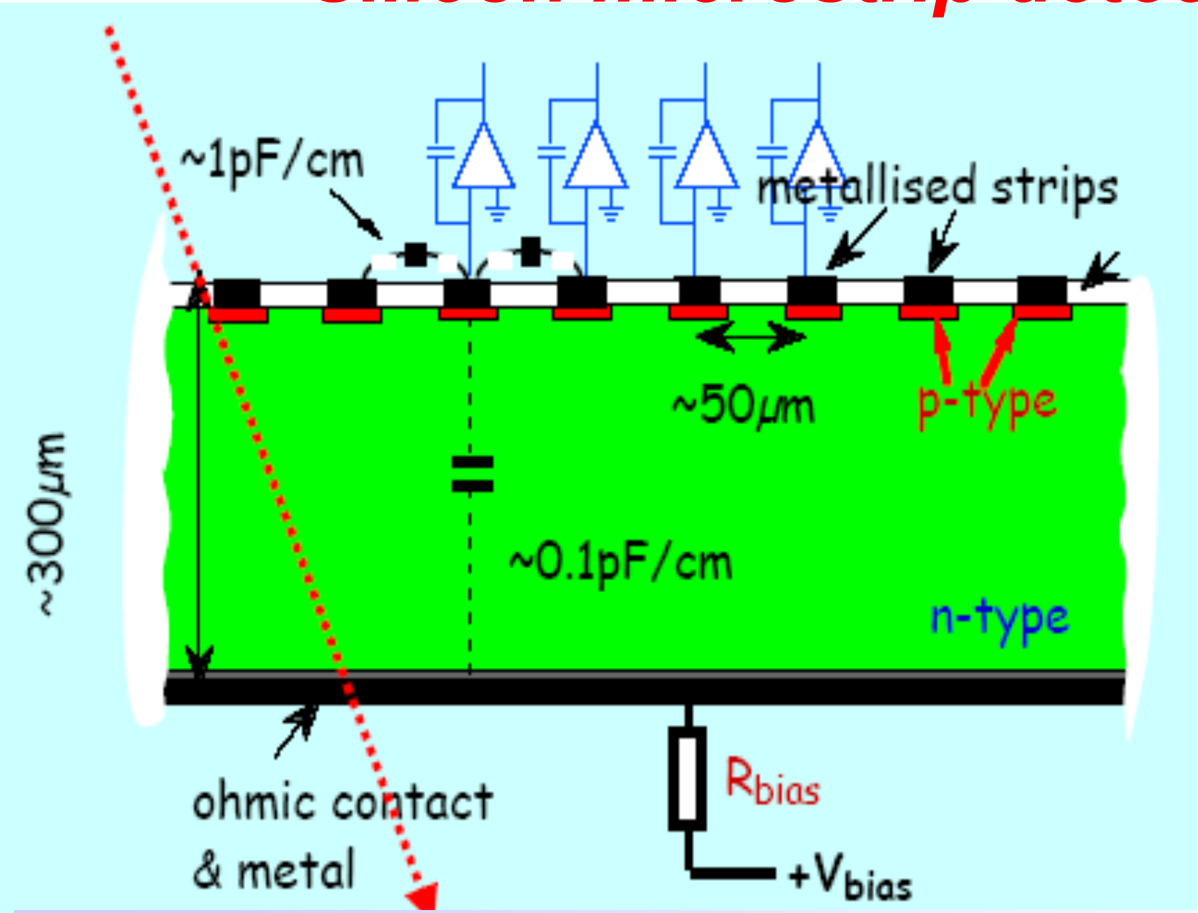

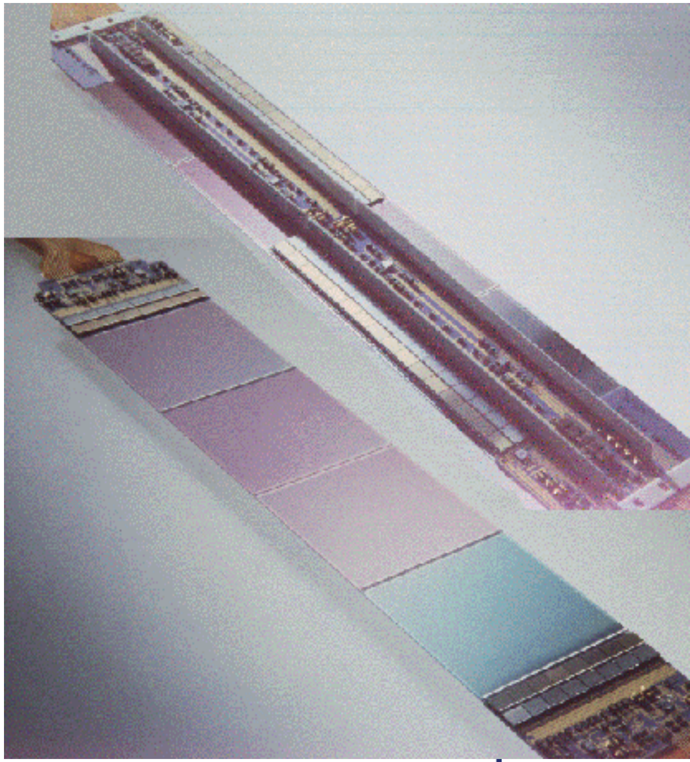

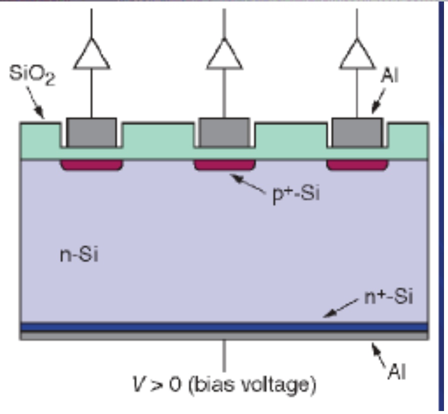

Charge Collection time

- Drift velocity of charge carriers $v \approx \mu E$, so drift time, $t_d = d/v = d/\mu E$

Typical values: d=300 μm, E= 2.5 kV/cm,
with μ_e= 1350 cm^2 / V·s and μ_h= 450 cm^2 / V·s

$\Rightarrow$ $t_d(e)$= 9ns , $t_d(h)$= 27ns

Silicon Detector

Every electrode is connected to an amplifier → Highly integrated readout electronics.

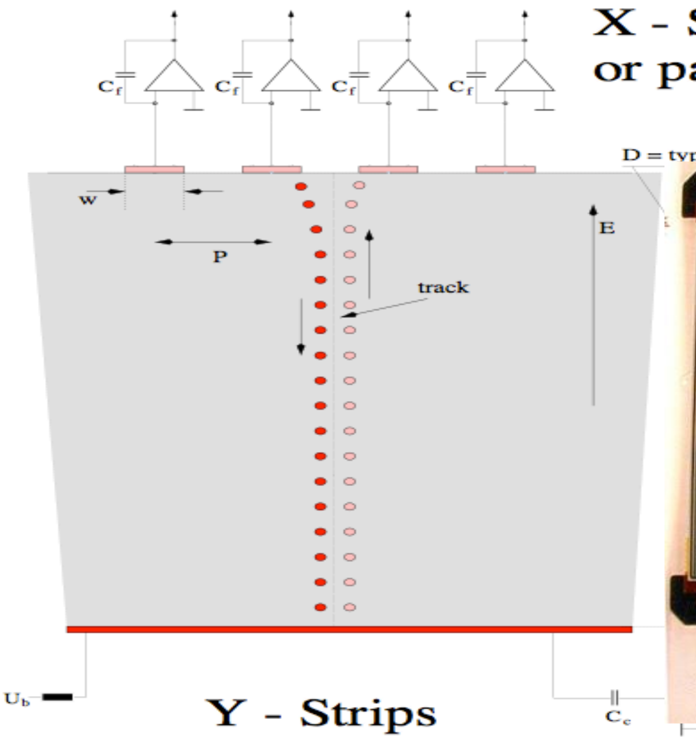

CMS Outer Barrel Module

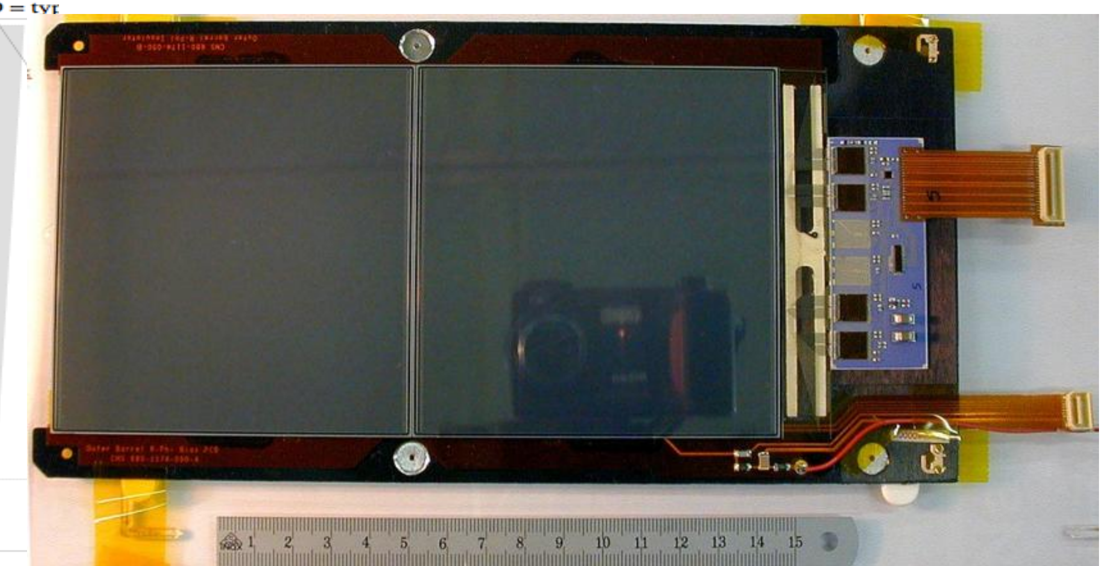

UNIVERSITÉ DE STRASBOURG

Micro-connexions Ø 17-25 µm

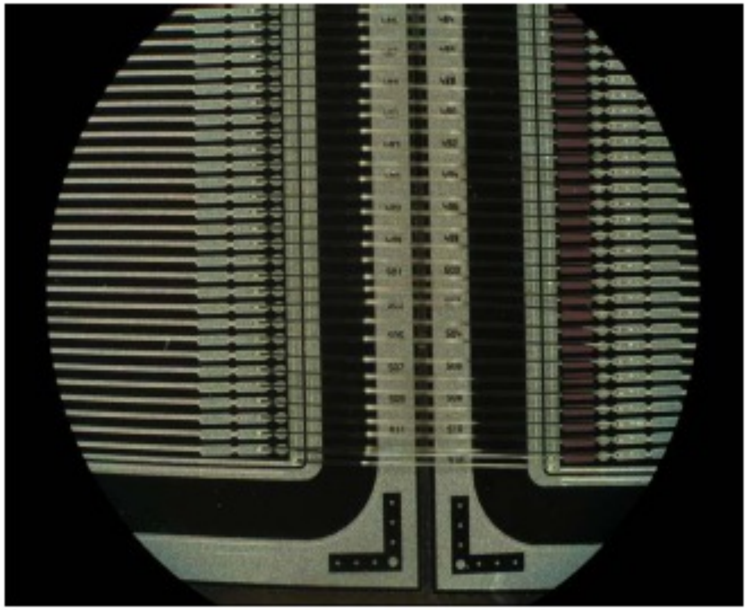

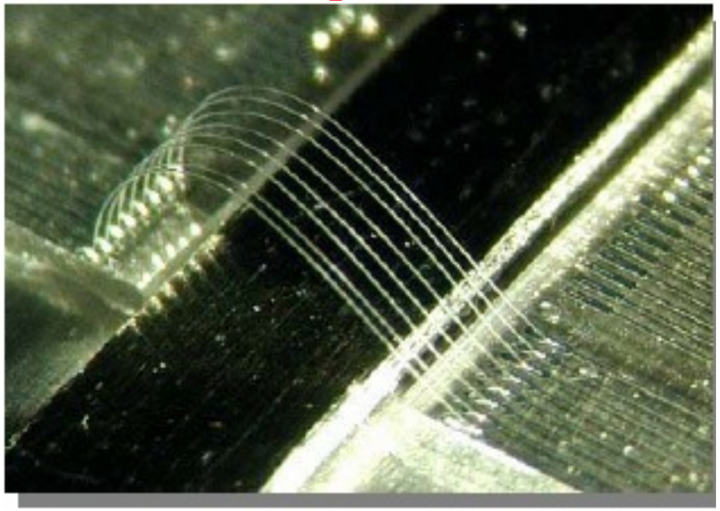

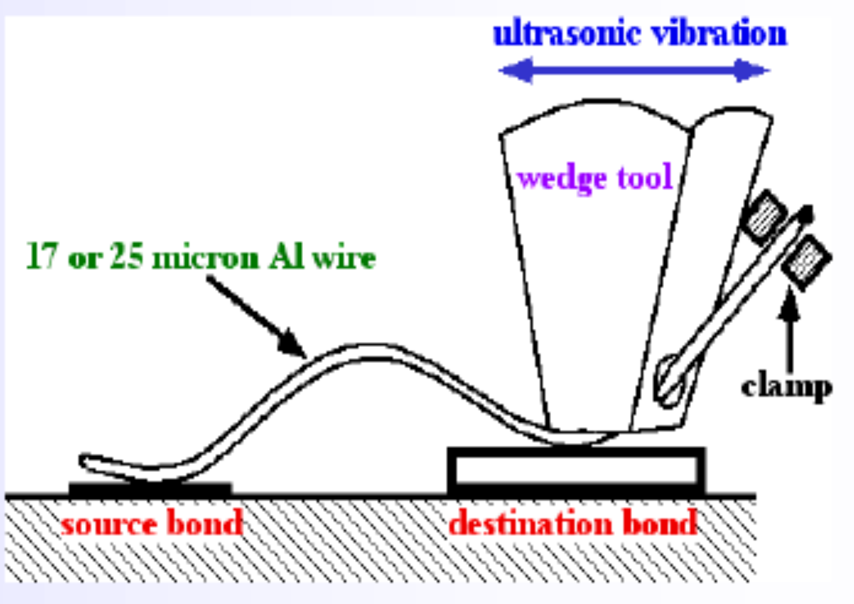

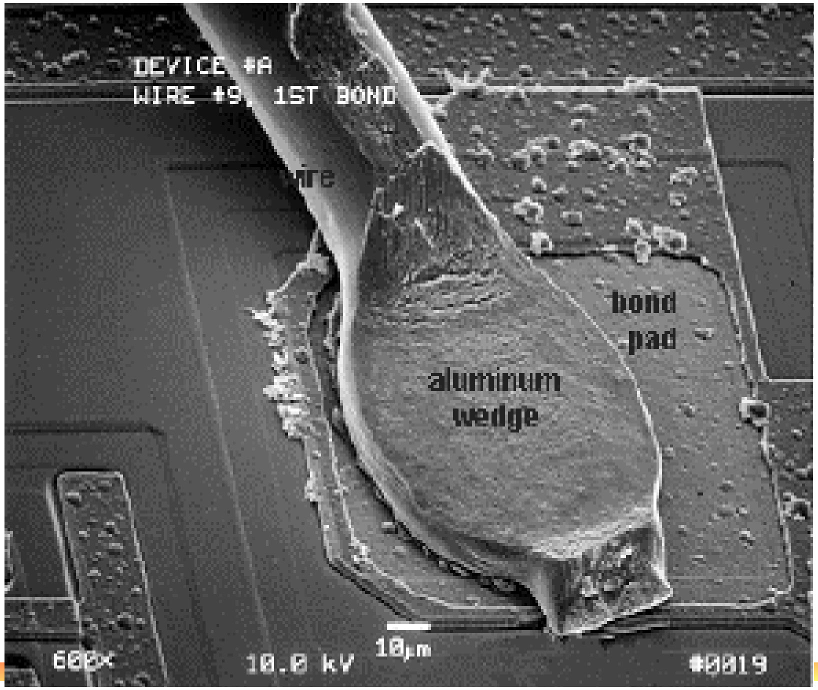

Hit resolution

The position resolution will depend on how many strips the charge is deposited on

Binary read-out

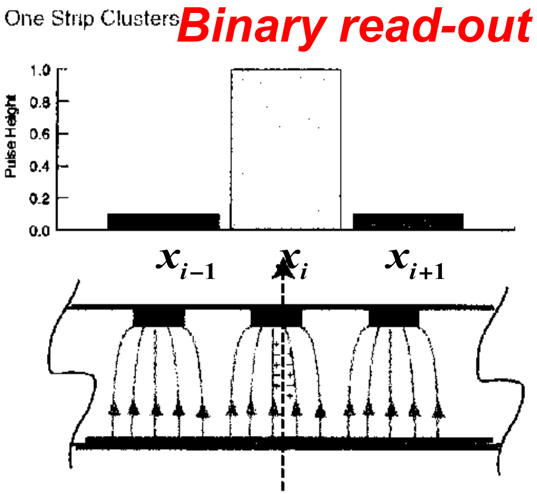

For 1 strip clusters the resolution is simply:

$$x = x_{i,(amplitude>seuil)}; \quad \Delta = x_i - x_{i-1}$$

$$\sigma_{hit} = \frac{\Delta}{\sqrt{12}}$$

$$\sigma^2 = \int_{-\infty}^{+\infty} P(x)(x-\mu)^2\,dx = \frac{1}{\Delta}\int_{-\Delta/2}^{+\Delta/2} x^2 dx$$

$$= \frac{1}{\Delta}\left[\frac{1}{3}x^3\right]_{-\Delta/2}^{+\Delta/2} = \frac{\Delta^2}{12}$$

Analog read-out

Centre of gravity

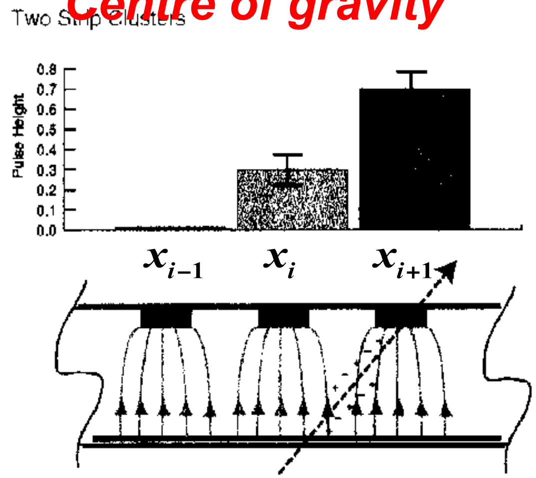

For 2 strip clusters the centroid calculation gives the resolution of :

$$x = \sum_{i=1}^{3} a_i x_i / A; \quad A = \sum_i a_i$$

$$\sigma_{hit} \propto \frac{\Delta}{2}\frac{Noise}{Signal}$$

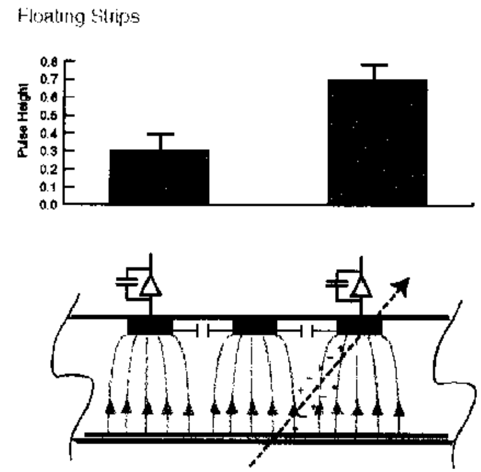

Because of capacitive coupling between strips, we don' t need to readout every strip to maintain good position resolution, BUT, because of stray capacitance to the back plane, some charge from the floating strip can be lost, causing problems.

The Charge Signal

extra slide not shown

Collected Charge for a Minimum Ionizing Particle (MIP)

- **Mean energy loss**
  dE/dx (Si) = 3.88 MeV/cm
  ⇒ 116 keV for 300μm thickness

- **Most probable energy loss**
  ≈ 0.7 ×mean
  ⇒ 81 keV

- **3.6 eV to create an e-h pair**
  ⇒ 72 e-h / μm (mean)
  ⇒ 108 e-h / μm (most probable)

- **Most probable charge** (300 μm)

  ≈ 22500 e ≈ 3.6 fC

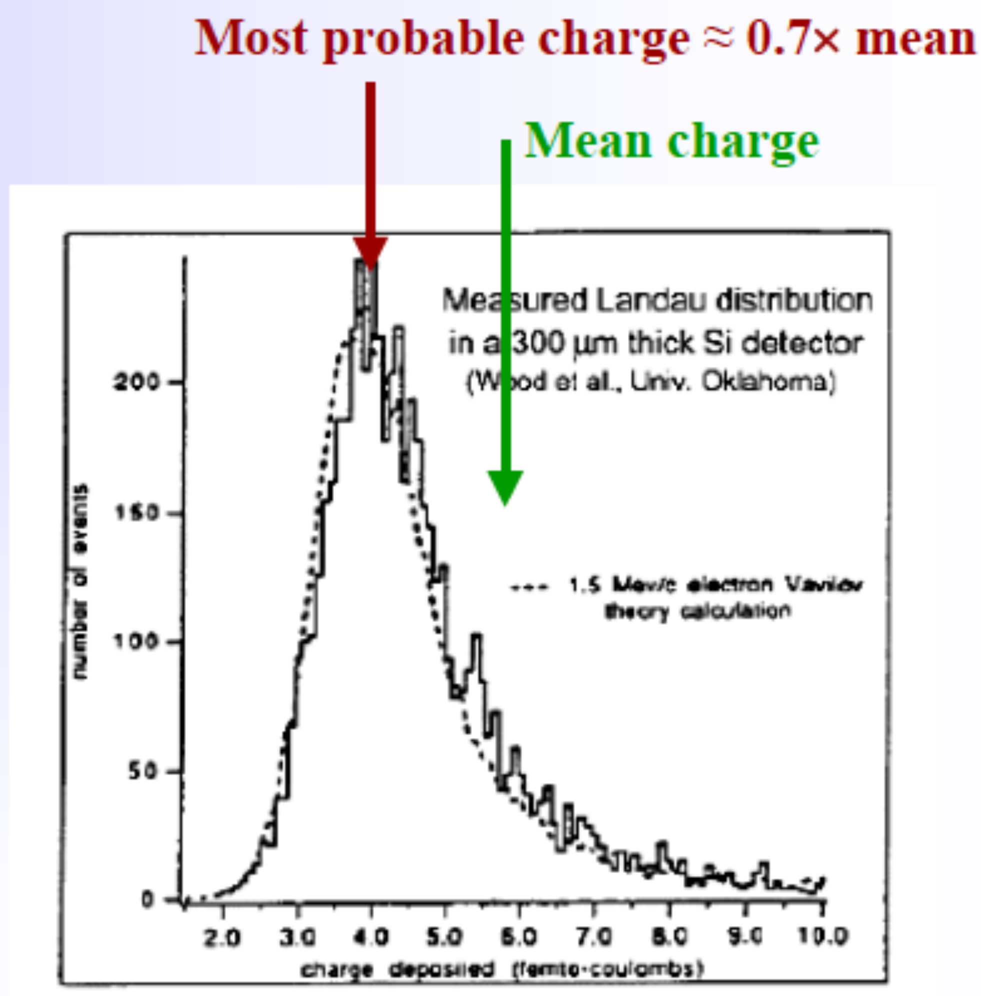

Signal to noise ratio (S/N)

- **Landau distribution** has a low energy tail
  - becomes even lower by noise broadening

Noise sources: (ENC = Equivalent Noise Charge)

- Capacitance $ENC \propto C_d$
- Leakage Current $ENC \propto \sqrt{I}$
- Thermal Noise (bias resistor) $ENC \propto \sqrt{k_B T / R}$

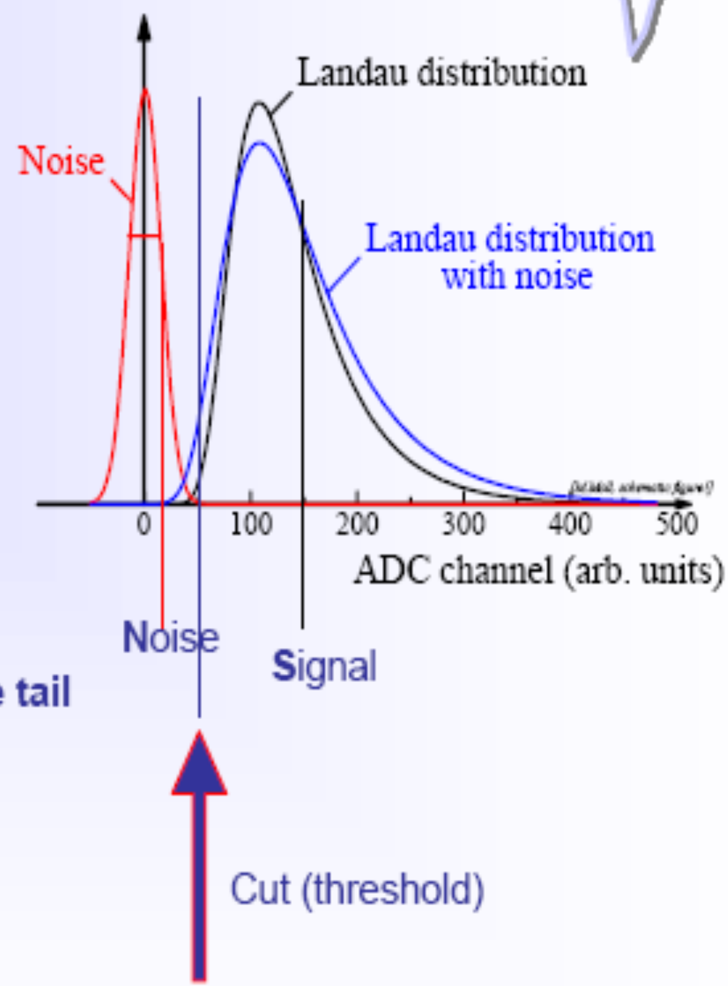

- **Good hits selected by requiring N_{ADC} > noise tail**
  If cut too high ⇒ efficiency loss
  If cut too low ⇒ noise occupancy
- **Figure of Merit: Signal-to-Noise Ratio S/N**
- **Typical values >10-15, people get nervous below 10.**
  Radiation damage severely degrades the S/N.

Silicon microstrip detector

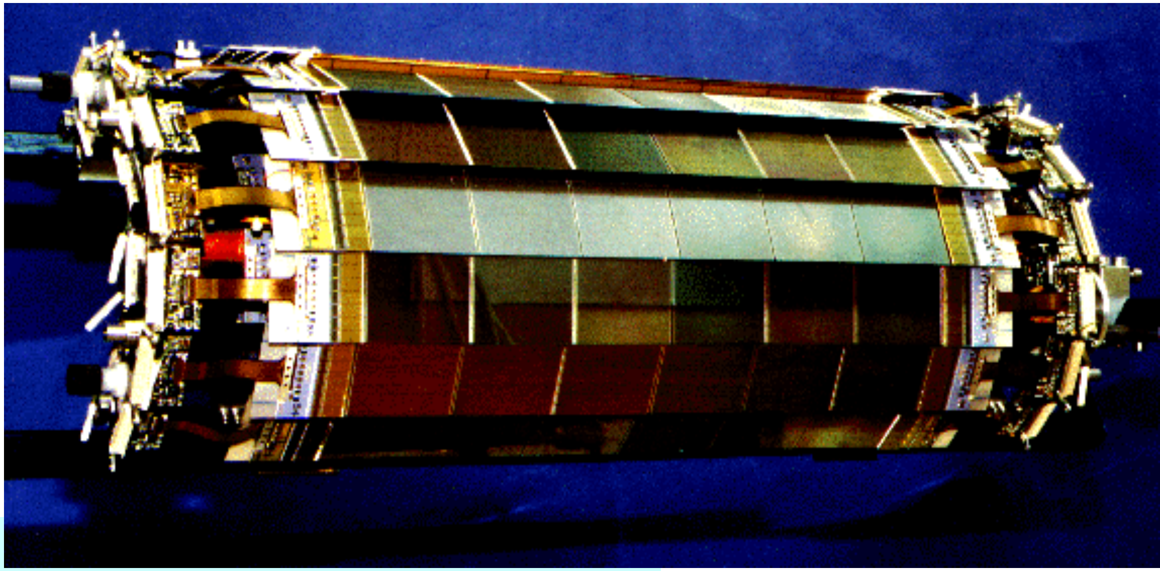

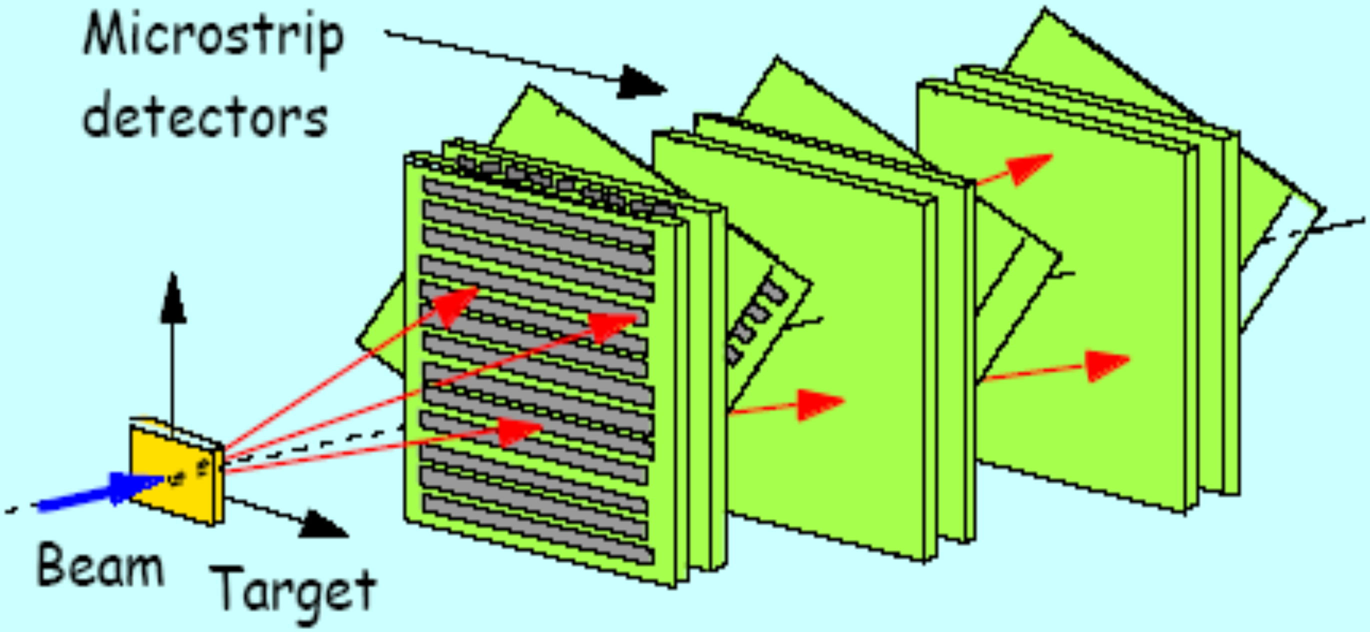

G.Hall

DELPHI, LEP

CMS Tracker

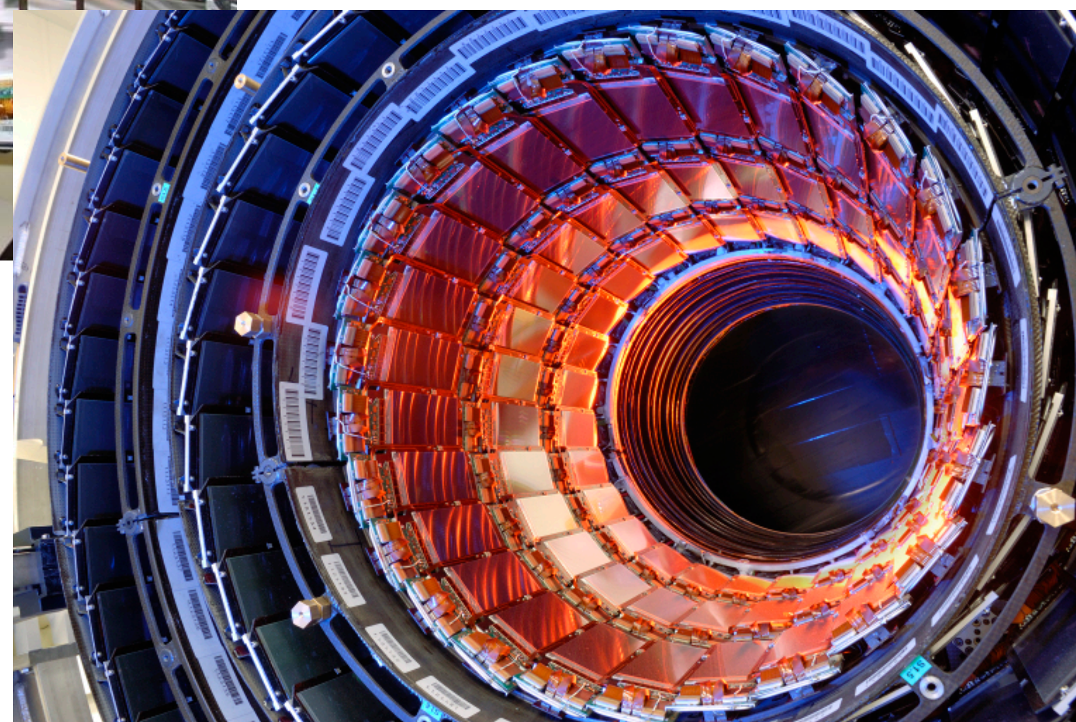

Pixel detectors

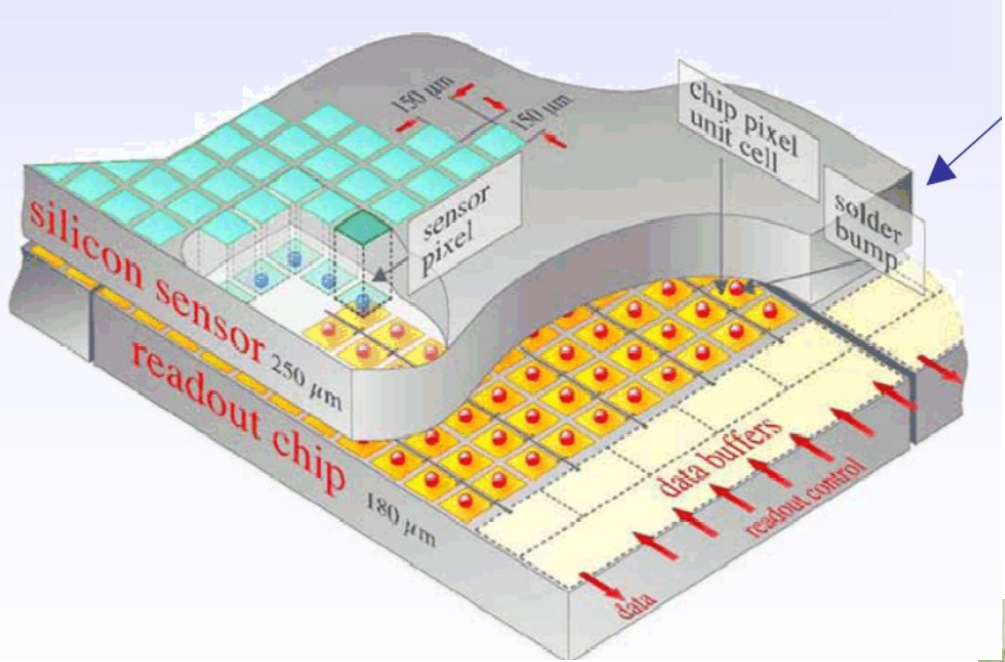

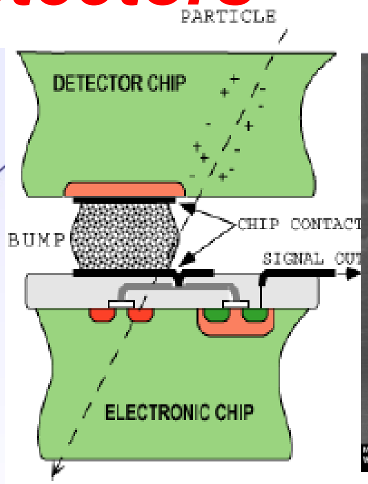

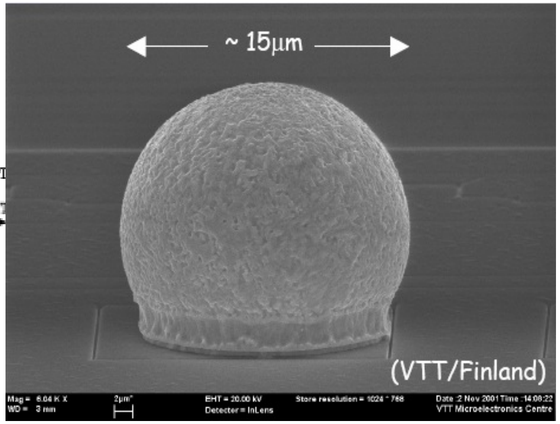

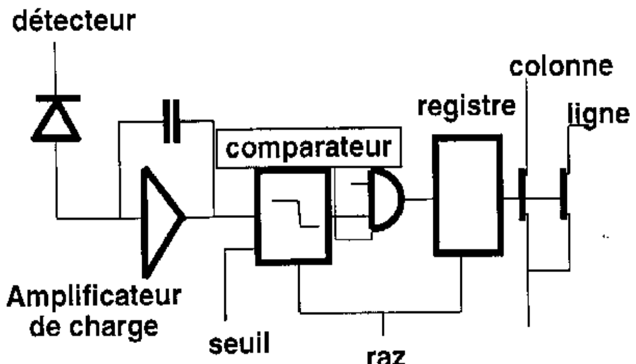

Pixel electronics: complex!

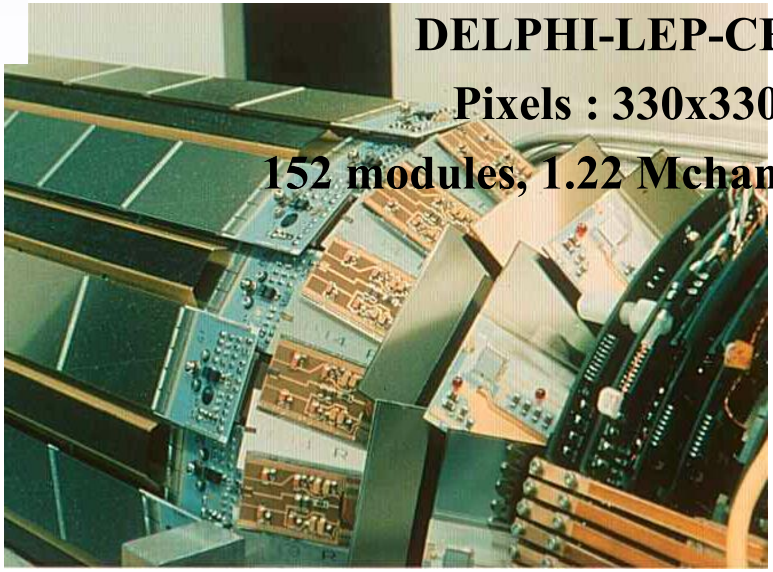

DELPHI-LEP-CERN
Pixels : 330x330 µm
152 modules, 1.22 Mchannels

UNIVERSITÉ DE STRASBOURG

iPHC
Institut Pluridisciplinaire Hubert CURIEN STRASBOURG

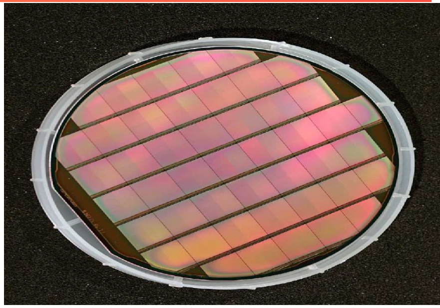

Monolithic Active Pixel Sensors IPHC

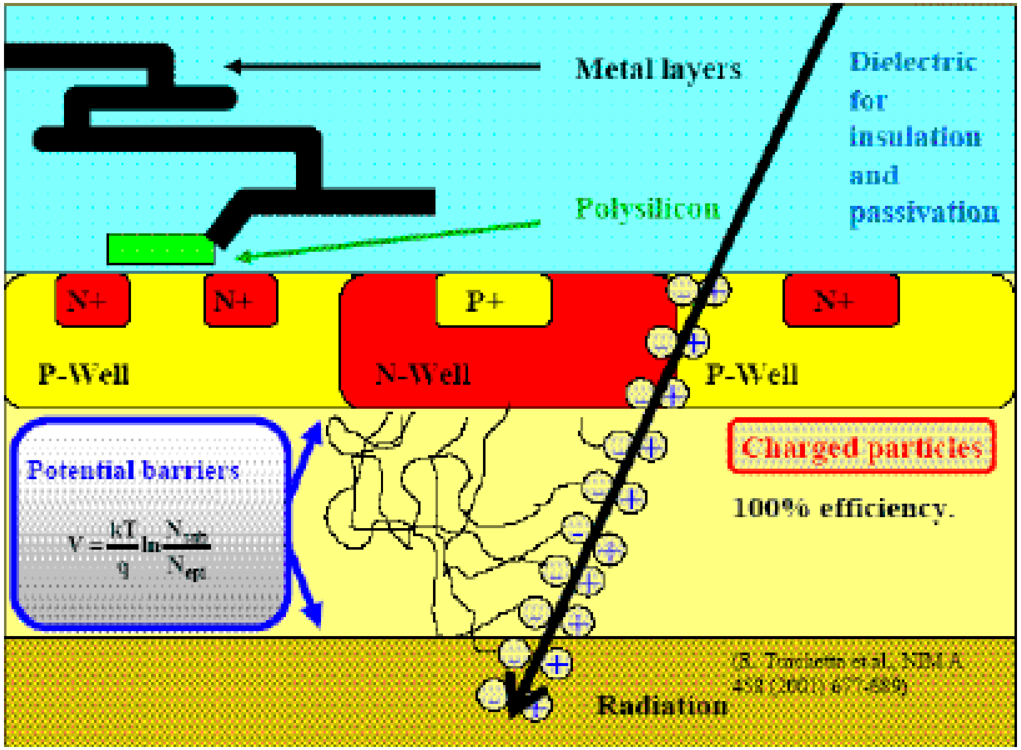

- charge collected at n-well / p-epi diode
- thermal diffusion of free charge
- reflection at potential barriers between areas with different doping concentration
- no depletion voltage applied
  ⇒ potential formed by different doping concentrations only

UNIVERSITÉ DE STRASBOURG

Detection of nuclear gammas

Semiconductors

Materials used for detectors

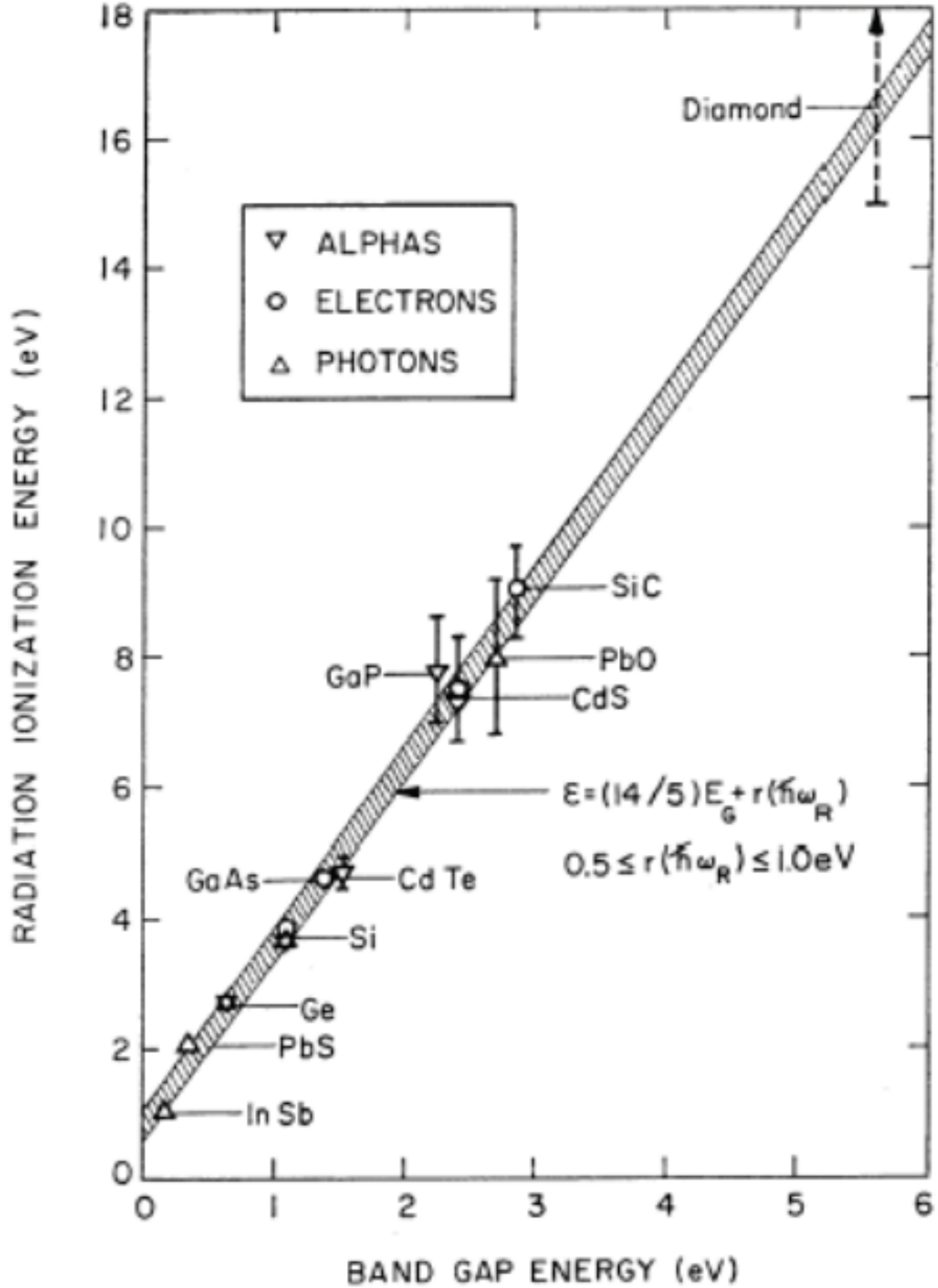

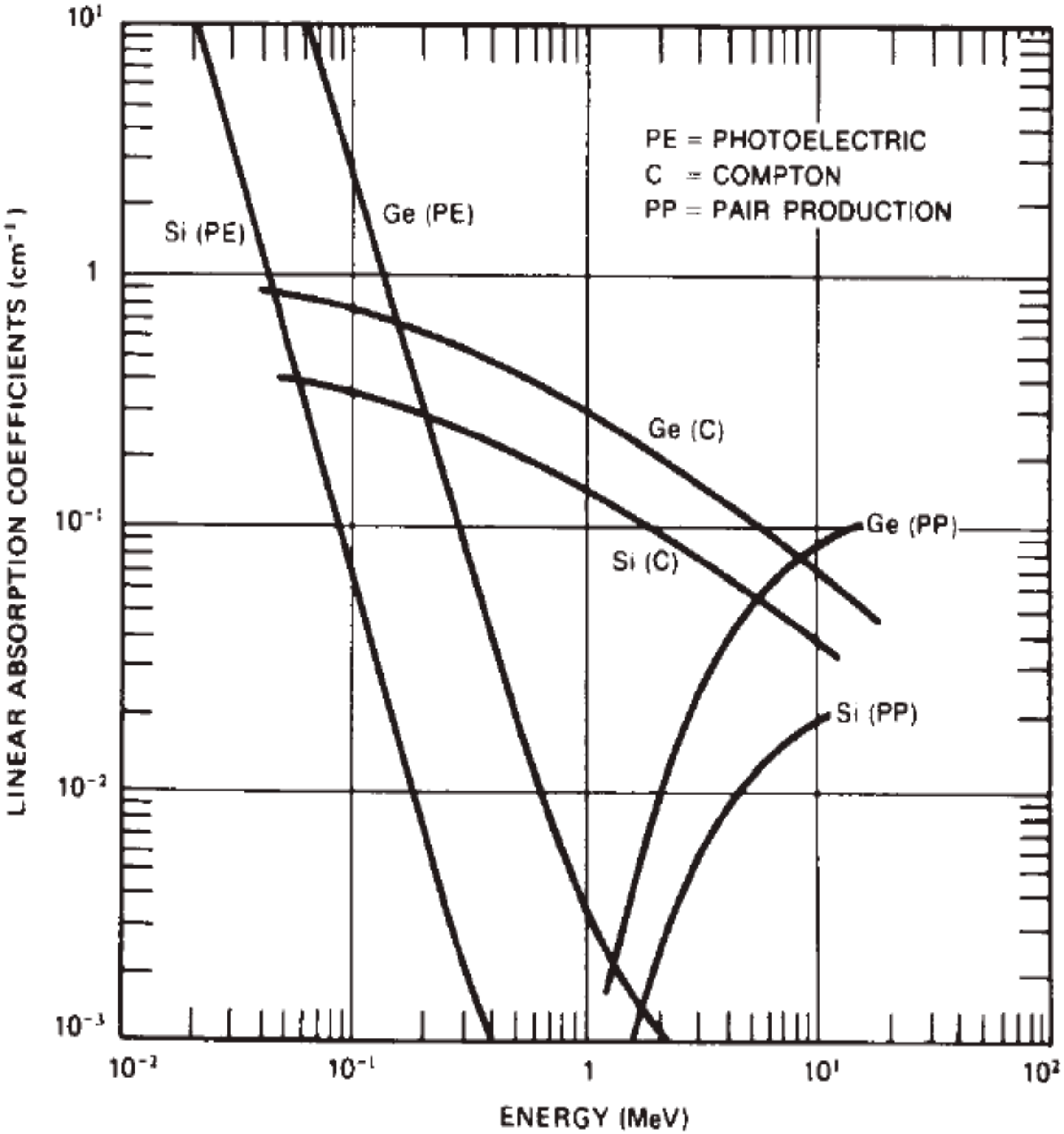

High Purity Germanium

Energy measurement of gammas

($|N_A-N_D| \cong 10^{10}\ cm^{-3}$):

- E_{gap} = 0.74 eV ⇒ operation temperature : T= 77K
- w_{eh}=2.98 eV ⇒excellent resolution
  - E_γ = 1 MeV, dE ≅ 1 keV
  - "High" photo peak efficiency

UNIVERSITÉ DE STRASBOURG

Large volume detectors

- **Depletion zone :**

$$d\Big|_{V_{bias}} = x_n + x_p = \sqrt{\frac{2\varepsilon\left(\phi_0 + V_{bias}\right)}{e}\frac{\left(N_A + N_D\right)}{N_A N_D}}$$

$$N = N_A \ll N_D;\; \phi_0 \ll V_{bias}$$

$$d\Big|_{V_{bias}} = \sqrt{\frac{2\varepsilon V_{bias}}{eN}}\;;\; N = N_A \text{ ou } N_D = \text{net impurity of material}$$

$$N = 10^{+13}\, atoms/cm^3;\; V_{bias} = 3000\,Volt;$$

$$d\Big|_{V_{bias}=3000Volt} = 2.2\,mm$$

- **High purity :**

$$N_A \; ou \; N_D = 10^{+10}\, atoms/cm^3;\; V_{bias} = 1000\,Volt;\; \varepsilon = 16\cdot\varepsilon_0;$$

$$\varepsilon_0 = 8.85\cdot 10^{-12}\, F/m;\; F = Coulomb/Volt\;;\; e = 1.6\cdot 10^{-19}\, Coulomb$$

$$d\Big|_{V_{bias}=1000Volt} = 1.8\,cm$$

$$d\Big|_{V_{bias}=2000Volt} = 2.5\,cm$$

$$d\Big|_{V_{bias}=3000Volt} = 3.1\,cm$$

Germanium detectors

Operation temperature: T= 77K (Liquid Nitrogen)

Configuration : co-axial

Electronics is mounted very close to the Crystal

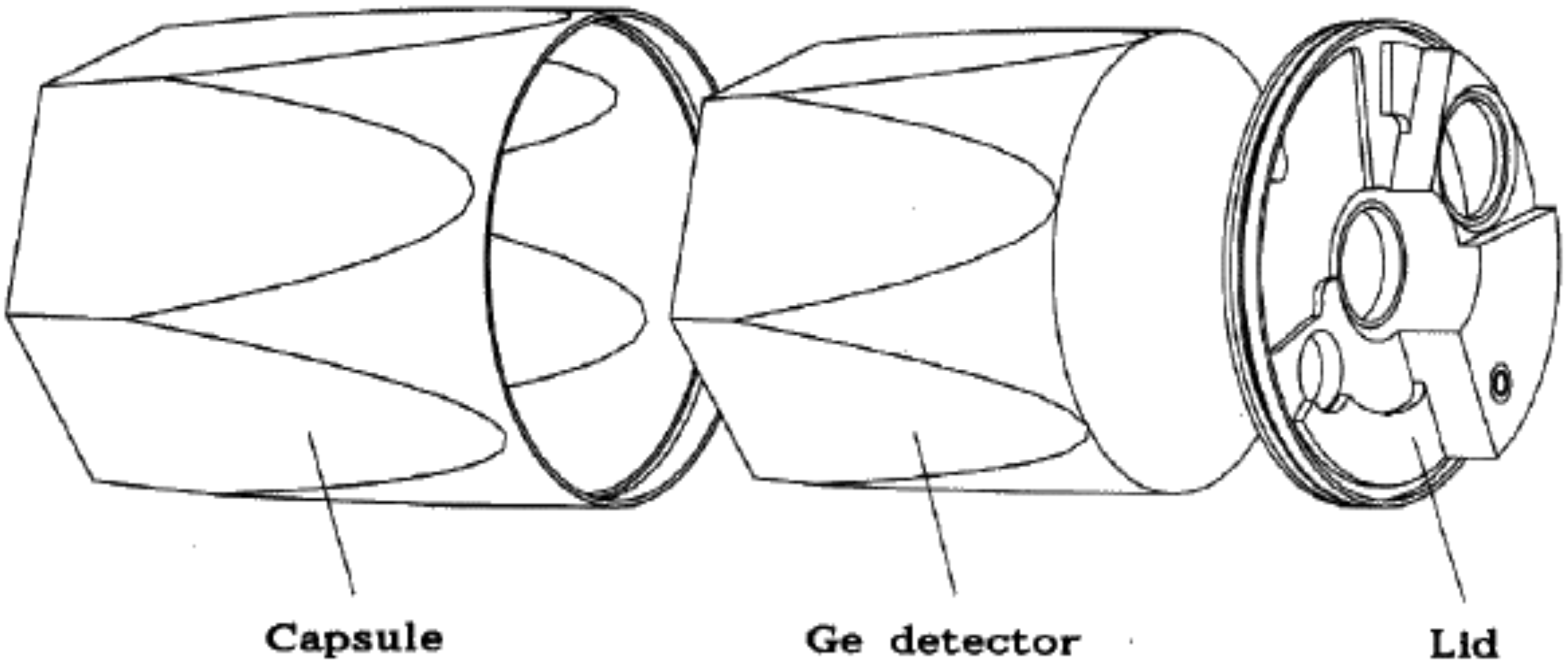

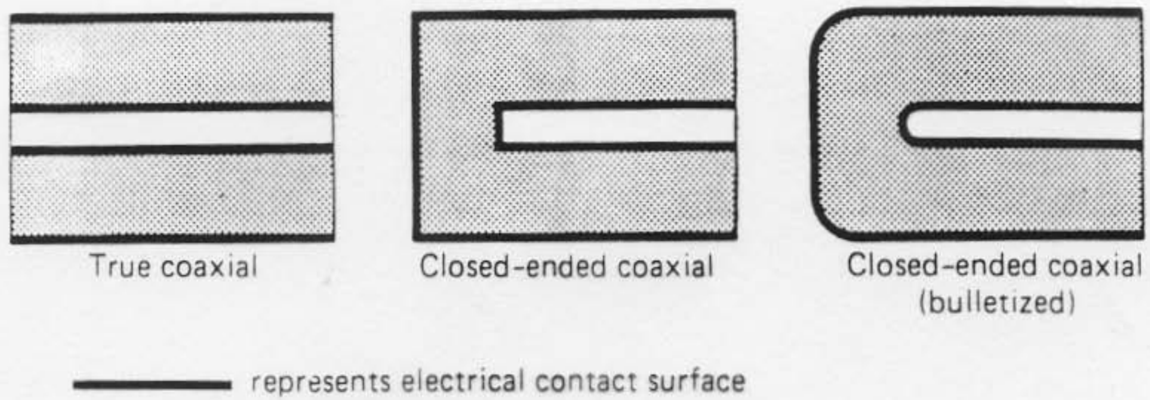

p^+: implanted Boron
n^+: diffused Lithium

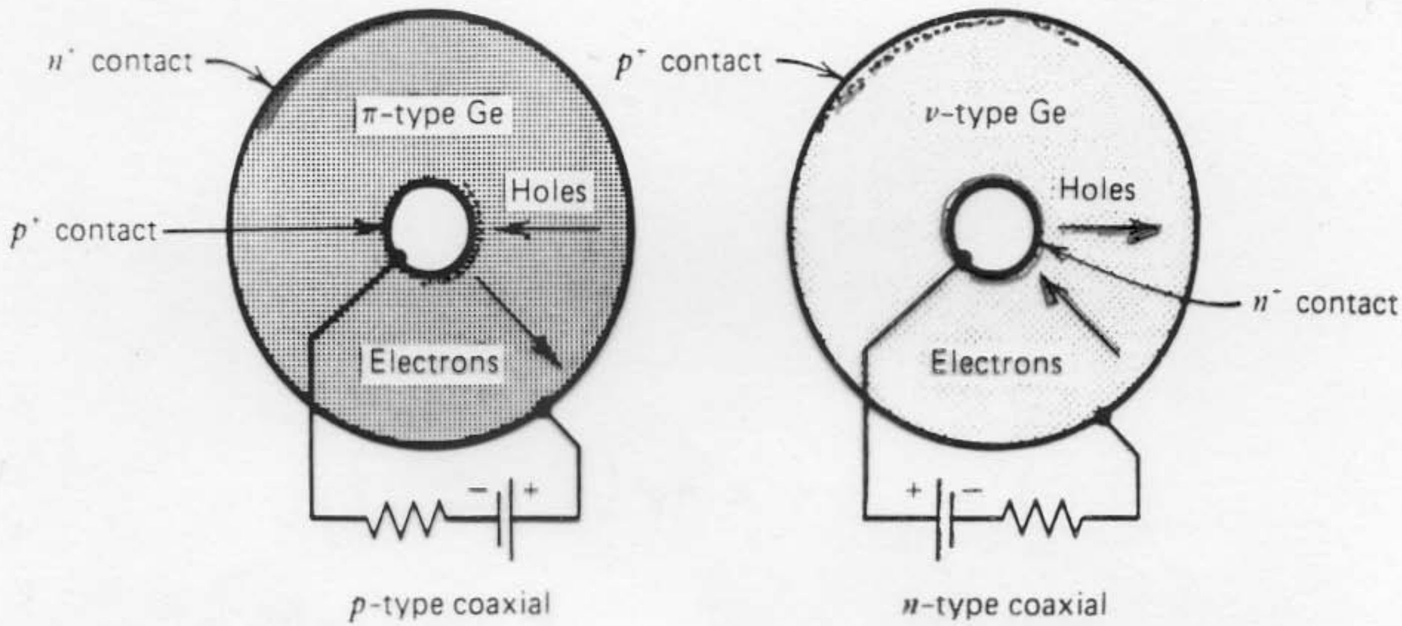

Typical mounting of an Germanium detector (here a Ge(Li))

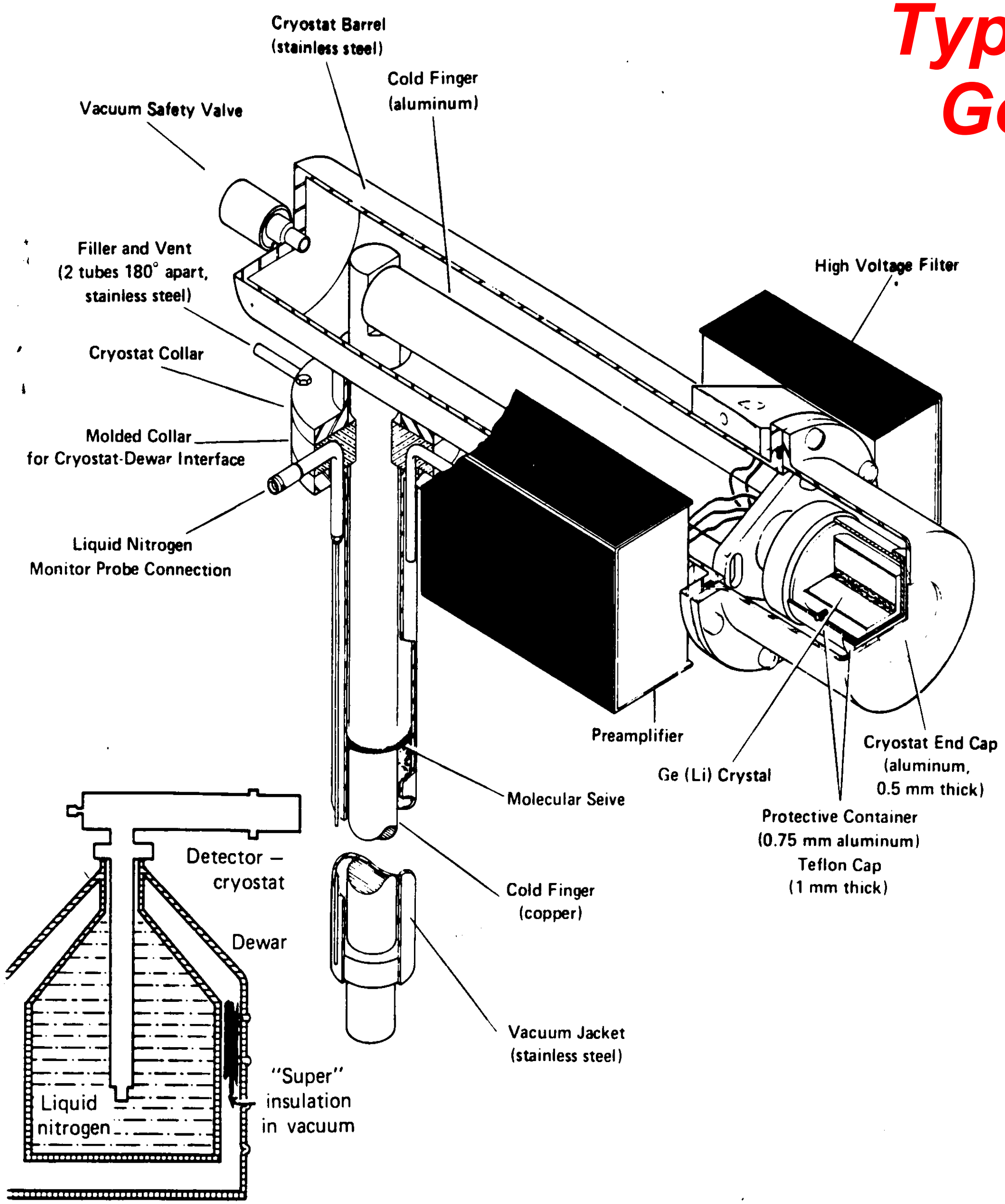

Spectrum of ^{60}Co with HPGe

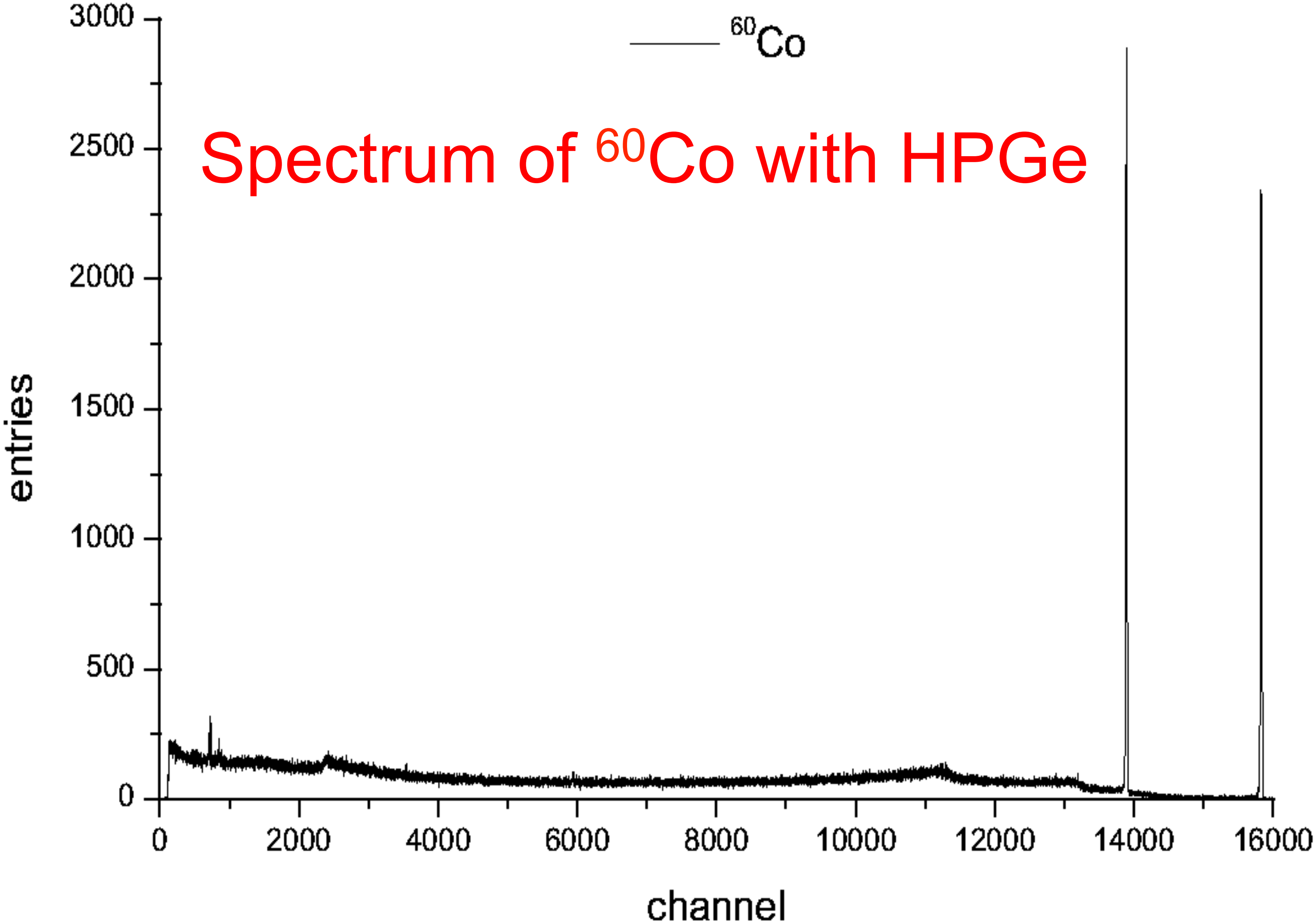

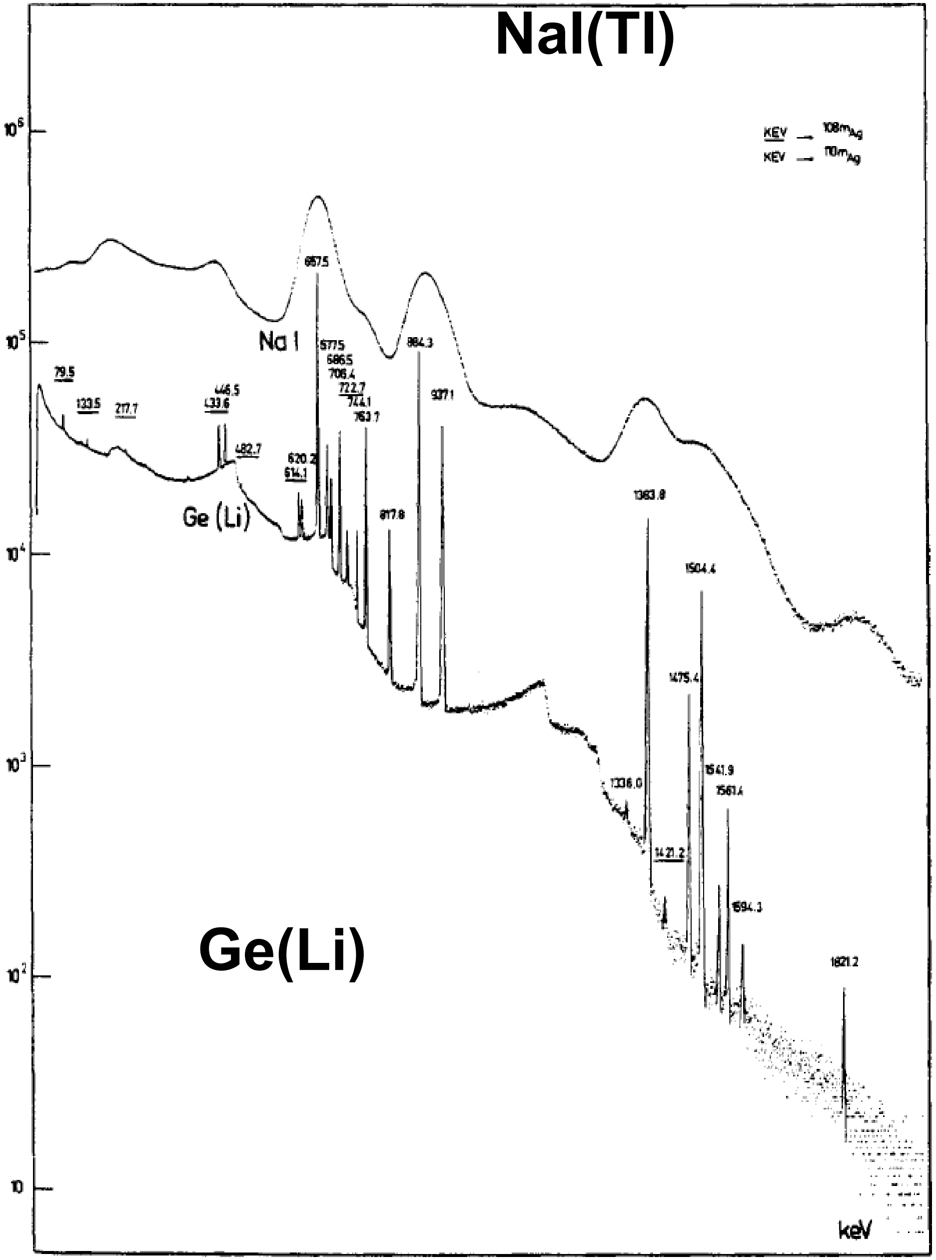

$$N_{eh} = \frac{E}{w}\varepsilon_{collection}$$

$$dN_{eh} = \sqrt{N_{eh}} = \sqrt{\frac{E}{w}\varepsilon_{collection}}$$

Statistics : Poisson

$\Rightarrow \sigma^2 = \mu; \quad \mu = \text{mean}; \sigma^2 = \text{variance}$

$$dE / E = dN_{eh} / N_{eh} \sim \frac{1}{\sqrt{N_{eh}}} = \frac{1}{\sqrt{\frac{E}{w}\varepsilon_{collection}}}$$

$\varepsilon_{collection} \approx 100\%; \; w = 2.98\,eV \quad E = 1\,MeV$

$\Rightarrow dE / E \approx 0.0017;$ Resolution $R = 2.35 \times dE / E = 0.4\%$

Fano factor:

$\sigma^2 = F_{ano}\mu;$

$F_{ano} \simeq 0.12\,(Ge, Si); \quad \sqrt{0.12} = 1/2.9$

$$dE / E = dN_{eh} / N_{eh} \sim \frac{\sqrt{F}}{\sqrt{N_{eh}}} = \frac{1}{\sqrt{\frac{E}{wF}\varepsilon_{collection}}}$$

$dE / E = 0.0006;$ Resolution $R = 2.35 \times dE / E = 0.14\%$

NaI:

$w = 25\,eV / photon_{\text{scint}}$ Light collection: 0.5 PM: $Q.E. \approx 0.20$

$dE / E \approx 1.6\%$ Resolution $R = 2.35 \times dE / E = 3{,}7\%$ à $1\,MeV$

Calorimetry

Calorimeters

- At very high energies the momentum resolution of any magnetic spectrometer will deteriorate rapidly
- Interactions at high energies
  - Electromagnetic showers (electrons, gammas, π^0…
  - Hadronic showers, all hadrons!
- Working principle
  - The energy of the incident particle is transformed into a large number of secondary particles which can be measured
  - The number of secondaries is proportinal to the energy
  - Ionisation, scintillation Cerenkov…

Elm : Conversion of photons into e^+e^- Bremsstrahlung

Had : Nuclear interactions, fragmentation

Showers in calorimeters

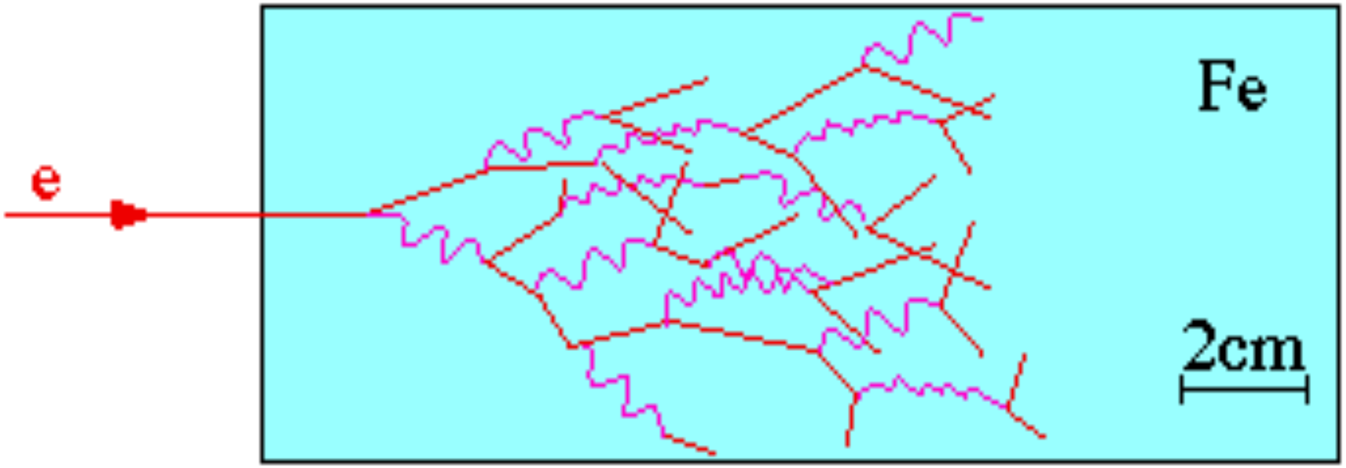

Electromagnetic shower

radiation length X_0

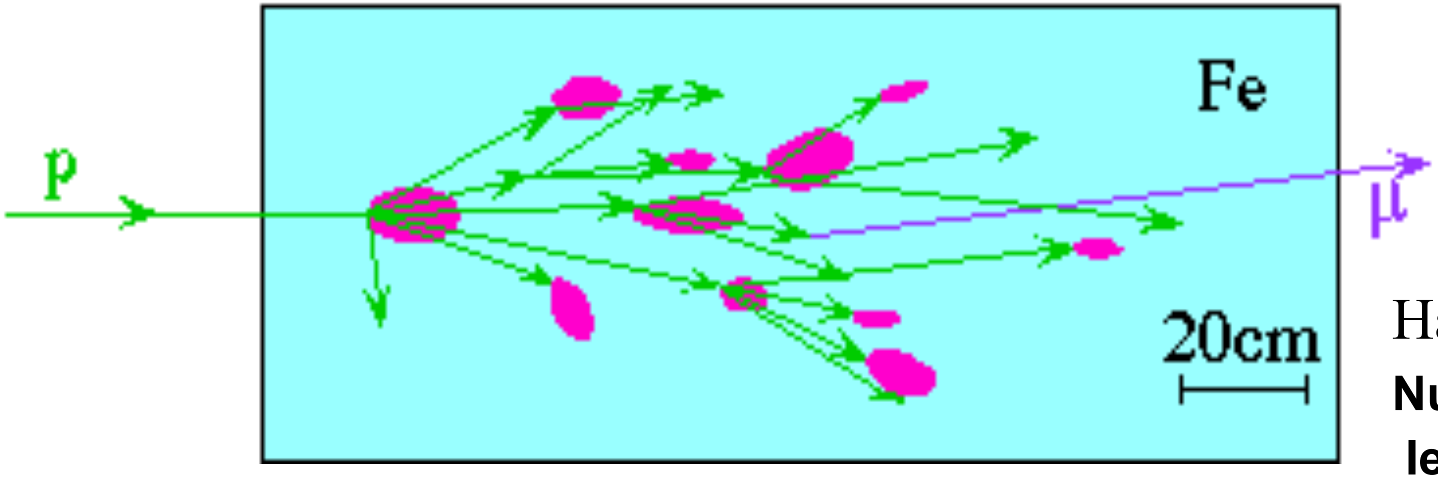

Hadronic shower

Nuclear interaction length Λ

UNIVERSITÉ DE STRASBOURG

Energy resolution

$$\frac{\sigma(E)}{E} = \frac{a}{\sqrt{E}} \oplus b \oplus \frac{c}{E}$$

Also spatial and angular resolution scale like $1/\sqrt{E}$

stochastic term
(see above)

'constant term'

- inhomogenities
- bad cell inter-calibration
- non-linearities

Quality factor !

'noise term'

- Electronic noise
- radioactivity
- pile up

Electromagnetic shower

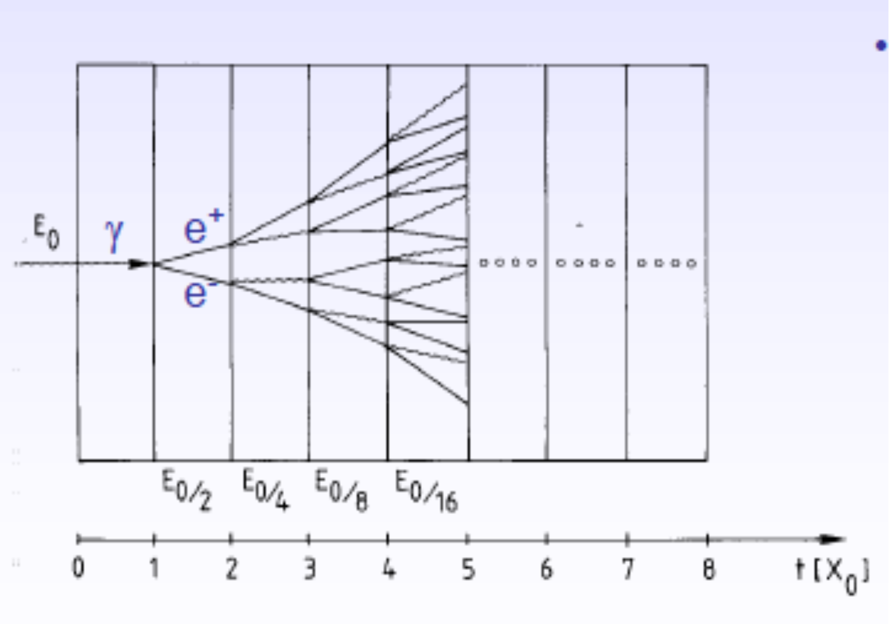

$N(t) = 2^t \qquad E(t)/particle = E_0 \cdot 2^{-t}$

Process continues until $E(t)<E_c$

$$N^{total} = \sum_{t=0}^{t_{max}} 2^t = 2^{(t_{max}+1)} - 1 \approx 2 \cdot 2^{t_{max}} = 2\frac{E_0}{E_c}$$

$$t_{max} = \frac{\ln E_0/E_c}{\ln 2}$$

PbW0$_4$ CMS, X$_0$=0.89 cm

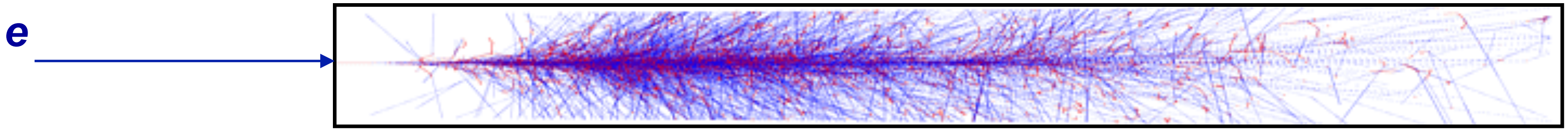

$$t_{max} = \ln \frac{E_0}{E_c} \frac{1}{\ln 2}$$

95% in a cone of R_M

$$R_M = \frac{21\,\text{MeV}}{E_c} X_0 \quad [g/cm^2]$$

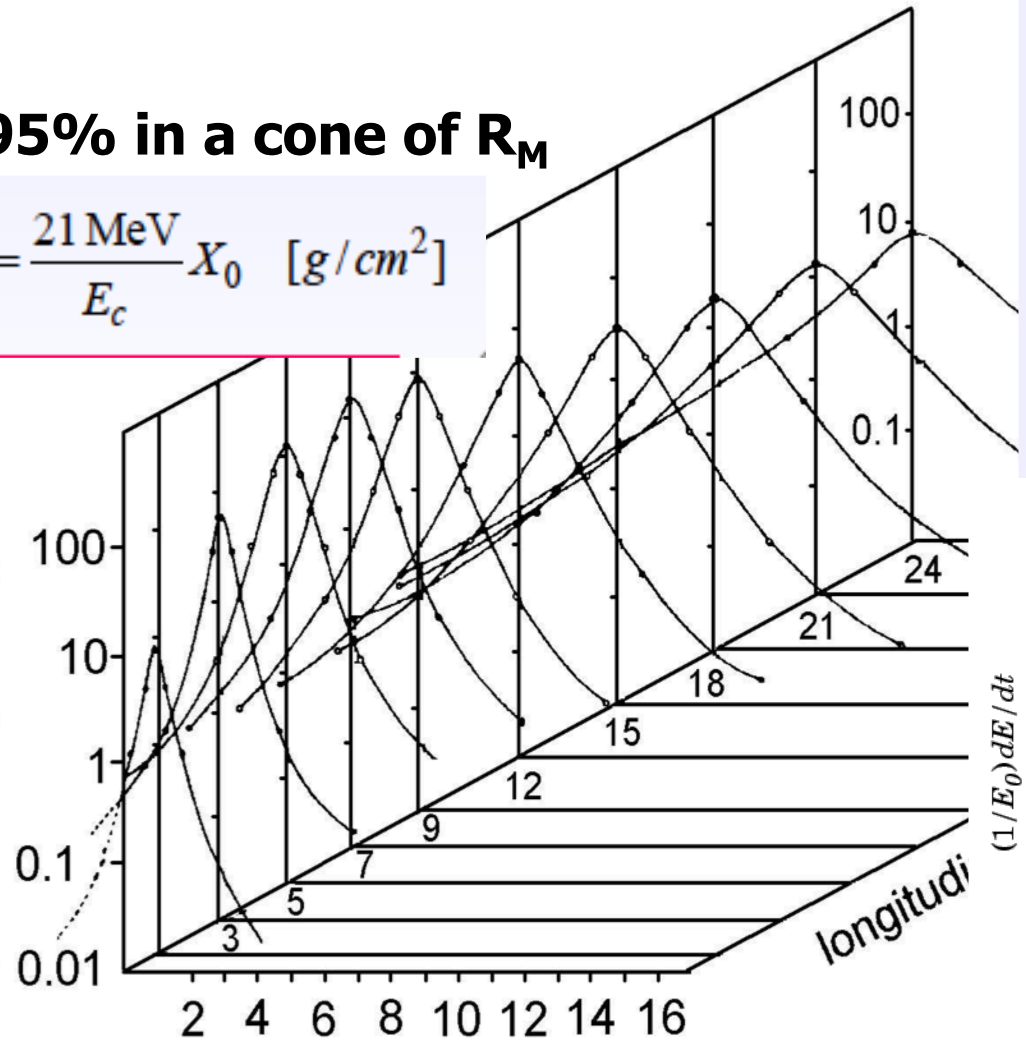

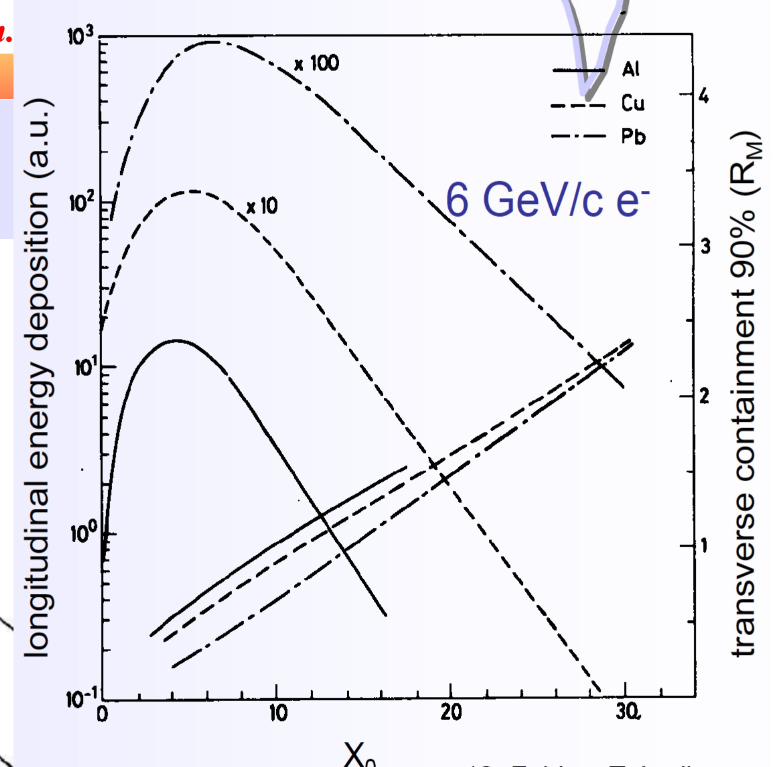

(C. Fabjan, T. Ludlam,

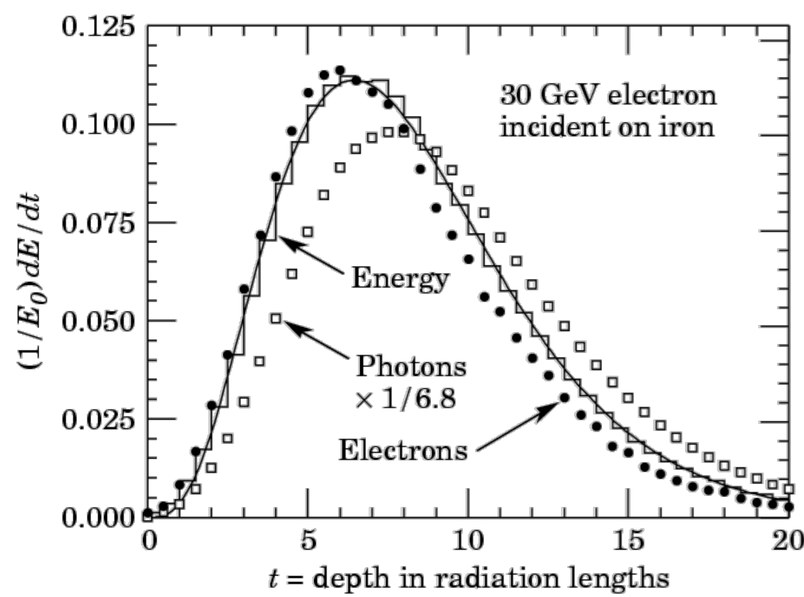

Radiation length

milieu	*Z*	*A*	X_0 (g/cm^2)	X_0 (cm)	E_C (MeV)
hydrogène	1	1.01	63	700000	350
hélium	2	4	94	530000	250
lithium	3	6.94	83	156	180
carbone	6	12.01	43	18.8	90
azote	7	14.01	38	30500	85
oxygène	8	16	34	24000	75
aluminium	13	26.98	24	8.9	40
silicium	14	28.09	22	9.4	39
fer	26	55.85	13.9	1.76	20.7
cuivre	29	63.55	12.9	1.43	18.8
argent	47	109.9	9.3	0.89	11.9
tungstène	74	183.9	6.8	0.35	8
plomb	82	207.2	6.4	0.56	7.4
air	7.3	14.4	37	30000	84
silice (SiO_2)	11.2	21.7	27	12	57
eau	7.5	14.2	36	36	83

ATLAS and CMS EM Calorimeters

CMS: $PbWO_4$ Scint. Crystal Calorimeter

Entire shower in active detector material
- High density crystals (28 X_0)
- Transparent, high light yield
- No particles lost in passive absorber
- High resolution: ~3% / $\sqrt{E}$ (stochastic)

Granularity
- Barrel: $\Delta\eta \times \Delta\phi = 0.017^2$ rad
- Longitudinal shower shape unmeasured

Read out with avalanche photo diodes

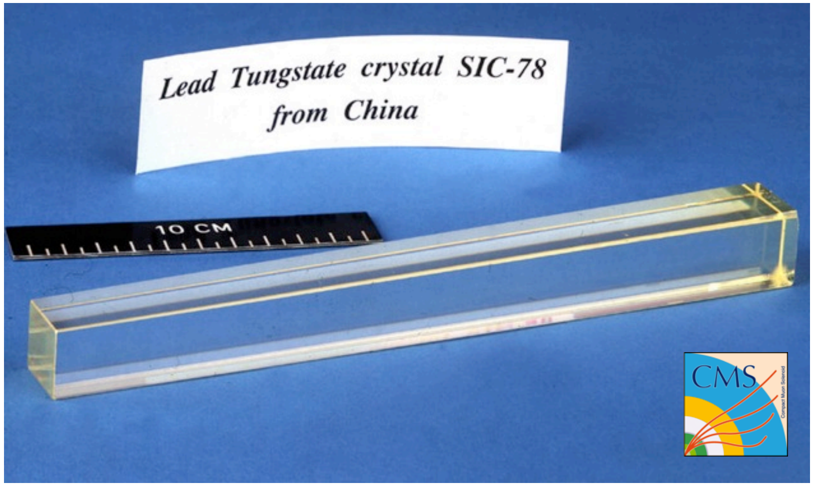

ATLAS: LAr Sampling Calorimeter

- Passive, heavy absorber (Pb, 1.1–1.5 mm thick [barrel]) inter-leaved with active detector material (liquid argon)
  - Overall 22 X_0
  - Accordion structure for full ϕ coverage
  - Resolution: ~10% / $\sqrt{E}$ (stochastic)
- Granularity
  - Barrel: $\Delta\eta \times \Delta\phi = 0.025^2$ rad (main layer)
  - Longitudinal segmentation (3 layers)

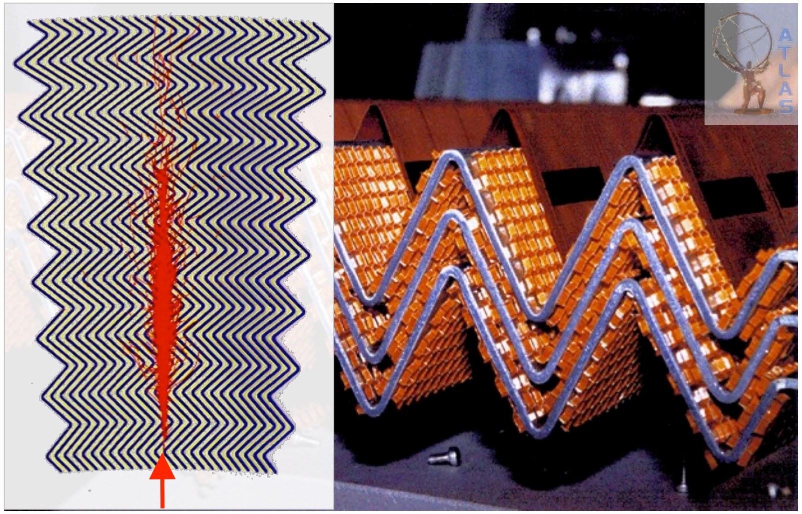

UNIVERSITÉ DE STRASBOURG

The Electromagnetic Calorimeter - ECAL

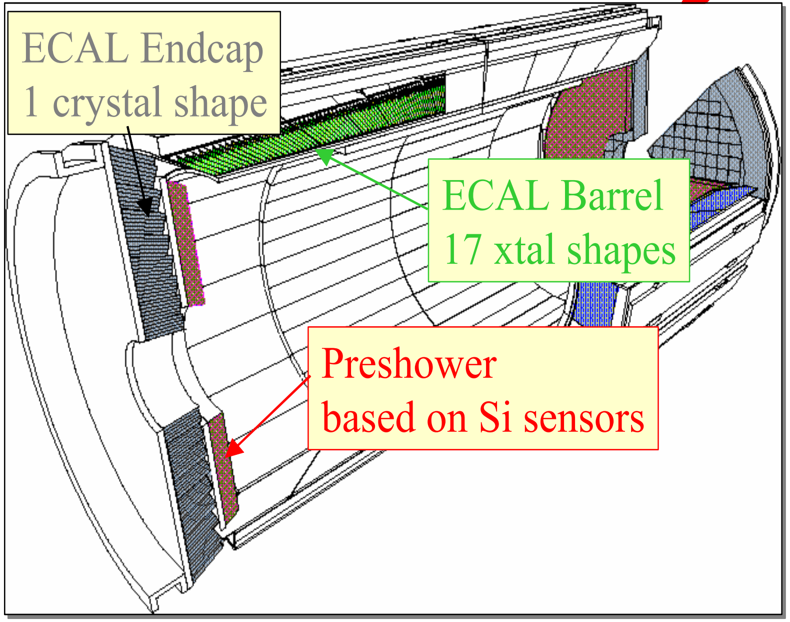

78,000 crystals

2.2 x 2.2 x 23cm (barrel)

3 x 3 x 22cm (endcaps)

Characteristics of $PbWO_4$
$X_0 = 0.89$cm
$\rho = 8.28$g/cm^3
R_M (Molière radius) = 2.2cm

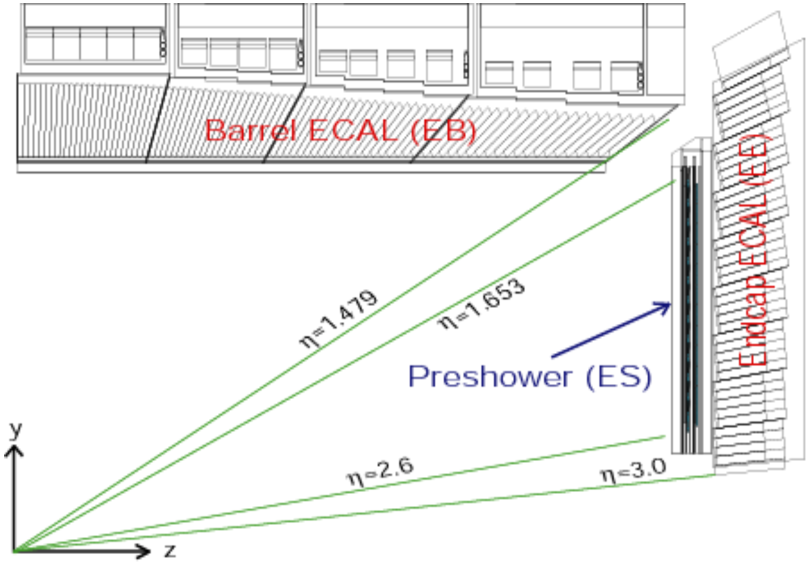

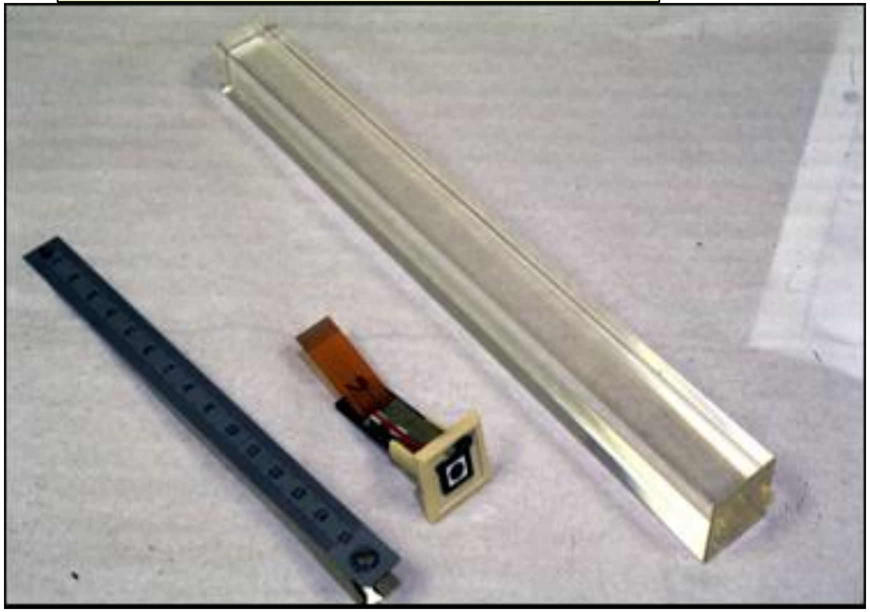

The Electromagnetic Calorimeter - ECAL

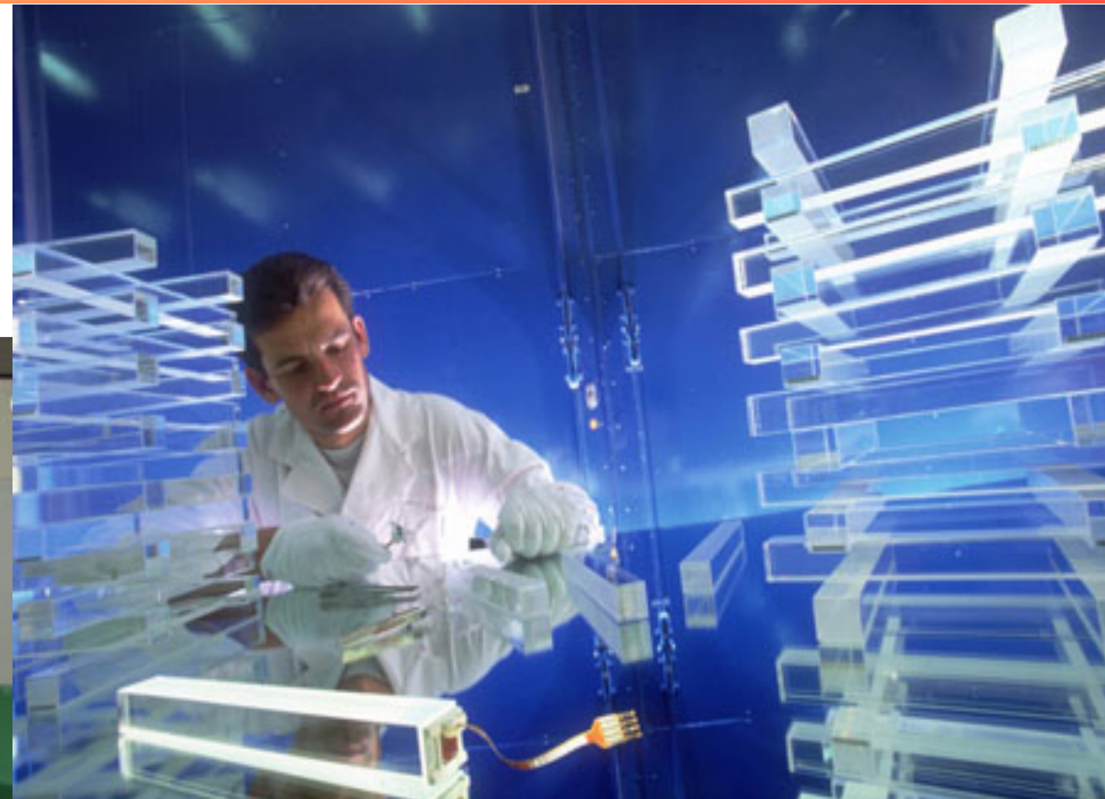

UNIVERSITÉ DE STRASBOURG

Energy resolution

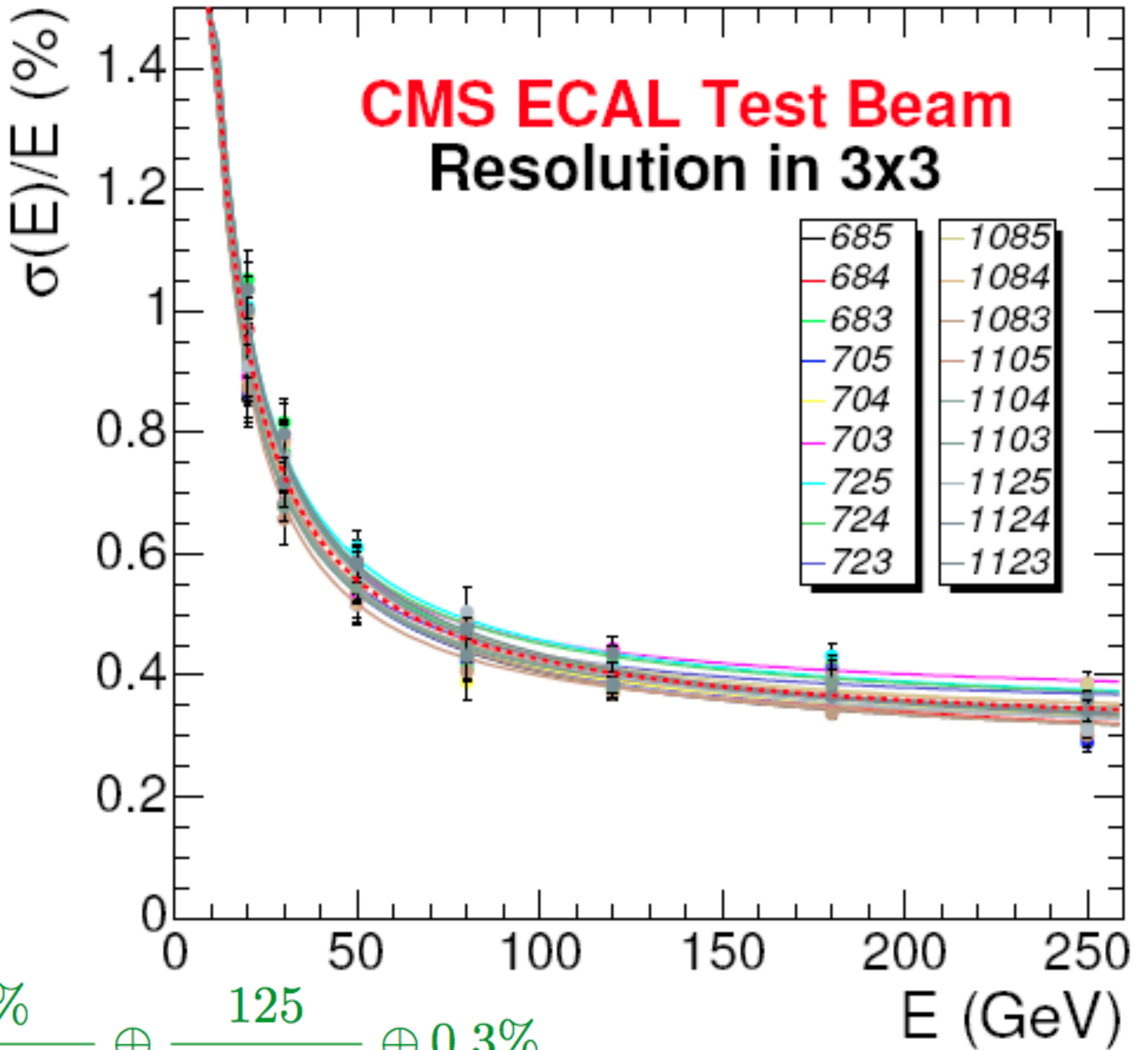

$$\frac{\sigma}{E} = \frac{2.8\%}{\sqrt{E(\mathrm{GeV})}} \oplus \frac{125}{E(\mathrm{MeV})} \oplus 0.3\%$$

Sampling calorimeters

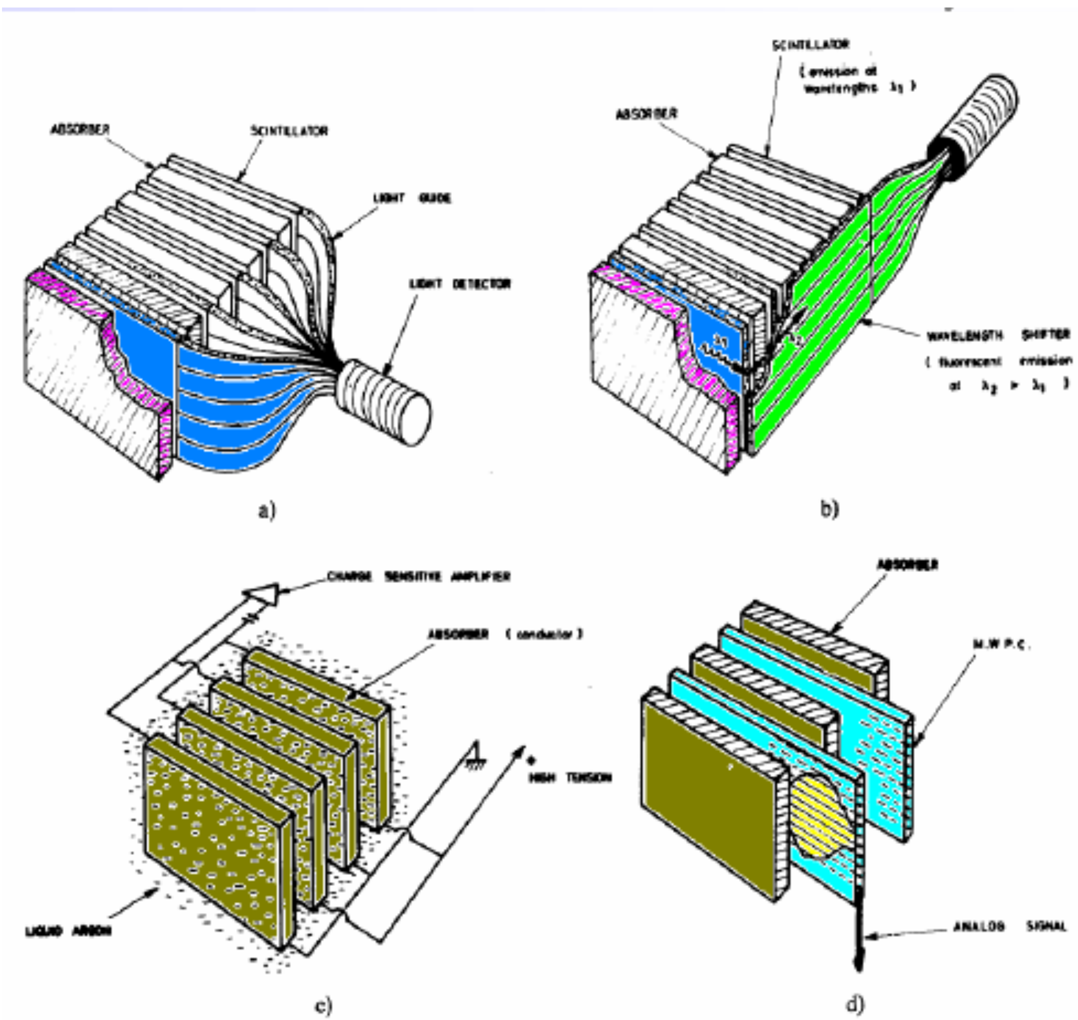

Absorber
Detector
Absorber
Detector
Absorber
Detector

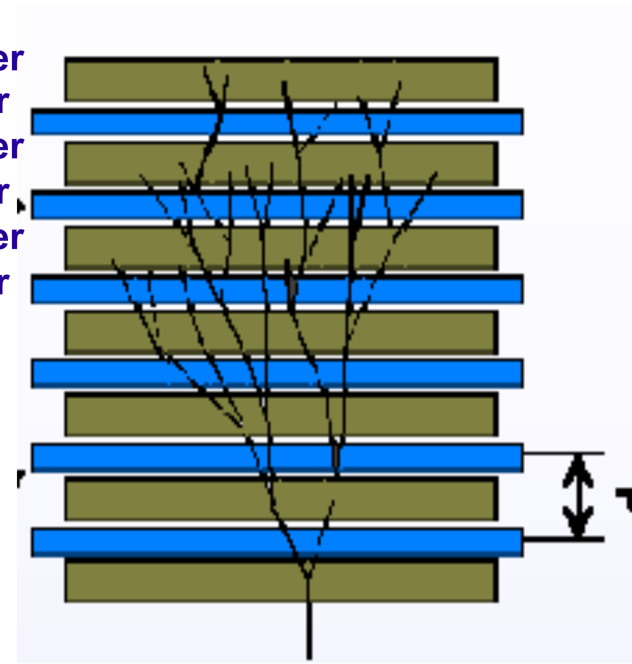

ATLAS Liquid Argon EM Calorimeter

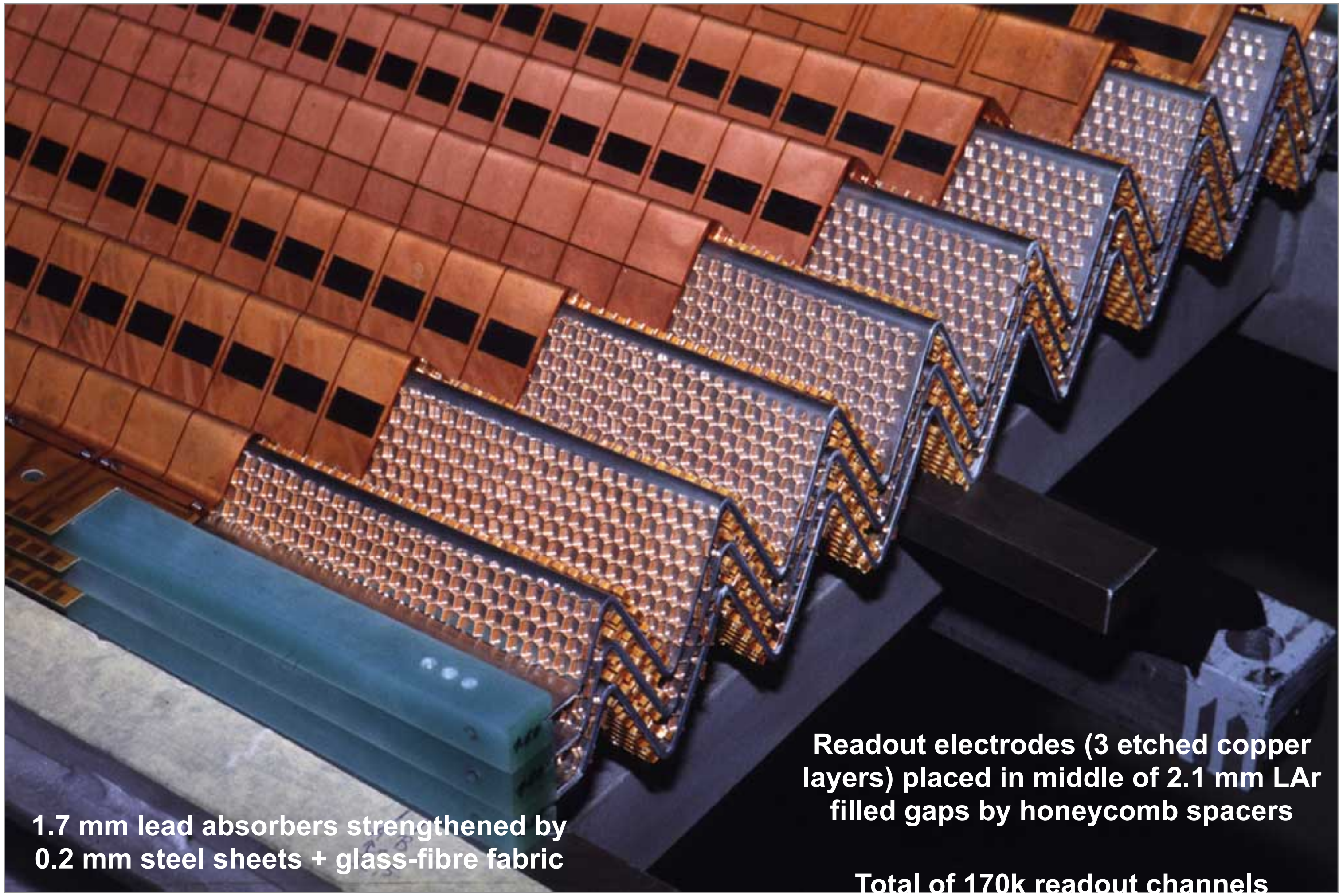

ATLAS electromagnetic Calorimeter

Accordion geometry absorbers immersed in Liquid Argon

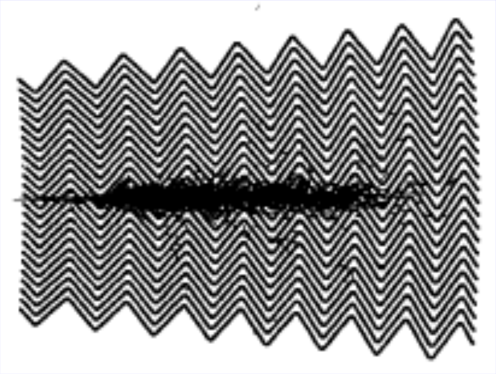

Liquid Argon (90K)

+ lead-steal absorbers (1-2 mm)

+ multilayer copper-polyimide readout boards

→ Ionization chamber.

1 GeV E-deposit → 5 x10^6 e^-

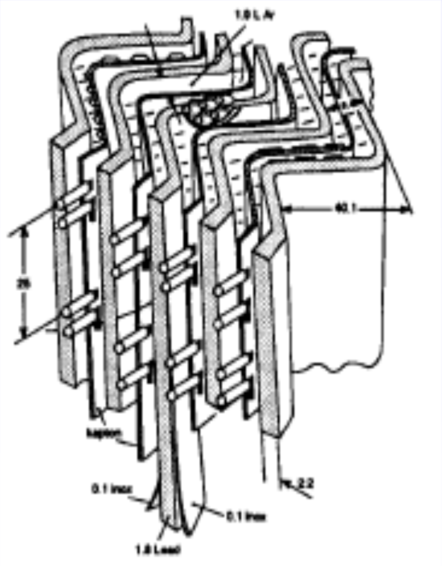

- Accordion geometry minimizes dead zones.
- Liquid Ar is intrinsically radiation hard.
- Readout board allows fine segmentation (azimuth, pseudo-rapidity and longitudinal) acc. to physics needs

Test beam results $\sigma(E)/E = 9.24\%/\sqrt{E} \oplus 0.23\%$

Spatial resolution ≈ 5 mm / √E

Hadronic showers

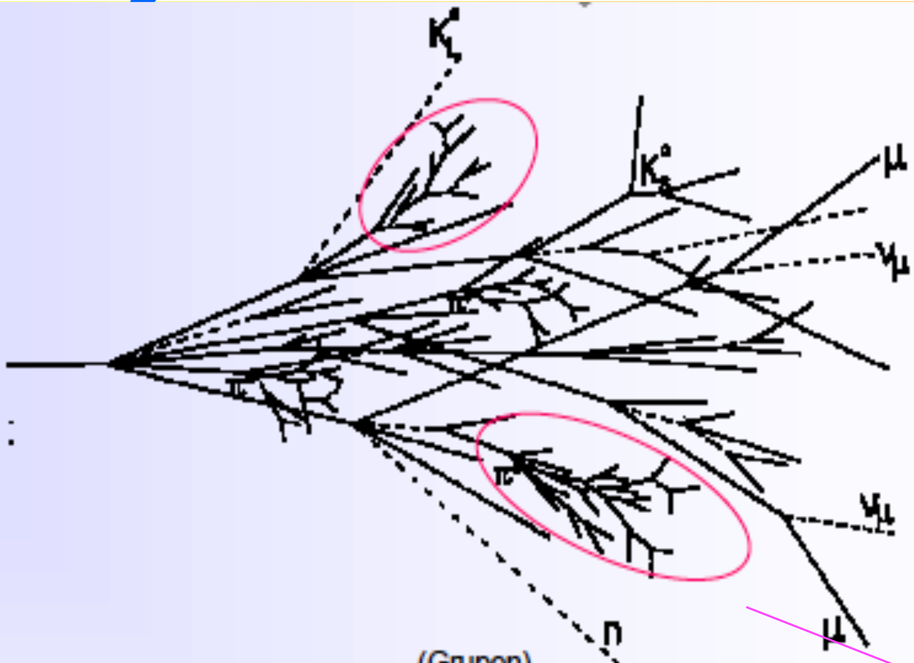

(Grupen)

hadronic + electromagnetic

- charged hadrons p,$\pi^\pm$,$K^\pm$,
- nuclear fragmets ….
- breaking up of nuclei (binding energy)
- neutrons, neutrinos, soft γ's, muons

neutral pions $\rightarrow 2\gamma$

$\rightarrow$ electromagnetic cascades

$$n(\pi^0) \approx \ln E(GeV) - 4.6$$

example $E = 100$ GeV: $n(\pi^0) \approx 18$

invisible energy $\rightarrow$ large energy fluctuations $\rightarrow$ limited energy resolution

Hadronic shower

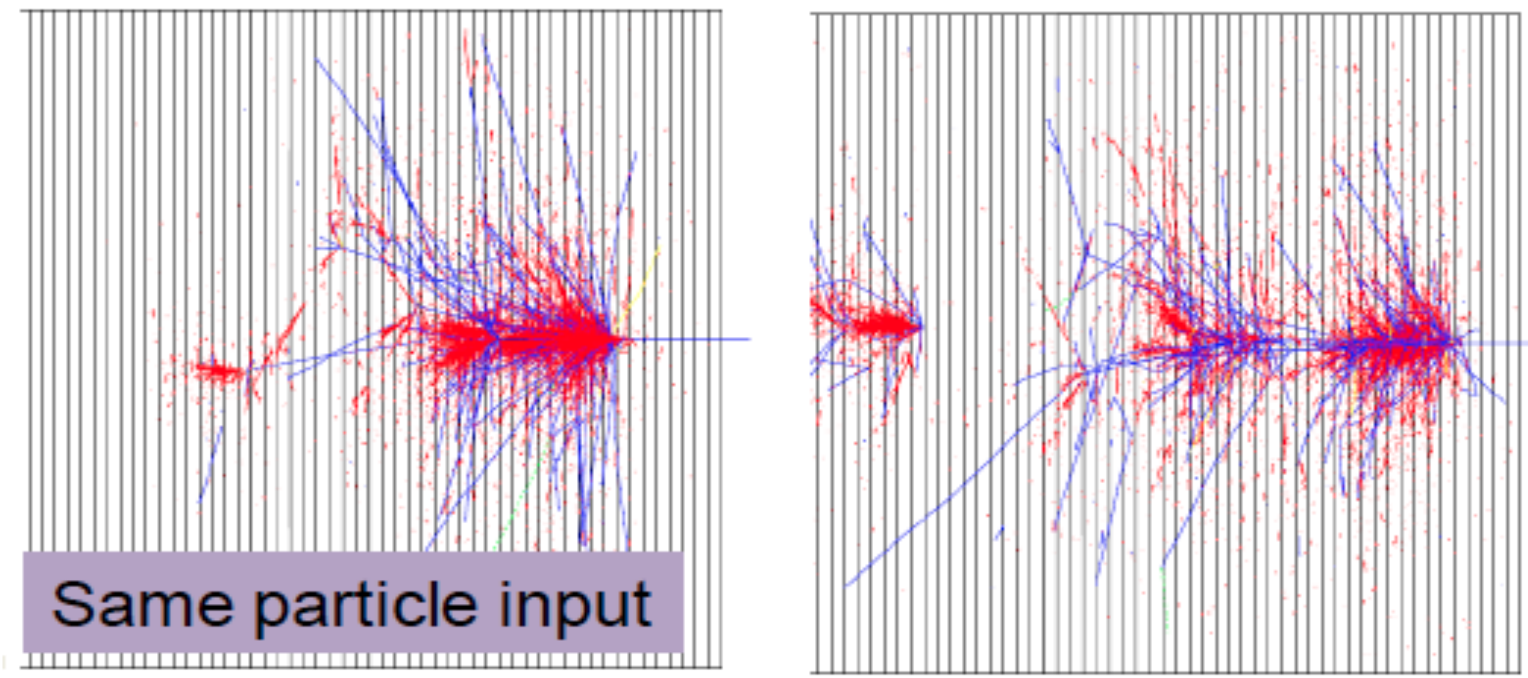

red - e.m. component
blue - charged hadrons

Hadronic showers

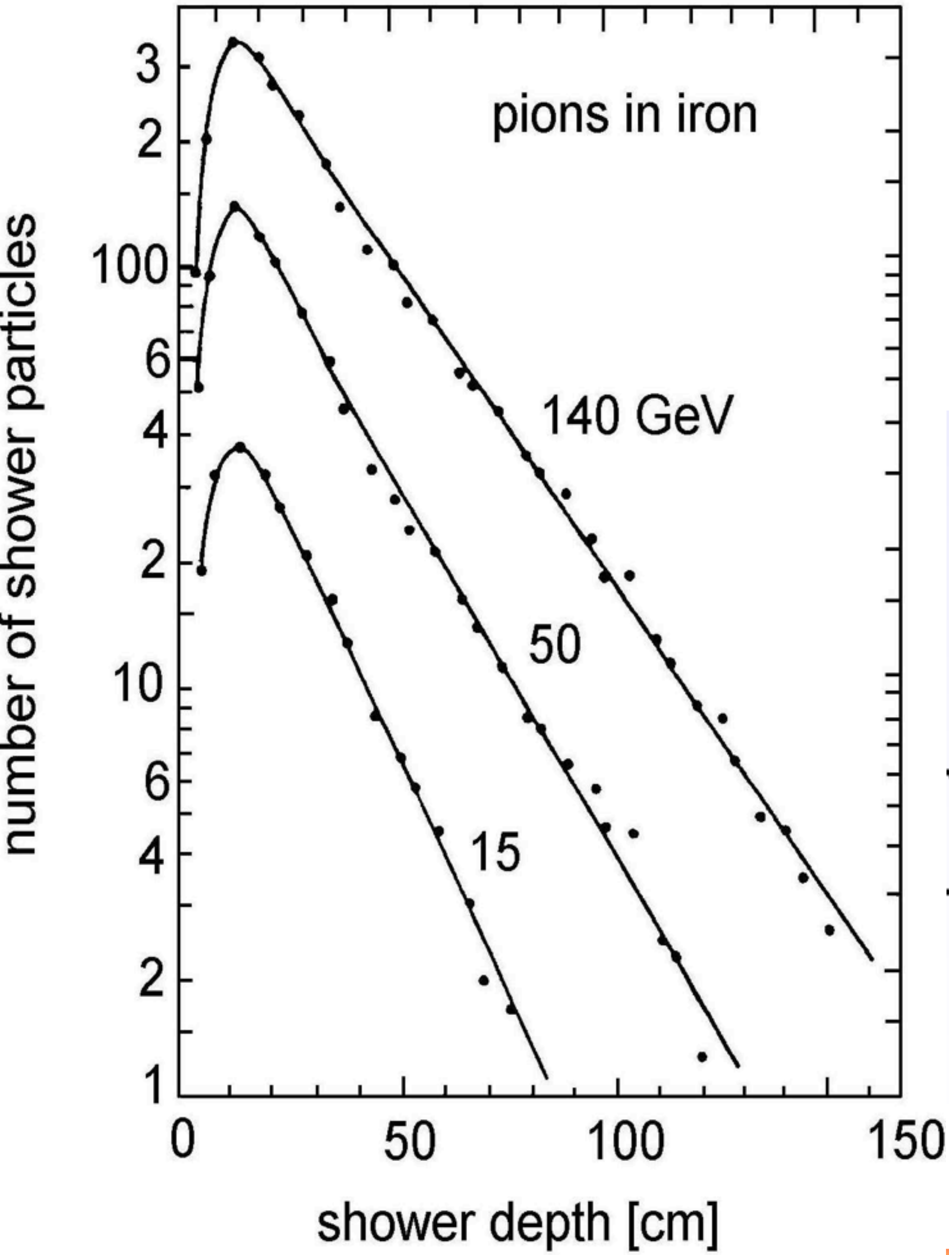

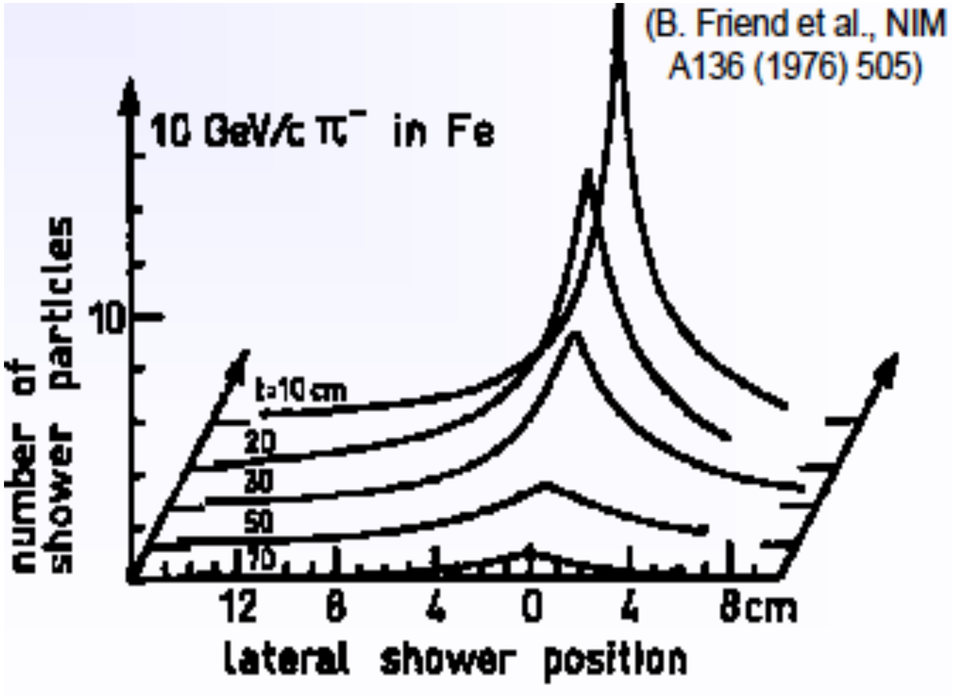

Material	Z	A	ρ [g/cm³]	X_0 [g/cm²]	λ_I [g/cm²]
Hydrogen (gas)	1	1.01	0.0899 (g/l)	63	50.8
Helium (gas)	2	4.00	0.1786 (g/l)	94	65.1
Beryllium	4	9.01	1.848	65.19	75.2
Carbon	6	12.01	2.265	43	86.3
Nitrogen (gas)	7	14.01	1.25 (g/l)	38	87.8
Oxygen (gas)	8	16.00	1.428 (g/l)	34	91.0
Aluminium	13	26.98	2.7	24	106.4
Silicon	14	28.09	2.33	22	106.0
Iron	26	55.85	7.87	13.9	131.9
Copper	29	63.55	8.96	12.9	134.9
Tungsten	74	183.85	19.3	6.8	185.0
Lead	82	207.19	11.35	6.4	194.0
Uranium	92	238.03	18.95	6.0	199.0

For Z > 6: $\lambda_I > X_0$

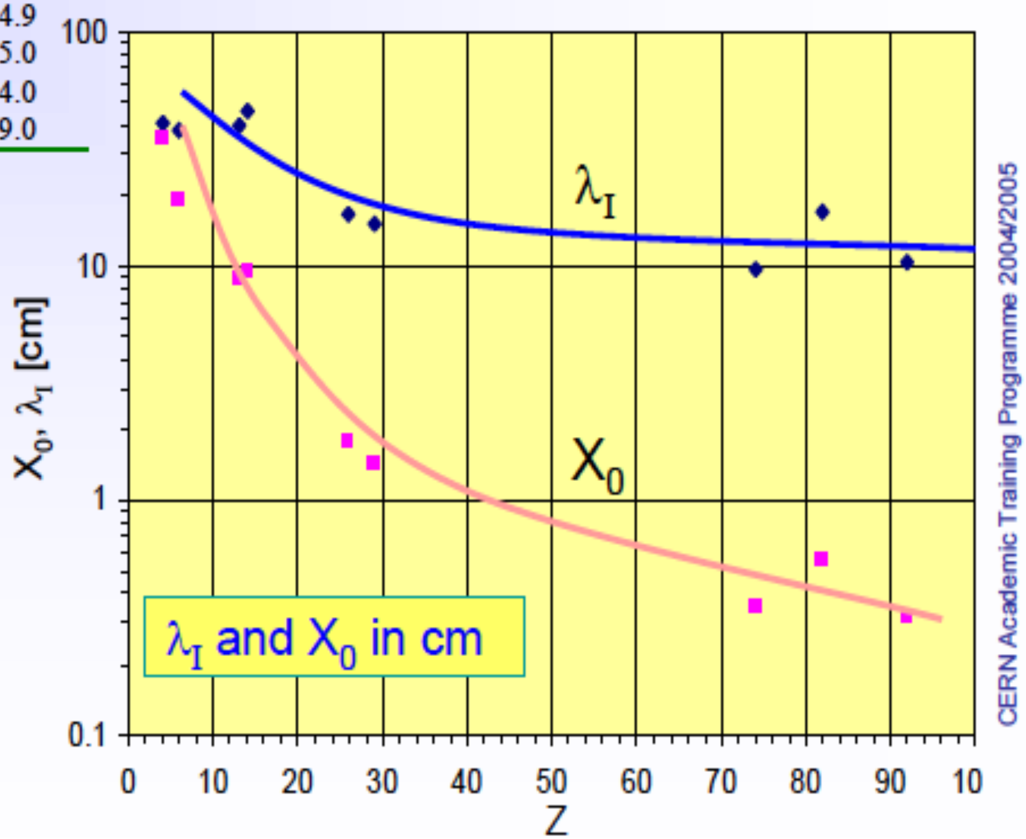

CMS Hadron calorimeter

Brass absorber + plastic scintillators

2 x 18 wedges (barrel)
+ 2 x 18 wedges (endcap)
~ 1500 T absorber
5.8 λ_i at $\eta = 0$.

Scintillators fill slots and are read out via WLS fibres by HPDs (B = 4T!)

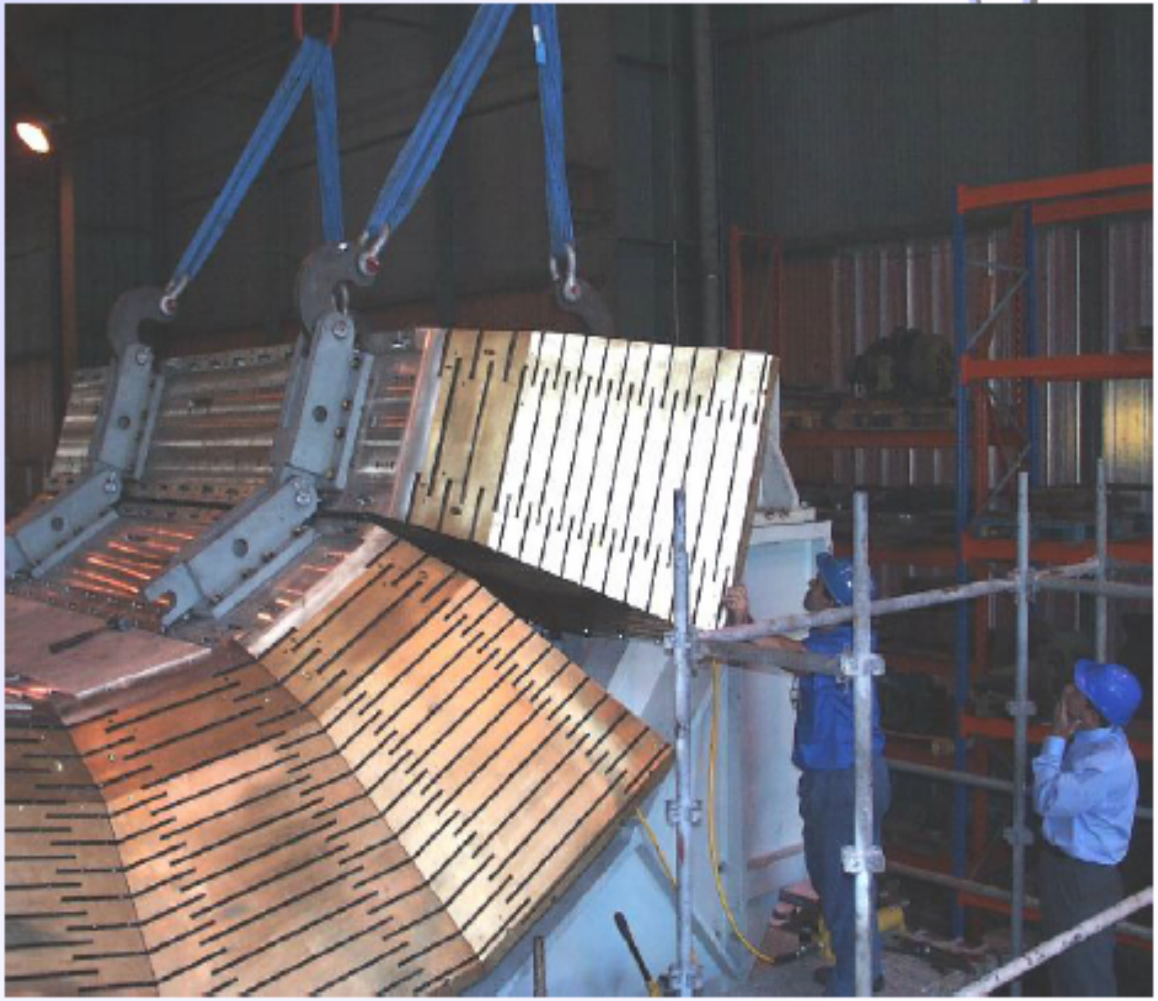

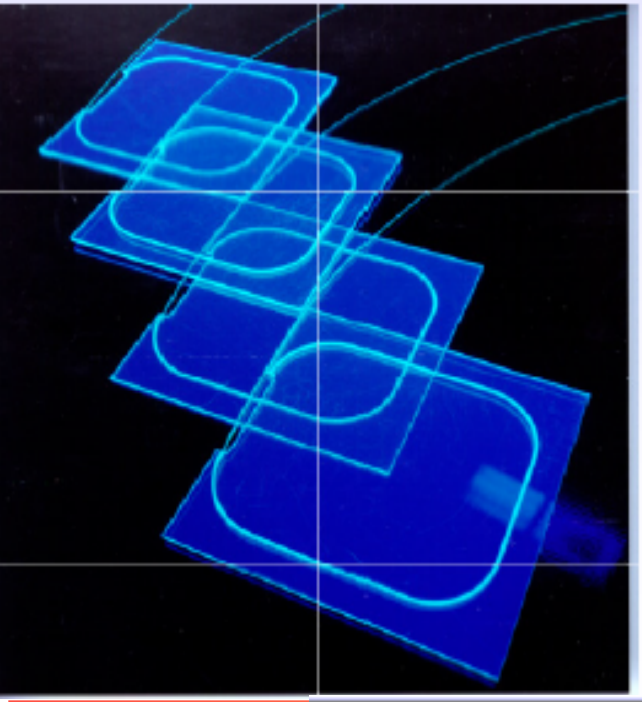

Test beam resolution for single hadrons

$$\frac{\sigma_E}{E} = \frac{65\%}{\sqrt{E}} \oplus 5\%$$

The Hadron Calorimeter - HCAL

- CMS HCAL is constructed in 3 parts:
  - Barrel HCAL (HB)
    - Brass (laiton) plates interleaved with plastic scintillator embedded with wavelength-shifting optical fibres (photo top right)
  - Endcap HCAL (HE)
    - Brass plates interleaved with plastic scintillator
  - Forward HCAL (HF)
    - Steel wedges stuffed with quartz fibres (photo bottom right)
- ~10000 channels total

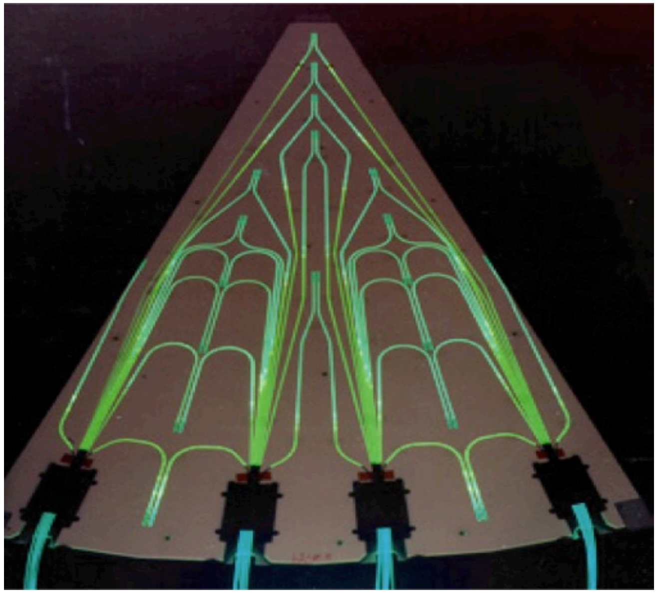

The atmosphere as a big calorimeter

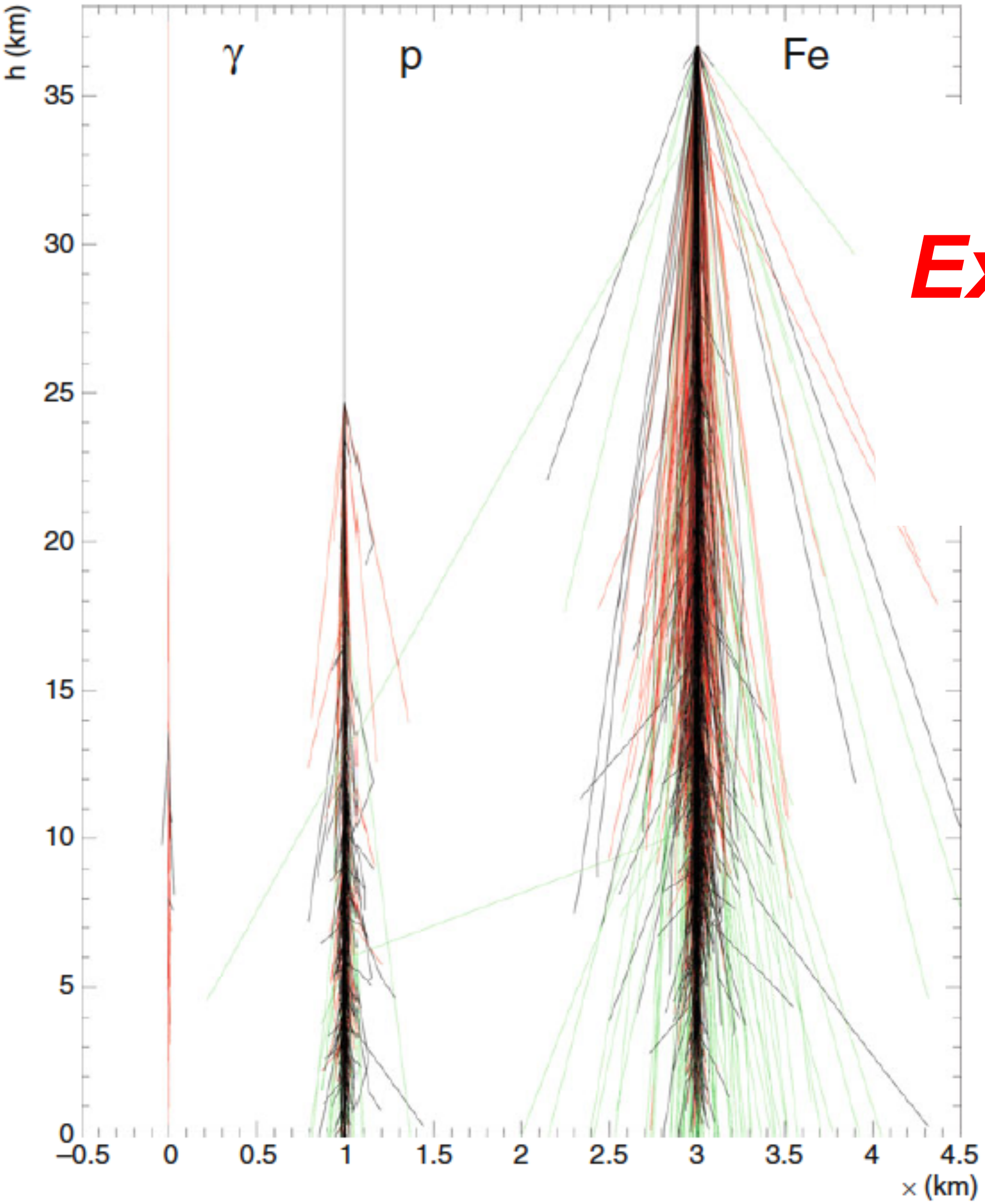

Fig. 1.11 Side view of trajectories of particles of energy ≥10 GeV of a photon, a proton and an iron nucleus initiated shower having a total primary energy of 10^5 GeV each. The electromagnetic component is shown in *red*, hadrons are *black* and muons *green*. The widely spread particles in the lower region of the atmosphere in the hadron showers are mostly muons (courtesy of KASCADE group)

Extensive Air shower 10^{14} eV

The atmosphere as a big calorimeter

extensive air shower

Differences in the shower developments give hints to the energy and mass of the primary

Energy of an UHECR

- **Detectors on the ground**
  - **Sampling in one plane**
- **Fluorescence:**
  - **sampling of the scintillation light**
  - **Information about shower development**
  - **X_{max} is sensitive to the mass of the incoming particle : $X_{max} \sim \Lambda\, ln(E_0/A)$**

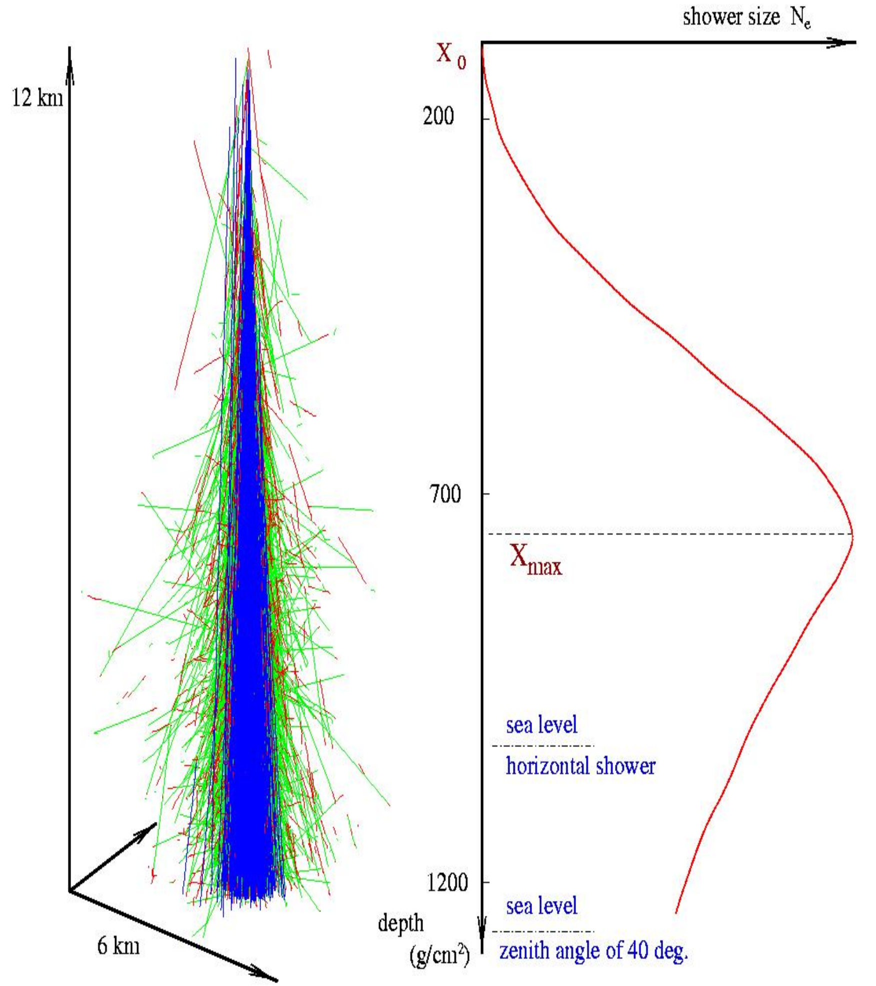

Cerenkov and Transition radiation

Cerenkov effect

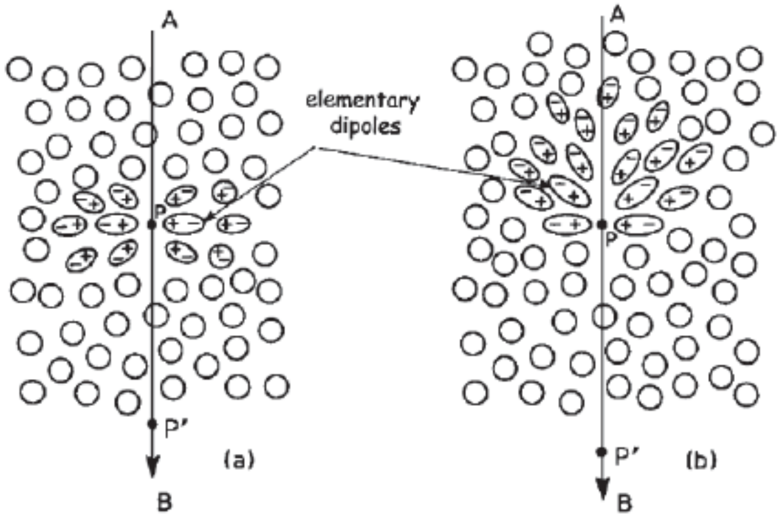

$v_p/c < c/n(\lambda)$ $v_p/c > c/n(\lambda)$

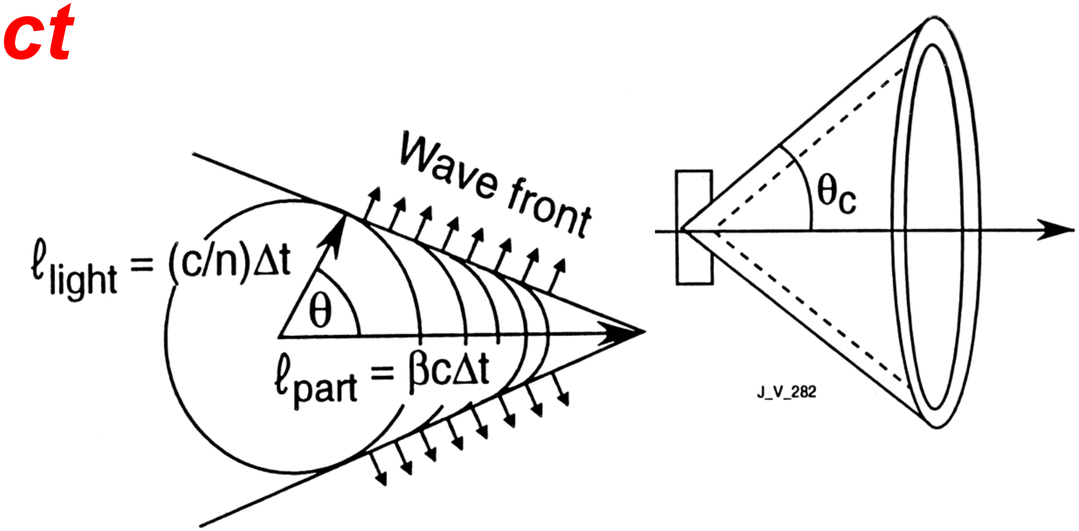

- **Coherent superposition of the radiation of the atoms**
- **Mainly blue light**
- **Very few photons**
- **Very small energy loss**
- **Identification of particles!**

$$v = \beta c > c/n$$

$$\cos\theta_C = \frac{c \cdot \Delta t / n}{\beta c \cdot \Delta t} = \frac{1}{\beta n}$$

$$\Rightarrow \quad \beta > \frac{1}{n} \; ; \; \cos\theta_c^{max} = \frac{1}{n}$$

$$\lambda_{photons} \approx 200 - 700\, nm$$

Exercise

Blue light in a reactor

1. **What produces the light?**
2. **Water *n*=1.333. calculate the minimal energy of an electron to produce Cerenkov light**

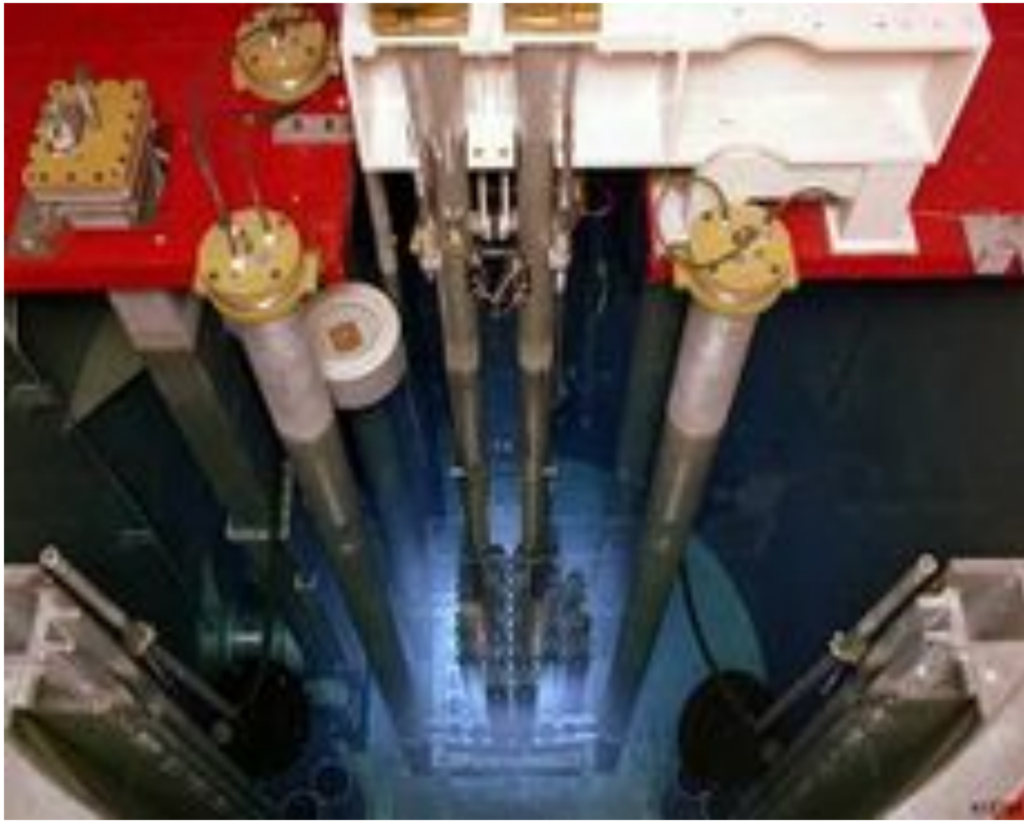

Cerenkov Detectors

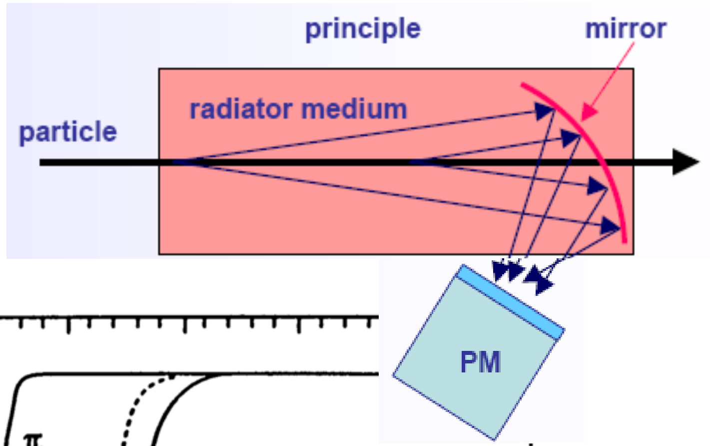

medium	n	θ_{max} (deg.)	N_{ph} (eV^{-1} cm^{-1})
air*	1.000283	1.36	0.208
isobutane*	1.00127	2.89	0.941
water	1.33	41.2	160.8
quartz	1.46	46.7	196.4

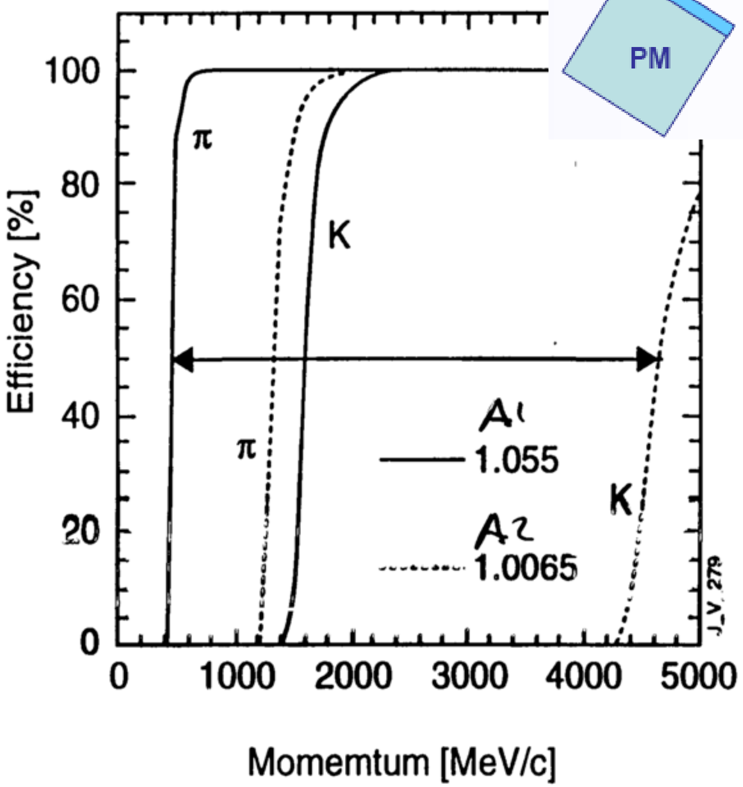

$$N_{ph} \approx 1 - \frac{1}{n^2\beta^2} = 1 - \frac{1}{n^2}\cdot\left(1 + m^2/p^2\right)$$

Ring Imaging Cerenkov

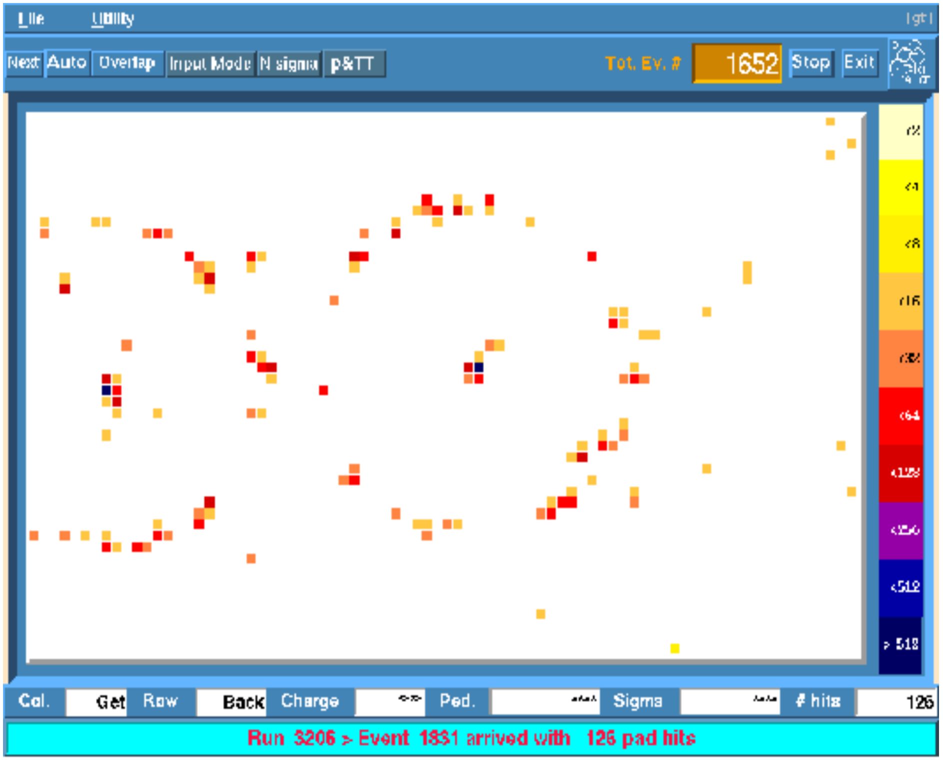

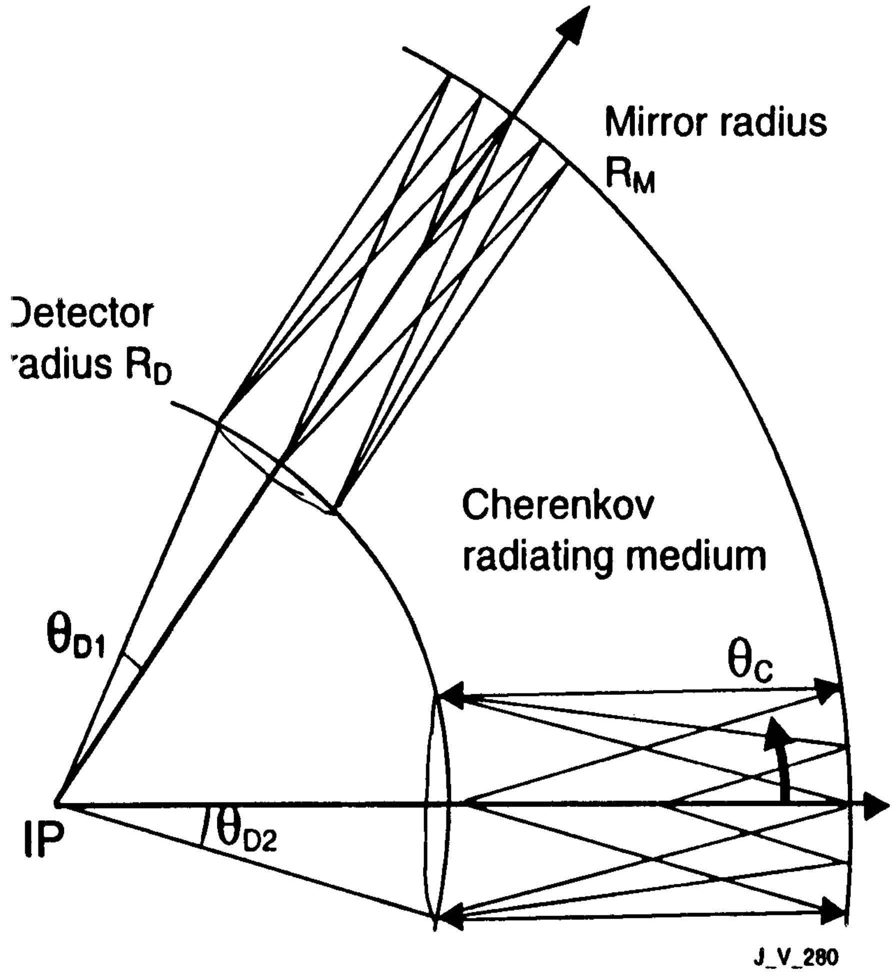

Ring Imaging Cerenkov

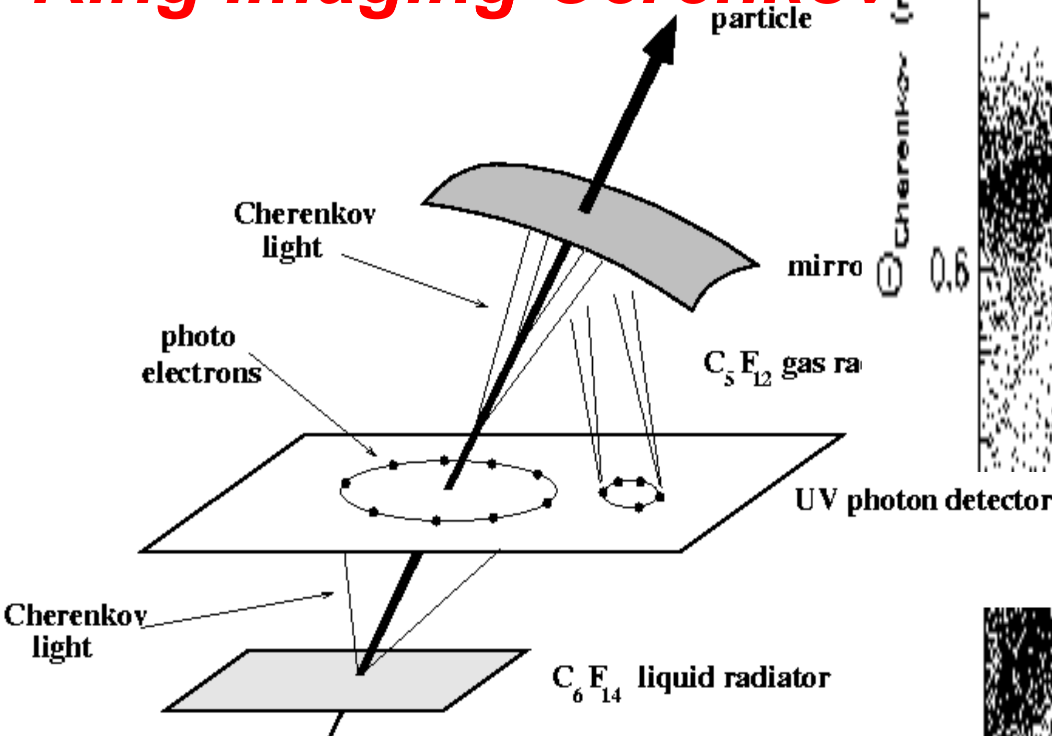

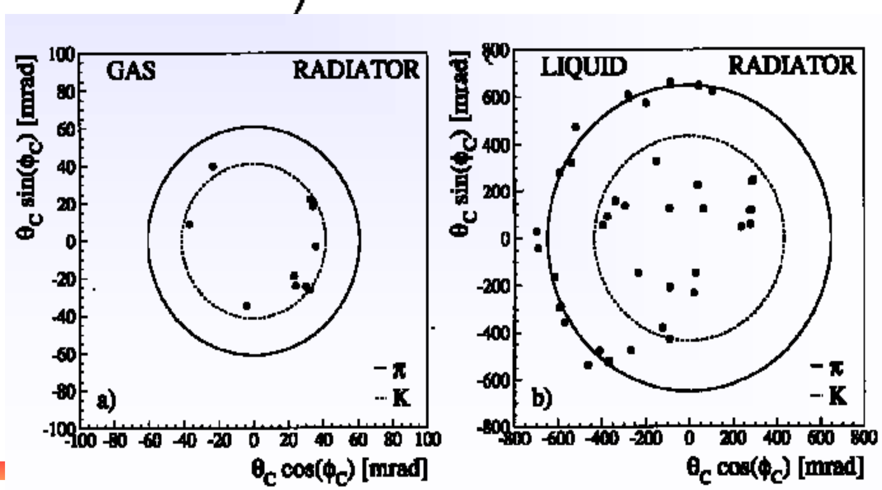

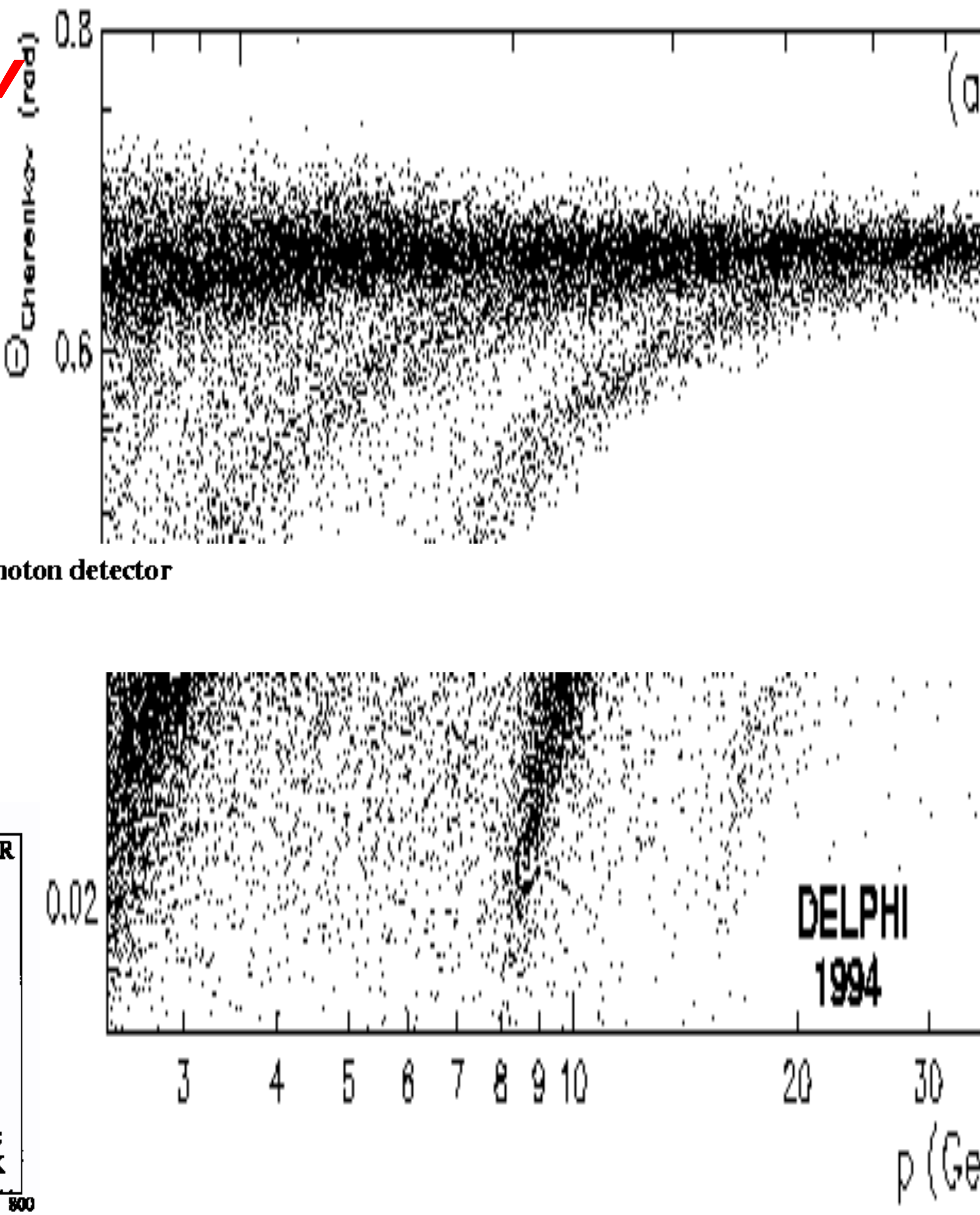

LHCb RICH

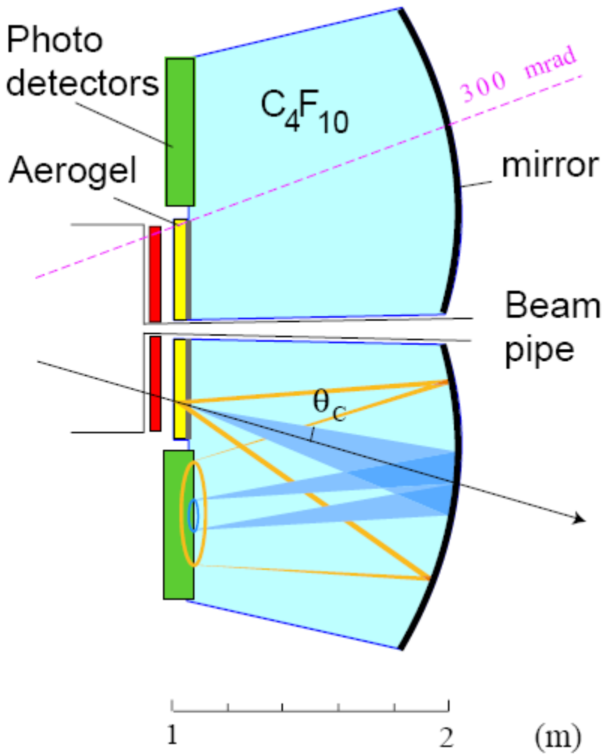
Photo detectors
C4F10
300 mrad
Aerogel
mirror
Beam pipe
θc
Track
1
2
(m)

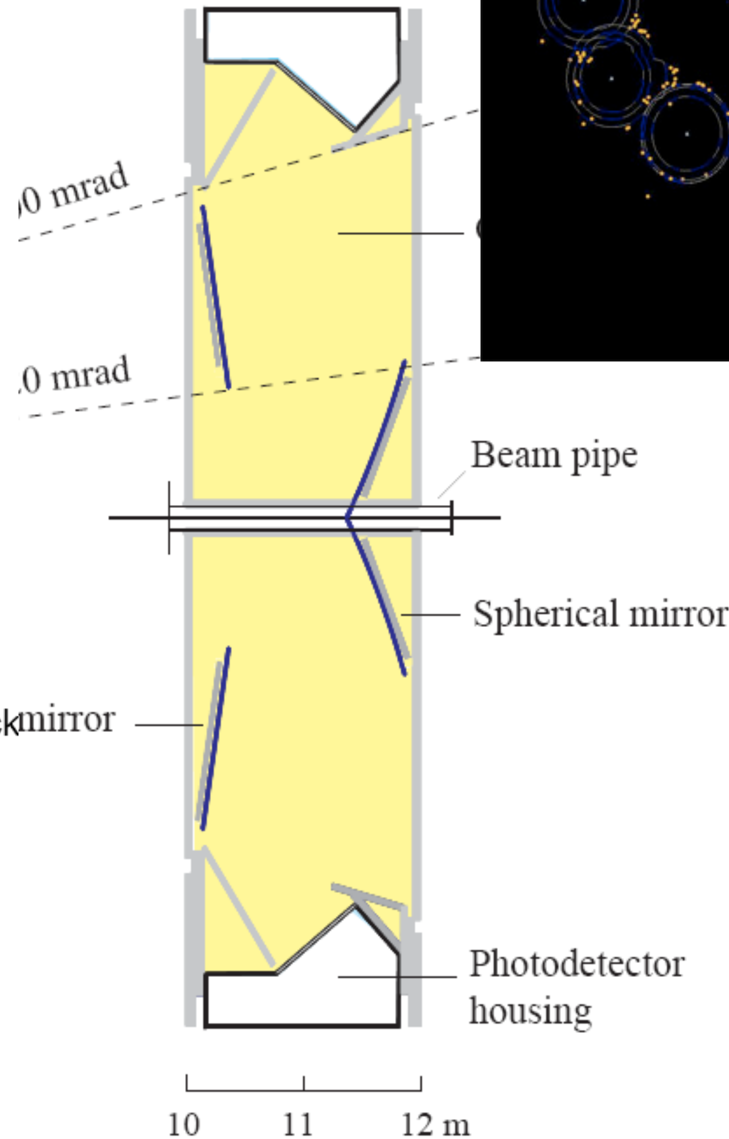
0 mrad
0 mrad
Beam pipe
Spherical mirror
mirror
Photodetector housing
10
11
12 m

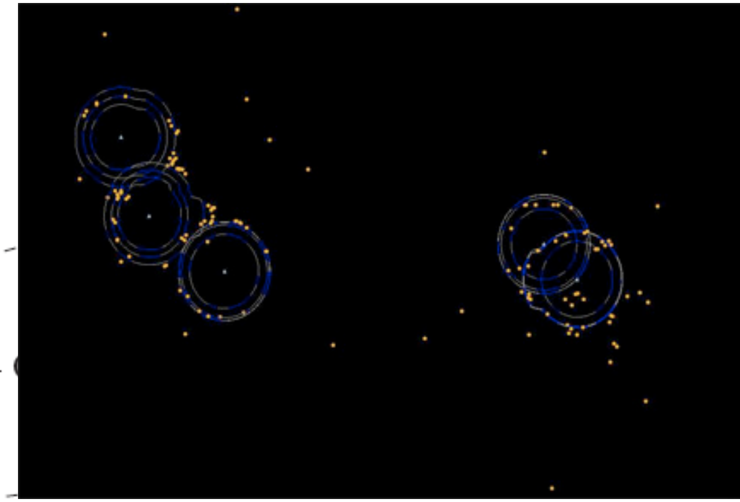

Transition radiation

- Effect can be explained by re-arrangement of electric field
- A charged particle approaching a boundary creates a electric dipole with its mirror charge
- The time-dependent dipole field causes the emission of electromagnetic radiation

Photon radiation when charged ultra-relativistic particles traverse the boundary of two different dielectric media (foil & air)

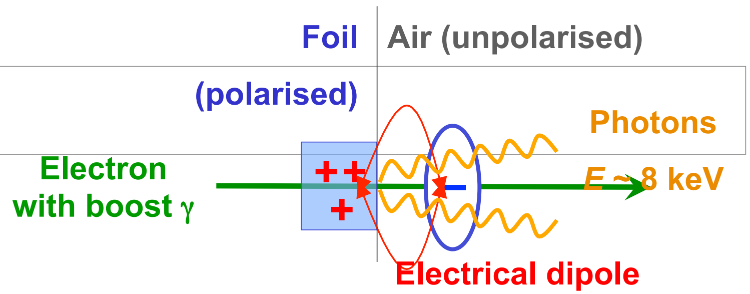

➡ **Significant radiation for γ > 1000 and > 100 boundaries**

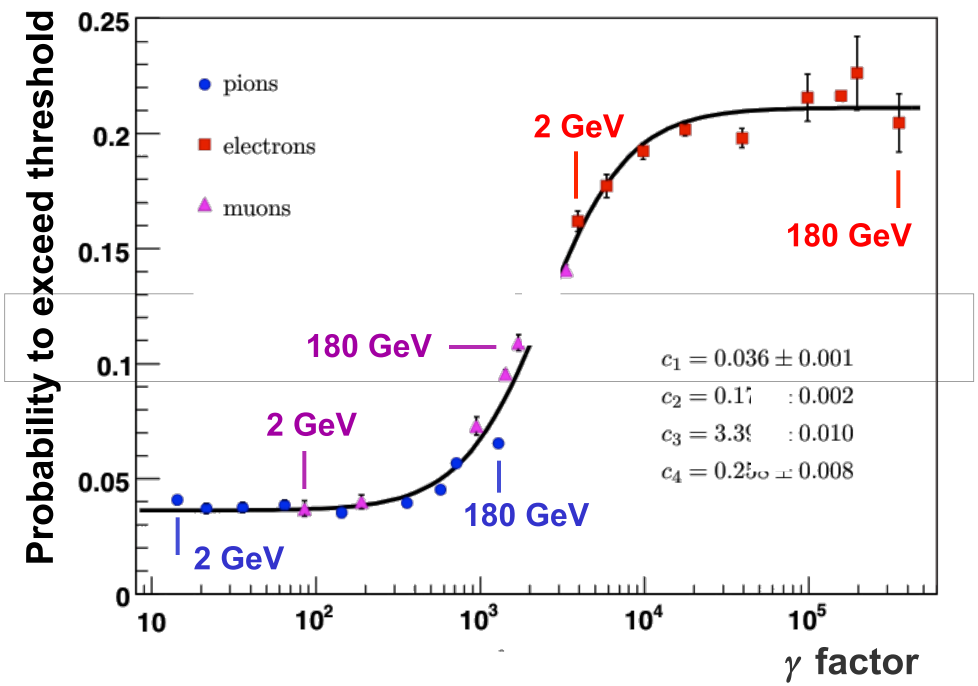

From D. Froidevaux, ASP 2010

Transition Radiation Detectors

$$W = \frac{1}{3}\alpha\hbar\omega_p\gamma \qquad W \propto \gamma$$

$$\omega_p = \sqrt{\frac{N_e e^2}{\varepsilon_0 m_e}} \quad \left(\begin{array}{c}\text{plasma}\\ \text{frequency}\end{array}\right) \quad \hbar\omega_p \approx 20\text{eV} \ \text{(plastic radiators)}$$

$$N_{ph} \approx \frac{W}{\hbar\omega} \propto \alpha \approx \frac{1}{137}$$

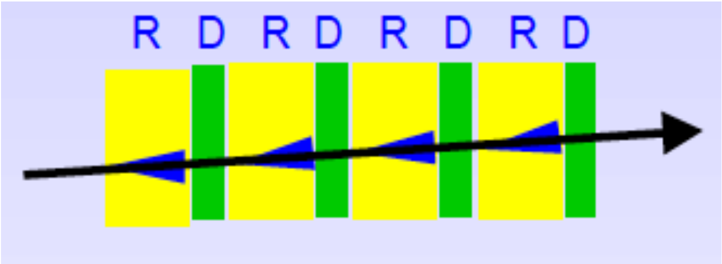

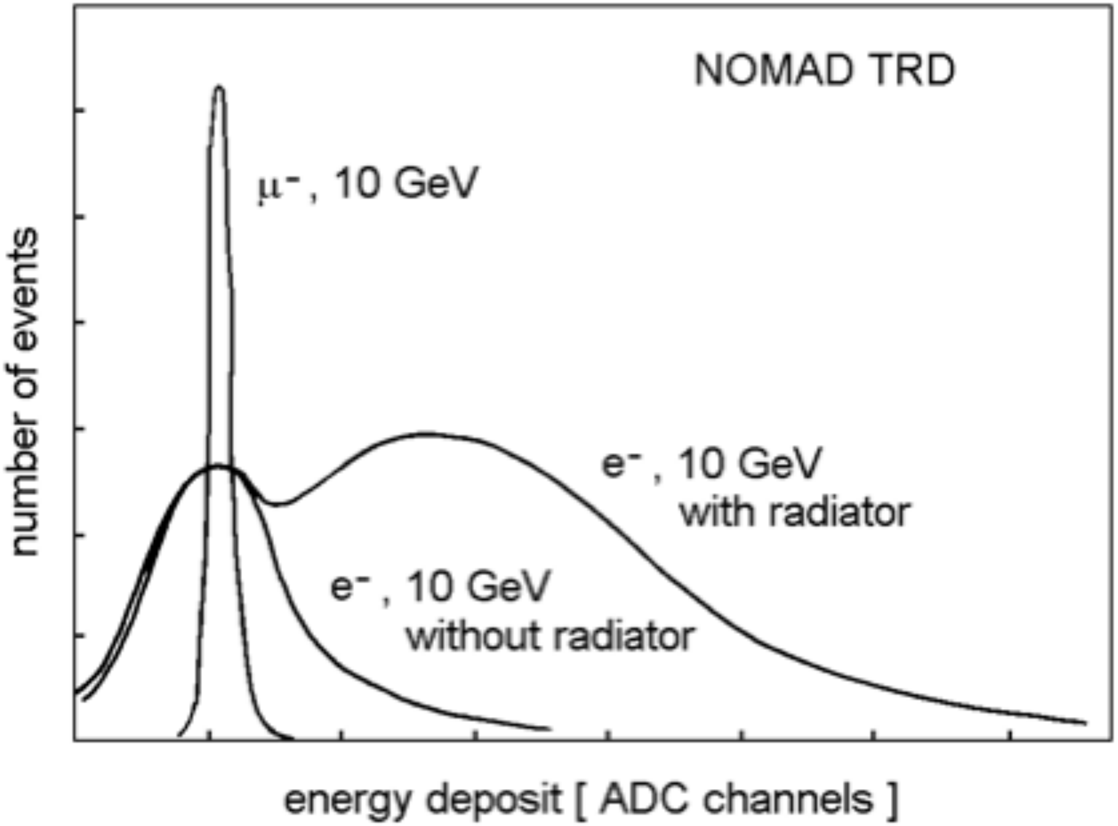

ATLAS TRT

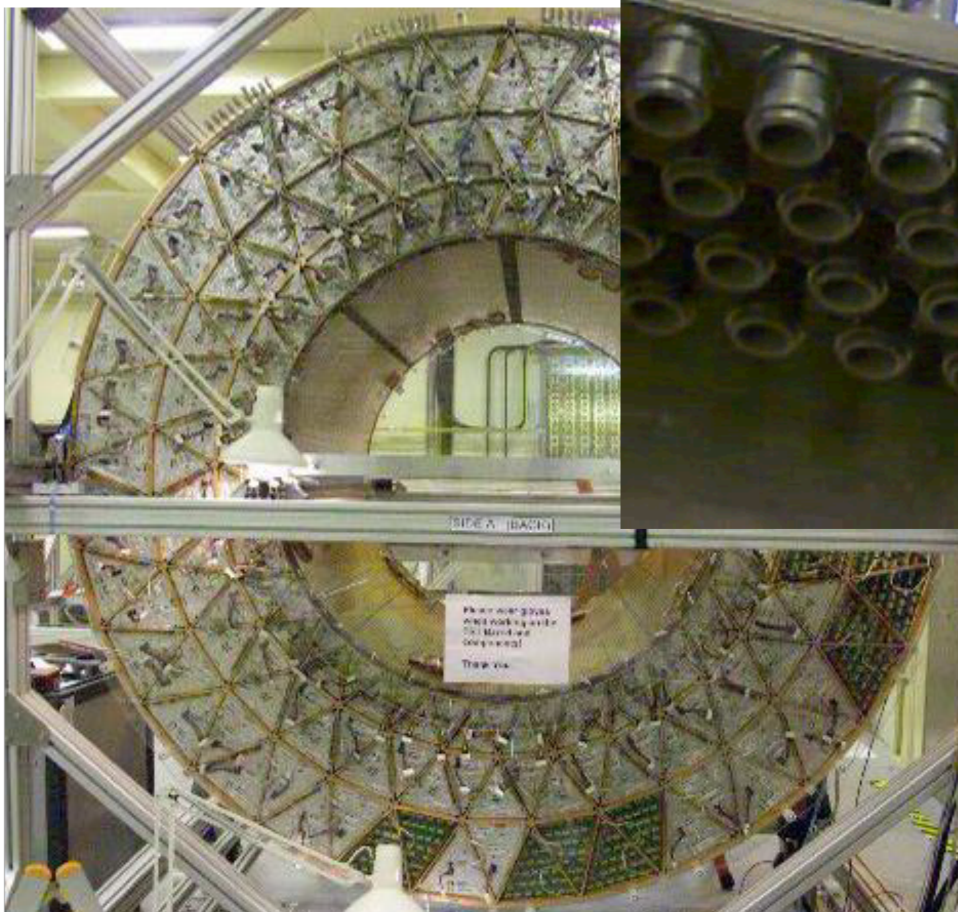

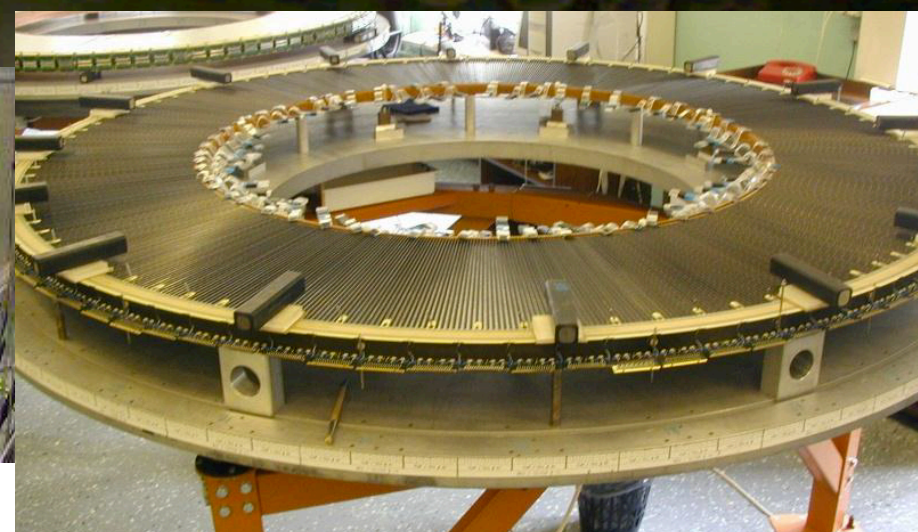

Experiments

- Detector systems, some examples
  - (Dark matter searches)
  - Nuclear physics
  - (Detectors in Space)
  - Experiments at the LHC
  - Astroparticle physics experiments
- Large collaborations: Where are the students?

UNIVERSITÉ DE STRASBOURG

Nuclear Physics gamma spectroscopy

Anti-Compton spectrometer

BGO

Large efficiency

Less energy resolution

Shielding, Pb ou W

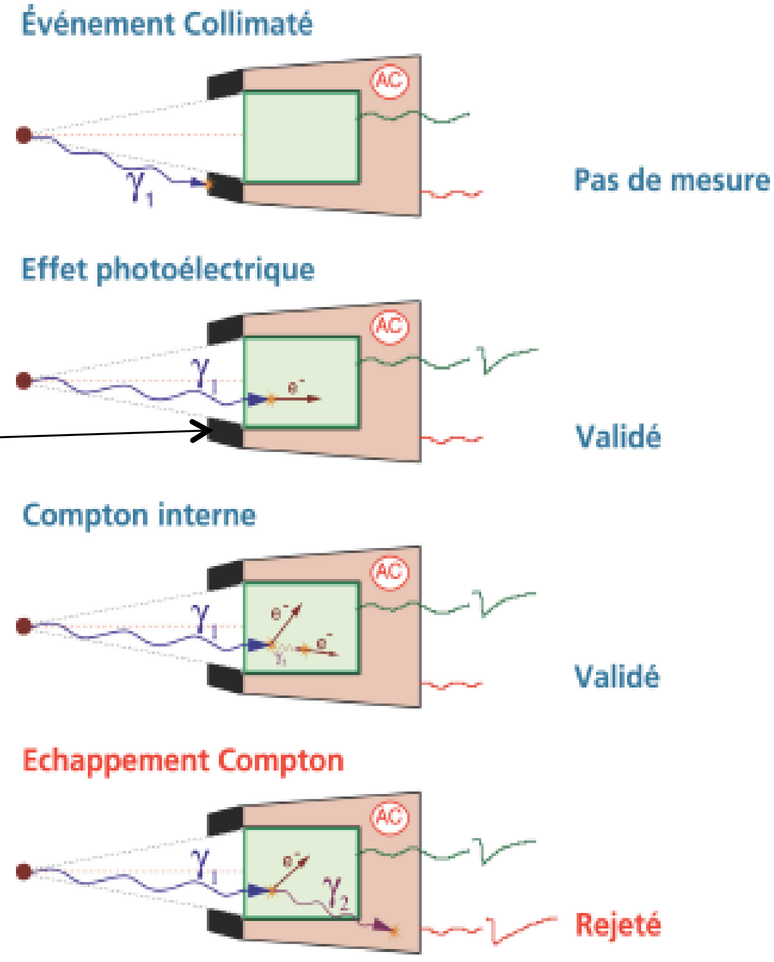

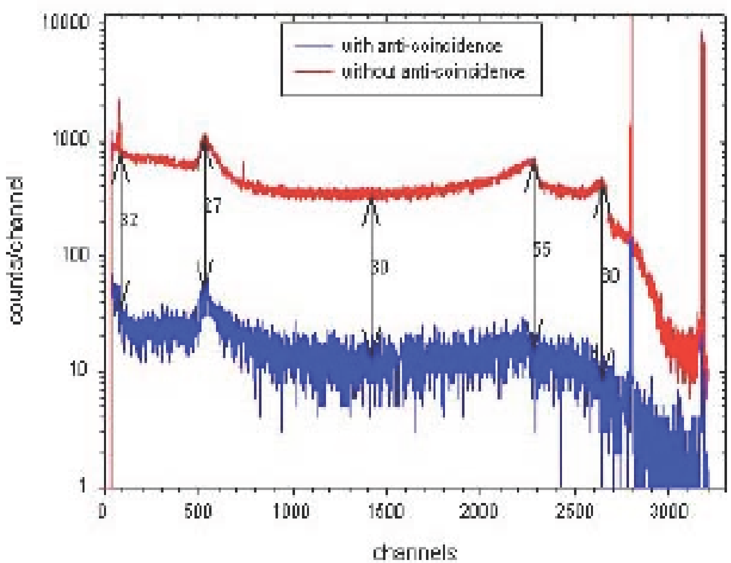

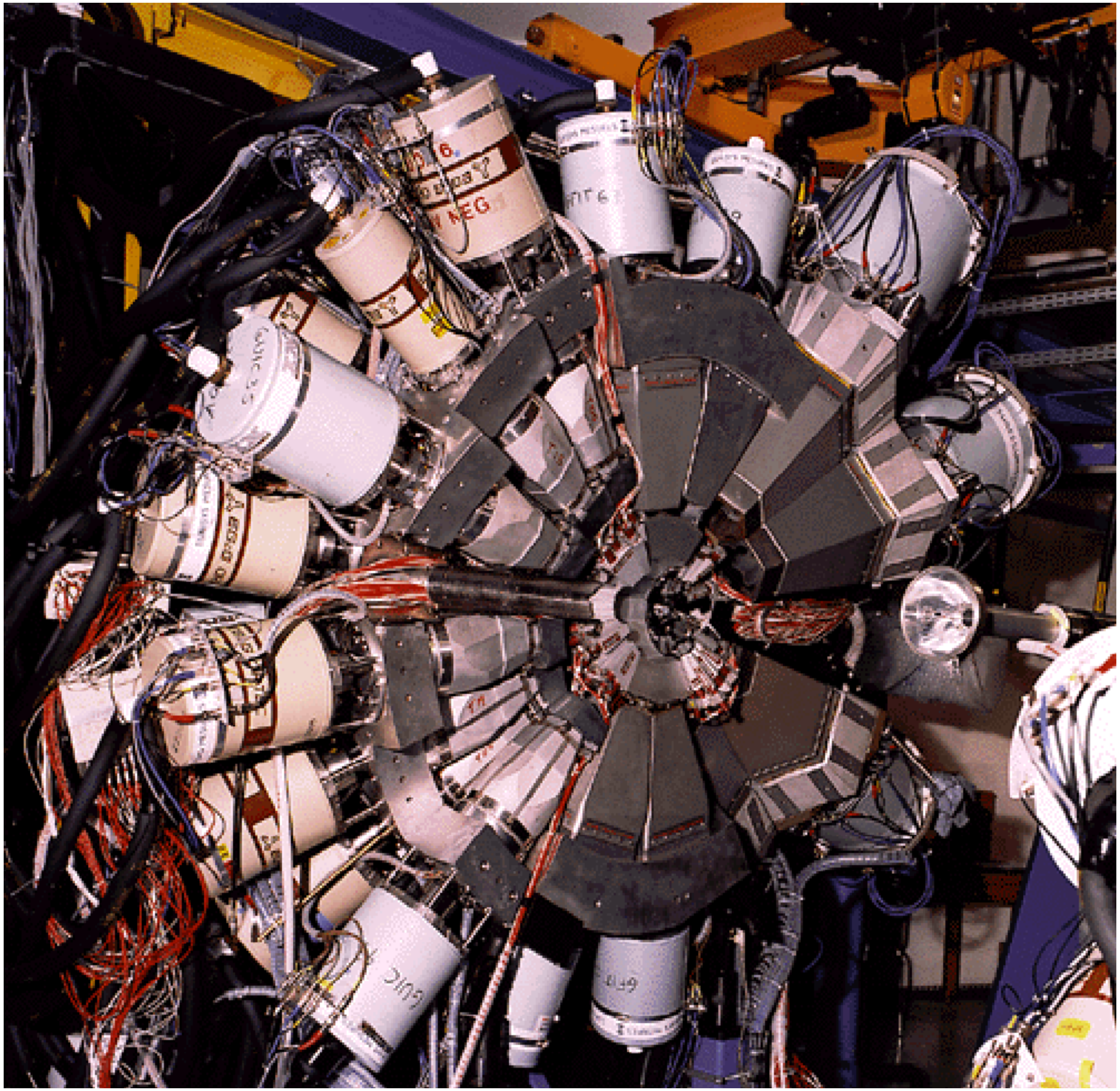

Euroball at Strasbourg

Several years ago

The idea of γ-ray tracking

Compton Shielded Ge

ε_{ph} ~ 10%
N_{det} ~ 100

Ω ~ 40%
θ ~ 8°

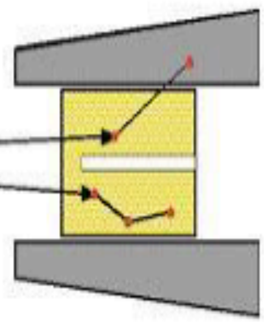

large opening angle means poor energy resolution at high recoil velocity.

Previously scattered gammas were wasted.
Technology is available now to track them.

Ge Tracking Array

ε_{ph} ~ 50%
N_{det} ~ 100

Ω ~ 80%
θ ~ 1°

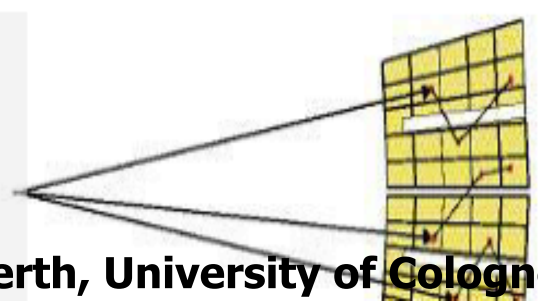

Combination of:

- segmented detectors
- digital electronics
- pulse processing

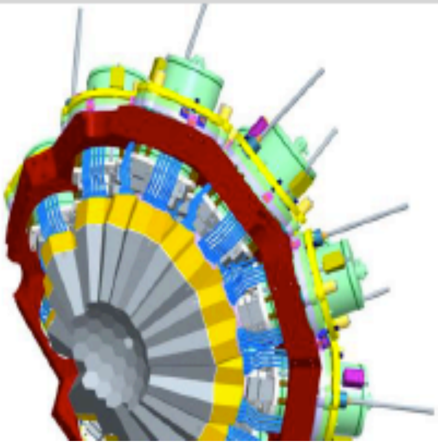

AGATA detectors and the AGATA triple-cluster

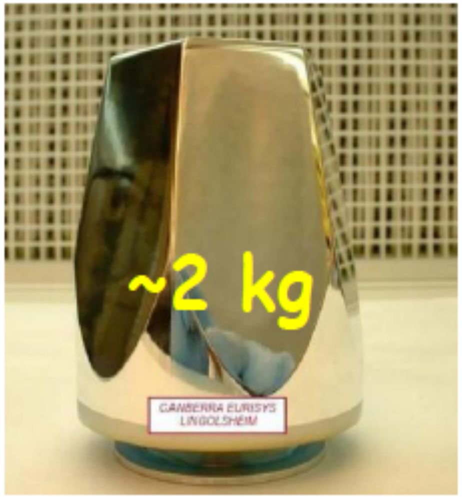

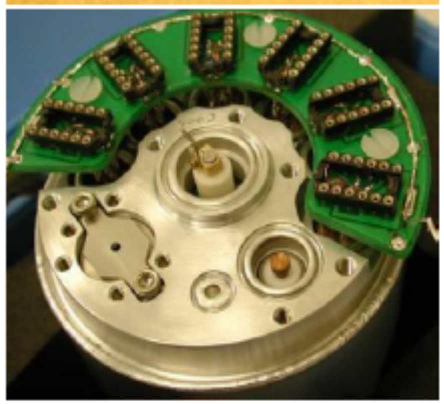

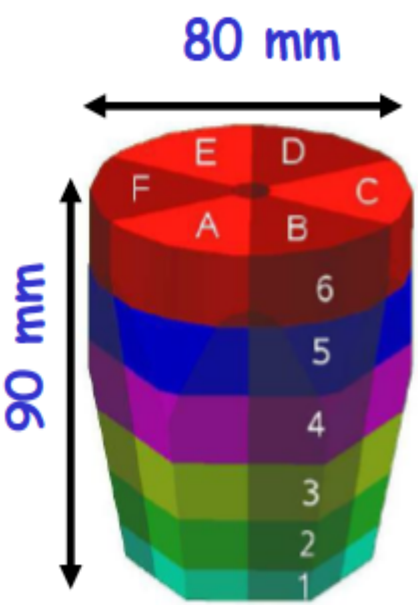

6x6 segmented cathode

Symmetric detectors
- 3 in use since 6 years
- Used in single cryostats or as a triple cluster

Asymmetric detectors
- 31 ordered
- 15 accepted
- 4 clusters operational

Segmented Ge detectors

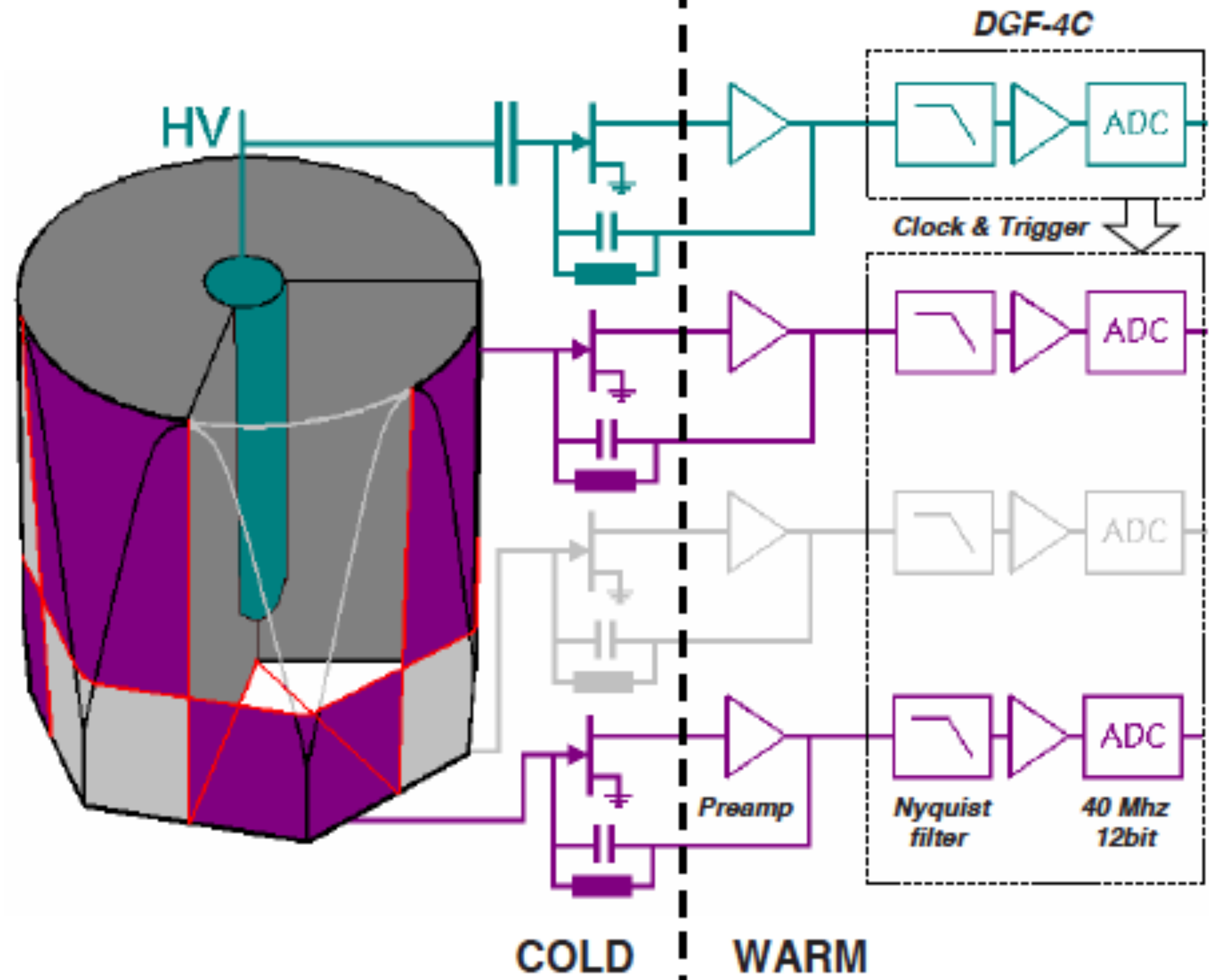

Jürgen Eberth, University of Cologne

Signal Formation
Ge-HP

Cylindrical Geometry

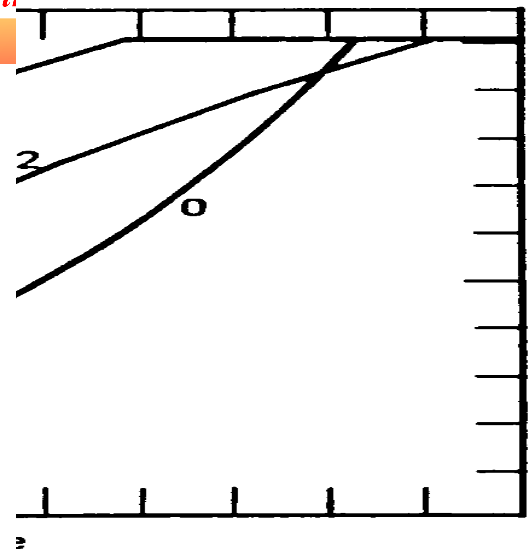

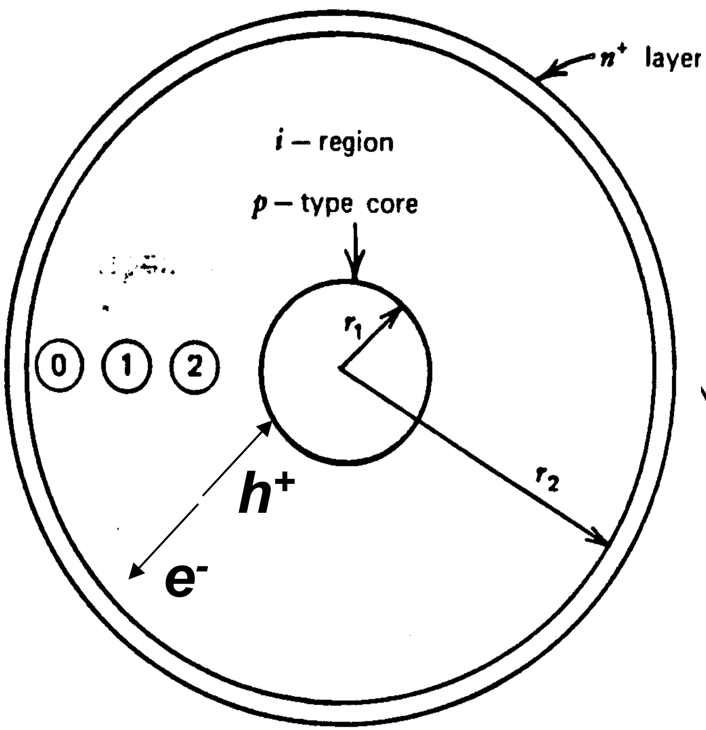

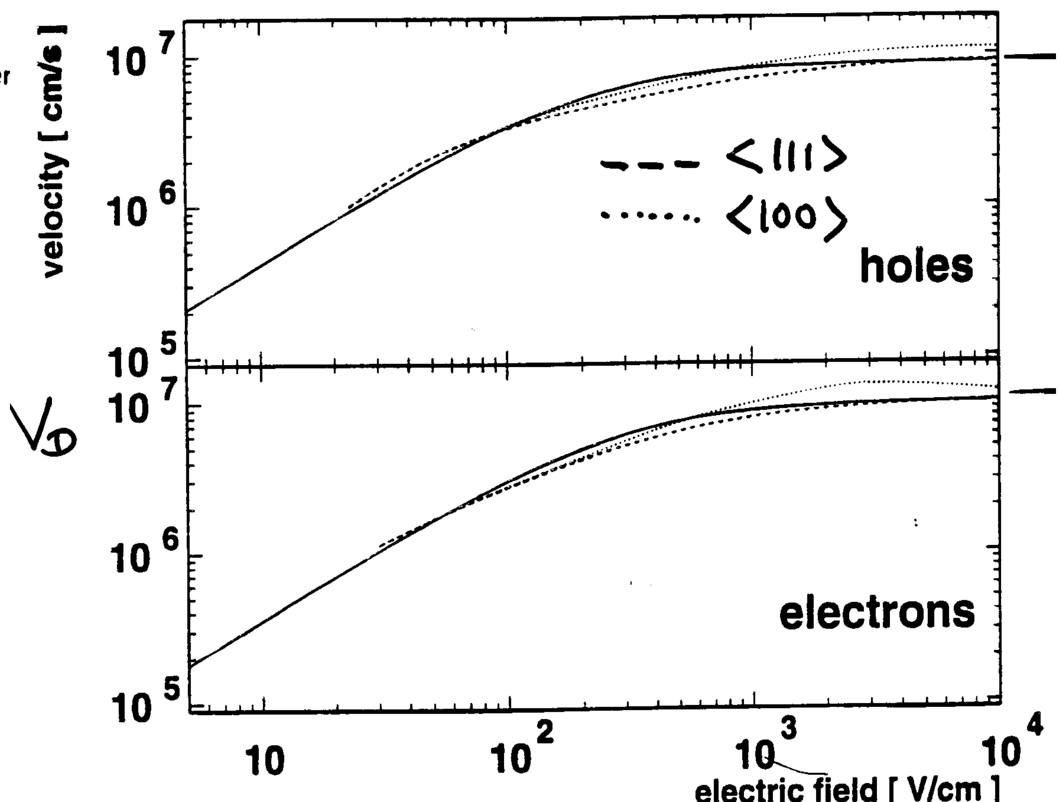

Multiple Interactions

Ge-HP

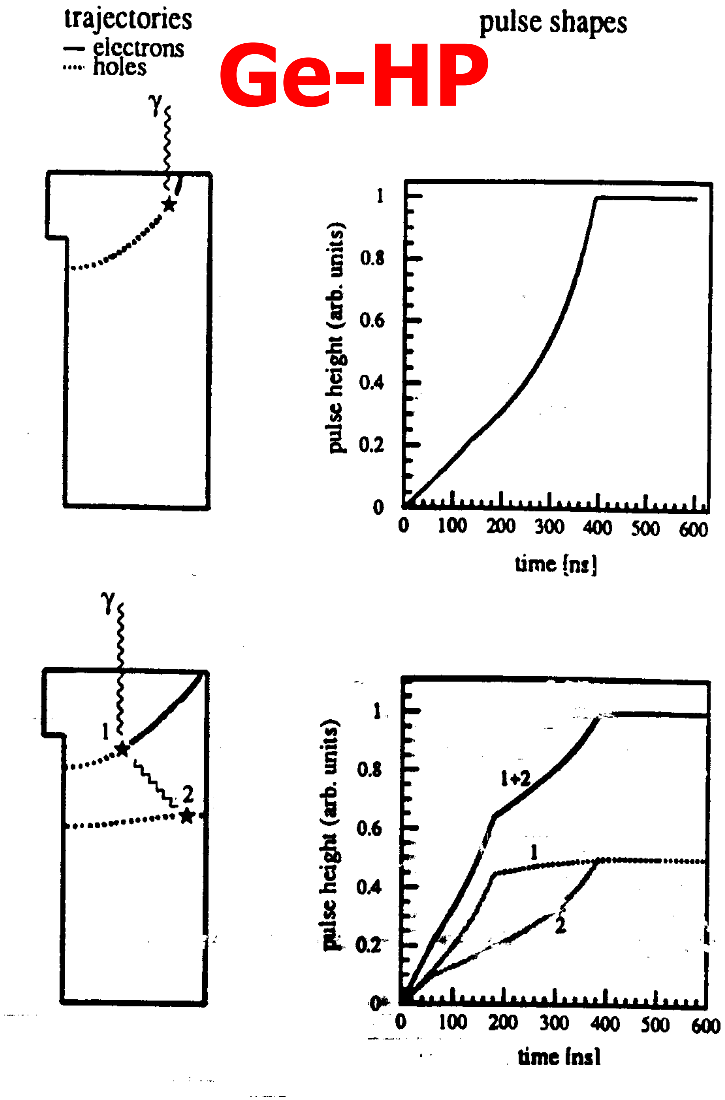

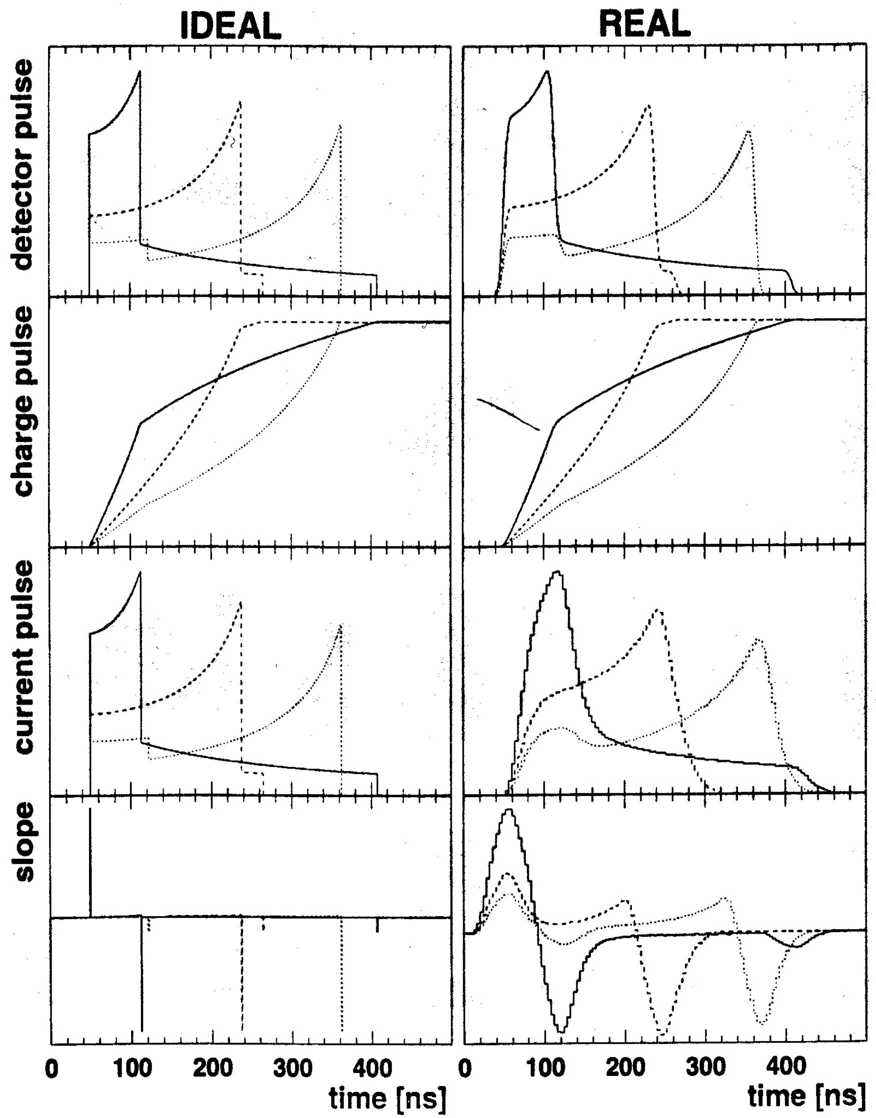

Ingredients of Gamma-Ray Tracking

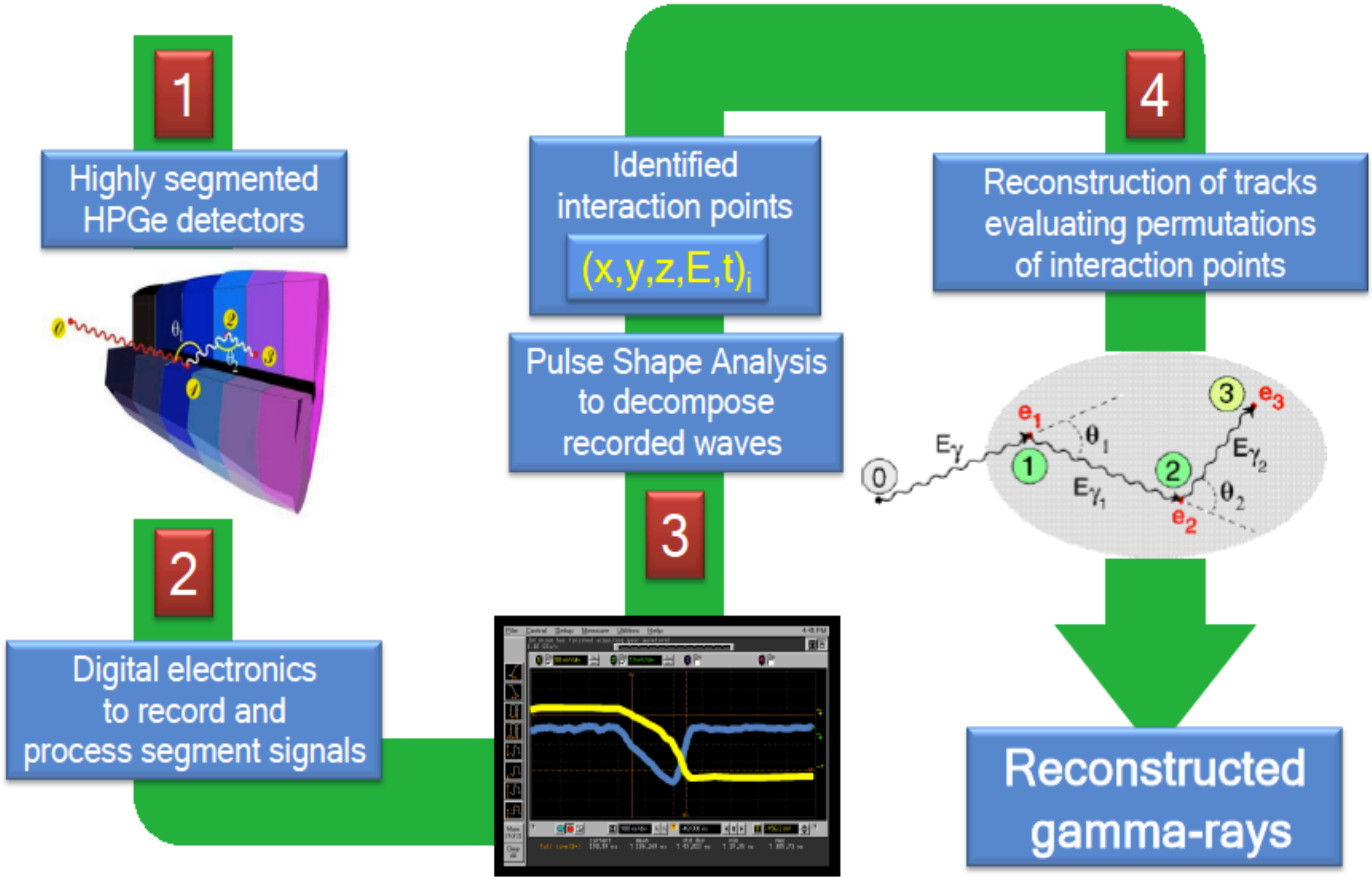

Space experiments

PAMELA

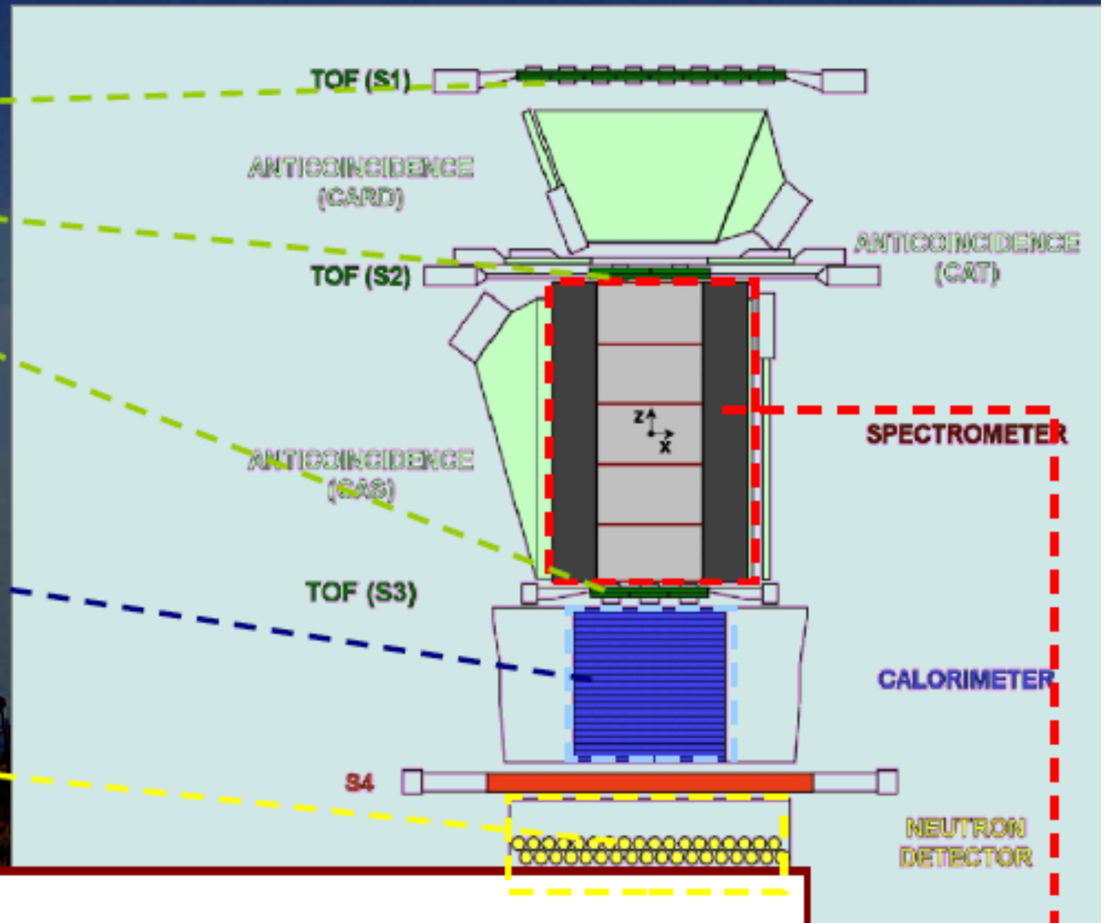

Time-Of-Flight (TOF)

plastic scintillators + PMT:

- Trigger
- Upward-going rejection
- Mass identification up to 1 GeV
- Charge value from dE/dL

Electromagnetic calorimeter

W/Si sampling (16.3 X_0, 0.6 λ_I)

- Discrimination e^+ / p, p-bar / e^- (shower topology)
- Direct E measurement for e^-/e^+

Neutron detector

polyethylene + ^{3}He counters:

- High-energy e/h discrimination

Spectrometer

microstrip Si tracking system (TRK) + permanent magnet

6 plans

- Charge sign (particle/antiparticle discrimination)
- Momentum
- Charge value from dE/dL
- 6 planes of double-sided (X-Y) microstrip Si sensors.
- Spatial resolution: 3÷4 mm.

GF: 21.6 cm² sr
Masse: 470 kg
Taille: 130 · 70 · 70 cm³
Consommation: 360 W

Particle Identification

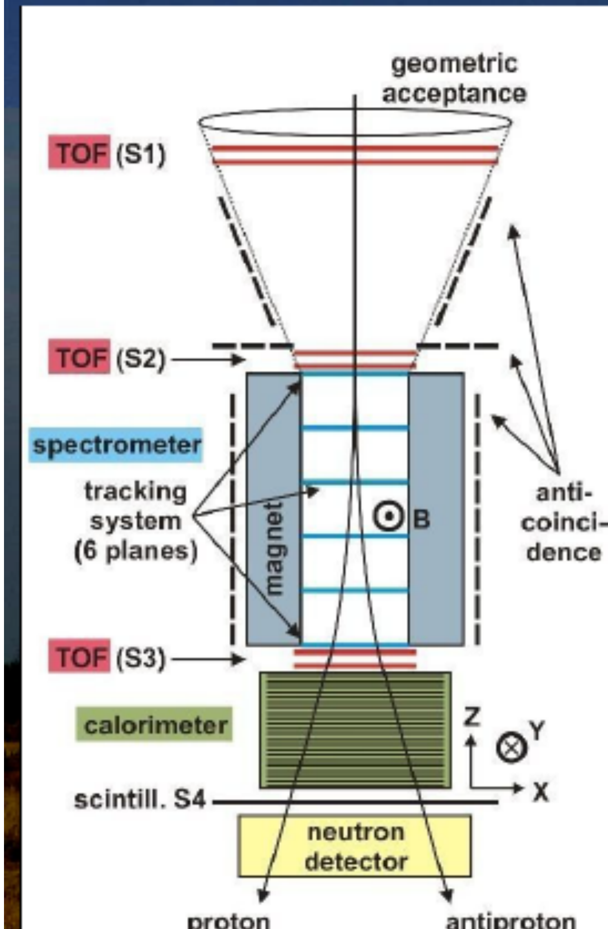

- Rigidity (p/Ze) from tracker
- dE/dx or E from time-of-flight or calorimeter
- Redundancy

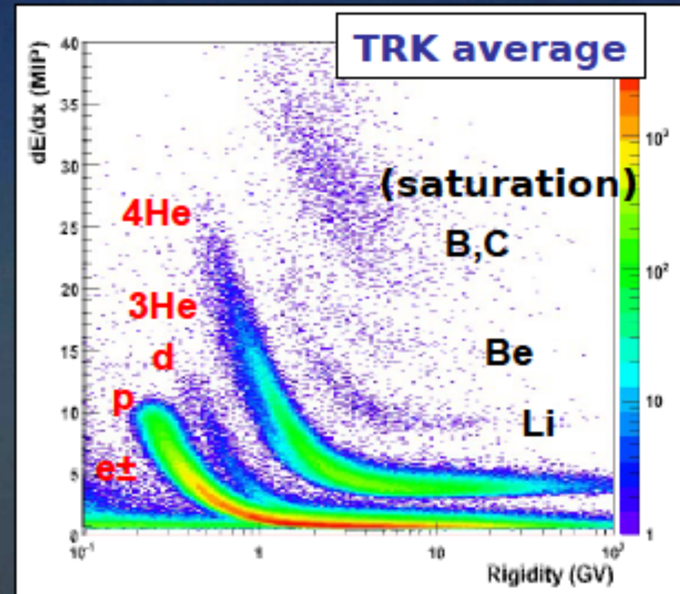

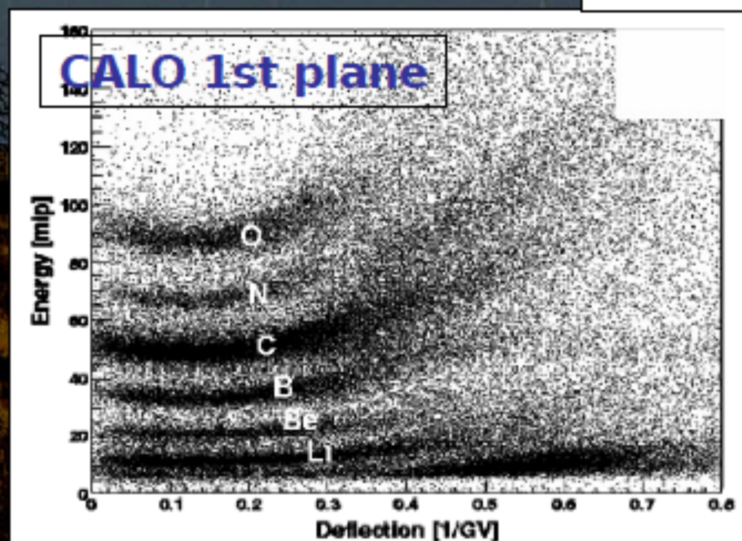

PID at low momentum : e/π/K/p

Use physics process sensitive to particle mass or speed :
-Transition radiation (sensitive to γ=E/m): distinguish electron from heavy charged particles
- TOF : measure particle speed : two particles of same energy have different speed if different mass
- dE/dx : dependence on γ and β
- Rich detectors : linked to particle speed in the medium
Most of the time need to combine two techniques and/or with p momentum

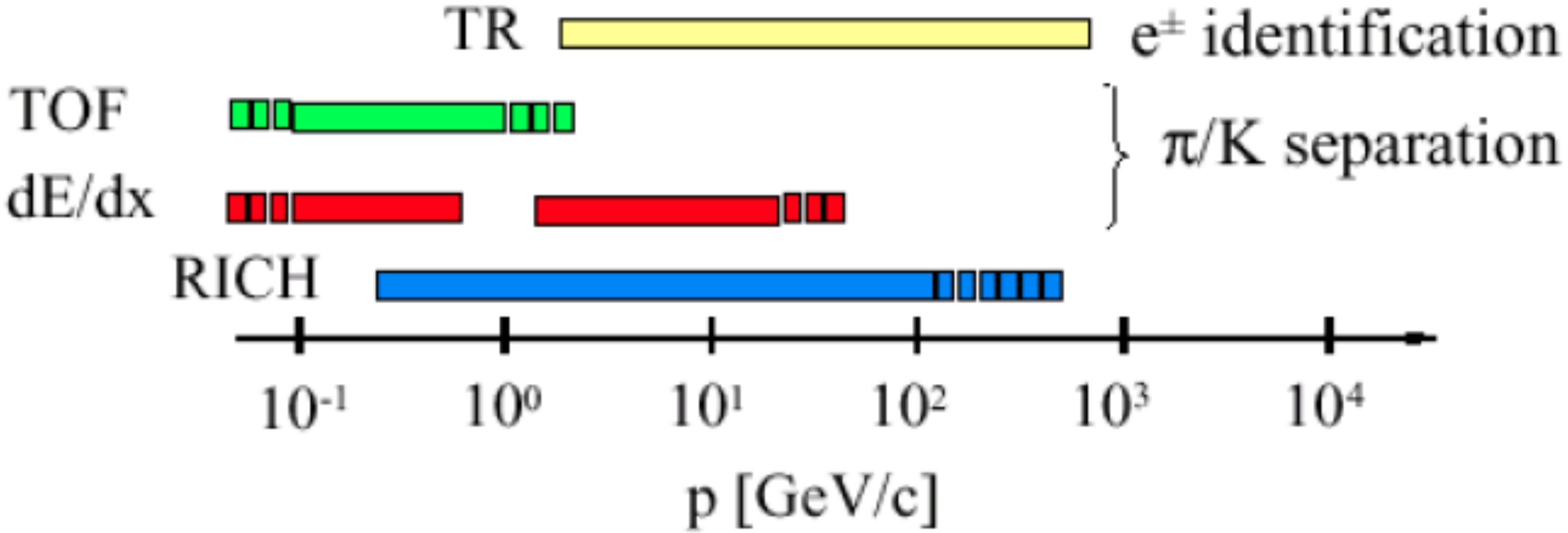

Time of flight measurement

L. Serin ESC2011

Particle ID using Time Of Flight (TOF)

$$t = \frac{L}{\beta c}$$

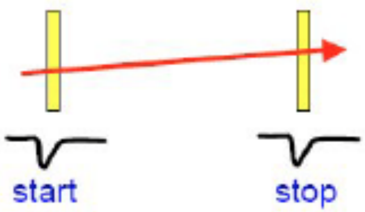

Combine TOF with momentum measurement $(p = m_0 \beta\gamma)$

$$m = p\sqrt{\frac{c^2 t^2}{L^2} - 1}$$

Mass resolution $\frac{dm}{m} = \frac{dp}{p} + \gamma^2\left(\frac{dt}{t} + \frac{dL}{L}\right)$

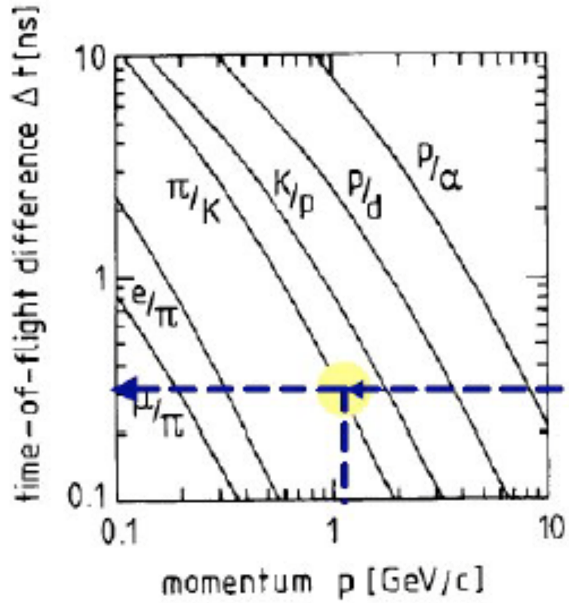

Δt for L = 1 m path length

σ_t = 300 ps
π/K separation up to 1 GeV/c

TOF difference of 2 particles at a given momentum

$$\Delta t = \frac{L}{c}\left(\frac{1}{\beta_1} - \frac{1}{\beta_2}\right) = \frac{L}{c}\left(\sqrt{1 + m_1^2 c^2 / p^2} - \sqrt{1 + m_2^2 c^2 / p^2}\right) \approx \frac{Lc}{2p^2}\left(m_1^2 - m_2^2\right)$$

Used in ALICE with time resolution about 100 ps with multigaps RPC

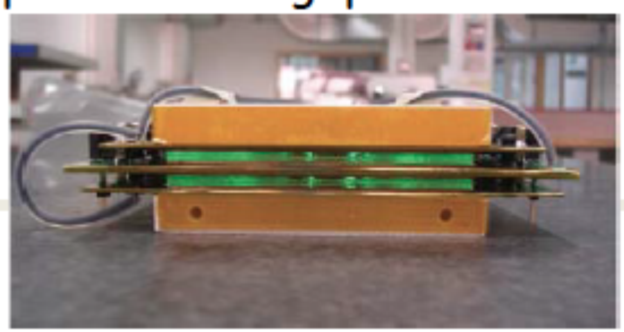

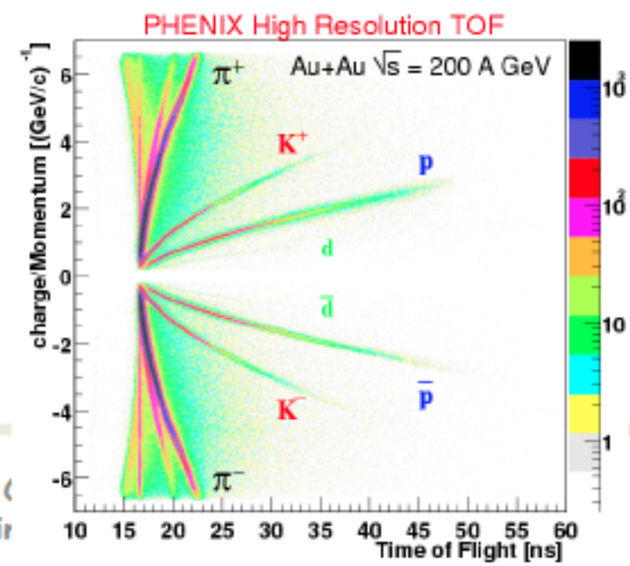

Lifetime tagging

Tracks have significant impact parameter, d_0, and maybe form a reconstructed secondary vertex

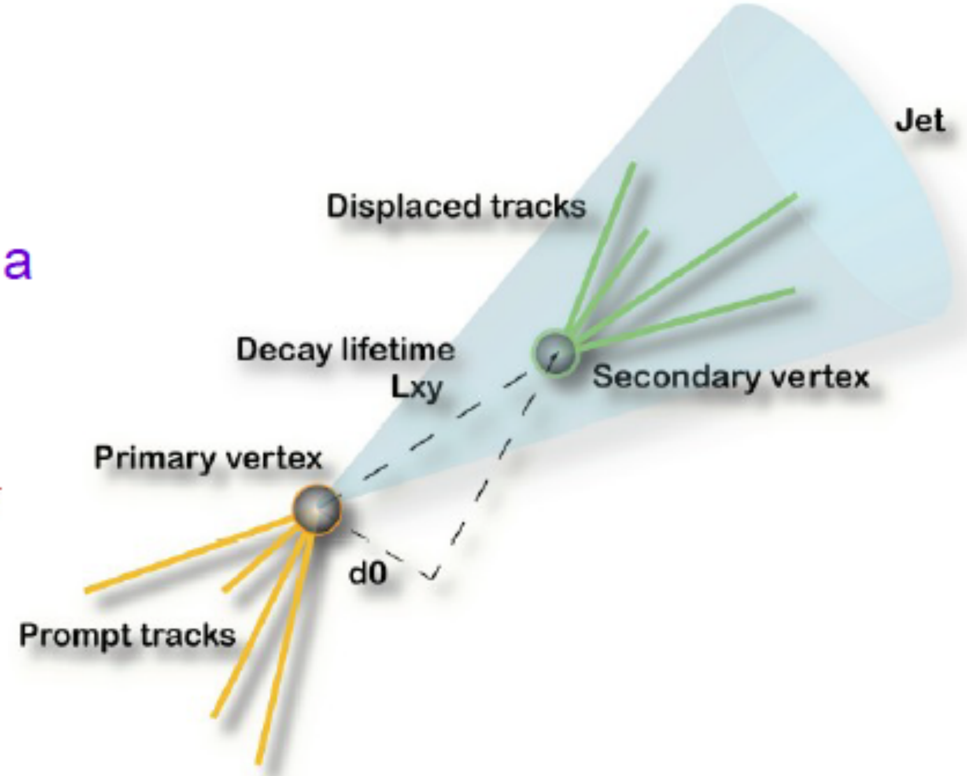

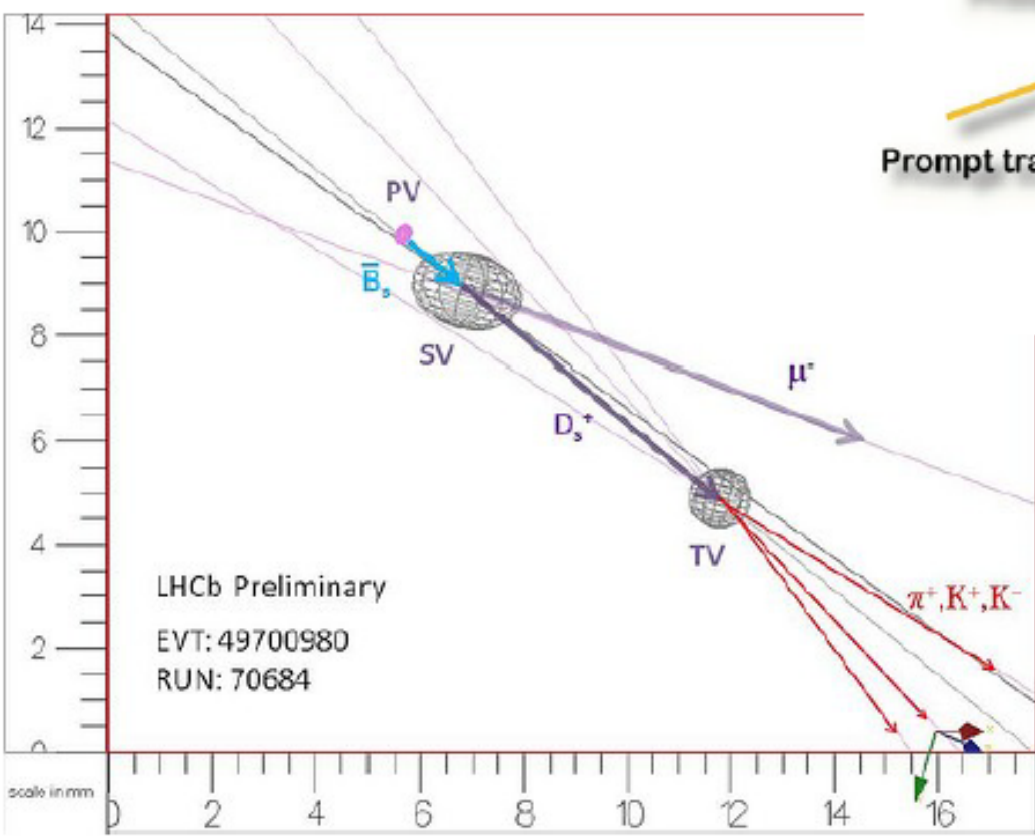

Example of a fully reconstructed event from LHCb, with primary, secondary and tertiary vertex.

Tagging

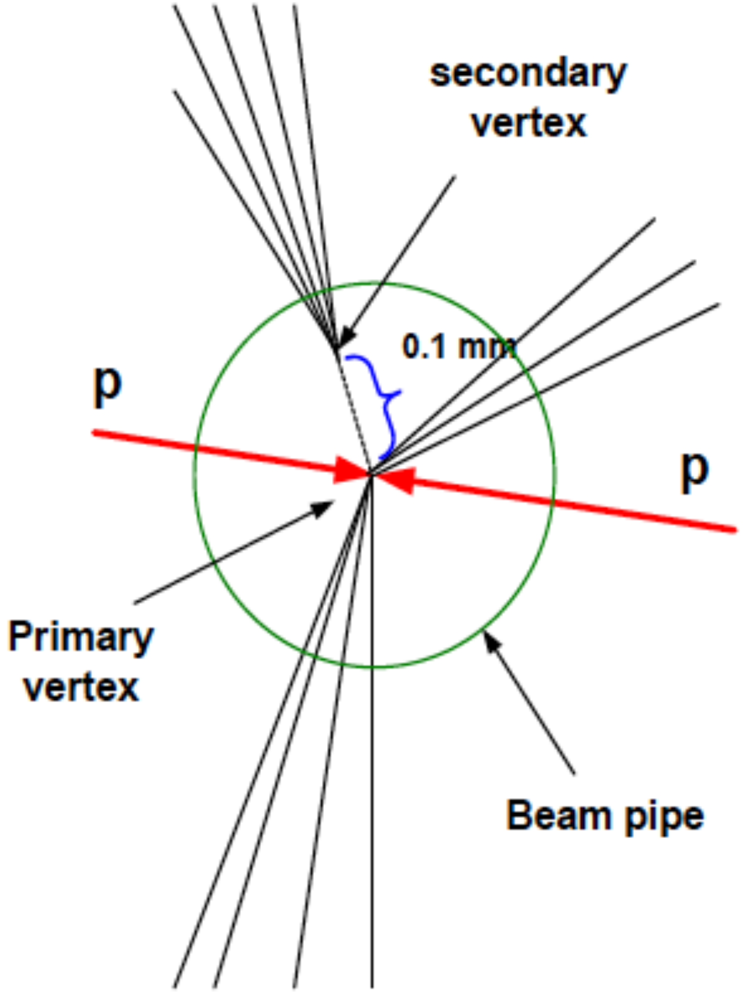

Identification of particles by their lifetime:
e.g.:

$D^{\pm}$	$\tau = 1040 \cdot 10^{-15}$ s
	$c\,\tau = 312\ \mu m$
D^0	$\tau = 410 \cdot 10^{-15}$ s
	$c\,\tau = 123\ \mu m$
$B^{\pm}$	$\tau = 1671 \cdot 10^{-15}$ s
	$c\,\tau = 501\ \mu m$
B^0	$\tau = 1536 \cdot 10^{-15}$ s
	$c\,\tau = 460\ \mu m$

➔ excellent vertex resolution needed!

UNIVERSITÉ DE STRASBOURG

Collider experiments
LHC

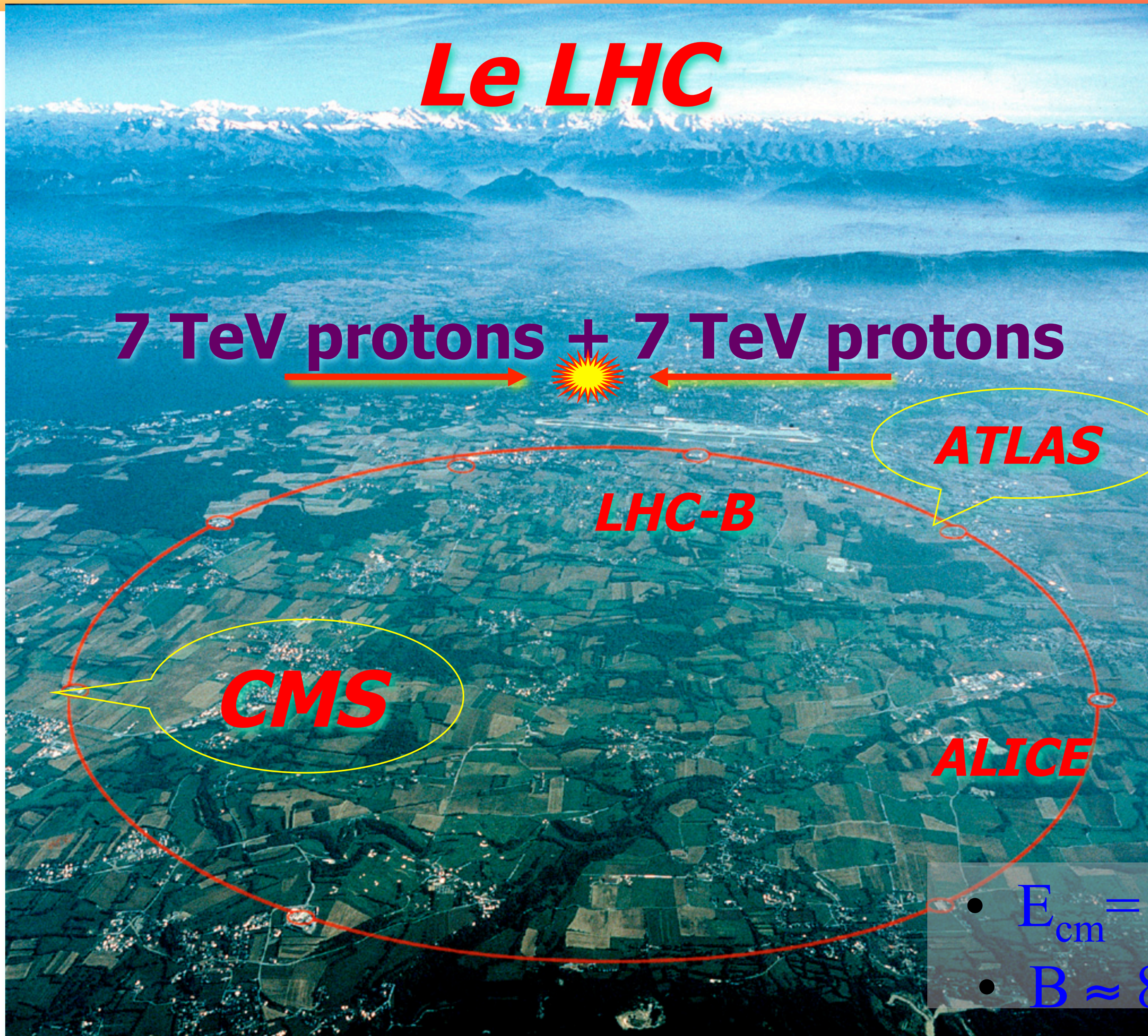

- E_{cm}=14 TeV
- B ≈ 8 Tesla

Le LHC

- E_{cm}=14 TeV
- B ≈ 8 Tesla

Experiments at colliders

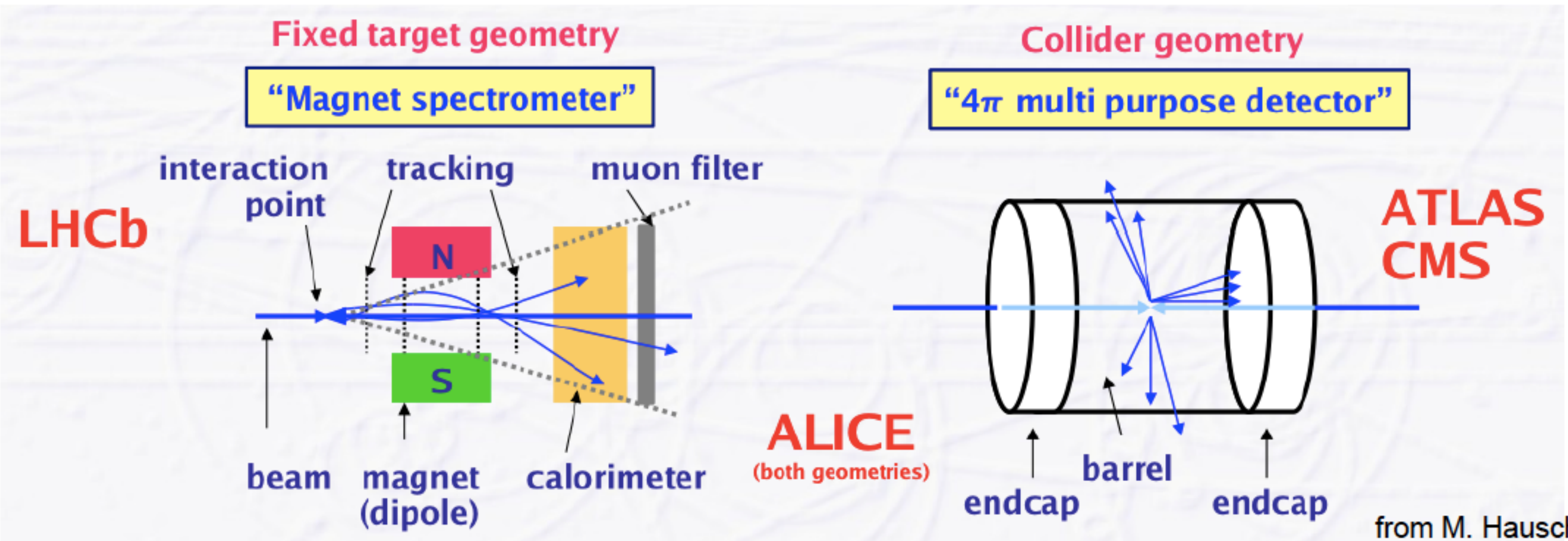

from M. Hauschild

But LHCb is NOT a fixed Target experiment !

$$E_{CM}^{\text{collider}} = 2E = \sqrt{s}$$

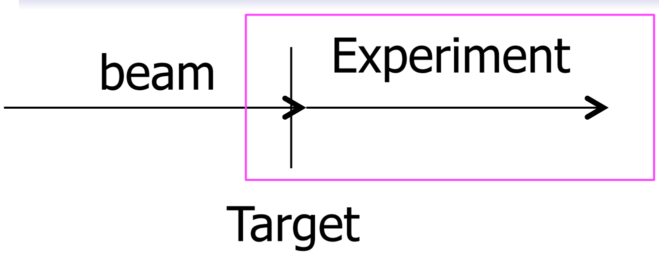

$$E_{CM}^{\text{fixed target}} = \sqrt{2Mc^2E + M^2c^4 + m^2c^4} \cong \sqrt{2Mc^2E}$$

UNIVERSITÉ DE STRA

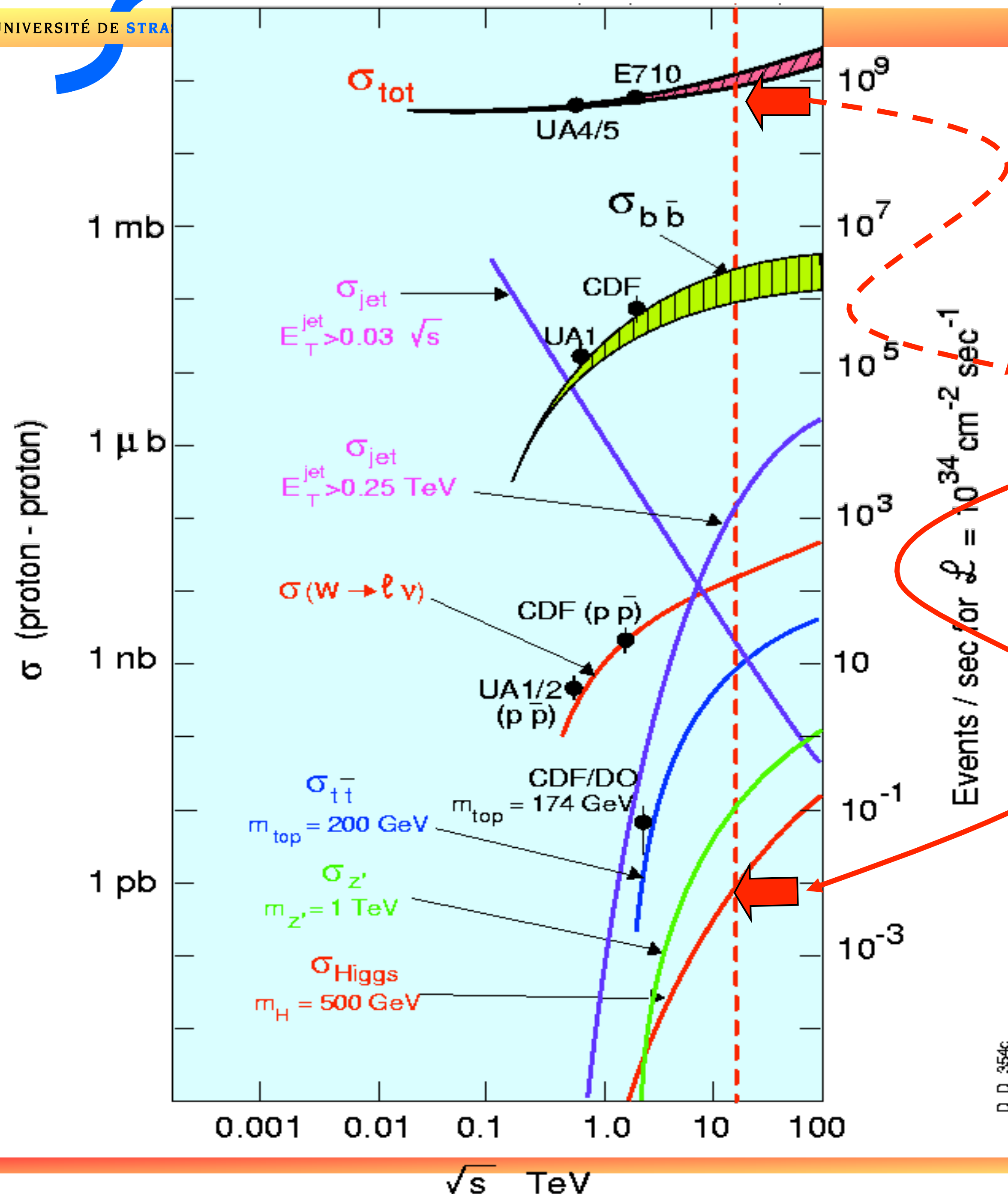

pp Collisions at LHC

$$\sigma_{\text{tot pp}} = 40 - 100\,mb$$

$$\sigma_{\text{H(500GeV)}} \approx 1\,pb$$

$$\mathcal{L} = 10^{34}\,cm^{-2}s^{-1}$$

Beam crossing rate: 40 MHz

25 interactions per crossing

$$\dot{N}_{tot} = 10^{9}\,s^{-1}$$

$$\dot{N} = 10^{-2}\,s^{-1}$$

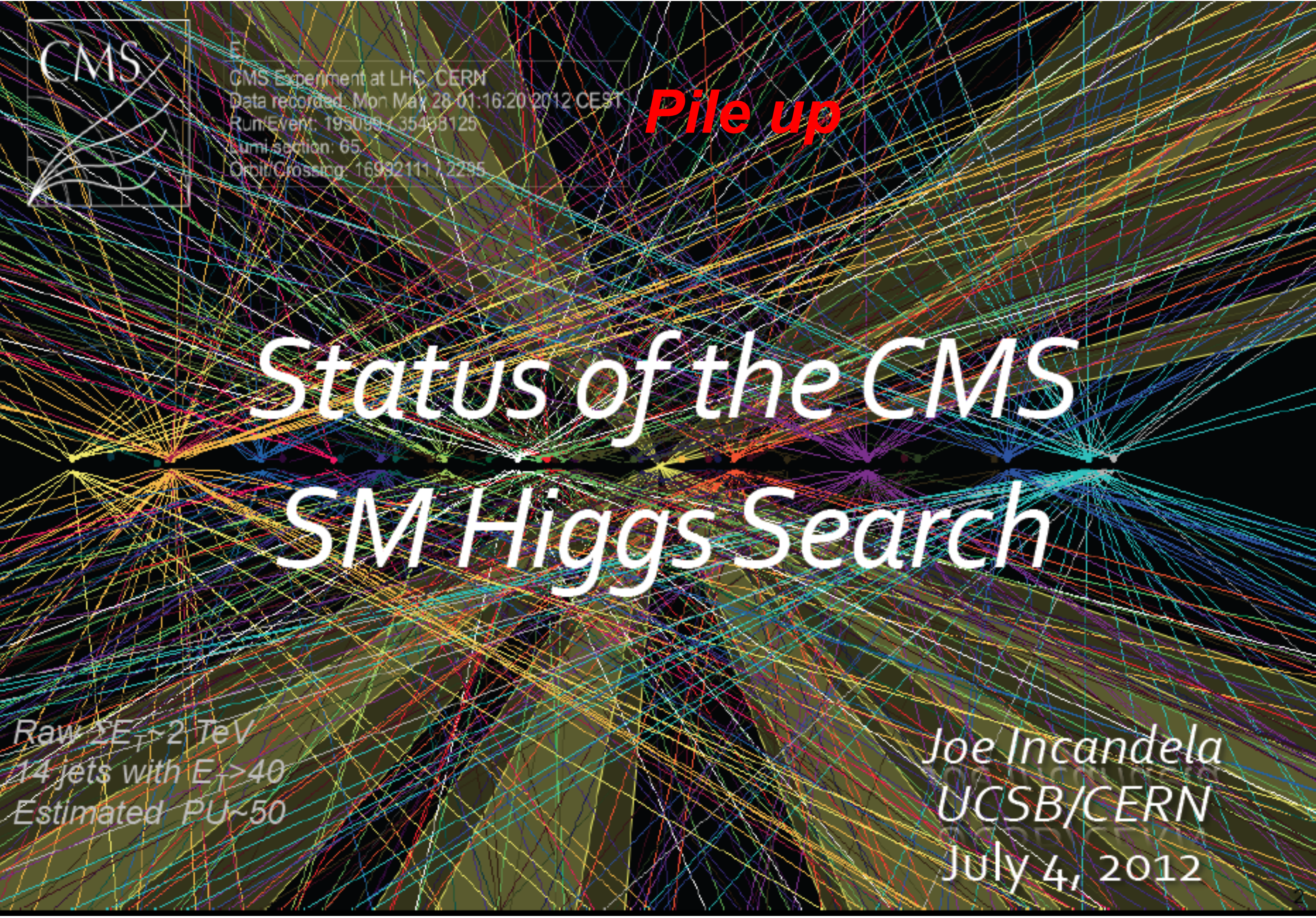
CMS
CMS Experiment at LHC, CERN
Data recorded: Mon May 28 01:16:20 2012 CEST
Run/Event: 195099 / 35438125
Lumi section: 65
Orbit/Crossing: 16992111 / 2295
Pile up
Status of the CMS
SM Higgs Search
Raw ΣE_T~2 TeV
14 jets with E_T>40
Estimated PU~50
Joe Incandela
UCSB/CERN
July 4, 2012

Radiation levels at LHC in ATLAS

***

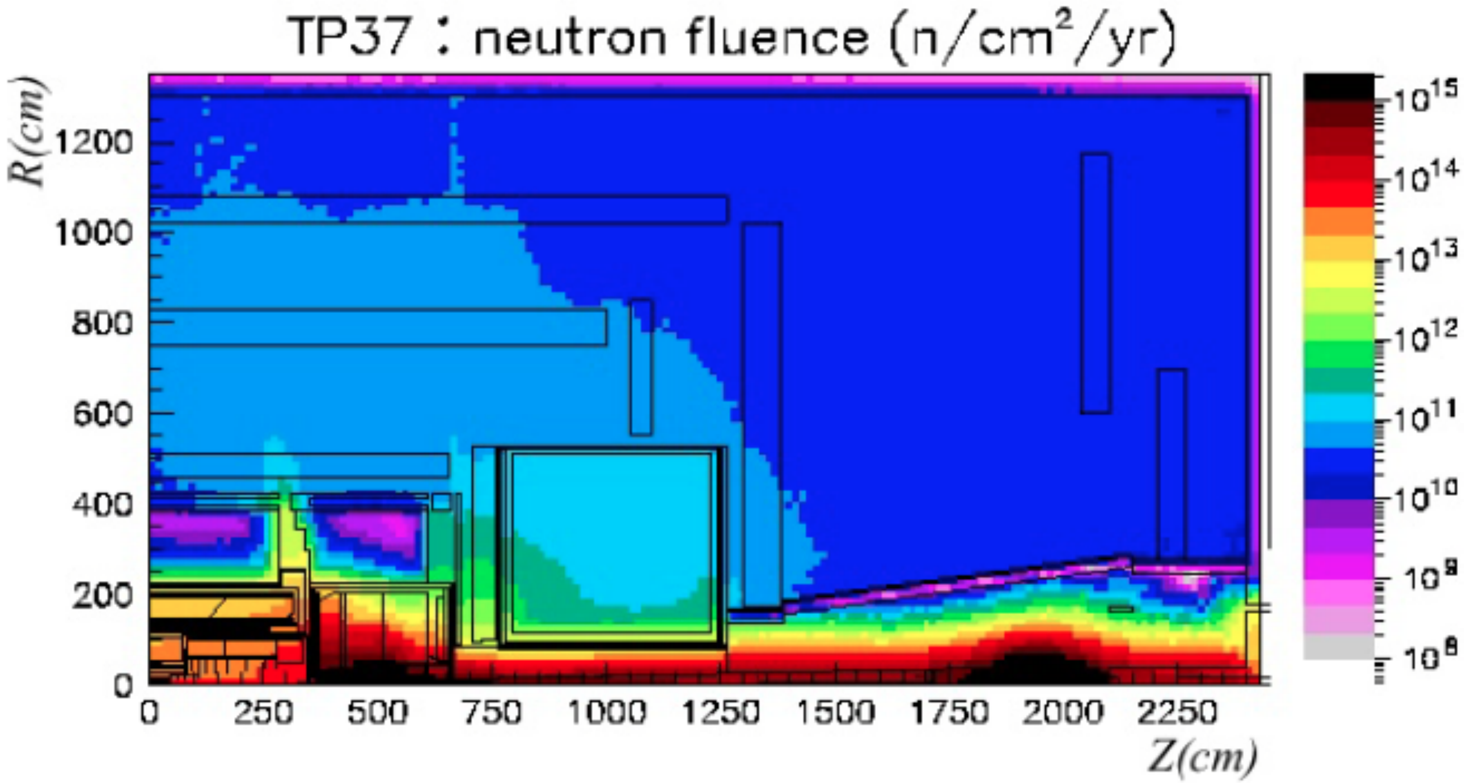

At r=11 cm, photons flux of 30 MRad !

100 Rad ~ 6.2410^{12} MeV/kg deposited energy (1J/kg)

Strong constraint on detector technology and electronics : ageing in gaseous detectors , pollution in liquids detectors, light loss (transparency) in scintillators/cerenkov, atom displacement in solid detectors

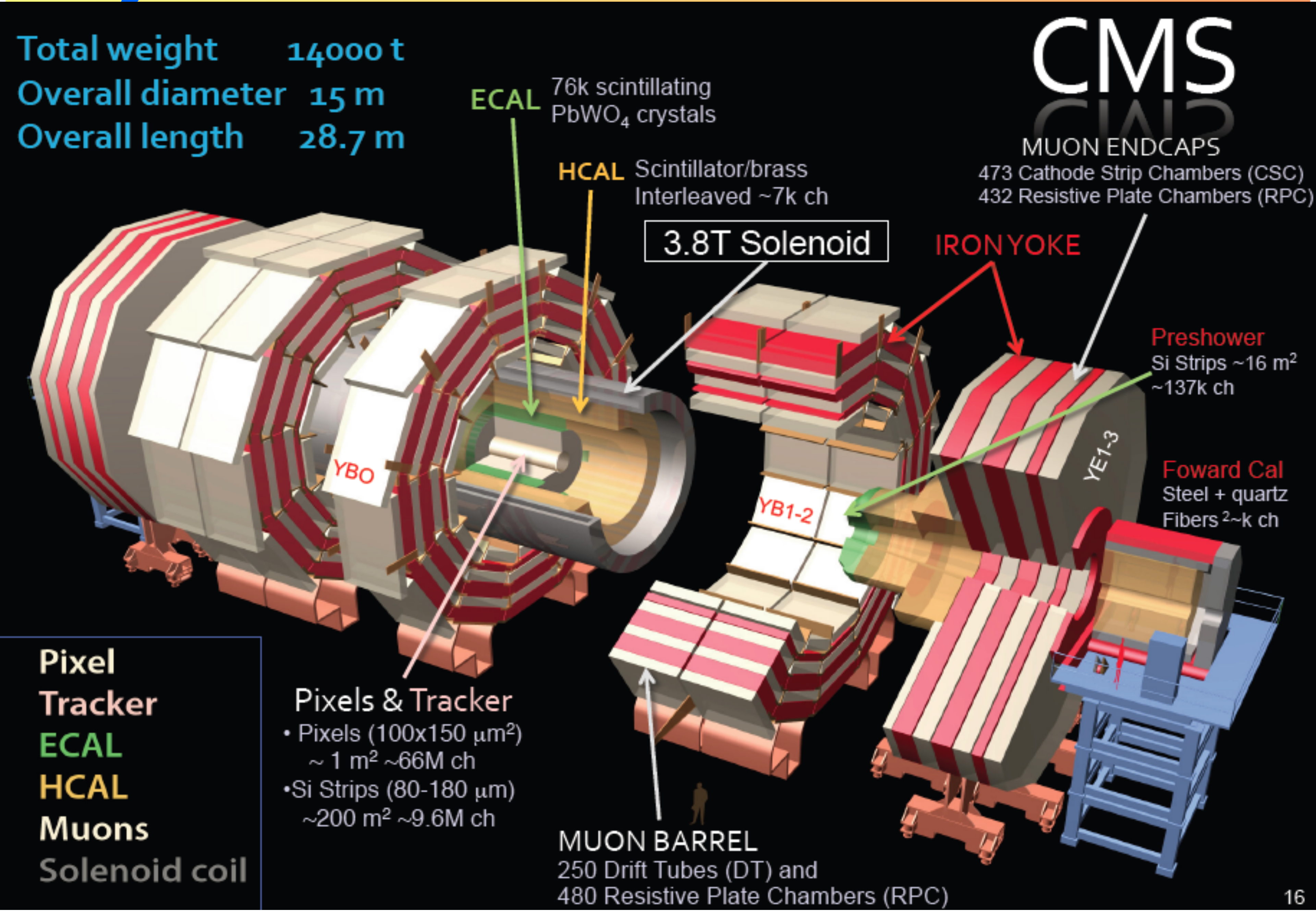
Total weight 14000 t
Overall diameter 15 m
Overall length 28.7 m
CMS
ECAL
76k scintillating
$PbWO_4$ crystals
HCAL
Scintillator/brass
Interleaved ~7k ch
3.8T Solenoid
IRON YOKE
MUON ENDCAPS
473 Cathode Strip Chambers (CSC)
432 Resistive Plate Chambers (RPC)
Preshower
Si Strips ~16 m²
~137k ch
YE1-3
YBO
YB1-2
Foward Cal
Steel + quartz
Fibers ²~k ch
Pixel
Tracker
ECAL
HCAL
Muons
Solenoid coil
Pixels & Tracker
• Pixels (100x150 μm²)
~ 1 m² ~66M ch
•Si Strips (80-180 μm)
~200 m² ~9.6M ch
MUON BARREL
250 Drift Tubes (DT) and
480 Resistive Plate Chambers (RPC)

Compact Muon Solenoid

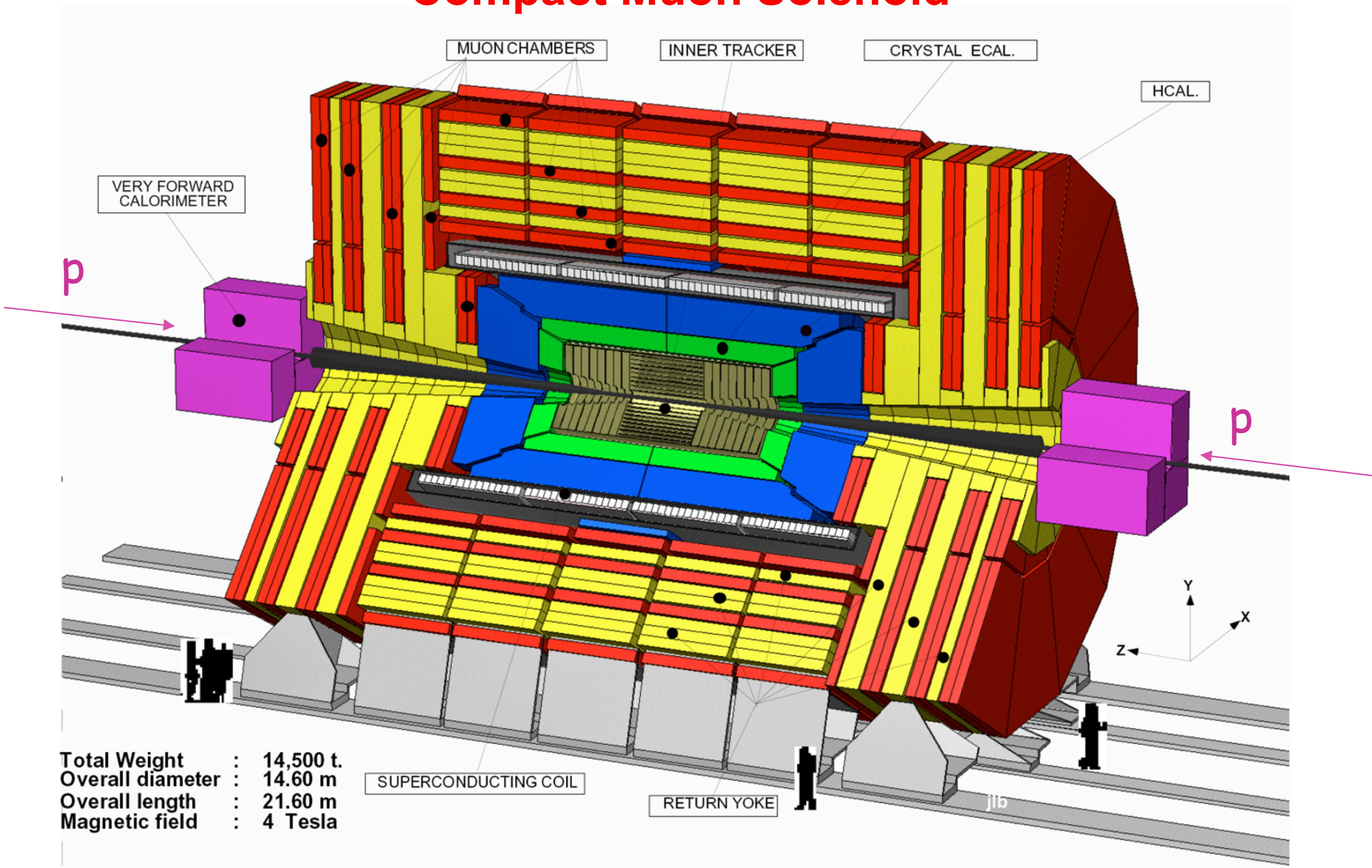

How huge are ATLAS and CMS?

ATLAS superimposed to the 5 floors of building 40

CMS

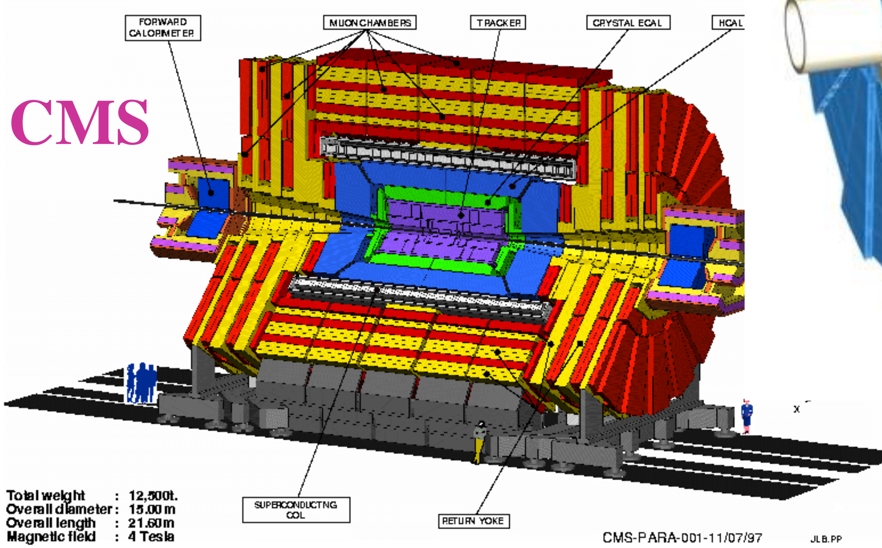

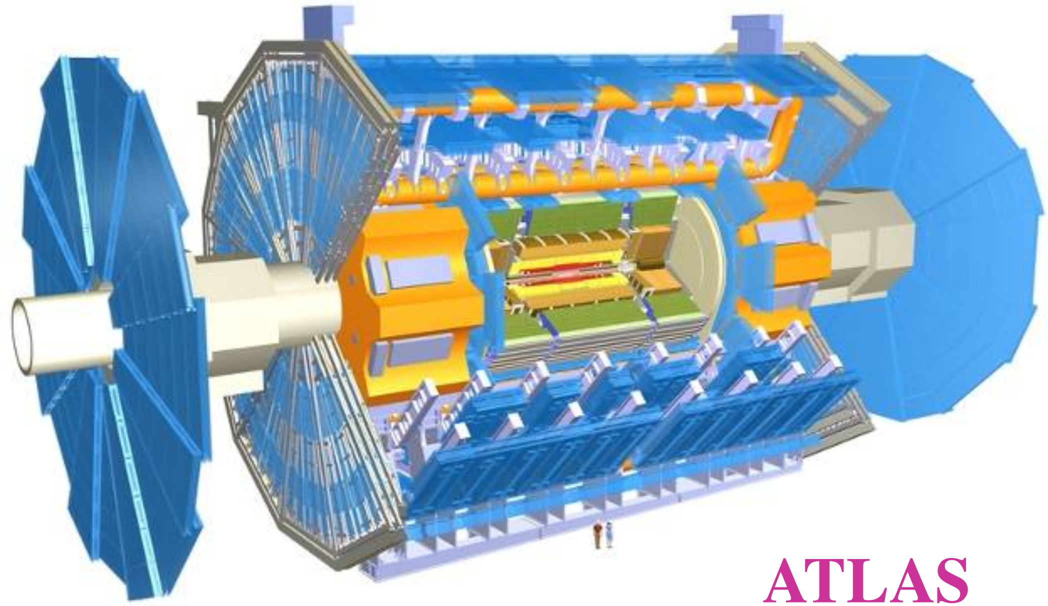

ATLAS

	ATLAS	CMS
Overall weight (tons)	7000	12500
Diameter	22 m	15 m
Length	46 m	22 m
Solenoid field	2 T	4 T

LHC... L'INFINIMENT PETIT VU EN GRAND

Exposition du 13 au 25 octobre 2008 au Palais Universitaire de Strasbourg.
Ouvert du lundi au samedi de 9h à 18h, Entrée libre

CMS END CAP

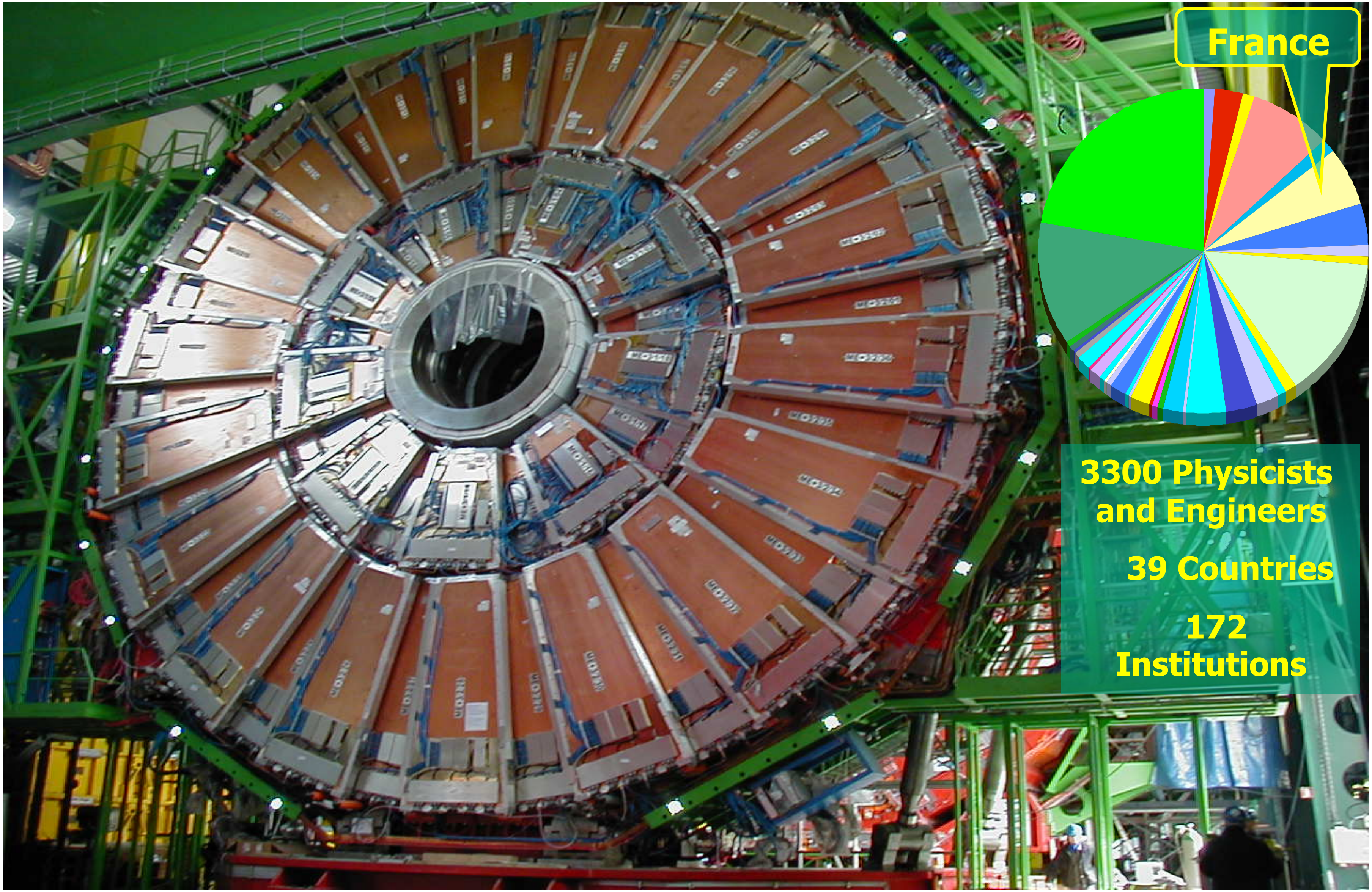
France
3300 Physicists
and Engineers
39 Countries
172
Institutions

CMS Design Goals

- **A good and redundant *muon system*** (= many layers – if one layer fails we can fall back on the others**)**
- **The best possible *electromagnetic calorimeter***
- **A high quality *central tracking***
- **A *hadronic calorimeter* that has good energy resolution and that is as hermetic as possible**
- **Affordable! (= ~500 MCHF)**

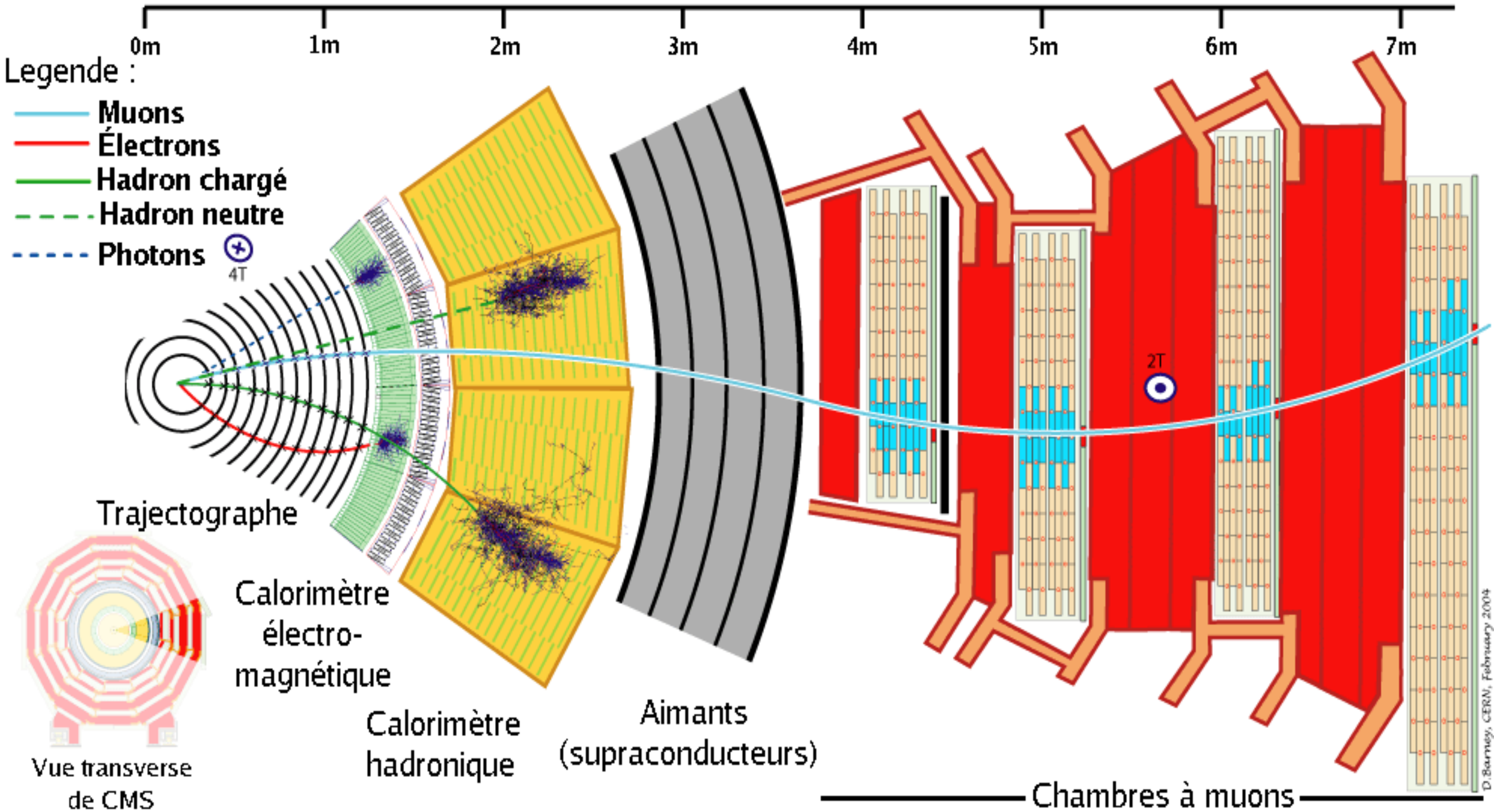

Transverse slice through CMS detector

https://cms-docdb.cern.ch/cgi-bin/PublicEPPOGDocDB/RetrieveFile?docid=97&version=1&filename=CMS_Slice_elab.swf

UNIVERSITÉ DE STRASBOURG

Reconstruction of transverse momentum in a magnetic field

Exercise !!!

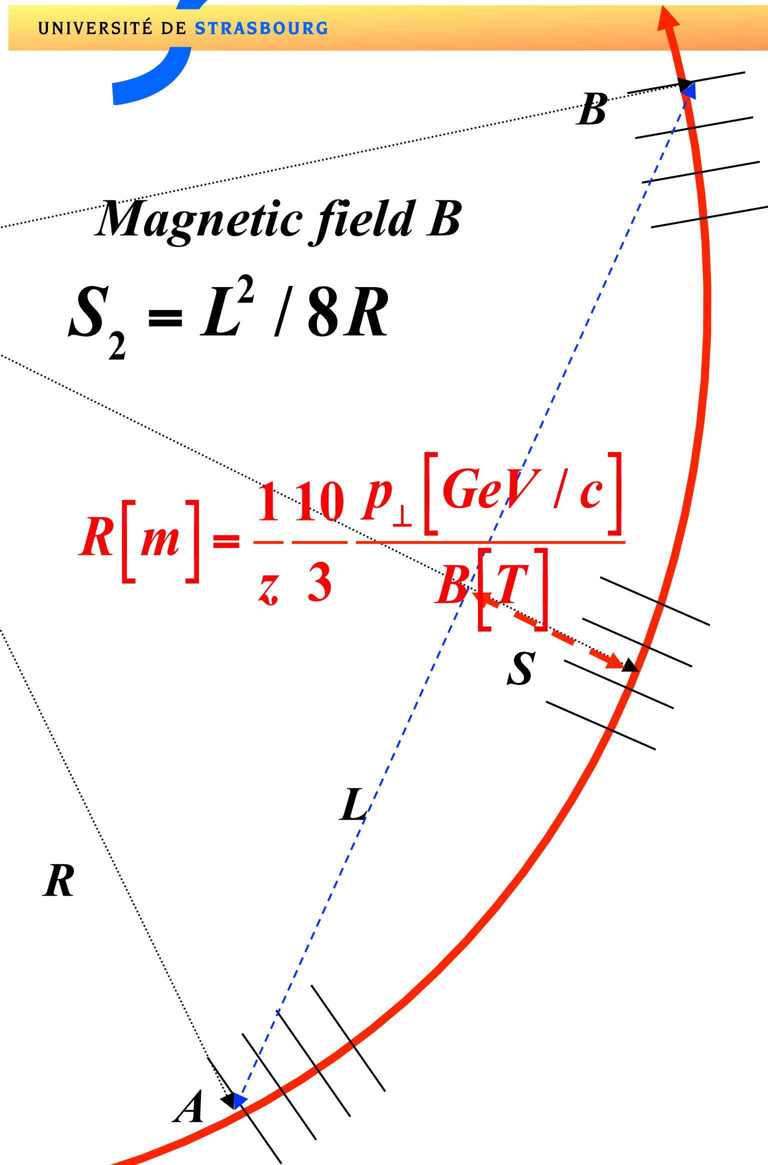

$$S_2 = L^2 / 8R$$

$$R[m] = \frac{1}{z}\frac{10}{3}\frac{p_\perp[GeV/c]}{B[T]}$$

- Mouvement of a charge z in a uniform magnetic field
- Momentum resolution *dp/p*
- Spatial resolution of the sagitta *dS/S*

$$\frac{dS}{S} = \frac{dp_\perp}{p_\perp} = \frac{80}{3 \cdot z}\frac{1}{BL^2} p_\perp dS$$

$$[B] = Tesla;\ [L] = m; [p_\perp] = GeV/c$$

If the trajectory is measured with *N* points:

$$\left.\frac{\sigma(p_T)}{p_T}\right|^{meas.} = \frac{\sigma(x) \cdot p_T}{0.3 \cdot BL^2}\sqrt{720/(N+4)} \quad \text{(for N} \geq \sim 10)$$

Resolution and multiple scattering

$$\left.\frac{\sigma(p_T)}{p_T}\right|^{meas.} = \frac{\sigma(x)\cdot p_T}{0.3\cdot BL^2}\sqrt{720/(N+4)}$$ (for N ≥ ~10)

$$\frac{\sigma(p)}{p_T} \propto \sigma(x)\cdot p_T$$

$$\sigma(x)\Big|^{MS} \propto \theta_0 \propto \frac{1}{p}$$

$$\left.\frac{\sigma(p)}{p_T}\right|^{MS} = \text{constant}$$, i.e. independent of p !

More precisely: $$\left.\frac{\sigma(p)}{p_T}\right|^{MS} = 0.045\frac{1}{B\sqrt{LX_0}}$$

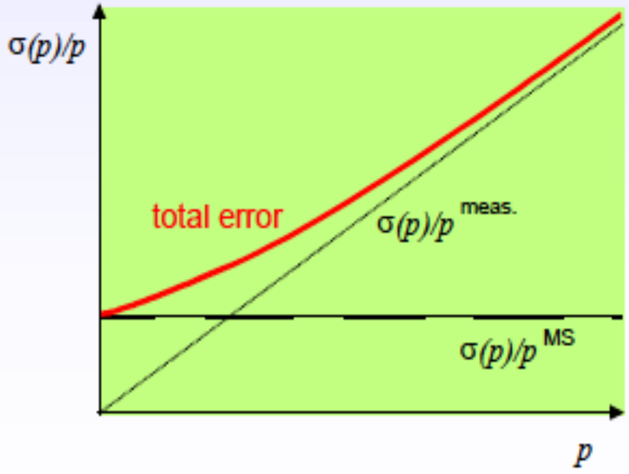

Example:

p_t = 1 GeV/c, L = 1m, B = 1 T, N = 10

$\sigma(x)$ = 200 µm: $$\left.\frac{\sigma(p_T)}{p_T}\right|^{meas.} \approx 0.5\%$$

Assume detector (L = 1m) to be filled with 1 atm. Argon gas (X_0 = 110m),

$$\left.\frac{\sigma(p)}{p_T}\right|^{MS} \approx 0.5\%$$

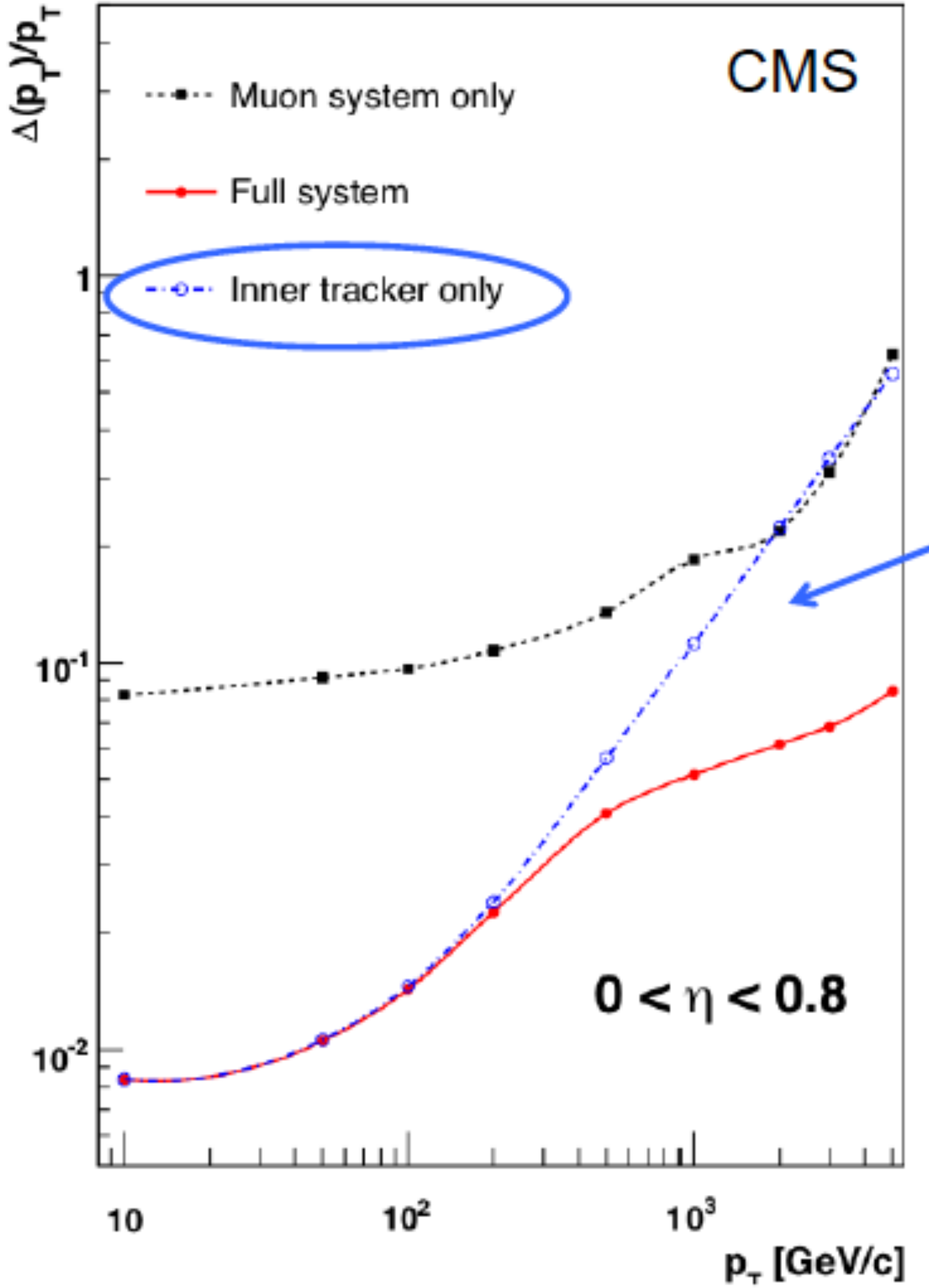

$$\frac{dp_\perp}{p_\perp} = \alpha \times p_\perp dS$$

$$\oplus\left(\text{multiple scattering}\right)$$

CMS Tracker

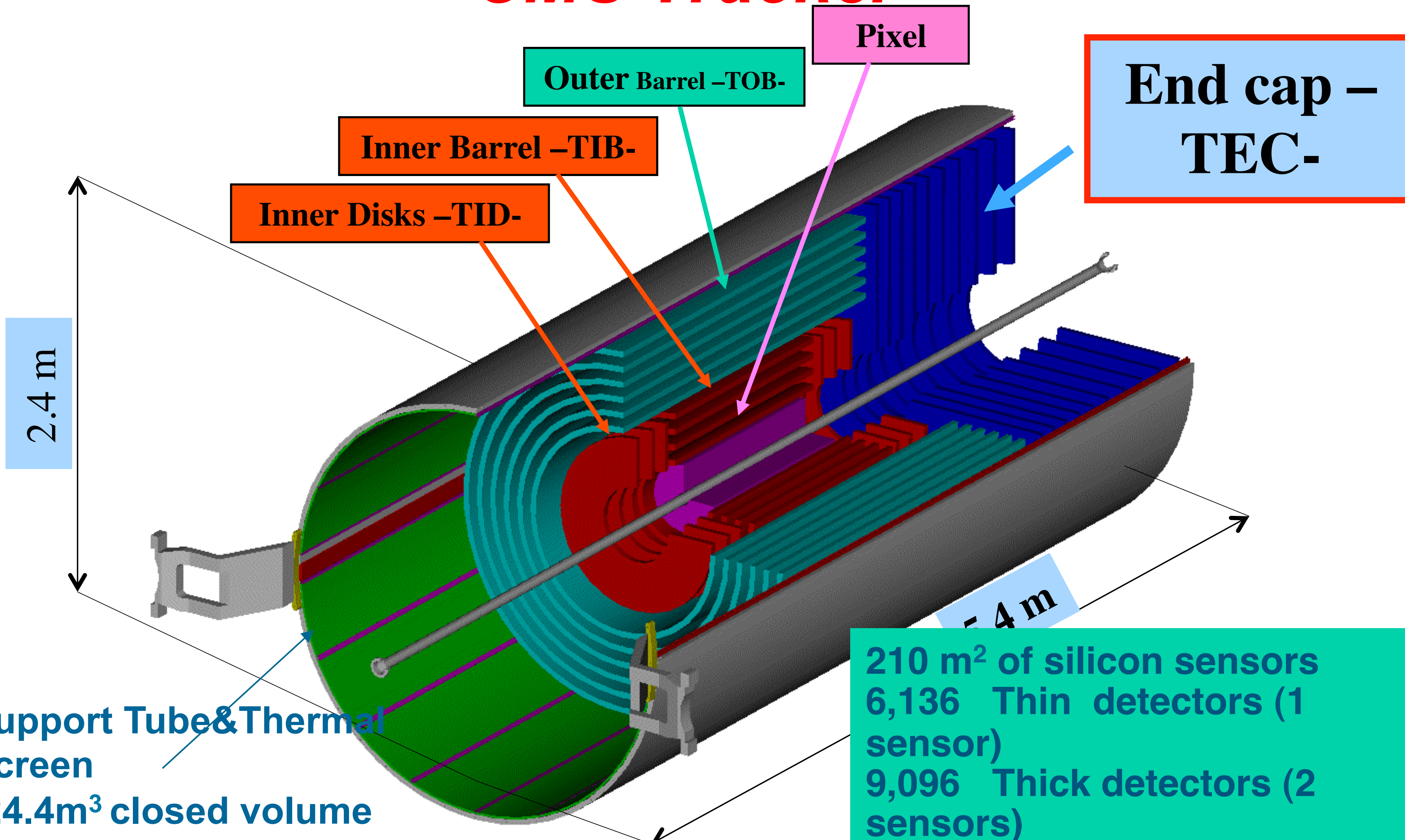

Support Tube&Thermal Screen

- 24.4m^3 closed volume
- operating temperature –10°C

210 m^2 of silicon sensors
6,136 Thin detectors (1 sensor)
9,096 Thick detectors (2 sensors)
9,648,128 electronics channels

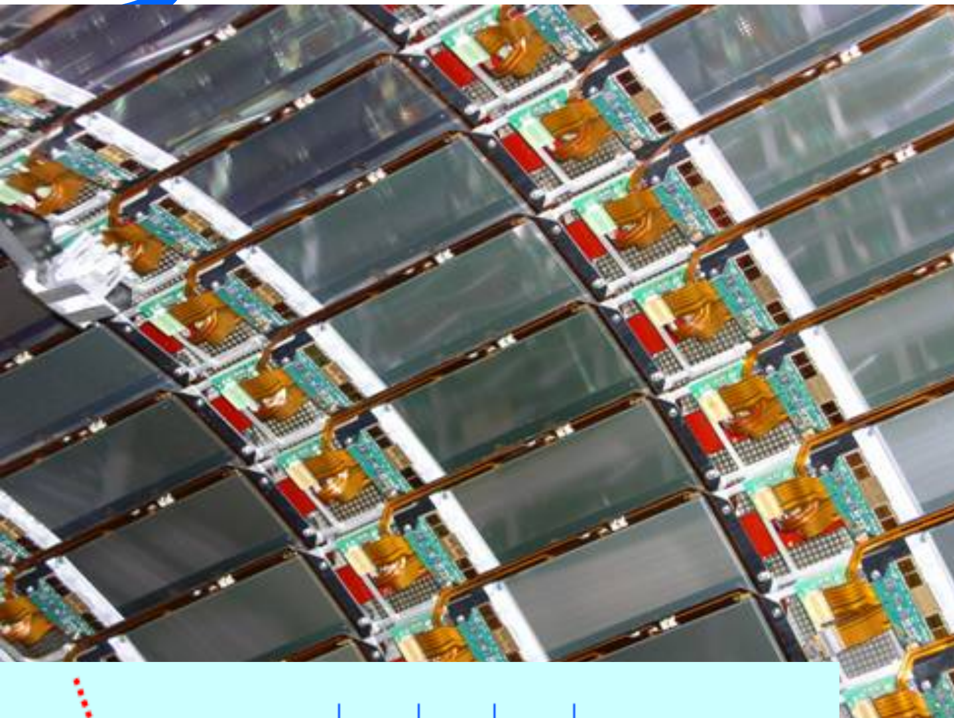

Silicon strip detectors

TIB Barrel

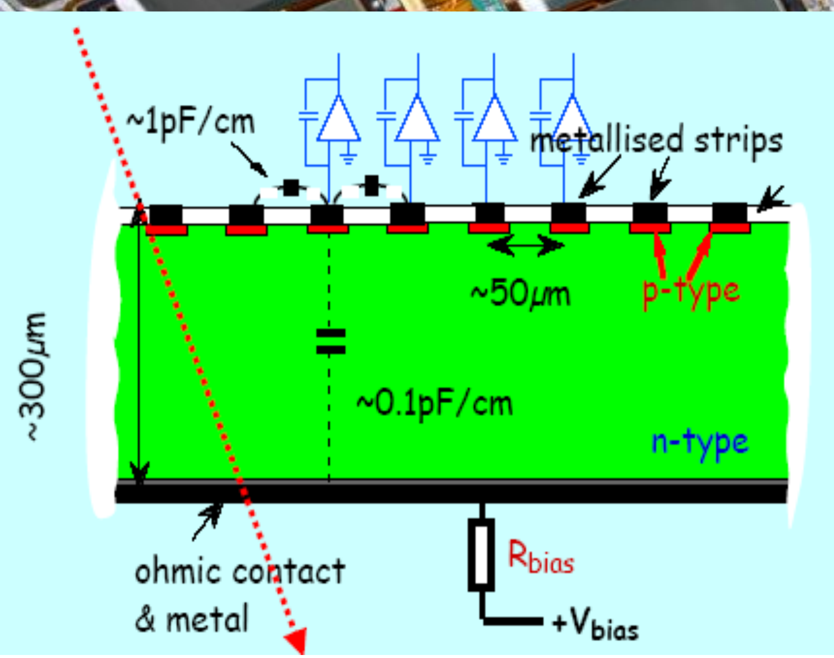

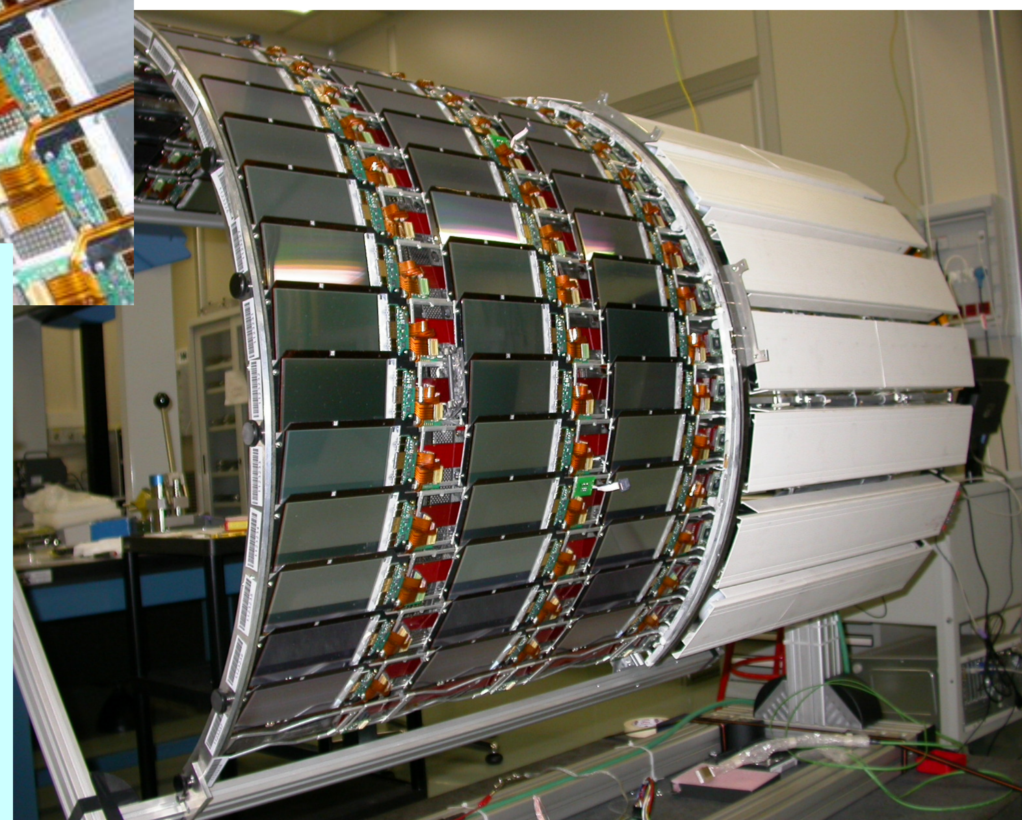

Construction of CMS

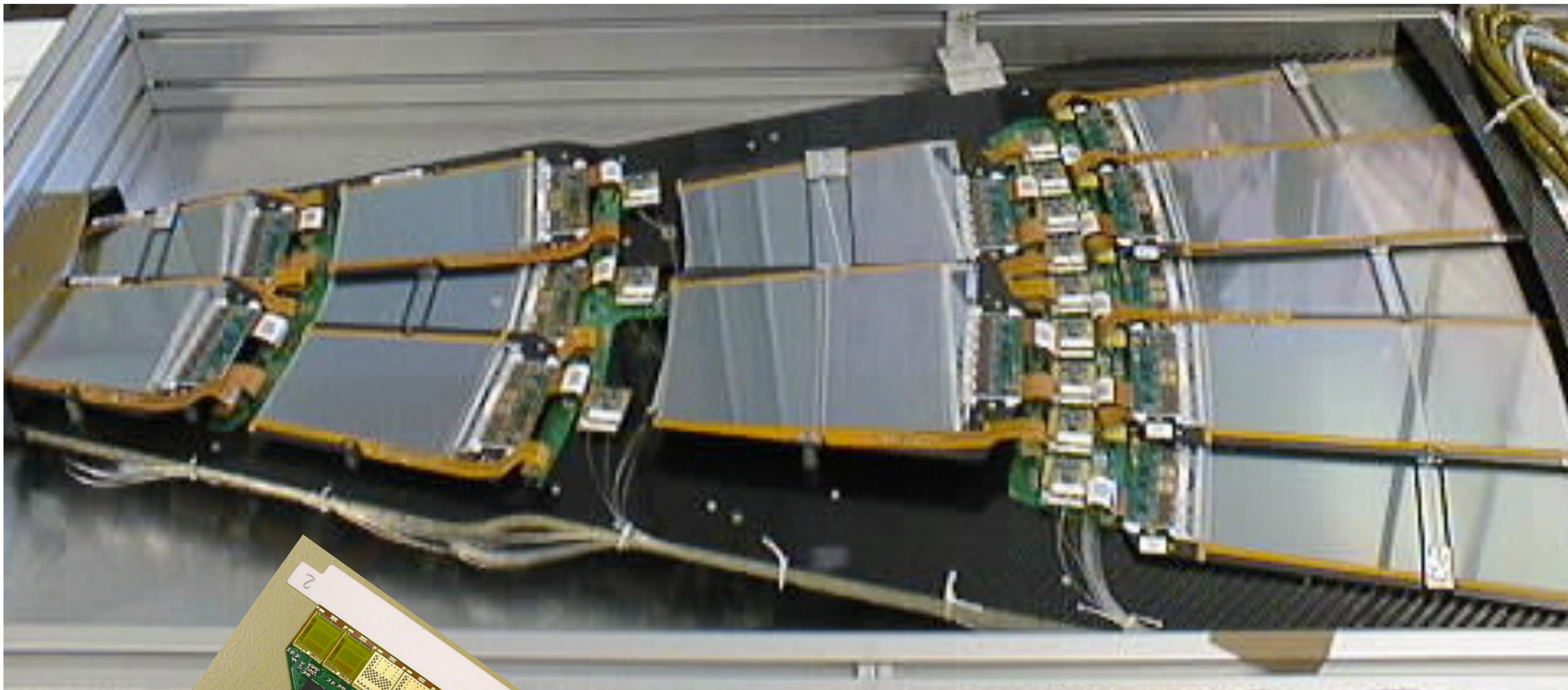

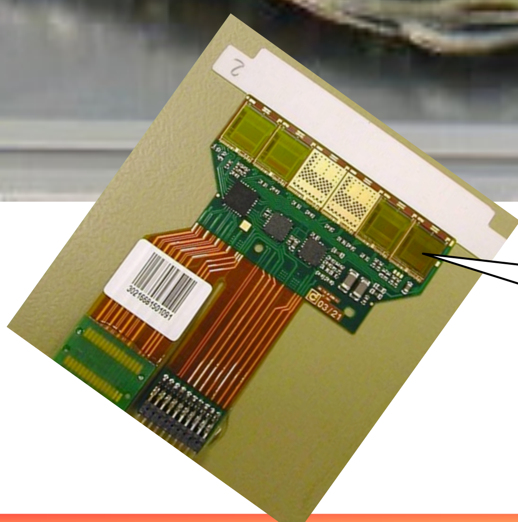

Radiation hard highly integrated electronics
128 channels, Amplifier, analogue memory, multiplexer

The Electromagnetic Calorimeter - ECAL

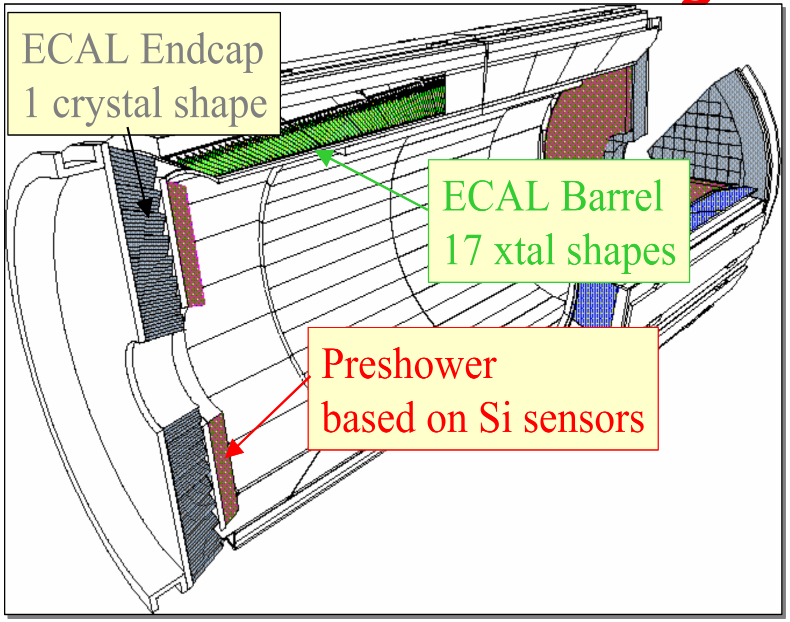

Characteristics of $PbWO_4$
$X_0 = 0.89cm$
$\rho = 8.28 g/cm^3$
R_M (Molière radius) = 2.2cm

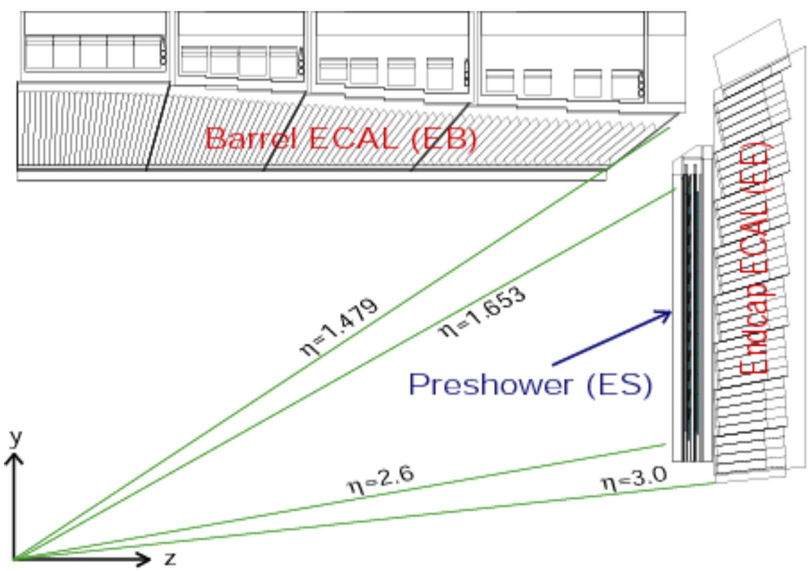

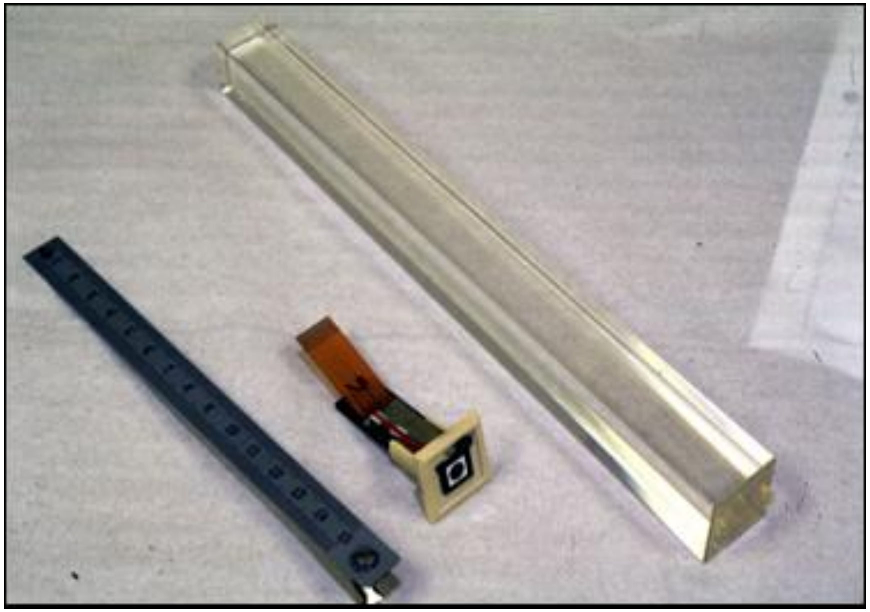

Ulrich.Goerlach@iphc.cnrs.fr, ASP Particle detectors 2012

Material in front of your expensive elm calorimeter

Weight: 4.5 tons

Weight: 3.7 tons

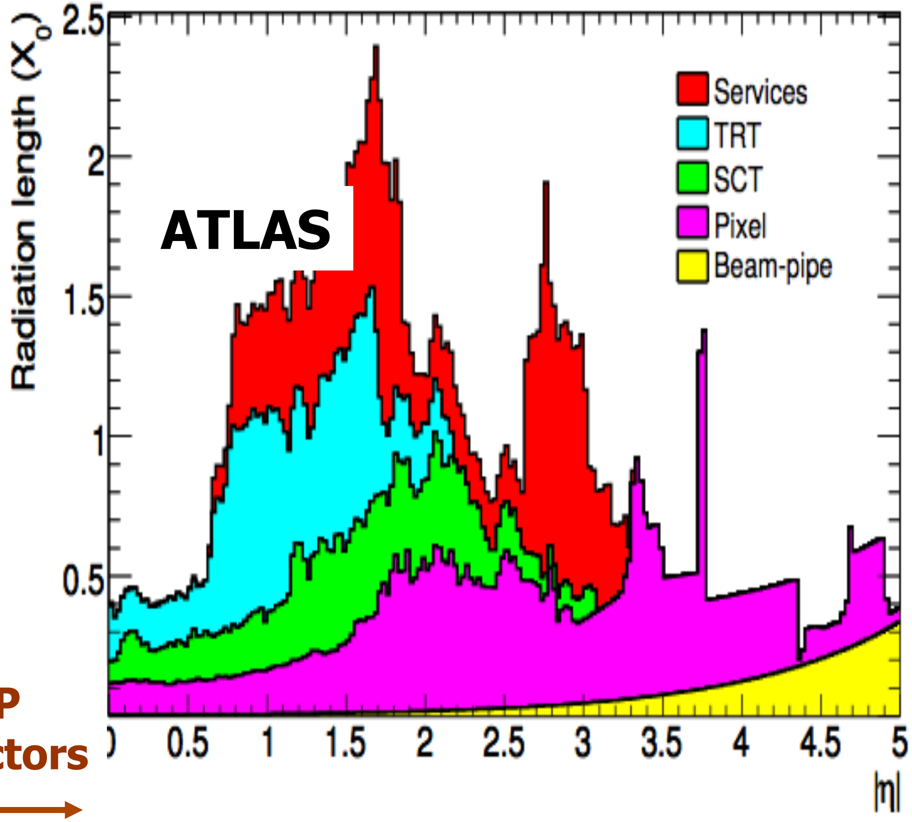

LEP
detectors

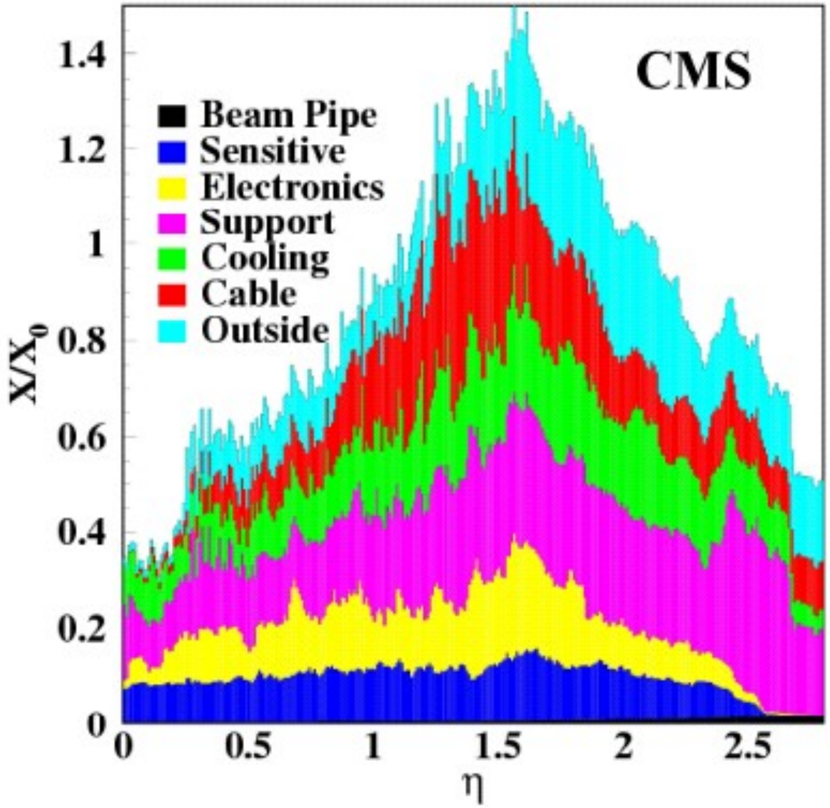

- **Conversion of Photons,**
- **Bremsstrahlung of electrons,**
- **Multiple scattering of all charged particles**

The Hadron Calorimeter - HCAL

- CMS HCAL is constructed in 3 parts:
  - Barrel HCAL (HB)
    - Brass (laiton) plates interleaved with plastic scintillator embedded with wavelength-shifting optical fibres (photo top right)
  - Endcap HCAL (HE)
    - Brass plates interleaved with plastic scintillator
  - Forward HCAL (HF)
    - Steel wedges stuffed with quartz fibres (photo bottom right)
- ~10000 channels total

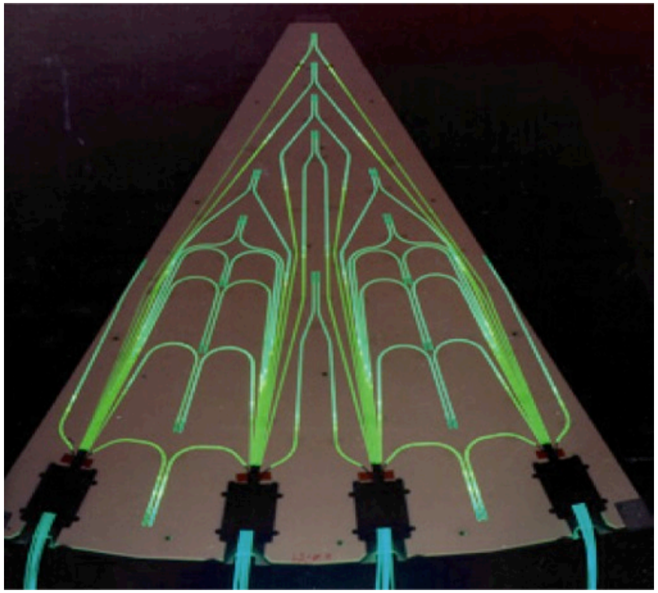

The Muon Chambers

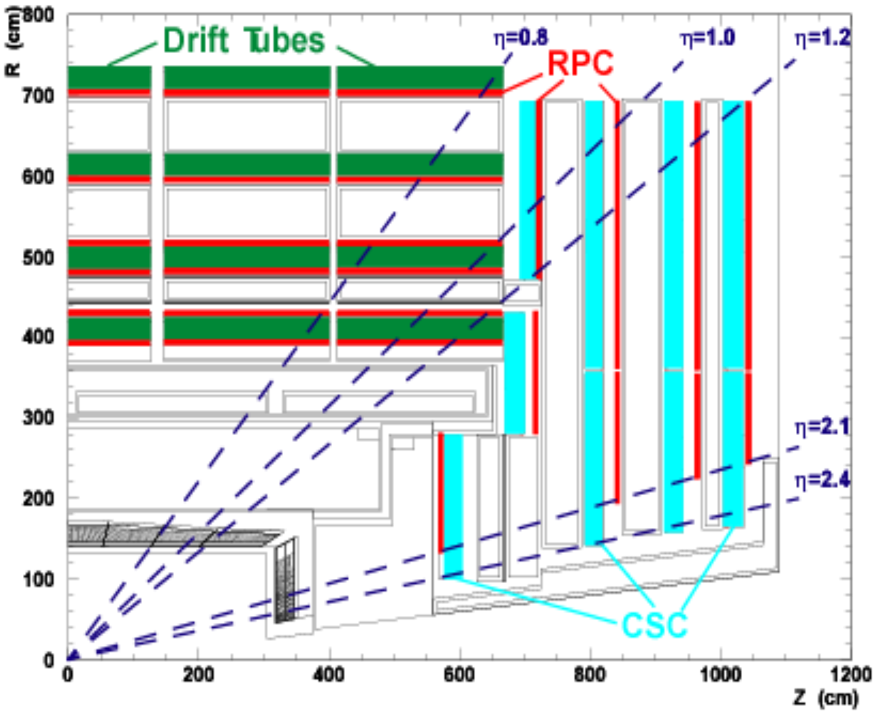

Position measurement:
Drift Tubes (DT) in barrel
Cathode Strip Chambers (CSC) in endcaps

Trigger:
Resistive Plate Chambers (RPCs) in barrel and endcaps

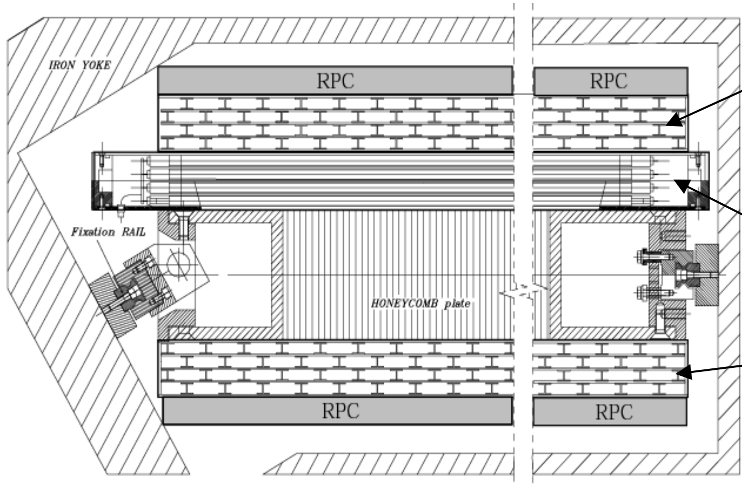

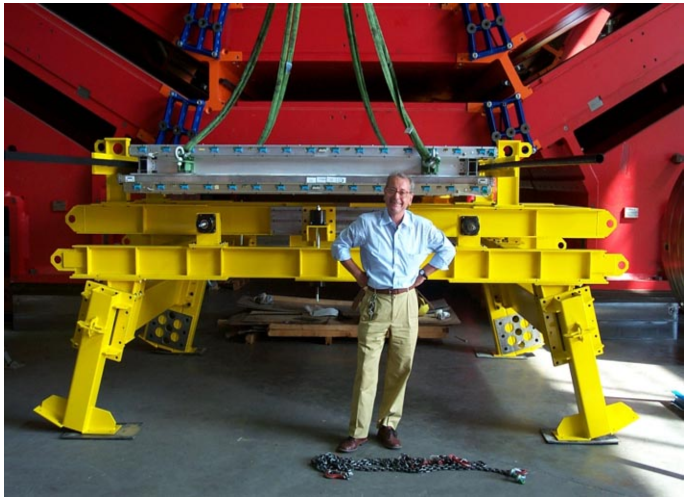

195000 DT channels
210816 CSC channels
162282 RPC channels

The Trigger and Data Acquisition System

Data Acquisition Main Parameters	
Collision rate	40 MHz
Level-1 Maximum trigger rate	100 kHz
Average event size	1 Mbyte
No. of electronics boards	10000
No. of readout crates	250
No. of In-Out units (200-5000 byte/event)	1000
Event builder (1000 port switch) bandwidth	1 Terabit/s
Event filter computing power	5 10^6 MIPS
Data production	Tbyte/day

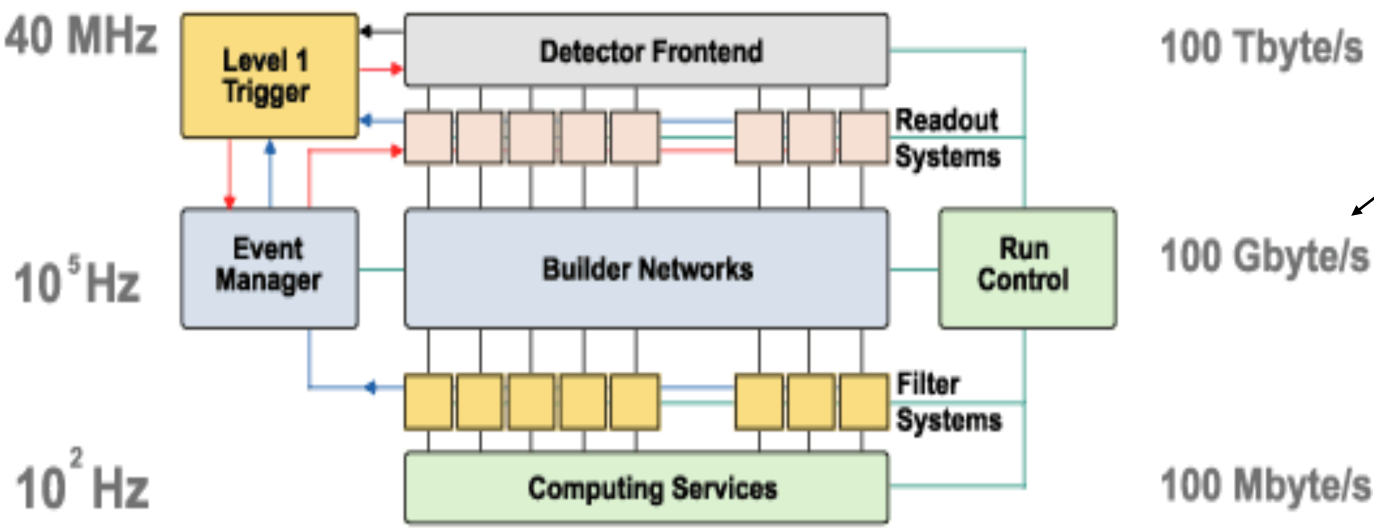

Trigger and Data Acquisition baseline structure

~same as whole world's telecom network!

CMS Basic Parameters

Physical Parameters

Length	21.6m
Diameter	14m
Mass	12500 Tonnes
Magnetic field	4 Tesla

Channel Count

Sub-Detector	Number of channels
Pixels	66×10^{6}
Silicon microstrips	11.4×10^{6}
ECAL crystals	0.076×10^{6}
Preshower strips	0.137×10^{6}
HCAL	0.01×10^{6}
Muon chambers	0.576×10^{6}
TOTAL	78.2×10^{6}

Trigger and Data Acquisition Parameters

Parameter	Value
Bunch-crossing frequency	40 MHz
Average # of collisions / bunch-crossing	20
"interaction rate"	$\sim 10^{9}$
Level-1 trigger rate	100 kHz
Average event size	1 Mbyte
Event builder bandwidth	100 Gbytes/sec
Event filter computing power required	10^{6} SI95
Event rate saved to mass storage	100 Hz
Data production	10 Tbytes/day

Ulrich.Goerlach@iphc.cnrs.fr, AS

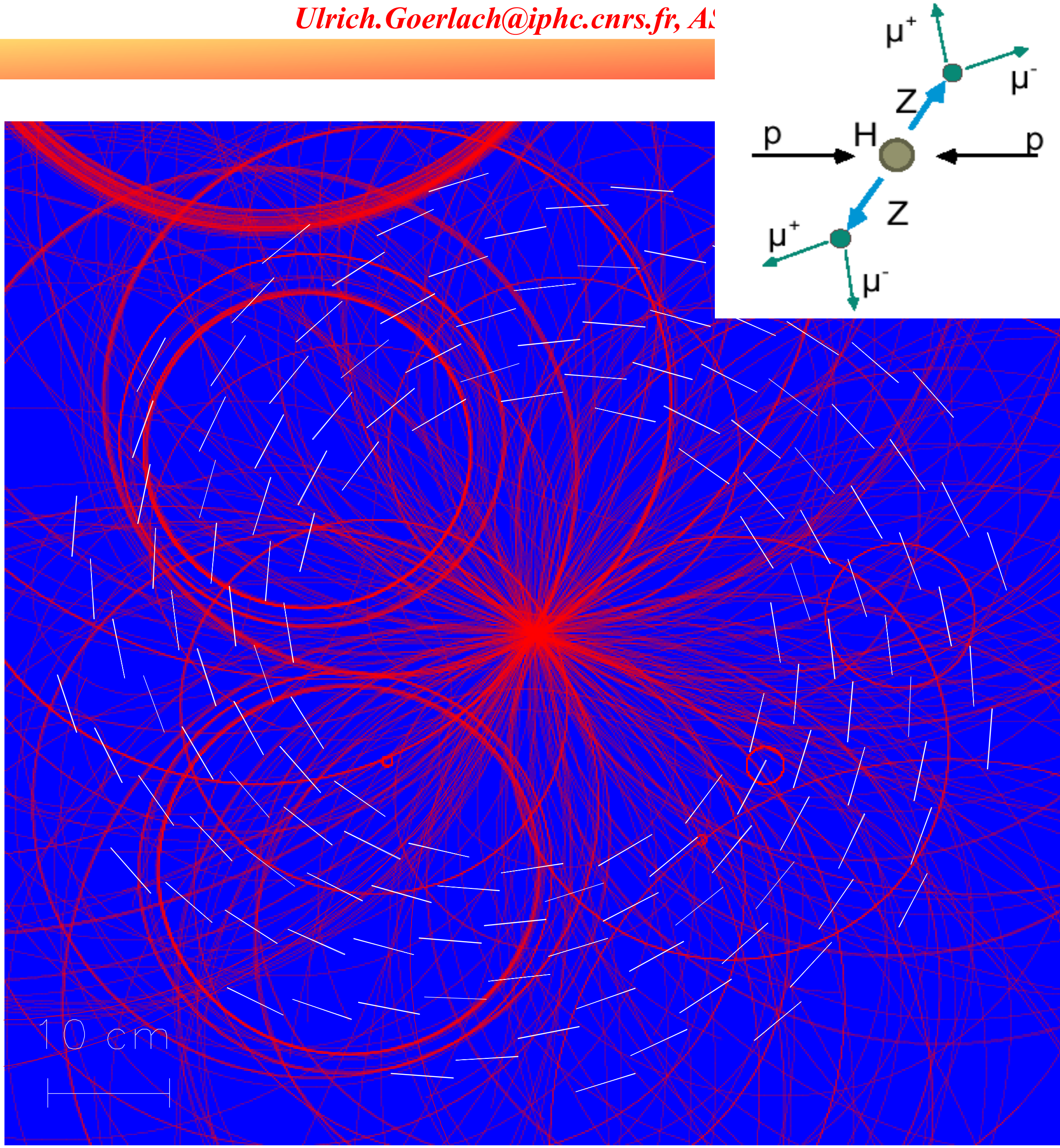

View along beam line of the inner tracking, with a H→ 4μ event superimposed. The μ are very high energy, so leave straight tracks originating from the centre and travelling to the outside

Make a "cut" on the Transverse momentum Of the tracks: p_T>2 GeV

Find 4 straight tracks.

View along beam line of the inner tracking, with a H→ 4μ event superimposed. The μ are very high energy, so leave straight tracks originating from the centre and travelling to the outside

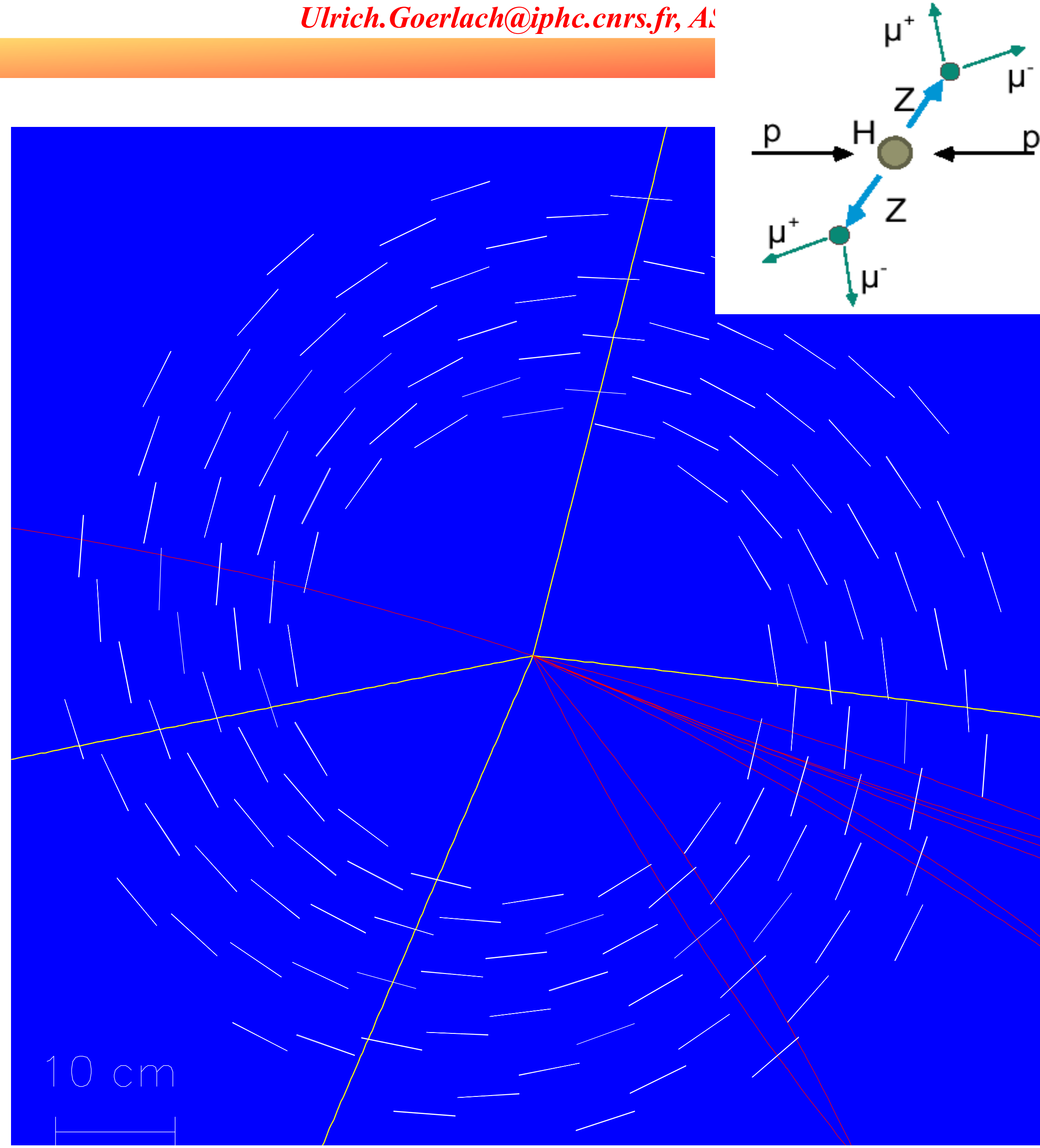

Make a "cut" on the Transverse momentum Of the tracks: p_T>2 GeV

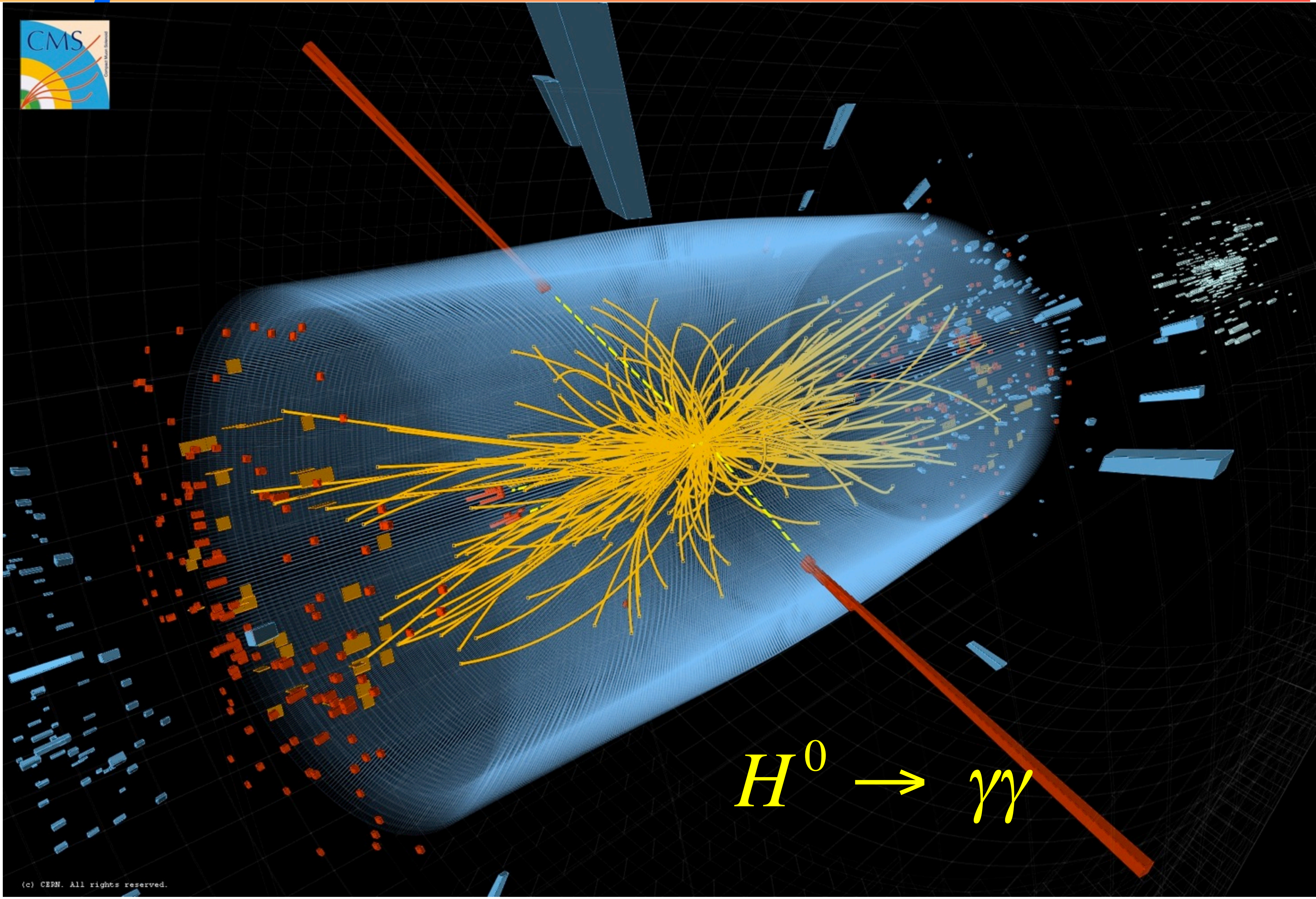

$$H^0 \rightarrow \gamma\gamma$$

Simulation in 1997!

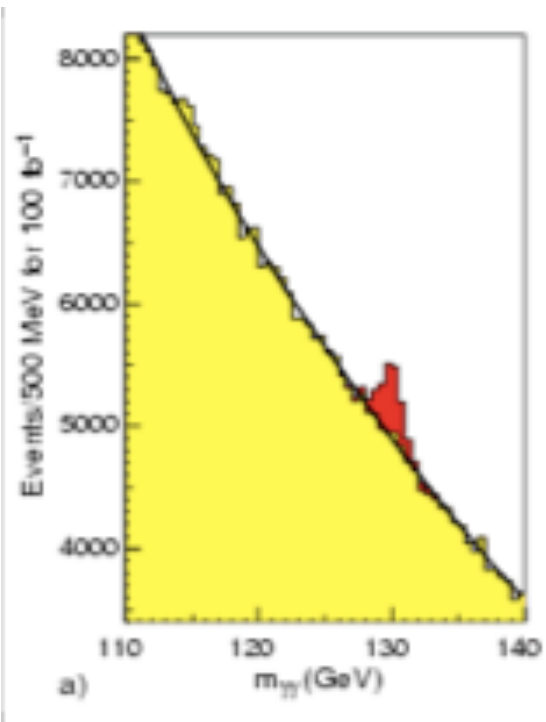

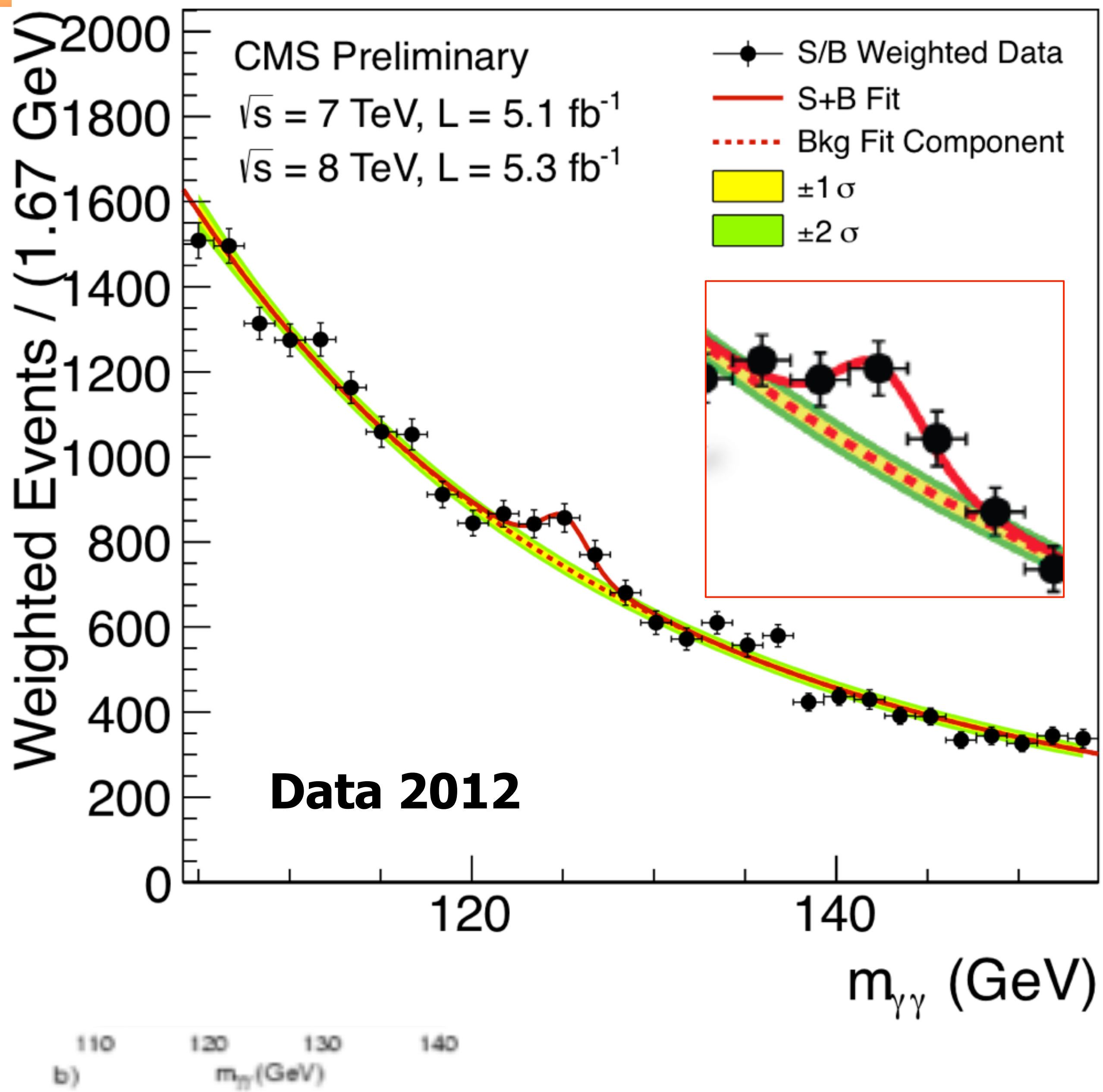

Large colaborations: Where are the students?

- Sub divided in smaller groups
  – Detector, subdetector
  – Analysis: different topics
  – Students belong to instituts
- International environment
  – Communication skills !
  – Mobility
  – Good students become well known in the collaboration very fast!
- Management
  – Physicists are (generally) not trained for that changes with time...
  – Sometimes there are problems, one has to sort them out..
- Students are an extremely important factor
- job opportunities outside particle physics

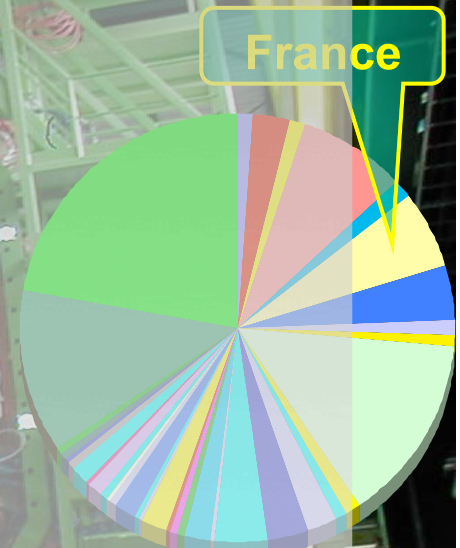

3300 Physicists and Engineers

39 Countries

172 Institutions

Astroparticle detectors

UNIVERSITÉ DE STRASBOURG

Super-Kamiokande

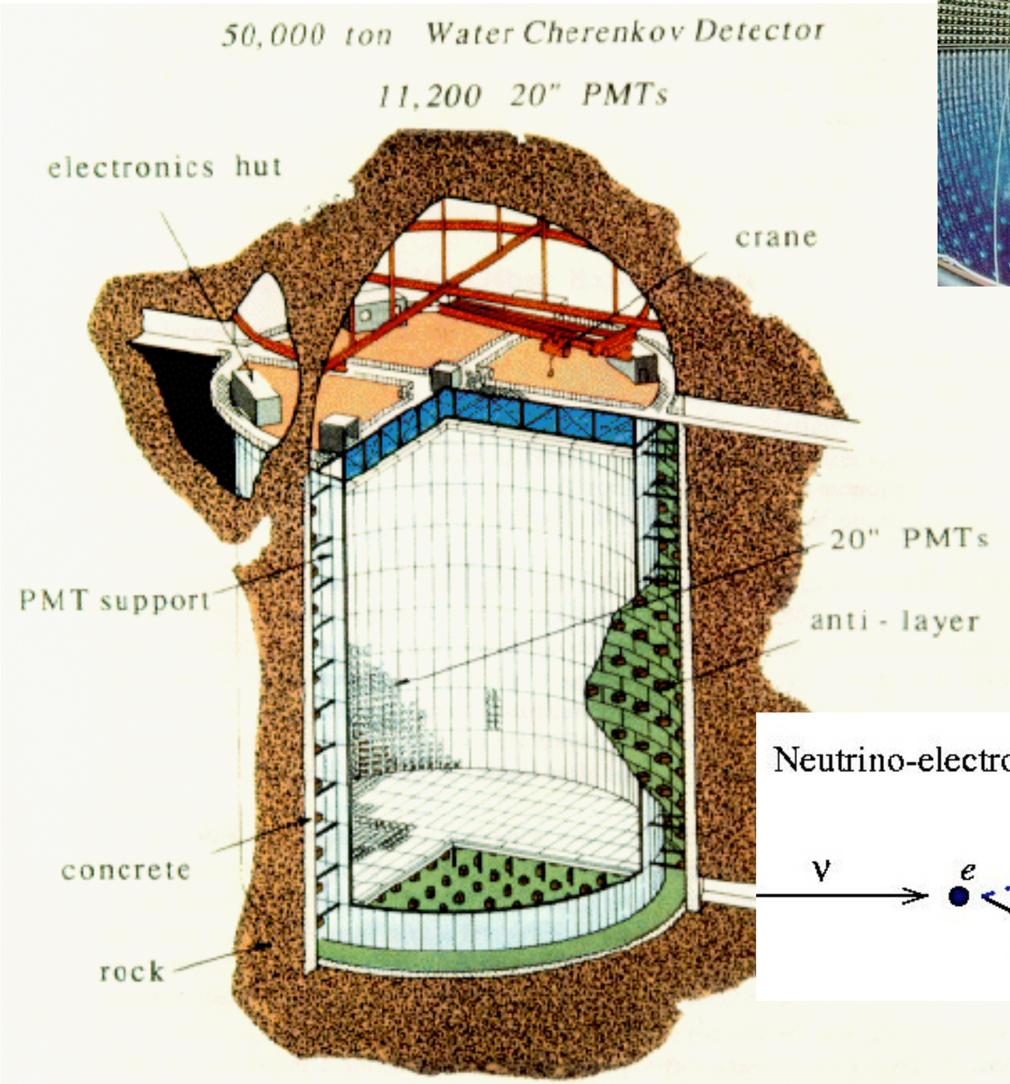

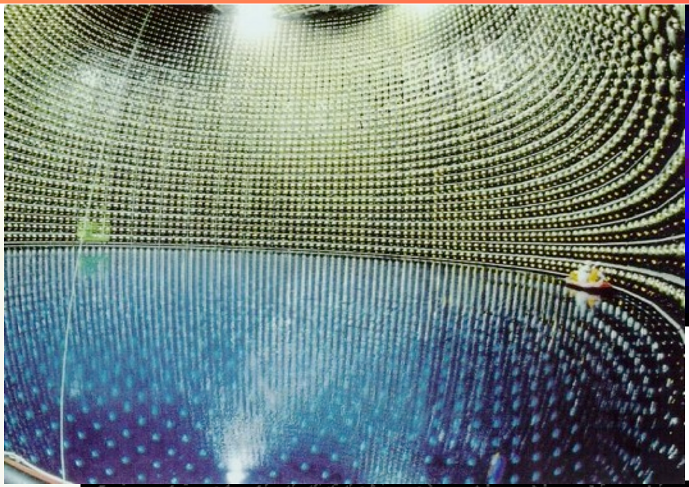

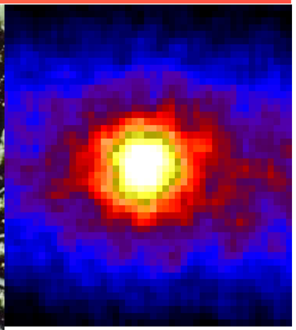

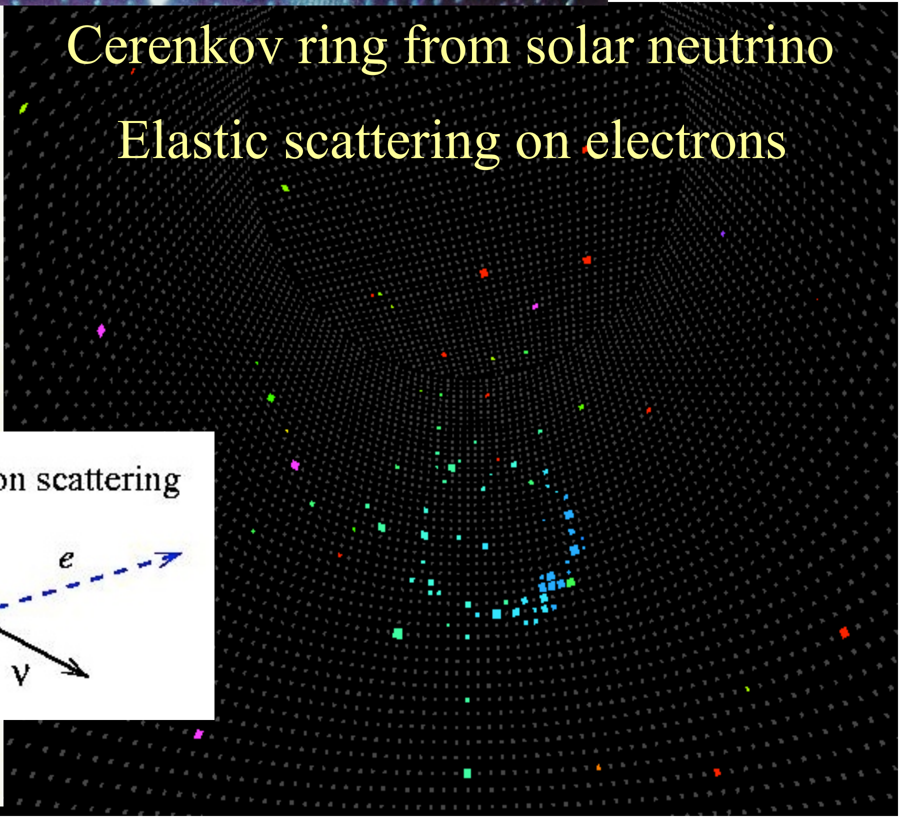

L'expérience (Super)-Kamiokande :

Masatoshi Koshiba,
(Kamioka Nucleon Decay)
Experiment

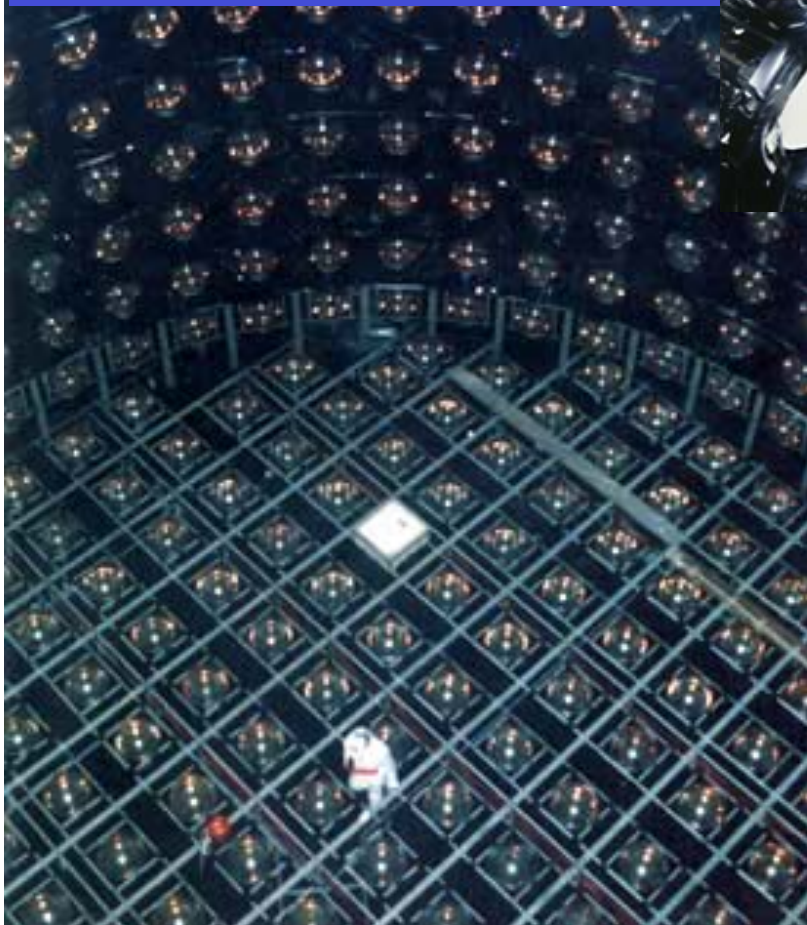

Prix Nobel 2002

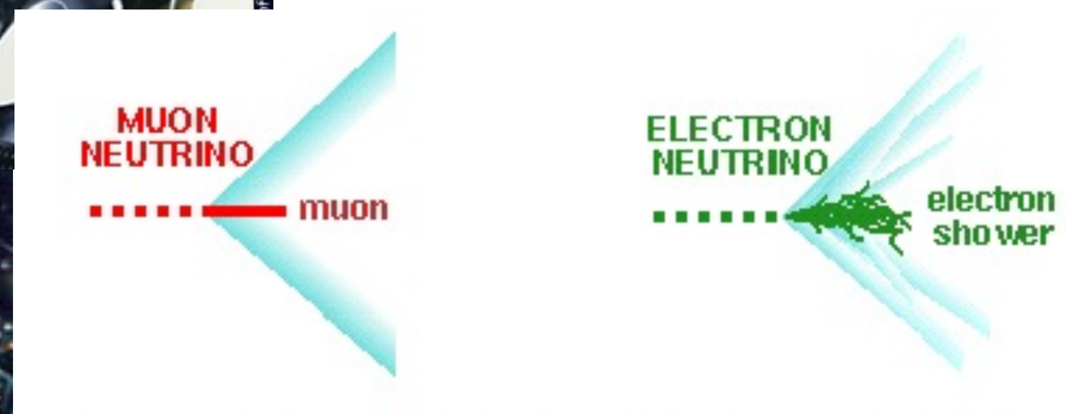

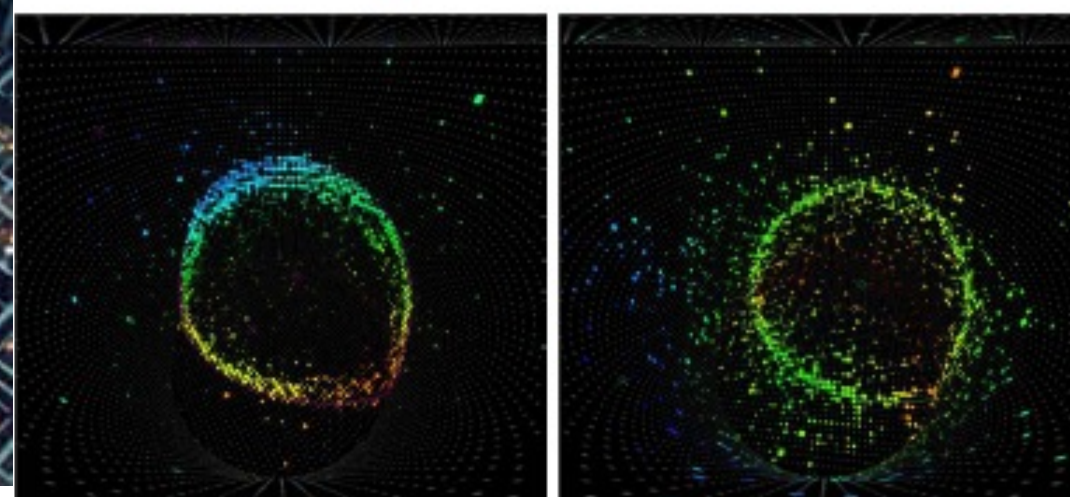

High energy atmospheric showers

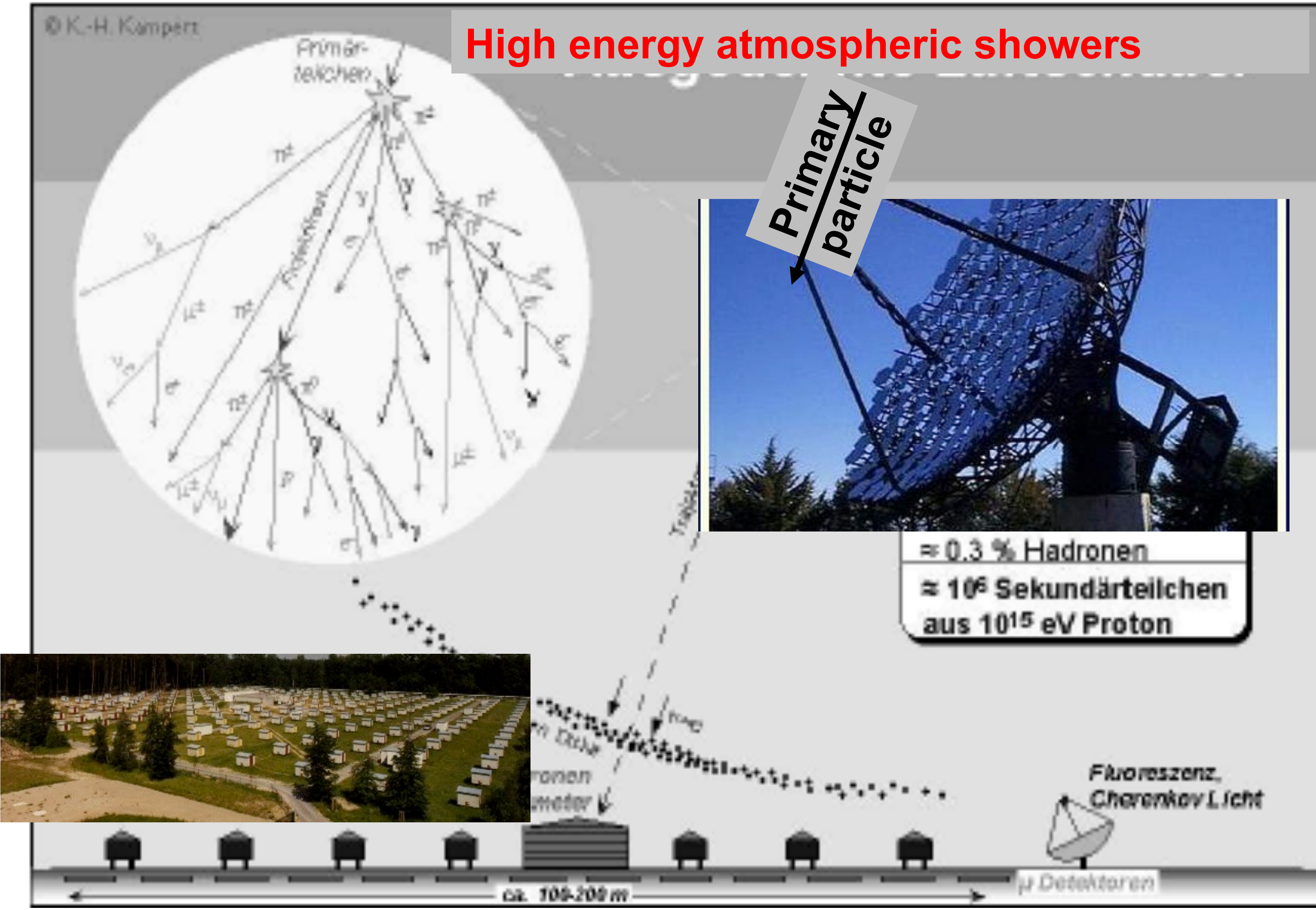

Pierre AUGER Observatory– southern site

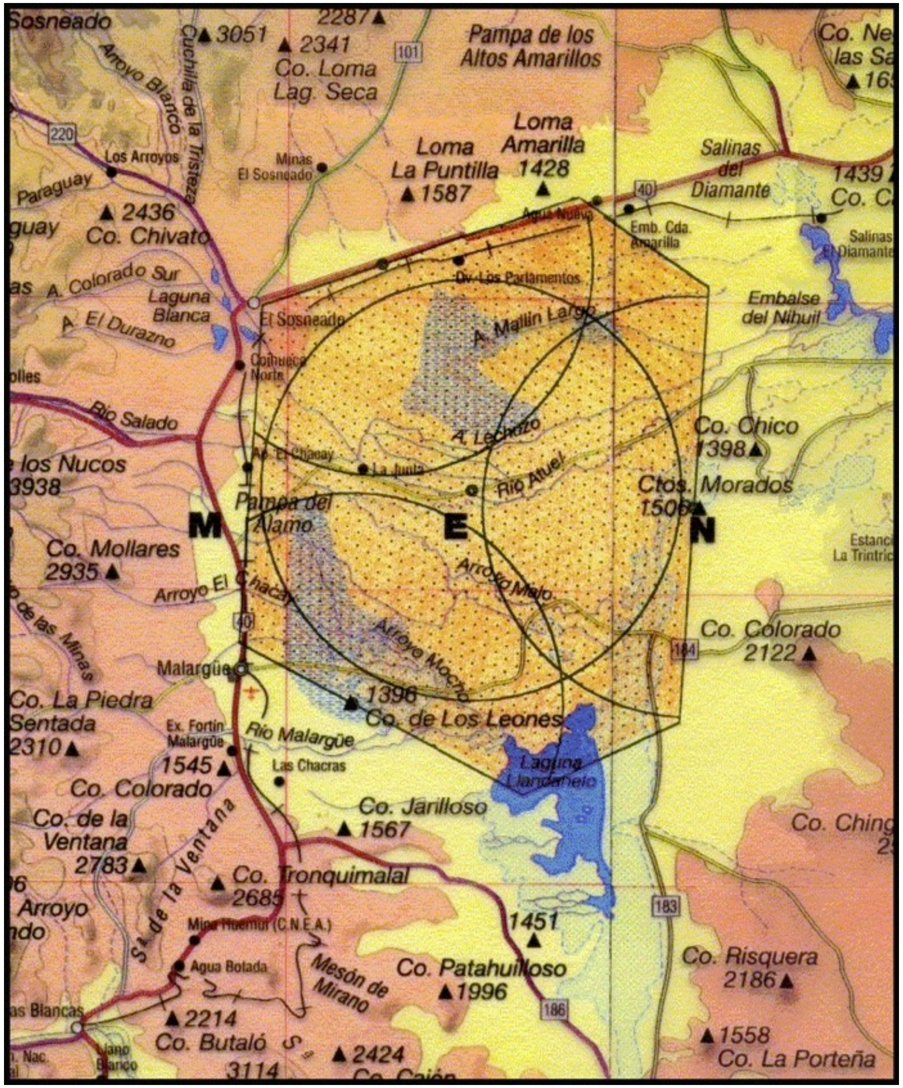

- 1600 detectors at 1,5 km
- 3000 km^2
- 24 telescopes in 4 points

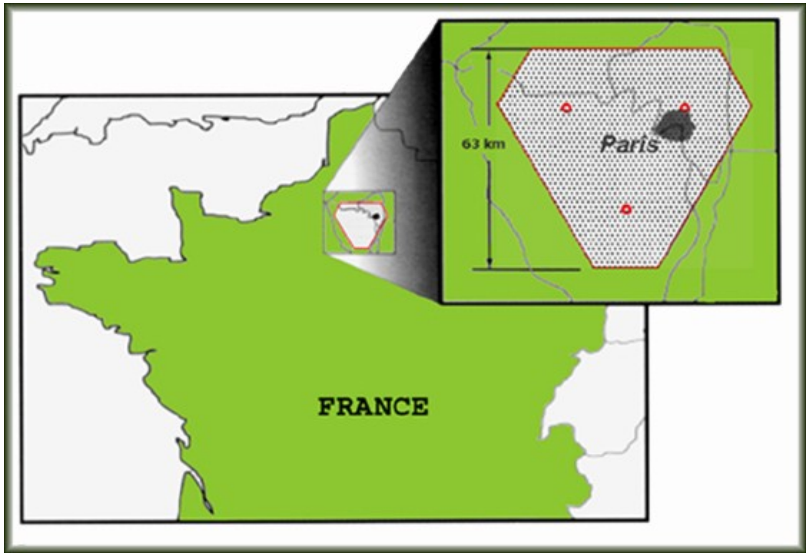

AUGER

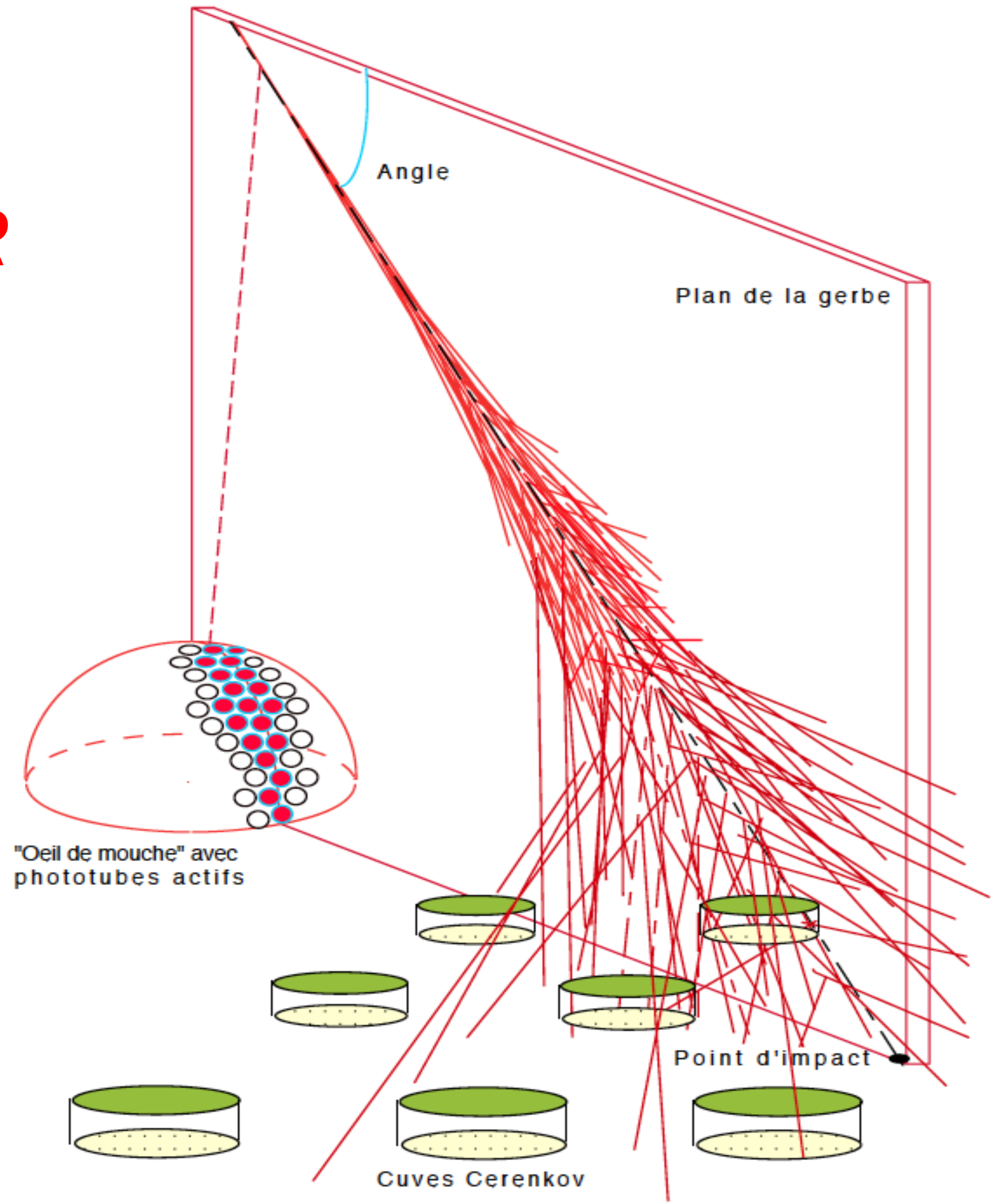
Angle
Plan de la gerbe
"Oeil de mouche" avec
phototubes actifs
Point d'impact
Cuves Cerenkov

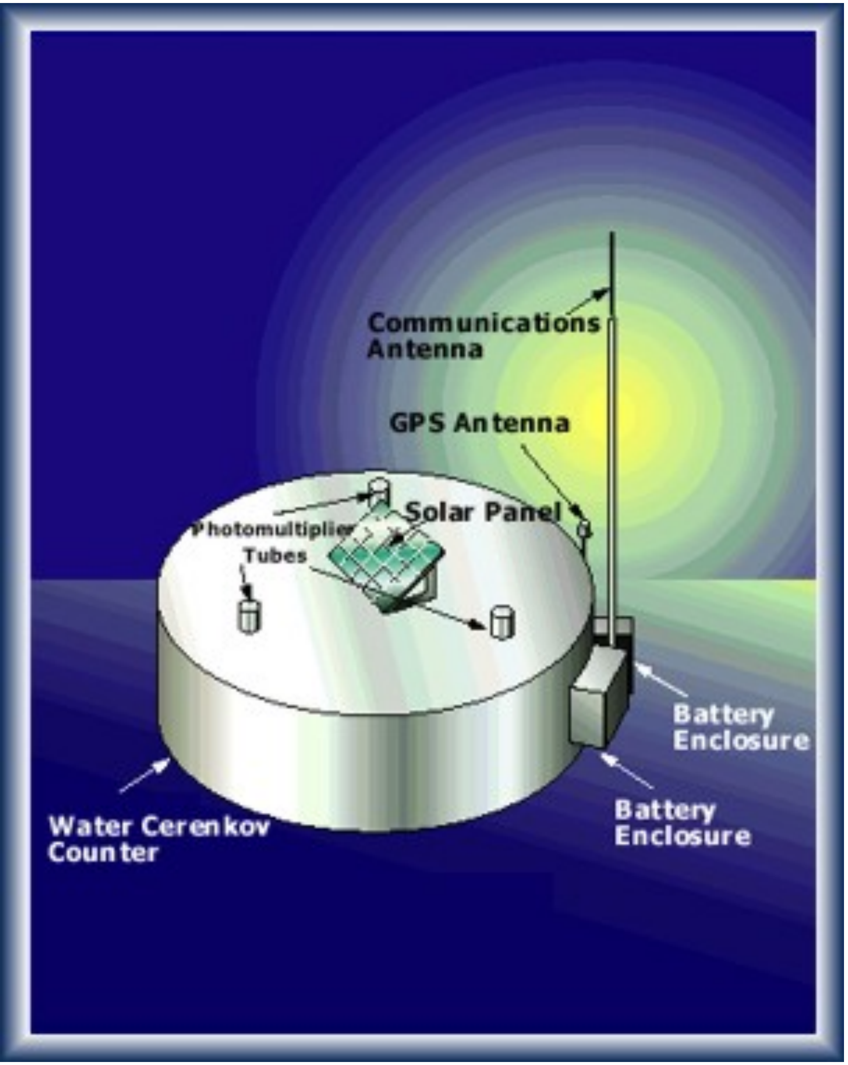

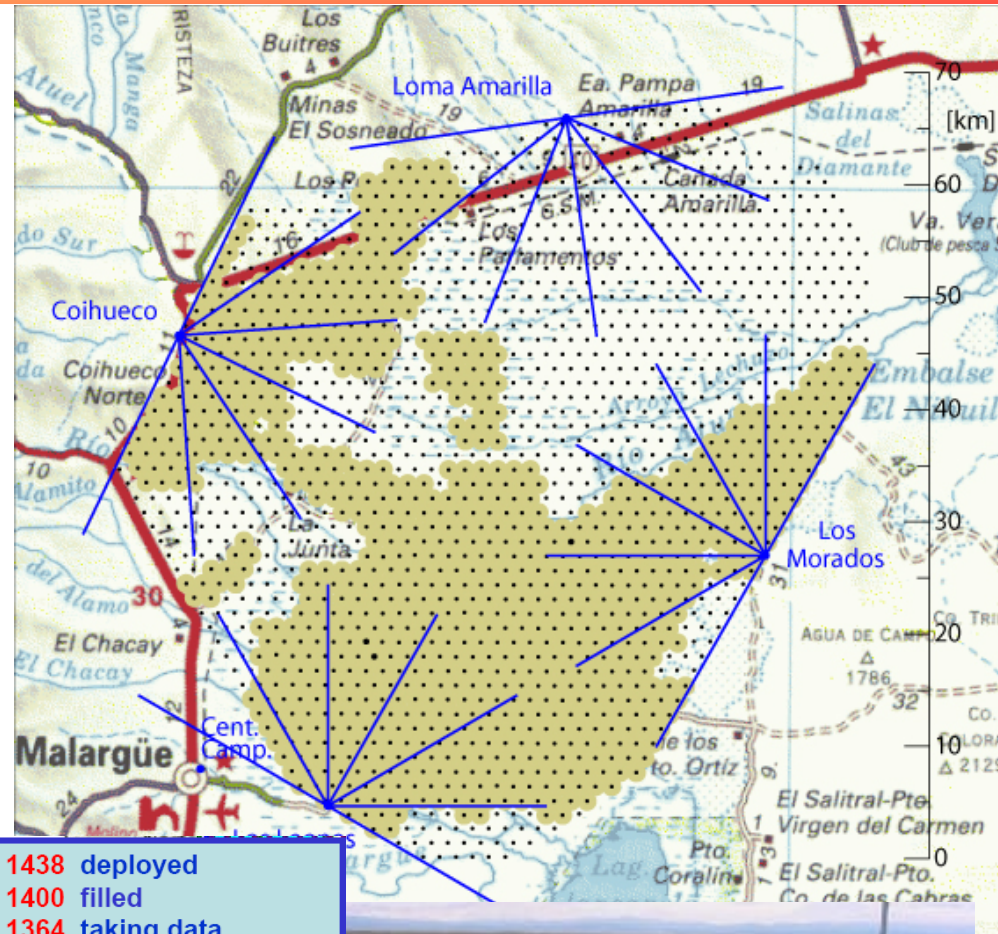

1438 deployed
1400 filled
1364 taking data

090707 ~ 85%

All 4 fluorescence buildings complete, each with 6 telescopes

1st 4-fold on 20 May 2007

AIM: 1600 tanks

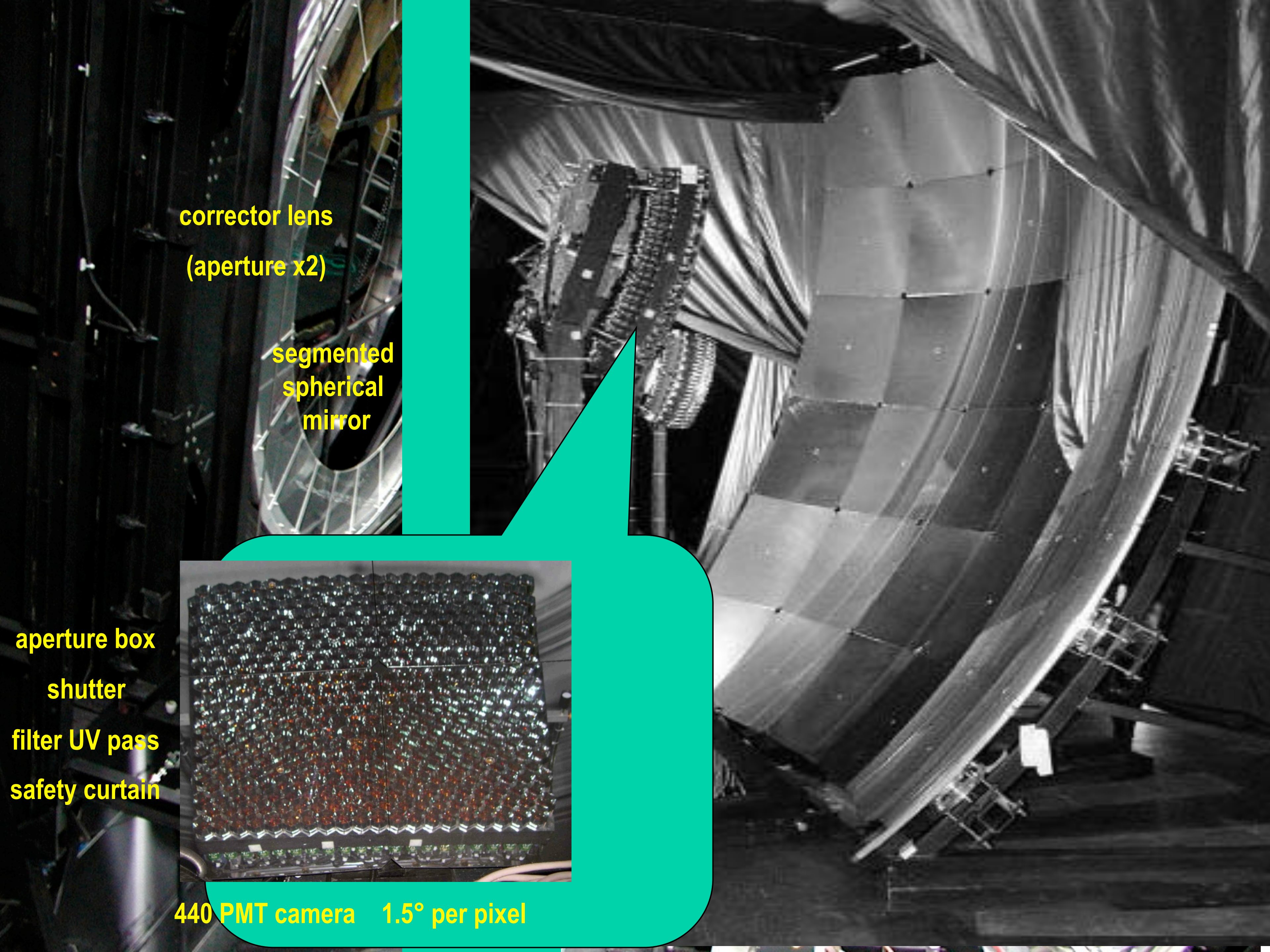
corrector lens
(aperture x2)
segmented
spherical
mirror
aperture box
shutter
filter UV pass
safety curtain
440 PMT camera
1.5° per pixel

Conclusions

- All particle detectors in nuclear, particle and astroparticle physics are based on the physics of the interaction of particles and radiation with matter
- It is possible to measure and reconstruct the interaction of elementary particles also in the very difficult environments of proton proton collisions at the LHC
- Many of the experiments today are large and complex, both in their concept and in the new technologies employed
- They are run by very large collaborations of scientists, engineers and also of students over 10-20 years
- We live in exciting times and there is a lot more ahead of us, many opportunities for students

Message to students

- It is fun to work on these experiments and their data